# The Role of CD40 in Epithelial Cell Fate


## Christopher John Dunnill


**A thesis submitted in partial fulfillment of the requirements for the degree of Doctor of Philosophy**


**The University of Huddersfield**

**School of Applied Sciences**


**September 2013**

# Abstract

CD40 belongs to the tumour necrosis factor receptor (TNFR) family and its ligation by membrane-presented CD40 ligand (mCD40L) causes extensive apoptosis in malignant cells, while sparing their normal epithelial counterparts which, can respond to CD40 ligation by proliferation, thus representing an intriguing paradox in TNFR biology. Although the apoptotic potential of mCD40L is well-documented, the precise intracellular signalling pathways of cell death remain largely unknown. Moreover, due to the practical constraints imposed by the necessity to deliver surface-CD40L for therapeutic purposes, deciphering the molecular nature of the CD40 signalling 'black-box' may permit the design of novel therapeutic approaches. This thesis aimed to unravel for the first time the precise cell signalling pathways responsible for mCD40L-mediated apoptosis and attempted to determine the mechanisms underpinning the tumour-specificity of CD40 ligation.

The first part of this thesis focused on optimisation of cell models for the delivery of the mCD40L signal to epithelial cells (via co-culture with third party cells and based on the urothelial cell culture system). A number of assays were optimised for the detection of several apoptosis hallmarks (membrane integrity loss, caspase activation, DNA fragmentation and mitochondrial cytochrome c release). Immunoblotting techniques were improved for the sensitive detection of intracellular CD40-signalling mediators, followed by the optimisation of methodologies for retrovirus transduction-mediated delivery of short hairpin RNA (shRNA) molecules for functional (knockdown) experiments.

Expression studies and knockdown experiments reinforced the role of TRAF3 as a key mediator of apoptosis and cemented its essential role in both JNK/AP-1 activation and subsequent induction of pro-apoptotic Bak and Bax, with Bak and particularly Bax loss alone demonstrating as essential for apoptosis. The project also revealed for the first time the proximal events in the CD40 pathway that provided a link between TRAF3 induction and JNK/AP-1 activation followed by Bak/Bax induction. A series of functional experiments involving RNAi-mediated knockdown and/or pharmacological inhibition of critical target proteins suggested that mitogen activated protein kinases (MAPKs) ASK1 and MKK4 (but not MKK7) drive the activation of JNK/AP-1 and CD40-mediated death. Because of the well-documented sensitivity of ASK1 towards oxidative stress and its direct regulation by reactive oxygen species (ROS), a CD40-ROS paradigm was explored. It was found that oxidative stress is essential in CD40-mediated apoptosis as pharmacological inhibitors of ROS attenuated cytotoxicity. Additionally, the work provided novel evidence for a functional role for the NADPH oxidase (Nox) enzyme in apoptosis, as pharmacological inactivation of Nox attenuated ROS induction and blocked apoptosis, signifying that ROS-mediated oxidative stress is Nox-dependant. More specifically, it was found that CD40 ligation caused phosphorylation of p40phox, a Nox-2 subunit previously reported to interact with TRAF3, but not in the context of apoptosis induction. These observations implied that TRAF3-mediated CD40-Nox interactions may be crucial for CD40-induced apoptosis. Importantly, the observation that adequate ROS elevation, to permit efficient thioredoxin (Trx) down-regulation and ASK1 activation, was only observed following receptor ligation by pro-apoptotic mCD40L, but not by non-apoptotic soluble agonist, led to the hypothesis that pharmacological interference with Trx may compensate for the lack of signal strength and sensitise cells to apoptosis. Strikingly, combinatorial treatment of carcinoma cells with a specific Trx-1 inhibitor and agonistic anti-CD40 antibody showed efficient synergy and resulted in extensive apoptosis. The combinatorial treatment appeared functionally equivalent to mCD40L and employed ASK-1/JNK signalling to induce apoptosis.

Finally, to enhance our understanding of the role of malignant transformation in CD40 susceptibility, the effect of over-expression of the telomerase catalytic sub-unit (hTERT) in normal epithelial cells was assessed. It was found that, unlike normal human urothelial (NHU) cells where CD40 ligation did not cause apoptosis (but appeared to be cyto-protective), para-malignant hTERT NHU expressers were highly susceptible to CD40-killing and to an extent equivalent to that observed in carcinoma-derived cells. By comparing normal, para-malignant and tumour-derived cells, the study added to increasing evidence that during malignant transformation cells exhibit higher basal ROS levels, which functions as 'double-edged sword' that renders them more susceptible to signals that elevate ROS past a lethal pro-apoptotic threshold, such as that triggered by CD40.

Collectively, this thesis has unravelled for the first time the molecular nature of pro-apoptotic CD40 ligation revealing a key signalling axis triggered CD40 ligation that involves TRAF3, Nox-2 (p40phox), ROS, ASK1, MKK4, JNK, Bak/Bax and intrinsic apoptosis, whilst the new knowledge of the signalling pathway has now provided novel avenues for exploiting CD40 as a target for anti-cancer therapy.

## Contents Page

**Figures**

## Copyright declaration

# Acknowledgements

A wealth of gratitude must first go to my Supervisor Dr Nik Georgopoulos at the University of Huddersfield who has been not only ‘fantastic’ mentor but a great friend. Nik has set a high standard of academic quality which caused me to reach deep into my potential and self-belief.

In kind, I would like to thank Loretta Stoklosa and Mr Albashir Mohammed for being great friends during my most difficult times of study.

Some appreciation must also go to Professor Jennifer Southgate at the University of York who provided primary normal urothelial cell samples to further enhance my research potential and also the Huddersfield Royal infirmary for providing such samples. Last but not least I’d like to thank The University of Huddersfield, School of Applied Sciences for giving me the funding to participate in my PhD qualification.

*This thesis is dedicated to my beloved mother who was sadly taken by cancer in 2011 and also to 'Nanna Peggy' who passed shortly after.*

*'In loving memory, I will always keep you next to my heart'.*

***RIP***

*Frances Johnson 18.04.1953 - 01.10.2011*

*Margaret Johnson 30.6.1924 - 08.11.2011*

# 1.0 Introduction

# 1.1 Apoptosis

## 1.1.1 General

Apoptosis, or programmed cell death (PCD), is a highly organised sequence of biological and energy-dependent events that are essential for an organism's existence. Apoptotic cell death follows a multi-step process, which quietly removes unwanted or irreparable cells without interfering or causing damage to surrounding tissue (Elmore, 2007).

## 1.1.2 Cell morphological and biological changes during apoptosis

During apoptosis, cells demonstrate distinct morphological and biochemical features that divide it from a further characterised type of cell known as necrosis (see below). Initial features include cell shrinkage and condensation of the cytoplasm due to volume loss, which is partnered by chromatin condensation a process termed 'pyknosis'. Both cytoplasmic condensation and pyknosis are visible using tissue histology with low resolution microscopy (Figure 1-1). In continuation, the nucleus, DNA and organelles become fragmented, and the cell begins to show cytoplasmic 'blebbing'. The blebs form apoptotic bodies that contain fragmented constituents on the internal-, and phosphatidylserine on the external- cell membrane for 'engulf me' signals to neighbouring phagocytes (Figure 1-2). Since cells are taken up quietly during phagocytosis, there is no internal spillage of cell contents into the surrounding cells, which would normally cause inflammation and secondary tissue damage like that induced by necrosis.

Necrosis is also distinguishable due to apoptosis. Necrotic cell death, also known as accidental cell death (ACD), generally occurs in response to extreme stimuli and is characterised by a loss of cell membrane integrity, cell swelling, the formation of cytoplasmic vacuoles, swollen endoplasmic reticulum's, distended or ruptured mitochondria's, lysosomes and lysis. This results in internal cell spillage into surrounding tissue, immune cell recruitment and subsequent inflammation as briefly mentioned earlier – see Figure 1-2 (Hengartner, 2000, Elmore, 2007).

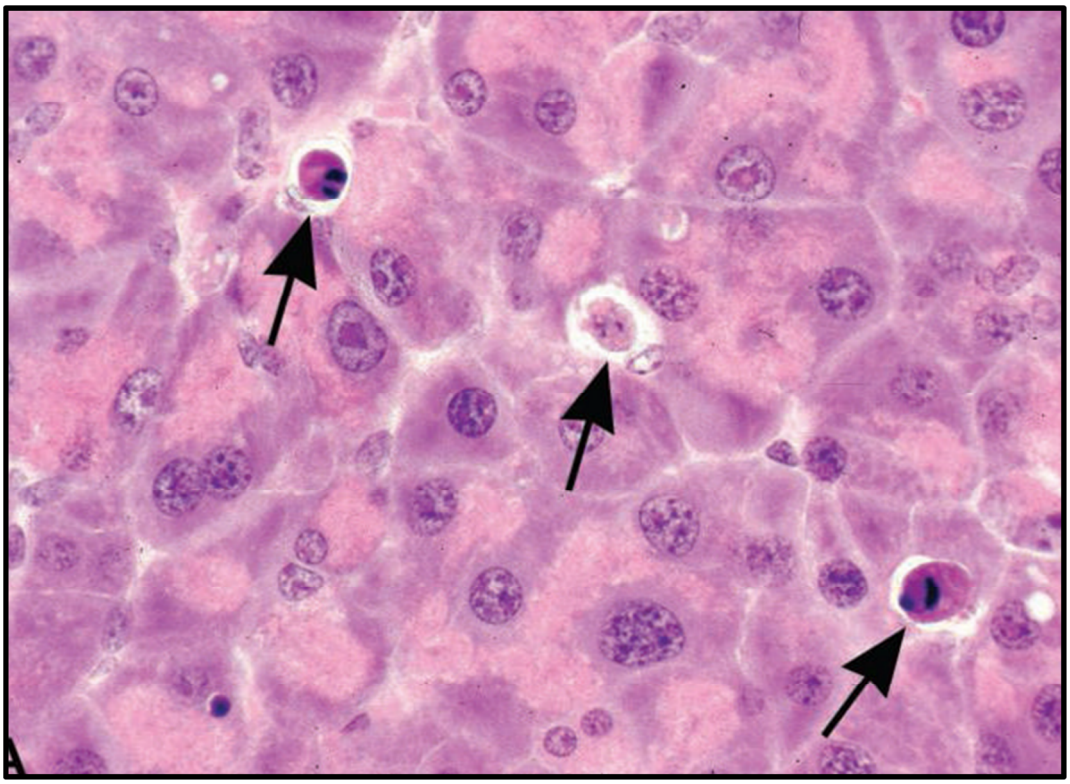

**Figure 1-1 A photomicrograph section of murine exocrine pancreas with apoptotic**

The arrows indicate apoptotic cells. Visible features are a condensed cytoplasm (deep pink) and nuclear pyknosis (deep blue). Figure Adopted from (Elmore, 2007).

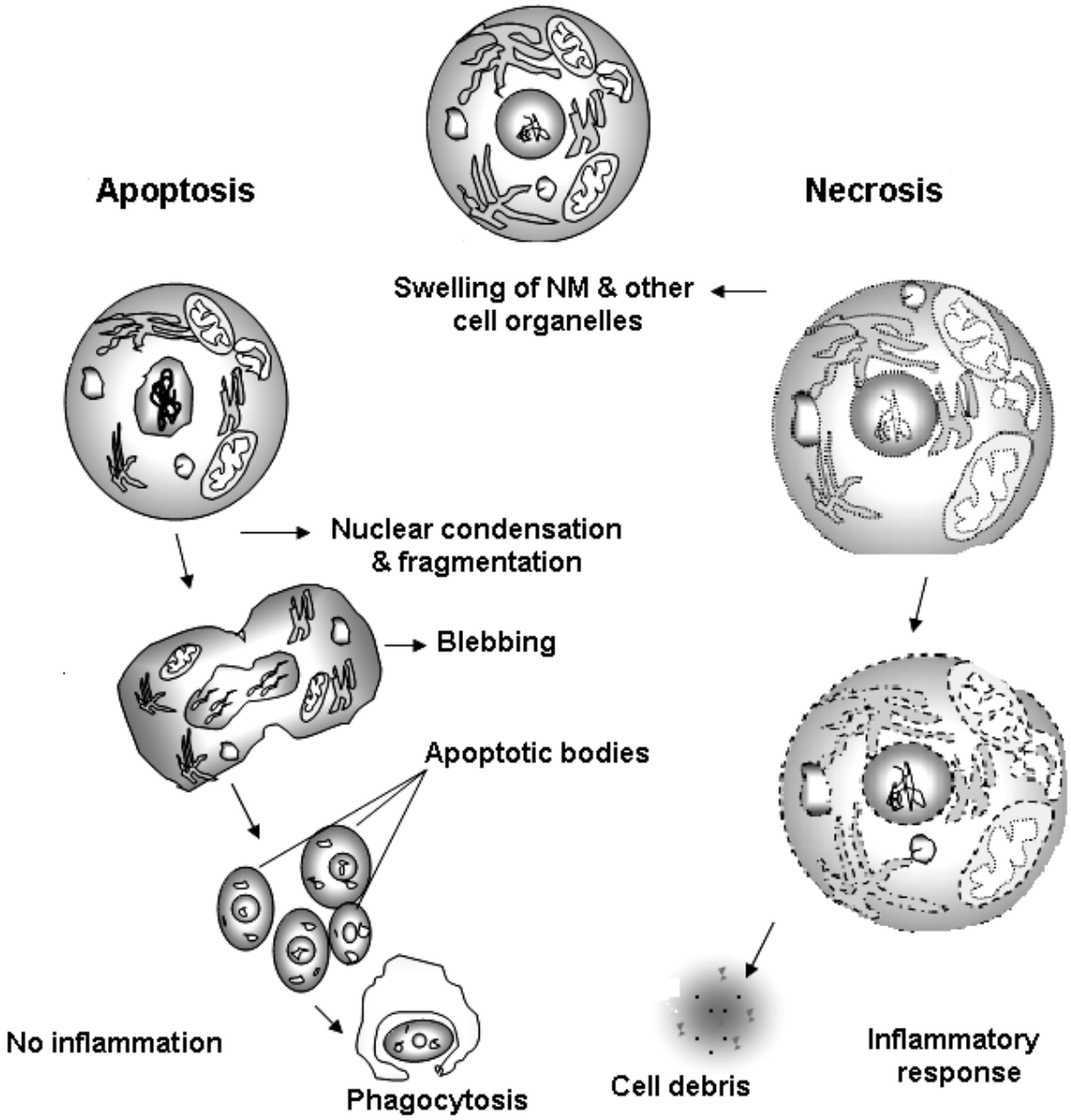


**Figure 1-2 A diagrammatic illustration of apoptotic and necrotic morphological changes**

Distinctive features of apoptosis include nuclear (chromatid) and cytoplasmic condensation, blebbing, the formation of apoptotic bodies and phagocytosis. Distinctive features of necrosis include swelling of the cytoplasm, organelles and nuclear membrane (NM), which results in cell lysis, internal cell content spillage and an inflammatory response. Figure adopted from (Rastogi and Sinha, 2010).

## 1.1.3 Physiological importance of apoptosis

The elimination of cells by apoptosis is equally important as their mitotic generation or regeneration and this is demonstrated by many biological processes including; the early tissue curvature of a developing embryo to the formation of an adult, the maturation of the immune system, morphogenesis, neural development and wound repair. Apoptosis is also equally fundamental to the removal of virally-infected, DNA damaged and carcinogenic cells. Moreover, throughout and following complete adult creation, there is an enormous overproduction of cells with those non-beneficiaries internally wired for self-removal. For instance, dendrites must make synaptic connections in order to prevent the activation apoptotic machinery during nerve expansion and equally fundamental is the removal of self-reactive B and T-cells during self-tolerance (Han et al., 2008, Elmore, 2007, Rastogi and Sinha, 2010). A plethora of diseases are associated with malfunctioning of the process of apoptosis, therefore demonstrating the biological importance of this process throughout all stages of an organism's existence (Figure 1-3).

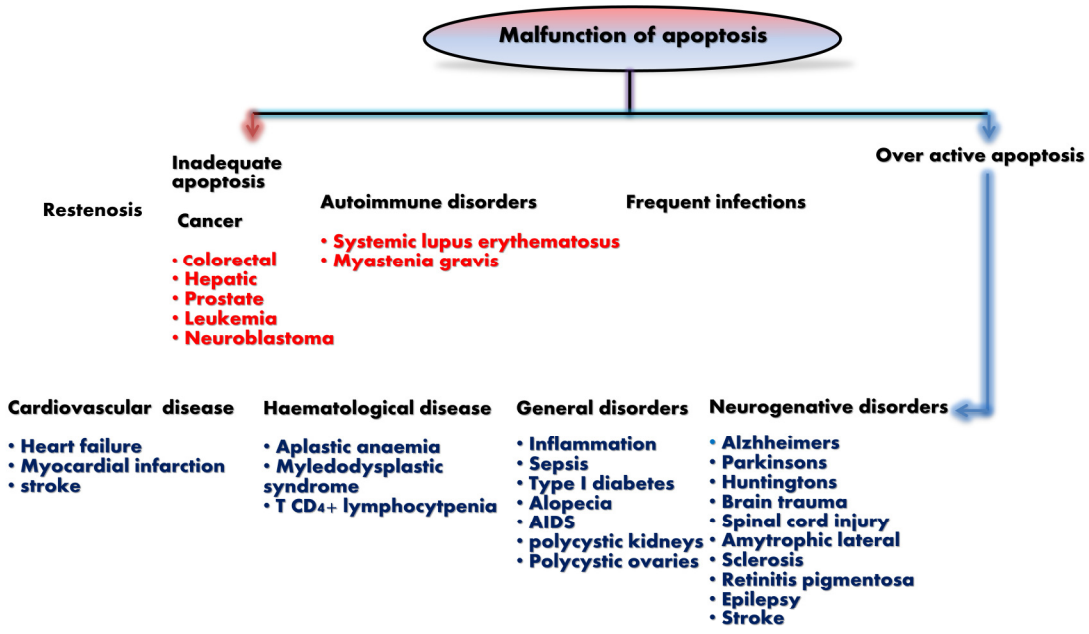


**Figure 1-3 Human diseases implicated in over or under active apoptosis**

Underactive or overactive apoptosis contributes to all the diseases listed in the Figure 1-4. Figure drawn based on information from (Han et al., 2008, Elmore, 2007, Rastogi and Sinha, 2010).

## 1.2 Pathways of apoptosis

There are three biological pathways that are recognised to induce apoptosis; the perforin/granzyme (section 1.2.2), the intrinsic or mitochondrial (section 1.2.3), and the extrinsic (section 1.3) pathways of apoptosis (Zitvogel et al., 2006). As will be discussed, each pathway is fundamental to cancer prevention, in addition to sharing a notion in active catalytic proteins known as the caspases, which are first discussed (section 1.2.1).

### 1.2.1 Caspases - key mediators of apoptosis

In the majority of cases, caspases are understood to play a key role in the induction of apoptosis (Hengartner, 2000, Elmore, 2007). All caspases are created as inactive enzymes known as zymogens containing a prodomain, a large p20 sub-unit and a small p10 sub-unit and before their activation are termed pro-caspases. Caspases are proteases that contain a cysteine residue in their active site and they cleave peptides at aspartic residues following recognition of four contiguous amino acids (Li and Yuan, 2008). A number of caspases have been identified and characterised into functional groups; initiator caspases, effector/executioner caspases or inflammatory caspases. As implied by their term, inflammatory caspases -1,-4,-5,-11,-12,-13 and -14 are not directly used for apoptosis but for inflammatory events. Initiator caspases -1,-2,-4 and -9 contain a death domain (DD) known as the caspase activation and recruitment domain (CARD), whereas caspases -8 and -10 contain a death effector domain (DED). In response to stimuli and after a series of protein interactions, which involve the formation large protein molecular complexes, the initiator caspases become ‘activated’ and directly cleave executioner caspases -3, -6 or -7 via a recognition sequence. This leads to a stream of proteolytic events that underpin the morphological and biological features of apoptosis – as previously shown in Figure 1-2 (Riedl and Shi, 2004, Taylor et al., 2003). The general structural and functional characteristics of the caspases are shown in Figure 1-4.

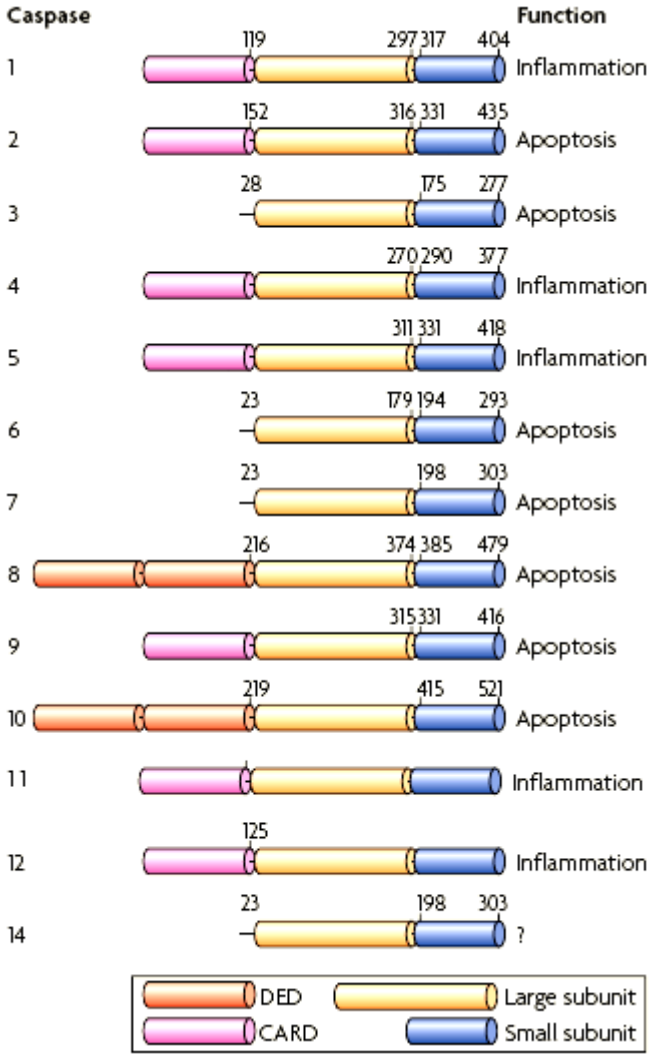


Figure **1-4 The structural and functional features of the Caspases**

Each caspase consists of different sub-units with large, small, DED and CARD sub-units sharing structural homology. Caspases -1,-4,-5,-11,-12,-13 and 14 mainly mediate inflammatory events, Caspases -3, -6, -7, -8, -9 and -10 mediate apoptosis. Figure adopted from (Taylor et al., 2008).

### 1.2.2 The perforin/granzyme pathway of apoptosis

The perforin/granzyme pathway is the most predominantly used pathway for the removal of infected or transformed cells. This pathway utilises T–cell receptor recognition of viral or tumour antigens displayed by MHC class I molecules. Upon antigen recognition, cytotoxic T-lymphocytes release a membrane-disrupting pore-forming protein known as perforin. Subsequently, the exocytosis of granzyme A and/or B induces apoptosis via two distinct mechanisms. Granzyme A targets nuclear proteins and DNA, causing single stranded DNA breaks and the induction of apoptosis. Granzyme B targets Bid for cell death executed by the intrinsic pathway of cell death (section 1.2.3) or caspase-10 for the activation of caspase -3, -6 and -7 (Trapani and Smyth, 2002).

### 1.2.3 The intrinsic (mitochondrial) pathway of apoptosis

The major source of energy (ATP) production that permits cell survival is also an essential gatekeeper between cell life and death, the mitochondrion. This organelle regulates the intrinsic pathway of apoptosis in response to survival factors, cell stress and injury. Changes occur in the permeability of the outer mitochondrial membrane (OMM) due to its interaction with Bcl-2 members, or through opening of permeability transition pores (PTPs) in response to oxidative stress. Oxidative stress is caused by a raised intracellular production of reactive oxygen species (ROS) and these molecules are becoming increasingly recognised as essential mediators for this type of cell death due to their ability to modify pro-apoptotic proteins (Ott et al., 2007, Circu and Aw, 2010, Biswas et al., 2006).

The aforementioned change in permeability is termed mitochondrial outer membrane permeabilisation (MOMP), which leads to the release of cytochrome c and SMAC/DIABLO. Cytochrome c causes the formation of the apoptosome via procaspase-9, Apaf-1 and ADP, which subsequently cause the activation of caspase-9. SMAC/DIABLO directly inhibit inhibitors of apoptosis (IAPs), which function to attenuate caspase activation, and thus caspase-9 is permitted to trigger activator executioner caspases-3/6/7. Following this, caspase-activated DNase (CAD), a DNA proteolytic enzyme, executes the final steps of the cell death. The intrinsic pathway thus includes many regulatory components such as transcriptional

and translational regulation of Bcl-2 members, death effector components and IAPs for caspase inhibition. However, cell death may also occur independently of caspases via the release of apoptosis inducing factor (AIF), which translocates from the intermembrane space to the nucleus causing DNA fragmentation and condensation by means of its interaction with Endo G. The fundamental regulators of MOMP however, are the Bcl-2 family of proteins and their discussion follows below in section 1.2.4 (Danial and Korsmeyer, 2004, Youle and Strasser, 2008). A detailed schematic diagram including key mediators and events of apoptosis are also shown in Figure 1-5.

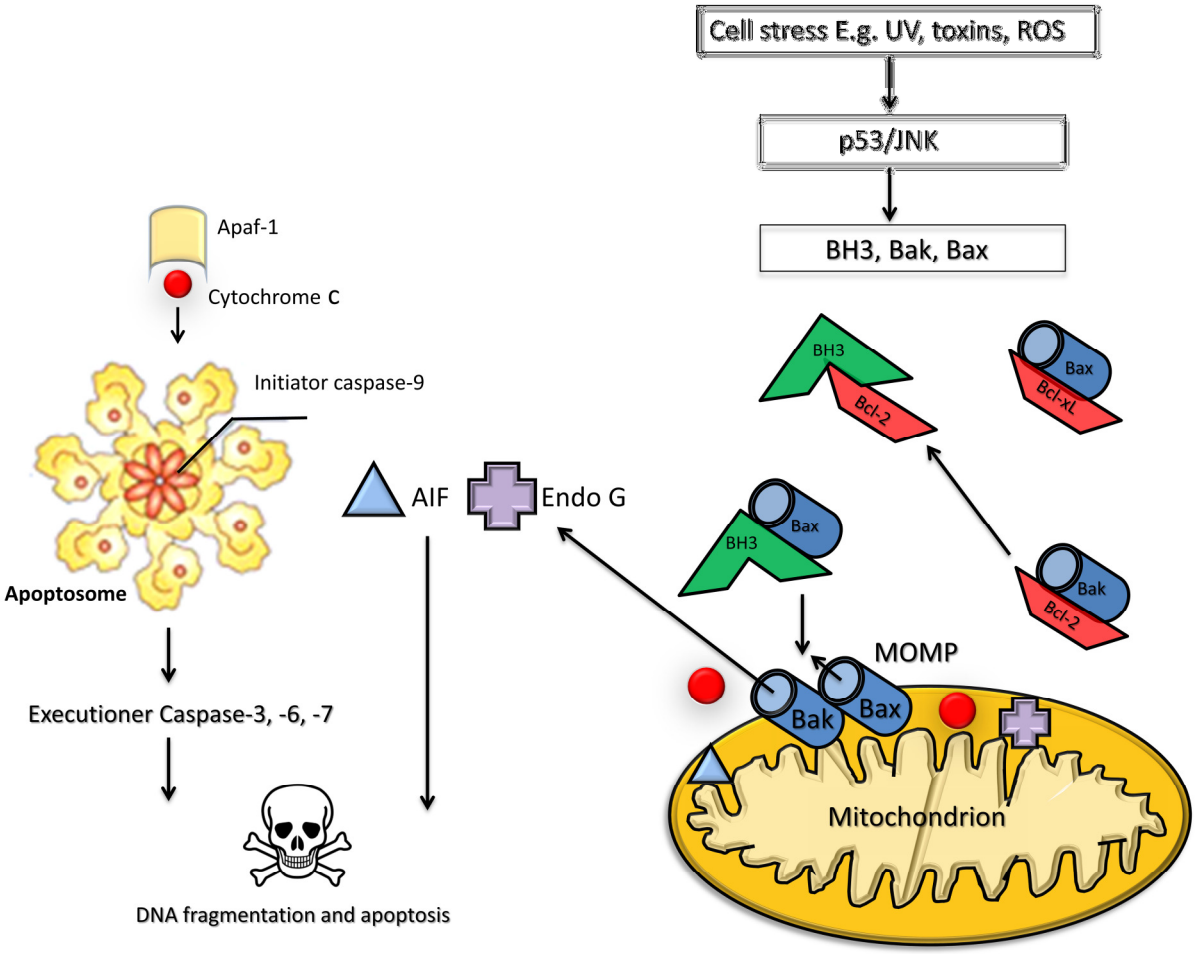


**Figure 1-5 The intrinsic pathway of apoptosis**

In response to cell stress p53 or c-Jun N-Terminal kinase transcriptionally regulate pro-apoptotic Bcl-2 members for the induction of apoptosis. In this example, BH3-only proteins facilitate Bax to the outer mitochondrial membrane (OMM) whilst also removing anti-apoptotic Bcl-2 from Bak. This causes Bak and Bax to create pores in the OMM a process known as MOMP, which releases cytochrome c, apoptosis inducing factor (AIF) and Endo G. Cytochrome c interacts with Apaf-1 and caspase-9 to form the apoptosome. The apoptosome causes pro-caspase-9 to become active caspase-9 which activates caspases -3,-6 or -7 for the induction of apoptosis. Additionally, AIF or Endo G can directly cause DNA fragmentation and apoptosis in a caspase-independent manner. Diagram drawn based on information from (Danial and Korsmeyer, 2004, Youle and Strasser, 2008).

### 1.2.4 Bcl-2 family members - master regulators of the intrinsic cell death pathway

MOMP is determined by a balance between pro-apoptotic and anti-apoptotic B-cell CLL/Lymphoma 2 (Bcl-2) proteins. Some anti-apoptotic members Bcl2, Bcl-w, Bcl-xL, A1 and Mcl-1 integrate into the outer mitochondrial membrane where they directly inhibit pro-apoptotic Bcl-2 members Bcl-2 antagonist killer 1 (Bak) and Bcl-2 associated x protein (Bax). Bak and Bax are accepted as the key two fundamental pro-apoptotic proteins that cause MOMP by the formation of proteolipid pores. This has been well demonstrated by the addition of BH3 peptides, which cause cytochrome c release, the induction of MOMP, and subsequent caspase activation. Bak and Bax, however, are accepted to remain redundant until triggered by a group of Bcl-2 members known as BH3-only proteins, which include Bad, Bid, Bim, Bmf, Bnip3, Hrk, Noxa and Puma (Esposti and Dive, 2003, Kuwana and Newmeyer, 2003, Scorrano and Korsmeyer, 2003).

The mechanisms that underlie the effects of Bak and Bax on MOMP through modern techniques have shown that at the molecular level; they are either blocked by anti-apoptotic Bcl-2 members, this until released by anti-apoptotic Bcl-2 inhibition by BH3-only proteins, or they are directly activated by BH3-only proteins (Vela et al., 2013). Recently, observations at the nanometer-scale have revealed that in the presence of Bid, Bax monomers form pores which distort the OMM phospho-lipid bilayer for cytochrome c release. Furthermore, this process is negatively regulated by the presence of anti-apoptotic Bcl-xL (Xu et al., 2013). Thus, more recent studies have confirmed the previous suggestions about the mechanisms underlying the regulation cell death by Bcl-2 proteins via an intrinsic pathway (Chipuk and Green, 2008); such that anti-apoptotic Bcl-2 members inhibit pro-apoptotic Bak and Bax, whereas BH3-only members inhibit anti-apoptotic Bcl-2 and facilitate pro-apoptotic Bcl-2 members Bak and Bax.

The induction of cell death during interactions of different Bcl-2 members thus depends on the presence of individual members, which ‘pushes’ the cell towards or away from an apoptotic threshold (Wyllie, 2010) as diagrammatically illustrated in Figure 1-6. In fact, the importance of the delicately balanced action of pro- versus anti-apoptotic Bcl-2 members becomes more obvious when it is disturbed during

disease, in particular cancer. Cancer cells may resist apoptosis by mutating Bcl-2 family members, for instance, mutations that lead to over-activation of anti-apoptotic Bcl-2 or Bcl-xL expression. On the contrary, they may also down regulate the expression of pro-apoptotic Bcl-2 members such as Bax, Bim and Puma. The genetic alterations that cancer cells evolve with to avoid cell apoptosis by the intrinsic pathway of cell death are viewed as a strong contributing factor towards carcinogenesis however, before this point p53 plays an essential role to protect cells from a fate of malignant 'havoc' and this is highly dependent on 'normal' functioning of the intrinsic pathways of apoptosis, as is further discussed below (Lowe et al., 2004, Hanahan and Weinberg, 2011).

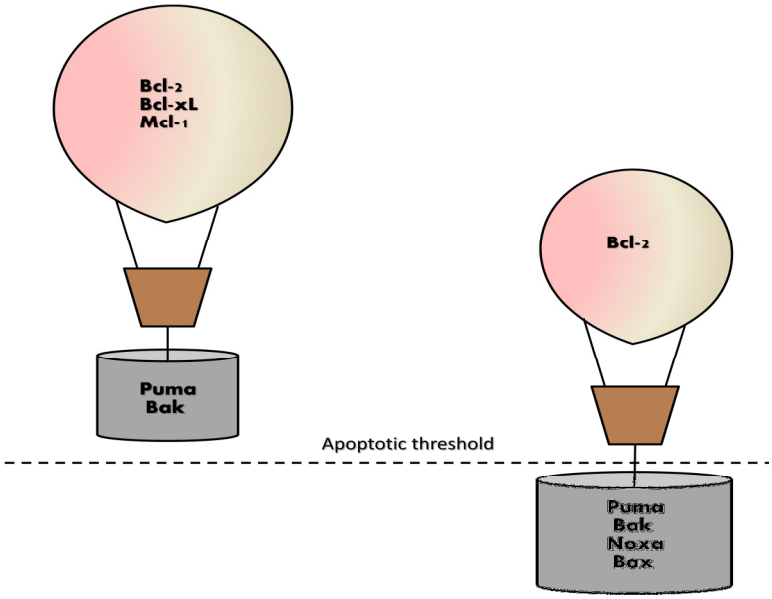


**Figure 1-6 Schematic diagram of the balance between anti-apoptotic and pro-apoptotic Bcl-2 signalling**

The decision between life and death depends on the balance between pro- and anti-apoptotic Bcl-2 members. The left balloon represents an example where anti-apoptotic Bcl-2 members are able to keep the cell above an apoptotic threshold. On the right the balloon pro-apoptotic members become too heavy for Bcl-2 members to deal with and the apoptotic threshold is crossed, subsequently the cell undergoes apoptosis. Diagram drawn based on information from (Wyllie, 2010, Lowe et al., 2004).

## 1.2.5 Intrinsic defence against malignancy

### 1.2.5.1 Hyperproliferative signalling

Underactive cell apoptosis combined with cell hyper-proliferation are major contributing factors towards carcinogenesis, the evolutionary process underlying the formation of cancers (Hanahan and Weinberg, 2011). The facilitation of this process is heavily linked to mutations of p53, the 'guardian of the genome', and/or retinoblastoma (Rb), the cell cycle 'gatekeeper'. There are well characterised recognition systems for oncogenic-over-proliferative signals that involve interaction between p53, Rb, Ras and Myc, which protect the cell from excessive mitotic division signals. Over-activated/oncogenic Myc signalling activates ARF, an inhibitor of MDM2, which normally acts as an inhibitor of p53 (by inducing its degradation). This frees p53 to induce apoptosis over senescence under the condition that its transcriptional regulation of pro-apoptotic BH3 signals prevail over anti-apoptotic Bcl-2 signals and that Myc represses p21 activation (Figure 1-7). Therefore, loss of p53 accounts for a key step in the loss of protection against apoptosis during aberrant cell proliferation (Igney and Krammer, 2002, Lowe et al., 2004, Sherr and McCormick, 2002, Zuckerman et al., 2009).

p21 is also transcriptionally regulated by p53 to prevent cell cycle entry through the G1-S phase functioning as a cyclin-dependant kinase (CDK) inhibitor, a member of a group of proteins which can attenuate the cell cycle. The expression of p21 prevents the phosphorylation of Rb, which permits the continuation of the cell cycle past the DNA repair checkpoint (G1-S phase). Therefore, loss of p53 also contributes to cell hyper-proliferation as cells are permitted to pass through G1-S DNA repair checkpoint. Additionally, elevated E2F signalling, which occurs due to aberrant signalling of the retinoblastoma-p16 pathway (Rb-p16) also elevates ARF expression to facilitate p53 mediated apoptosis or senescence, therefore, under normal circumstances the cell has tight control of hyper-proliferative signalling. Although this mechanism is somewhat cell type and context specific, this is one example of how cells are 'fine tuned' for the recognition of over mitogenic signals and thus cancer growth prevention (Igney and Krammer, 2002, Lowe et al., 2004, Sherr and McCormick, 2002, Zuckerman et al., 2009).

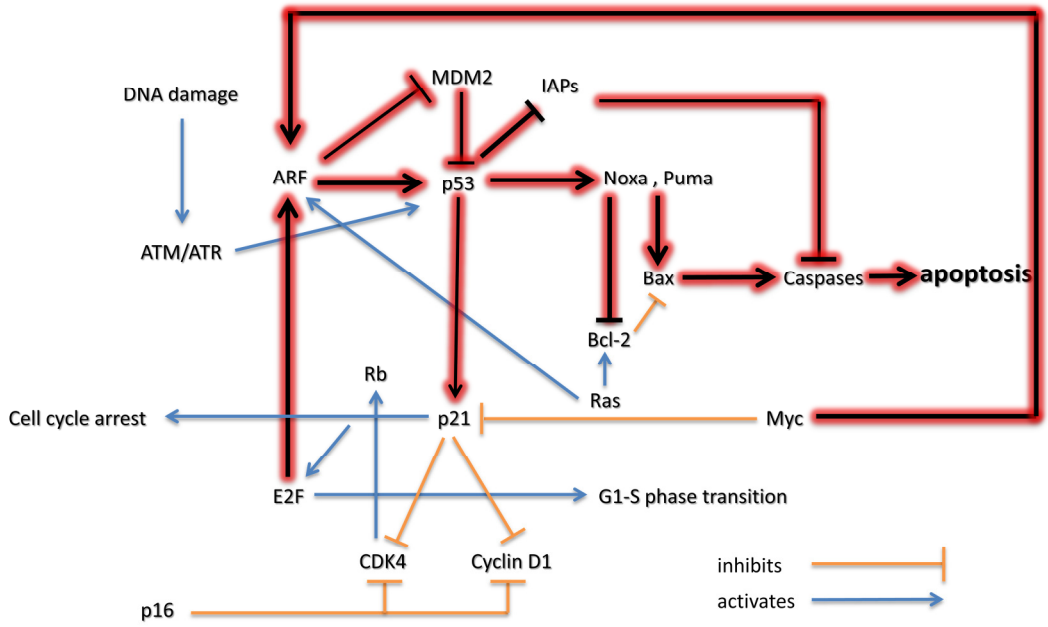


**Figure 1-7 An evidence based p53 signalling network for the protection against cell-overactive proliferation signals**

P53 protects against malignancy by inducing apoptosis in cells that have hyper-proliferative signals. In this example, E2F/Rb and Myc signals are sending aberrant cell proliferation signals, which strongly activate ARF. MDM2 a biological inhibitor of p53 is inhibited by ARF, which also increases p53 stabilisation. p53 in this example does not cause cell cycle arrest via p21 but promotes the expression of pro-apoptotic Bcl-2 members for the induction of apoptosis. Whether the cell commits apoptosis is upon many factors, including cell type and context. Furthermore, mutation of any cancer defensive proteins increases the risk of cancer in particular p53 and Rb. Diagram drawn based on information from (Igney and Krammer, 2002, Lowe et al., 2004, Sherr and McCormick, 2002, Zuckerman et al., 2009).

### 1.2.5.2 DNA damage

DNA damage by exogenous mutagens inactivates tumour suppressors or activates proto-oncogenes and p53 plays a key role in preventing the continuation of cells with such cancer promoting traits. Genomic damaging agents, such as UV light, activate ATM/ATR which further activates p53 to induce apoptosis or senescence. p53 loss therefore, allows a constitutive rate of genomic mutations that can occur as a result of tumour cell hyper-proliferation (which already have mutations) and/or external mutagens (Igney and Krammer, 2002, Lowe et al., 2004, Sherr and McCormick, 2002, Zuckerman et al., 2009).

In accordance with excessive mitogenic signals, p53 responds to such stresses by the upregulation of pro-apoptotic Bcl-2 proteins Noxa and Puma, which activate the intrinsic pathway of cell death. Therefore, the normal functioning of the intrinsic cell death pathways is essential to prevent oncogenic transformation. It is therefore overall unsurprising that over 50% of cancers are clinically represented by p53 loss (Hollstein et al., 1991). In addition p53 is also able to transcriptionally regulate the expression of 'death receptors' a sub-family of proteins that belong to the tumour necrosis factor receptor (TNFR) superfamily (Lowe et al., 2004). Death receptors induce apoptosis via the extrinsic pathway of apoptosis (see below). Yet, before this is discussed, there are other proteins that protect cells from cancer causing milieu, one of which is well studied in the field of cancer c-Jun N-terminal kinase (JNK). JNK is also termed a stress activated protein kinases and has the capability to induce cell survival or apoptotic responses dependent on the external stimuli. Although a more detailed discussion of JNK is provided elsewhere (section 4.2.4.2), it is worth noting that JNK plays a pro-apoptotic role in both intrinsic and extrinsic pathways of cell death by regulating death receptors, death receptor responses and the Bcl-2 protein interactions previously discussed (Dhanasekaran and Reddy, 2008).

## 1.3 The extrinsic pathway of apoptosis

### 1.3.1 The TNFR family

The tumour necrosis factor receptors (TNFRs) are a group of transmembrane proteins, which are critically involved in immune homeostasis and are hallmarked by a cysteine-rich domain. So far, over 40 members are identified and they may be divided into three groups: TNFR members that contain a DD (death receptors), TNFR members without a DD but contain a TRAF interacting motif (TIM) domain, and decoy receptors (Figure 1-8). Receptor binding by their cognate TNF ligand activates numerous signal transduction pathways that regulate cell proliferation, survival, differentiation and apoptosis. TNF ligands are predominantly expressed on T-cells and natural killer (NK) cells for the activation of apoptosis via intrinsic and extrinsic pathways (Hehlgans and Pfeffer, 2005, Pfeffer, 2003).

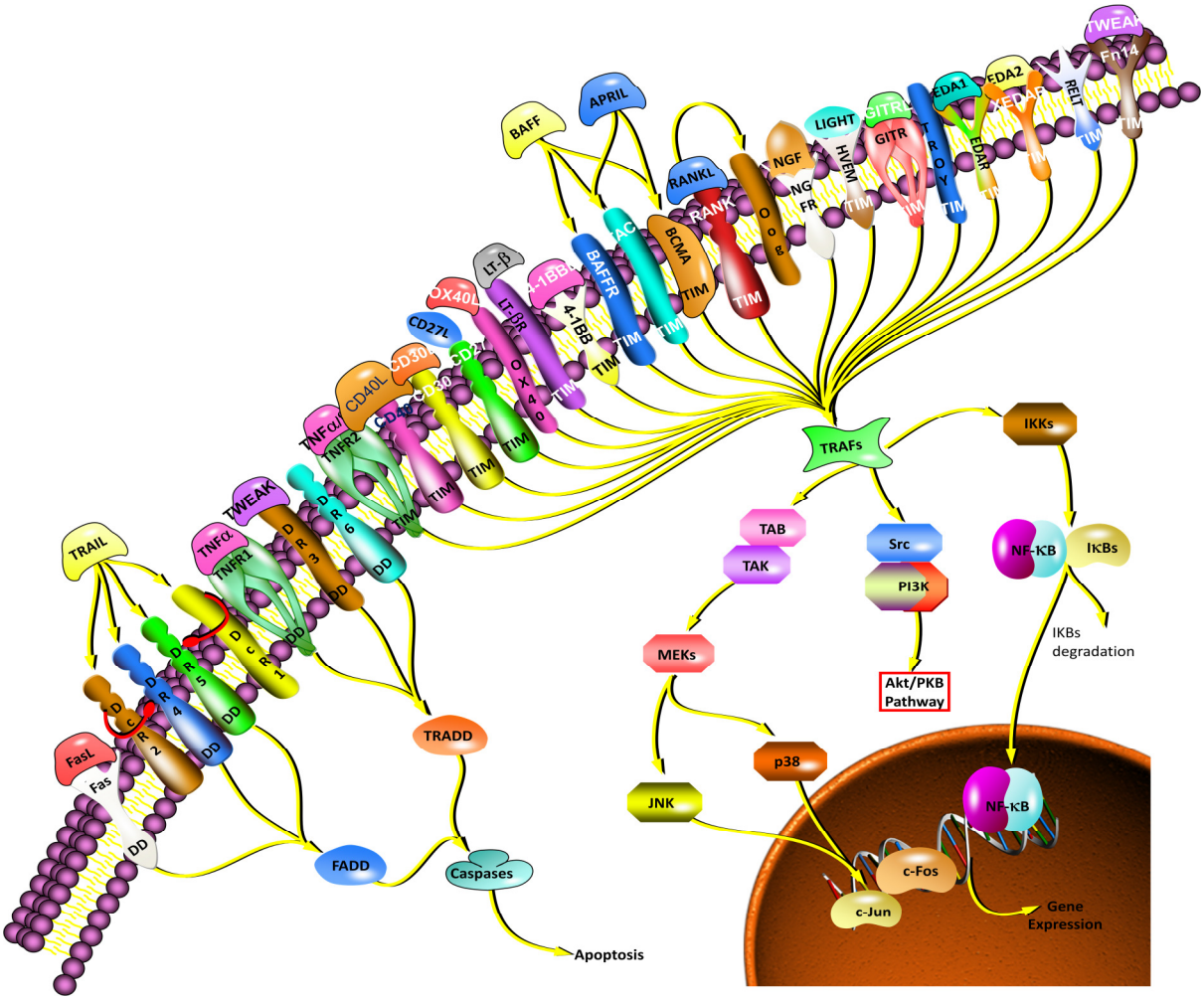


**Figure 1-8 The TNFR superfamily**

The TNFR superfamily is divided into three groups: death receptors, decoy receptors and TIM domain containing receptors. Death receptors contain death domains which induce apoptosis via FADD or TRADD. Decoy receptors harvest TRAIL ligands and prevent their signalling whereas TIM domain containing receptors recruit TRAF molecules. Figure adopted from (www.sourcebioscience.com).

### 1.3.2 TNFR mediated apoptosis: elimination of aberrant cells

In line with the elimination of any defective cell that threatens the body's homeostasis, cancer cells are removed by a vastly complex array of cells that create the immune system. Therefore, it is not surprising to also observe that the epidemiology of cancer is closely linked with a defective immune response (Penn, 1990). Although immunity-associated apoptosis represents a diverse topic of immunology, this study relates to the induction of apoptosis by the immunocyte presentation of TNF ligands, in particular T-cells and natural killer (NK) cells and in cases dendritic cells (DCs) (Hill et al., 2008b). In the case of T-cells, the activation of apoptosis relies on their recognition of tumour-associated antigens occurring as a result of genomic and proteomic alterations. Two distinct pathways are utilised to destroy cells that display T-cell receptor reactive proteins within their MHC class I molecules a) the perforin/granzyme pathway of apoptosis or b) the 'extrinsic' or 'death receptor' cell death pathway of apoptosis, mediated by TNFRs (Ghiringhelli et al., 2006), which is also employed by NK cells but in a non-TCRs-manner, as these cells recognise cells for disruption on the basis of down-regulation or absence of MHC class I expression. Although the aforementioned are currently recognised as the two main pathways for T-cells and NK cells to induce apoptosis, there is plenty of evidence to also suggest that cell death may also be induced directly by TNFR-mediated intrinsic pathways (Ghiringhelli et al., 2006, Georgopoulos et al., 2006, Chen et al., 2003).

### 1.3.3 'Death receptor' (DR) signalling

Death receptors such as Fas, TNFR-I and TRAIL-R contain a cytoplasmic protein motif known as the death domain (DD), which recruits proteins for apoptosis induction during immune cell death signalling. The mechanisms behind Fas and TNF-RI mediated apoptosis are well studied in this context and the key events are summarised in Figure 1-9. A detailed account of TRAIL is not provided here, as it is closely associated with the Fas mediated signalling events discussed below (Guicciardi and Gores, 2009).

#### 1.3.3.1 FAS (CD95) signalling

Upon receptor trimerisation by FasL, Fas recruits Fas associated DD (FADD) and procaspase-8 to form the death inducing signalling complex (DISC) (Figure 1-9). The receptor release of the DISC activates caspase-8 known as an initiator caspase and depending on caspase-8 intensity the cell takes two alternate apoptotic routes.

Early studies in lymphoid cell lines indicated that cells sensitive to anti-Fas-induced apoptosis could differ in the dependence on the mitochondria pathway. Thus effective killing does not require mitochondrial involvement in Type I cells, but does in Type II cells (Scaffidi et al., 1998). Consequently over-expression of the anti-death Bcl-2 or Bcl-xL could block Fas-mediated apoptosis in Type II cells, but not in Type I cells (Sun et al., 2002, Scaffidi et al., 1998). Thus, high levels of Caspase-8 activation directly activates the executioner caspase-3, whereas as low levels cleave Bid into tBid, which interacts with Bak and Bax. Bak and Bax create mitochondrial outer membrane permeability, cytochrome c and AIF release for death execution by the intrinsic pathway (Danial and Korsmeyer, 2004, Gupta, 2003, Hehlgans and Pfeffer, 2005).

### 1.3.3.2 TNF-RI Signalling

TNF-R1 trimerisation via TNFα ligand binding can mediate both death and survival signals. Receptor trimerisation releases silencer of death domain (SODD) to recruit TNF-R1-associated death domain (TRADD) to form either complex I or II. TRADD, receptor interacting protein (RIP1), TRAF2 and transforming growth factor beta (TGF-β) induce survival via nuclear factor kappa-light-chain-enhancer of activated B cells (NF-κB), or apoptosis via p38 or JNK by formation of a plasma membrane bound complex, termed complex I. Independent of TNFRI, TRADD and FADD mediate cytoplasmic complex II formation, and activate caspase-8 and -10 via DISC formation. However, complex II mediated cell death is dependent on the outweighing expression of either RIP1 or anti-apoptotic $FLIP_L$ (Danial and Korsmeyer, 2004, Gupta, 2003, Hehlgans and Pfeffer, 2005, Micheau and Tschopp, 2003).

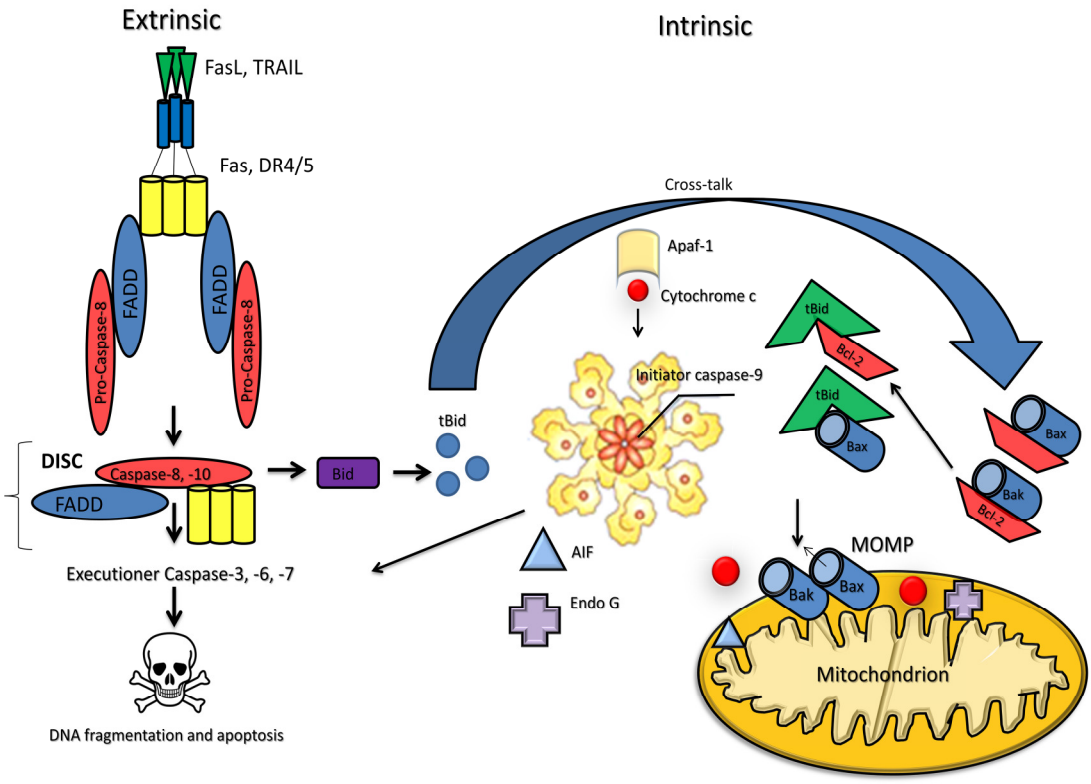


**Figure 1-9 The 'classical' extrinsic pathway of cell death (and its cross-talk with the intrinsic pathway)**

Death receptor ligation causes the recruitment of FADD and pro-Caspase-8 or -10. Pro-Caspase-8 or -10 and FADD form the death inducing signalling complex. The formation of the DISC during death receptor engagement activates pro-caspase 8/10. Caspase-8 activates caspase 3/6/7 and symmetrically events proceed as for the intrinsic pathways. Caspase-8 can also cleave Bid to create tBid which as for the intrinsic pathway modulates Bak and Bax outer mitochondrial membrane pore formation. Diagram drawn based on information from (Youle and Strasser, 2008).

## 1.4 TIM domain signalling

A second group of TNFRs include CD40, TNFRII, OX40, and Lymphotoxin (and others - see Figure 1-8) that do not contain a DD, but mediate their effects through tumour necrosis factor receptor associated factors (TRAFs) and mitogen activated protein kinases MAPKs (Xie, 2013). However, in comparison to the classical death receptors, relatively little is known about how these TNFR members lead to apoptosis and only recently evidence has been available.

This thesis is interested in the study of CD40 receptor, which plays an essential role in cancer immunity, by priming a number of immunocytes. Furthermore, evidence has emerged showing that CD40, unlike members of the TNFR such as Fas and TNFRI, can directly induce cell apoptosis in a tumour cell-specific fashion by an intrinsic pathway specific death mechanism and that this is independent of p53. Therefore, the remainder of this chapter will not only review the importance of CD40 in immunity, but also studies where it has shown to be a direct apoptotic signalling mediator in epithelial cancer (carcinoma) cells.

## 1.5 The CD40-CD40L dyad

### 1.5.1 CD40

The discovery of CD40 occurred in 1984 during investigations on receptors specifically expressed on transitional cell carcinomas (TCCs) of the bladder. Although the abundantly expressed 50kDa CD40 was discovered using SDS-PAGE and immunoprecipitation on TCC cells (Paulie et al., 1984), and soon after that on other epithelial cell types (Young et al., 1989), it was also found on the surface of B-Lymphocytes (B cells), thus providing evidence against the initial hypothesis that it was a tumour cell-specific cell surface antigen (Paulie et al., 1985).

CD40 is a 45-50kDa glycoprotein consisting of a stretch of 277 amino acids (aa) and is mapped to human chromosome 20q11-2-q13-2 (Armitage, 1994). CD40 expression is amplified in response to IFN-γ and TNF-α (von Leoprechting et al., 1999) and is documented to monocytes, dendritic cells, thymic cells (Hess and Engelmann, 1996), hematopoietic progenitor cells, urothelial cell carcinoma UCC cells (Bugajska et al., 2002), colorectal carcinoma (CRC) (Georgopoulos et al., 2007), ovarian carcinoma (Gallagher et al., 2002), cervical carcinoma (Eliopoulos et al., 2000a), breast carcinoma (Wingett et al., 1998), squamous epithelia, thymic epithelia (Galy and Spits, 1992), ectocervical epithelia, SV40-transformed keratinocytes (Tong and Stone, 2003), normal keratinocytes and their basal counterparts, hepatocytes and intrahepatic biliary epithelial/endothelial (Ahmed-Choudhury et al., 2003, Afford et al., 2001) and some malignant melanomas (MM) (Peguet-Navarro et al., 1997). The widespread expression of CD40 strongly implies that it may be highly involved in many processes that balance cell homeostasis (Young et al., 1998, Kawabe et al., 2011).

Being classed as a member of the TNFR superfamily (TNFRSF) (Armitage, 1994) means CD40 is also a Type I protein that contains multiple cysteine-rich repeats in its extracellular amino terminus, which spans for around a length of 40 aa. As mentioned previously, a large number of TNFSR members contain an intracellular protein motif known as the death domain (DD) and are known as death receptors. The intracellular domain of human CD40 does not contain a DD, but instead between amino acids 231-238 and 250-266 contain sites for the binding of TRAF molecules (known as a TIM domain) which is a signal specific manner dictate

cell responses – as discussed in section 4.1 (Bishop et al., 2007). Latent membrane protein 1 (LMP1) encoded by Epstein-Barr virus is a biological mimic of activated CD40 where it relays elevated and sustained signals that contribute to the transformation of B cells (Eliopoulos et al., 1996a).

### 1.5.2 CD40L

Human CD40 ligand (CD40L or CD154) is a 35kDa Type II protein that is 261 aa in length and is mapped to human chromosome Xq.24. CD40L belongs to the Tumour necrosis factor (TNF) family and was discovered and isolated from T-cell membranes (Armitage et al., 1992) where it is transiently activated within 1-2 hours under inflammatory conditions (Banchereau et al., 1994). CD40L acts as a co-stimulatory molecule on CD4+ve and CD8+ve activated T-cells, platelets, NK cells, monocytes, activated DCs and mast cells, for the priming of CD40 related immunity (Kawabe et al., 2011), many examples are included below.

## 1.6 CD40-CD40L interactions in immunity

### 1.6.1 B-cells

The interaction between CD40 and CD40L (CD40-CD40L) is important for B-cell homotypic adhesion, cytokine secretion (Armitage et al., 1992), proliferation, memory cell formation (Stamenkovic et al., 1989) and survival via anti-apoptotic Bcl-2 signals (Hirai et al., 2003). CD40 can activate the anti-tumour effects of B-cells against breast tumours and mesotheliomas (Jackaman et al., 2010) and studies have also shown that CD40 ligation can directly cause apoptosis in B-cell Lymphomas (Funakoshi et al., 1996, Law et al., 2005, Jundi et al., 2012). Mutational loss of CD40L causes hyper IgM syndrome, which characterised by lack of germinal centres in secondary lymphoid organs and B-cell class switching (Banchereau et al., 1994, Callard et al., 1993). This gives an immunocompromised resistance against pathogens in addition to an increased risk of pancreatic and liver cancer (Hayward et al., 1997) and this phenomenon may be reciprocated using *in vivo* models of CD40 -/- mice as they fail to respond to T-cell dependent antigens (Kawabe et al., 1994).

### 1.6.2 T-cells

CD40-CD40L is important for the normal interaction between B and T-cells, for viral infection immunity (Ruby 1995) and for cytokine and chemokine signalling (Altenburg et al., 1999). CD40-CD40L is used to prime and expand CD4+ve T-cells by regulating the expression of co-stimulatory molecules and by causing the secretion of the cytokines that are necessary to mount a cytotoxic T-cell response (Fonsatti et al., 2010). In addition, T-cells are unable to utilise T-cell receptors (TCR) against tumour-antigens without the co-stimulatory interaction, and thus CD40-CD40L is also fundamental to the prevention of carcinogenesis (Moran et al., 2013). CD40L-CD40 may also contribute to autoimmune T-cell pathogenicity in diseases such as diabetes (Baker et al., 2008) and arthritis (Munroe and Bishop, 2007). CD40 may be stimulated by agonistic anti-CD40 antibodies, and this causes antigen presenting cells (APC) to secrete IL-12 and present B7-1 and B7-2. Through administration of vaccines and CD40 agonists, this mechanism has been used to prime the T-cell response against specific tumour antigens (Mackey et al., 1997).

### 1.6.3 Neutrophils

CD40 activation primes neutrophils, and in combination with IL-2, allows their interactions with CD8 cells to eliminate multiple melanoma and lung tumours *in vivo* (Jackaman et al., 2008).

### 1.6.4 Macrophages

CD40-activated macrophages secrete IFN-γ, IL-12 and nitric oxide (NO), which mediate their anti-tumour activity against *in vitro* melanomas, ovarian carcinoma and lymphomas (Buhtoiarov et al., 2005). CD40-mediated activation of monocytes induces their anti-tumour potential against lung carcinomas *in vitro* (Imaizumi et al., 1999) and lung, colon adenocarcinoma and neuroblastoma in murine *in vivo* models (Turner et al., 2001).

### 1.6.5 Natural killer (NK) cells

CD40 interaction causes the proliferation of NK cells (Amakata et al., 2001, Atochina and Harn, 2005). NK cells engineered to express CD40L cause *in vivo* cytolysis of rat adenocarcinomas (Jyothi and Khar, 2000). Additionally, activation of NK cells by CD40 engagement can induce anti-tumour effects in *in vivo* murine melanomas and adenocarcinomas via the action of IL-12 and macrophage recruitment (Tai et al., 2005).

### 1.6.6 Dendritic cells (DC)

DC CD40 ligation by T-cell-CD40L, primes DC cells to become effective antigen presenting cells (APC), via upregulation of MHC class II molecules and CD80/CD86 (Ma and Clark, 2009) and CD40-CD40L co-simulation is essential for the activation of dendritic cells in response to pathogen associated molecular patterns (PAMPs) (Sacks and Noben-Trauth, 2002). Additionally, CD40L is functionally expressed by in response DC-CD40 ligation (Pinchuk et al., 1996). In such manner, DC have been shown *in vitro* to utilise membrane CD40L (mCD40L) in order to mediate their cytotoxic effect effects towards urothelial cell carcinomas (UCC) and colorectal carcinomas, therefore, CD40 is not only essential for DC activation, but for their ability to induce CD40-mediated cell cytotoxicity (Hill et al., 2008a).

## 1.7 Potential of targeting CD40 for immunotherapy

Because of its great capacity to activate the immune response, the use of agonistic CD40-targetting humanised mAbs is an attractive concept for the treatment of cancer, as such mAbs help 'boost' an immune response against solid tumour by activating dendritic cells and supporting an effective cytotoxic T-cell response (Khong et al., 2012). Particularly, the anti-CD40 CP-870,893 humanised monoclonal antibody (MAb) shows in phase I and II clinical trials for cancer treatment that in many cases, there is an improved cytotoxic T-cell response against tumour antigens (Drabick and Schell 2010; Fonsatti et al., 2010). The most promising results reported are when CD40 is delivered with chemotherapy which poses an interesting concept as this type of treatment normally depletes immunocytes (Khong et al., 2010). The protocols used for the delivery of CD40 mAbs are now however being adapted as in cases they can cause the ill wanted depletion of T-cells, although this still remains an attractive area of interest in the facilitation of the tumour-antigen T-cell response (Moran et al., 2013). The future delivery of CD40 agonists will use nanoparticles bearing conjugated anti-CD40, and drugs of choice dependent on the genotype of the tumour, in order to achieve low systemic toxicity (Khong et al., 2013).

## 1.8 The effects of CD40 engagement on cancer cells

### 1.8.1 CD40-mediated apoptosis and role of signal 'quality' in functional outcome

Hess and Engelmann (1996) were first to demonstrate that carcinoma cells are susceptible to CD40-mediated apoptosis and since there has been a number of investigations into the ability of CD40 to induce malignant cell death, particularly by Young and colleagues. Although this will be discussed further in following chapters also, the type of CD40 ligand (CD40L) or CD40 agonist delivery largely affects the response of carcinoma cell lines; in other words the 'quality' of the CD40 signal, reflected by the degree of receptor cross-linking which has a dramatic influence on the functional outcome of CD40 ligation. The importance of receptor cross-linking does not appear to be unique for CD40, as this is an observation reported for other members of the TNFRSF, such as Fas, which requires a minimum of a hexameric ligand (Schneider et al., 1998). Similar observations have been reported for TRAIL receptor activation (Steele et al., 2006). Such differences have been reported by exploiting the use of recombinant soluble ligand preparation of ligands such as FasL or TRAIL cross-linked in different ways, e.g. using a FLAG tag or a His-tag (Steele et al., 2006), many of which are commercially available (e.g. Enzo, Peprotech).

However, the critical role of signal strength on functionality of ligation is more pronounced in the case of CD40. In fact, unlike classical TNFRs where increased cross-linking induces higher levels of already observed apoptosis, in the case of CD40, treatment with weakly cross-linked agonists causes little (in many cases, if any apoptosis) and mainly growth-inhibition without pharmacological intervention (Tong et al., 2001, Hirano et al., 1999). In addition to agonistic anti-CD40 antibodies, the main soluble recombinant CD40L preparations used are the leucine zipper-based cross-linked CD40L (Morris et al., 1999) (by Immunex) as well as less cross-linked preparations, such as the FLAG-tagged CD40L (available by various commercial suppliers). Although sCD40L biologically mimics the action of mCD40L in some cell models, particularly in the case of B cells, it appears that more extensive cross-linking is required for biological activity in the induction of carcinoma cell apoptosis (Bugajska et al., 2002, Elmetwali et al., 2010b).

### 1.8.2 Effects of CD40 ligation in cancer cells

Various studies have shown that soluble CD40 ligand (sCD40L) combined with protein synthesis inhibitors (in most cases cycloheximide) and/or IFN-γ are toxic to CD40-transfected cervical and lung carcinoma cells. However, membrane-presented CD40 ligand (mCD40L) is highly cytotoxic independently of pharmacological intervention, as shown by Hess and Engelmann (1996) and more recently Bugajska et al (2002). It was further shown that sCD40L requires protein synthesis inhibition to kill CD40-transfected cervical carcinoma cells, however, ovarian cell lines show both apoptotic and non-apoptotic responses demonstrating the context specificity of CD40 killing (Eliopoulos et al., 2000a). Unaided sCD40Ls also relay growth inhibition in UCC, ovarian, cervical, squamous epithelia, transformed keratinocytes, ectocervical epithelia and rat fibroblastic cell lines. Furthermore, sCD40Ls enhance the toxic effects of Cisplatin, TNF-α, Fas and ceramide in UCC cell lines (Eliopoulos et al., 1996b) and of 5-Flurouracil and Mitomycin C in cervical and ovarian cell models (Vardouli et al., 2009). Additional reports have shown that sCD40Ls in combination with protein synthesis inhibitors or membrane CD40Ls are also toxic to UCCs (Bugajska et al., 2002, Davies et al., 2004). sCD40L has also shown to have direct anti-tumour effects in ovarian cell lines, ovarian cells obtained from ascites fluid and ovarian adenocarcinomas transplanted into severe combined immunodeficient mice (Ghamande et al., 2001) and still remains a promising tool for this type of cancer (Scarlett et al., 2009). It has been suggested that CD40 engagement may cause the autocrine expression of TNFs Fas and TRAIL, which mediate apoptosis via the extrinsic cell death pathway (Eliopoulos et al., 2000b). Conversely, reports have challenged this, implying CD40-mediated apoptosis is regulated by direct signalling pathways involving the activation of the intrinsic pathway of apoptosis (Georgopoulos et al., 2006, Elmetwali et al., 2010b).

CD40 engagement growth inhibits lymphoma cells and MMs (Baker 1998), however it can induce both proliferation and apoptosis among multiple myeloma cells (Qi et al., 2004). MMs during their transformation demonstrate to down regulate CD40 expression allowing their evasion of CD40L-T-cell mediated apoptosis (von Leoprechting et al., 1999). Furthermore, *in vitro,* an equal amount of CD40 engagement causes B-cell proliferation, whilst it growth inhibits epithelial and

carcinoma cells (Eliopoulos et al., 1996). CD40 may also contribute to the proliferative state of some cancers (Qi et al., 2004) and their angiogenesis (Huang et al., 2011), thus re-enforcing that CD40 responses are highly context specific. Perhaps the most unique feature of CD40 appears to be its ability to kill malignant cells whilst sparing normal human epithelial cells (NHU) (Bugajska et al., 2002).

### 1.8.3 Mechanisms of CD40-mediated apoptosis in epithelial (carcinoma) cells

A number of signalling mechanisms which are linked to direct ligand-receptor interaction have been proposed in the field of CD40-mediated apoptosis. Studies on *in vitro* cervical and ovarian carcinomas implied that the isoleucine zipper sCD40L (in the presence of protein synthesis inhibitors) causes the paracrine expression of Fas, TRAIL and TNF. These classical 'death receptors' were shown to induce cell apoptosis via the extrinsic pathway of cell death, as not only did antibody neutralisation, but also caspase-8 inhibition, attenuate CD40-mediated cytotoxicity (Eliopoulos et al., 2000a). Some agree that CD40 ligation by mCD40L *in vitro* using UCC cells, causes mounted TRAF3 expression, JNK activation and subsequent cell death. However, there is discrepancy over whether this is mediated via extrinsic or intrinsic pathways of apoptosis, or their cross-talk (Georgopoulos et al., 2006, Elmetwali et al., 2010b). At least in part, there has been a consistent implication for Bak and Bax expression and caspase-9 dependency; therefore, it is likely that intrinsic pathways play a key role in the overall event, due to their ability to create MOMP (Bugajska et al., 2002, Georgopoulos et al., 2006). Furthermore, there is a report that TRAF6 attenuation is essential for mCD40L to mediate its full apoptotic potential (Elmetwali et al., 2010b). Perhaps some discrepancy over the signalling mechanism underlying CD40-mediated cell death is attributed to the mechanism of mCD40L delivery. Some studies utilise a co-culture method, which involves the culturing of carcinoma cell with mCD40L expressing third party cells (Bugajska et al., 2002), whereas others utilises the paracrine expression of mCD40L by transfection with a replication defective recombinant adenovirus (Elmetwali et al., 2010b). Either way, the signalling events leading to JNK activation via TRAF3 are a pre-requisite for the further understanding of the CD40-mediated pathway of cell death.

### 1.8.4 Malignant transformation and susceptibility to CD40 ligation

The lack of consistency with regards to the use of cell models and ligand delivery strategies makes the full understanding of CD40-mediated cell apoptosis difficult. Through the use of a robust urothelial cell model, the Georgopoulos group however have provided many insights into biological factors that underlie the effects of CD40-killing. Their model utilised normal urothelial cells (NHU) and well-characterised, established malignant urothelial cell carcinoma (UCC) lines, as well as NHU derivatives with defined genetic alterations, referred to as 'para-malignant' cells (Crallan et al 2006). The use of this system has permitted studies that have attempted to address 1) the importance of the degree of receptor cross-linking on functional outcome, 2) the important intracellular signalling events that regulate CD40-mediated apoptosis and 3) the influence of malignant transformation on CD40-mediated effects on epithelial cells.

Fundamental was their observation that without pharmalogical intervention sCD40Ls are growth inhibitory and non-toxic to UCCs or normal human urothelial cells NHUs, whereas mCD40L is highly apoptotic and in a tumour cell-specific fashion (Bugajska et al., 2002, Eliopoulos et al., 1996a). Further exploration showed that the differential susceptibility between normal and malignant urothelial cells is directly attributed to events relating to changes observed during malignant transformation (Shaw et al., 2005). In this context, the human papillomamovirus-16 (HPV-16) gene E6 immortalises NHU cells *in vitro* and makes them equally susceptible to CD40 and to the same extent observed with UCC cell lines. It has been suggested that this may be most likely attributed to the ability of E6 to abrogated p53 function (Bugajska et al., 2002) and cause the activation of human telomerase, which consequently disrupts p16 expression and allows constitutive activation of the Rb pathway (Kiyono et al., 1998, Dickson et al., 2000). Using NHU paramalignant cell derivatives with inactivated p53 and p16 function the effects of mCD40L-CD40 ligation were studied. Interestingly, p53 loss-of-function cells did not show CD40 susceptibility, however loss of p16 function rendered urothelial cells partially susceptible to CD40 in comparison to HPV 16 E6 over-expressers and fully-malignant UCC cells. These findings have suggested that loss of p16 and thus possibly over-activation of the Rb pathway is a contributory factor in the sensitivity of cells to CD40 killing (Shaw et al., 2005). However, the reasons underlying the partial

susceptibility remain unknown and it is also important to understand what the other determinants of susceptibility are. For instance, as HPV E6 affects telomerase activity (Reznikoff et al., 1996), thus it is of interest to understand the role of telomerase over-activation in CD40 susceptibility.

## 1.6 Thesis aims

The overall aim of this project was to for the first time provide a detailed understanding in the CD40 signalling 'black-box' by unravelling the mechanisms of CD40 and its ability to induce cell death in malignant cells, whilst sparing their non-transformed counterparts. The work aimed at;

a) defining the key events that mediate cell death and identify the precise role of intracellular mediators in mCD40L killing

b) understanding the molecular 'nature' of the intrinsic pathway-related apoptosis

c) increasing our current knowledge of the importance of malignant transformation in the functional outcome of CD40 ligation

d) use the knowledge on the mechanisms indentified to develop novel tools for delivery of a soluble signal functionally equivalent to mCD40L for future therapeutic intervention.

More specifically:

- Chapter 3: A co-culture model was used to achieve mCD40L-CD40 interaction on epithelial (carcinoma) cells and a number of independent assays were optimised for the detection of CD40 apoptosis. The most robust and sensitive assays were selected for detailed and functional investigations.

- Chapter 4: Co-culture methods for mCD40L-CD40 ligation, immunoblotting, shRNA mediated siRNA protein knockdowns, pharmacological inhibitors and apoptosis assays were used to a) provide for the first time a detailed investigation of the functional involvement of proteins previously implicated in CD40 killing (e.g. TRAF3, JNK, Bak and Bax), and b) indentify key MAPK kinase signalling intermediates upstream or downstream of TRAF3/ JNK in order to delineate the exact signalling axis utilised by CD40.

- Chapter 5: Using co-culture methods for mCD40L-CD40 ligation, soluble CD40 agonists for CD40 ligation, pharmalogical inhibitors, immunoblotting, apoptosis assays, and cell viability assays in normal and malignant epithelial cells, the role of reactive oxygen species (ROS) in CD40 signalling was studied, which allowed a) the identification for the first time of the importance of ROS in explaining the tumour specificity of CD40 signalling and b) the design of a combinatorial approach that achieved the delivery of a pro-apoptotic signal functionally equivalent to mCD40L that consisted of soluble CD40 agonist in combination with pharmacological ROS pathway modifiers.

- Chapter 6: Using normal and paramalignant epithelial cells immortalised by the overexpression of the catalytic sub-unit of human telomerase (hTERT) and utilising apoptosis assays and immunoblotting. The aim was to build on the understanding of the importance of genetic alterations involved in carcinogenesis in influencing epithelial cell susceptibility to CD40 ligation.

# 2.0 Materials and Methods

## 2.1 General

All practical work was carried out at the School of Applied Sciences, Science building, Queensgate which is located at the University of Huddersfield.

## 2.2 Suppliers

Commercial suppliers and manufacturers are indicated at the first mention of the reagent or equipment in the text. A full list of all suppliers and manufacturers can be found in Appendix I.

## 2.3 Disposable plasticware

Single use plasticware, sterile or non-sterile, was obtained from Sarstedt, Fisher Scientific, Greiner Bio-One or Alpha Laboratories. Non-sterile, disposable plasticware was sterilised by autoclaving in a Prior Clave/London Autoclave at 121°C (2 Bar) for 15 minutes and then left to air dry at room temperature.

## 2.4 Stock solutions

All chemical reagents were either of analytical or tissue culture grade as appropriate for the experiment and were supplied by Sigma Aldrich unless otherwise stated. General laboratory stock solutions were prepared with deionised water ($dH_2O$). Solutions for use in tissue culture were prepared with ultra-pure water from a LabStar ultra violet purification unit. Heat stable solutions were sterilised by autoclaving at 121°C (1 bar) for 15 minutes or filter-sterilised using an Acrodisc (VWR) low-protein binding Tuffryn® HT syringe filters with a pore size of 0.2µm. Recipes for all stock solutions can be found in Appendix II.

## 2.5 Reagents

### 2.5.1 Primary antibodies

Primary antibodies used in this study are listed in Table 2-1. Antibodies when possible were titrated prior to use on known positive controls to establish optimal dilutions. Antibodies used were aliquoted and stored as recommended by the manufacturer. Working stocks were diluted in Tris buffered saline (TBS; Appendix II) with 0.1% (v/v) Tween (Tween20; Sigma Aldrich) and stored at 4℃. When blocking buffers were included in the antibody dilutions, these were specified under 'Dilution' (Table 2-1).

| Antigen | Catalogue no/ Clone | Host | Supplier (product of) | Dilution | Application | Molecular weight (kDa) |
|---|---|---|---|---|---|---|
| Human CD40L | AF617 | Rabbit | R&D systems | 1:500 in TBS Tween20 0.1% | FC, WB | 37 |
| TRAF3 | sc-949 / c20 | Rabbit | Insight Bio (Santa Cruz) | 1:250 in TBS Tween20 0.1% | WB, IP, IF, FCM and ELISA | 65 |
| TRAF1 | sc-7186 / h-186 | Rabbit | Insight Bio (Santa Cruz) | 1:500 in TBS Tween20 0.1% | WB, IP, IF and ELISA | 52 |
| TRAF6 | sc-8409 | Mouse | Insight Bio (Santa Cruz) | 1:500 in TBS Tween20 0.1% | WB, IP, IF, IHC(P) and ELISA | 60 |
| Phospho-SEK1/MKK4 (Ser457) | #4514 (C36C11) | Rabbit | New England Biolabs (NEB)/Cell Signalling Technology (CST) | 1:1000 in TBS, 5% w/v BSA, 0.1% Tween20 | WB, FC | 44 |
| Phospho-MKK7 (Ser271/Thr275) | #4171 | Rabbit | NEB (CST) | 1:1000 in TBS, 5% w/v BSA, 0.1% Tween20 | WB | 48 |

| | | | | | | |
|---|---|---|---|---|---|---|
| JNK/SAPK | #9258 | Rabbit | NEB (CST) | 1:1000 in TBS, 5% w/v BSA, 0.1% Tween20 | WB | 46, 54 |
| Phospho-ASK1 (Ser967) | #3794 | Rabbit | NEB (CST) | 1:1000 in TBS, 5% w/v BSA, 0.1% Tween20 | WB | 155 |
| Phospho-JNK/SAPK (Thr183/Tyr185) | 255 (G9) | Mouse | NEB (CST) | 1:500 in TBS, 5% w/v non-fat dry milk, 0.1% Tween20 | WB, IP IF, FC | 46 (phospho-JNK1) 54 (Phospho-JNK2/3) |
| Cytochrome C (H-104) | sc-7159 | Mouse | Insight Bio (Santa Cruz) | 1:500 in TBS Tween20 0.1% | WB, IP, IF and ELISA | 15 |
| Phospho-ASK1 (Thr845) | #3765 | Rabbit | NEB (CST) | 1:1000 in TBS, 5% w/v BSA, 0.1% Tween20 | WB | 155 |

| | | | | | | |
|---|---|---|---|---|---|---|
| ASK1 | #3762 | Rabbit | NEB (CST) | 1:1000 in TBS, 5% w/v BSA, 0.1% Tween20 | WB | 155 |
| BAX | 2282-MC-100 (YTH-2D2) | Mouse | R&D systems (Trevigen) | 1:500 in TBS 0.1% Tween20 | WB, IP | 23 |
| Bcl-2 | 2291-MC-100 (YTH-8C8 | Mouse | R&D systems (Trevigen) | 1:500 in TBS 0.1% Tween20 | WB, IP | 25 |
| BAK | AF816 | Rabbit | R&D systems | 1:500 in TBS 0.1% Tween20 | WB | 28 |
| Phospho-p40phox (Thr154) | #4311 | Rabbit | NEB (CST) | 1:500 5% w/v BSA, 0.1% Tween20 | WB | 40 |
| Human Thioredoxin | #2285S | Rabbit | NEB (CST) | 1:500 5% w/v BSA, 0.1% Tween20 | WB | 12 |
| β-actin Clone AC15 | A5441 - 2ML | Mouse | Sigma | 1:20,000 in0.1% Tween20 | WB | 42 |
| CD40 | Sc-13128/ (H | Mouse | NEB (CST) | 1:500 in0.1% Tween20 | WB | 43 |
| CK18 | C8541 | Mouse | Sigma-Aldrich | 1:2000 in0.1% Tween20 | WB | 45 |

| | | | | | | |
|---|---|---|---|---|---|---|
| CK18 | 081213 | Mouse | Invitrogen | 1:1000 in0.1% Tween20 | WB | 45 |

**Table 2-1 Primary antibodies**

A table listing all primary antibodies used in this study, their catalogue number, host origin, supplier or manufacturer, optimal dilution, type of blocking buffer and the range of their applications. (Symbols - WB: Western blotting, IP: Immunoprecipitation, IF:Immunofluorescence, FC: Flow cytometry).

### 2.5.2 Secondary antibodies

For detection of all monoclonal antibodies the Molecular probes Alexa Fluor® 680 Goat anti-mouse IgG (H+L) antibody was used (Invitrogen Cat # A21057). Detection of all polyclonal antibodies was achieved using the Goat anti-Rabbit IgG IRDYE800 antibody (Tebu-bio Cat # 039611-132-122). Fluorochrome conjugated secondary antibodies were titrated prior to use and are listed in Table 2-2.

| Antigen | Catalogue no/ Clone | Host | Supplier (product of) | Dilution | Application |
|---|---|---|---|---|---|
| Mouse IgG | A21057 | Rabbit | Invitrogen | 1:10,000 in TBS 0.1% Tween20 | WB |
| Rabbit IgG | 039611-132-122 | Goat | Tebu-bio | 1:10,000 in TBS 0.1% Tween20 | WB |

**Table 2-2 Secondary antibodies**

A table listing all secondary antibodies used in the current study their catalogue number, host origin, supplier or manufacturer, optimal dilution, type of blocking buffer and the range of their applications. (Symbols - WB: Western blotting). Fluorescence detection of antibodies at wavelengths 680nm and 800nm was performed using the Licor Odyssey Infra red imaging system. When not in use antibodies were stored in the dark at 4℃.

### 2.5.3 Agonists & antagonists

Pharmalogical agonists and antagonists (Table 2-3) were reconstituted in either tissue culture grade dimethyl sulphoxide (DMSO; Sigma) or sterile $dH_20$ according to the manufacturer's instructions and stored in single use aliquots at -20°C. Prior to use, compounds were titrated using a cell viability assay (CellTiter 96® $AQ_{ueous}$ One Solution Cell Proliferation Assay; Promega, UK Cat # G3581) determining the effective and non- toxic dosage (as shown in Figure 4-10).

| Compound | Target | Supplier | Stock concentration | Effective concentration |
|---|---|---|---|---|
| N-acetyl L-cysteine (NAC) | ROS | Sigma | 30mM (culture media) | 30mM |
| DPI | NADPH Oxidase | Sigma | 10mM (DMSO) | 10µM |
| SP600125 | JNK | Enzo | 20mM (DMSO) | 25 µM |
| NDGA | AP-1 | Sigma | 20mM (DMSO) | 10µM |
| PX-12 | Thioredoxin | Sigma | 20mM (DMSO) | 1-3µM |
| Diethyl Maleate | Gluthathione | Sigma | 6.45 Molar | 75µM |
| Staurosporine | Protein Kinases | Sigma | 100µM | 1-10µM |
| Caspase-8 Inhibitor | Caspase-8 | R&D systems | 20mM | 25µM |
| Caspase-9 Inhibitor | Caspase-9 | R&D systems | 20mM | 25µM |
| Caspase-10 Inhibitor | Caspase-10 | R&D systems | 20mM | 25µM |
| GeneralcaspaseInhibitor (Z-VAD) | Caspases | R&D systems | 20mM | 25µM |
| Hydrogen peroxide | N/A | Sigma | 9.79M | 100µM-3200µM |
| G28-5 | CD40 | N/A | 1.1mg/ml | 10µg/ml |

**Table 2-3: Agonists & antagonists**

Agonists and antagonists used in the current study, their target molecule, the supplier, the stock and effective concentrations.

## 2.6 Tissue culture

### 2.6.1 General

All tissue culture work was undertaken using aseptic techniques within a HEPA filtration CellGard class II biological safety cabinet manufactured by NUAIRE. Prior and after use, internal working areas within the hood were disinfected using 70% (w/v) ethanol (Fisher). To do so 99% Ethanol was diluted appropriately (150ml:350ml) with purified autoclaved $dH_20$. Internal hood spillages were disinfected using Mikrozid® (Gompel Healthcare Cat# 32644) and this was also used for a monthly routine sterilisation. Any unwanted cells, exhausted media or solutions were aspirated into a large conical flask containing 10% (w/v) Virkon and were then left for a minimum of 30 minutes before poured off and washed into sewage.

Cell culture reagents were all of tissue culture grade, and were a product of Sigma unless otherwise stated. To isolate cells from solution they were spun for 5 minutes at 1500 RPM (210 RCF) using a Hettich Zentrifugen Universal 320 bench top centrifuge. Cells counts were performed from cell suspensions using a Marienfield Neubauer improved bright line haemocytometer before cells were seeded at the required cell density. When cells were not being manipulated they were kept in an Iso class 5 Nuaire Autoflow direct heat $CO_2$ incubator with a HEPA filtration system at 37℃ in a 5% $CO_2$ humidified atmosphere (incubator contained $dH_20$ supplemented with Sigma clean (Sigma cat# S5525-40Z). Cultured Cells were routinely observed by phase contrast microscopy using an EVOS XL (PeqLab) inverted microscope at x100 magnification.

### 2.6.2 Cryo-preservation and recovery of cell lines

Cells were cryo-preserved and stored in liquid nitrogen in a Statebourne storage dewar at -196℃. For cryopreservation of cell lines, cultures were harvested as for passaging (section 2.6.3) and collected by centrifugation. The cell pellet was re-

suspended in the appropriate ice-cold growth medium containing 10% (v/v) FBS and 10% (v/v) dimethylsulphoxide (DMSO) at a cell density not less than $1x10^6$ cells/ml. Cells were aliquoted in a total of 1ml to polypropylene cryovials (Sarstedt) and then transferred to an ice-cold Nalgene "Mr Frosty" (Fisher) containing 250ml of isopropanol (Fisher) to control the cooling rate to 1°C per minute. Cells were then placed within a -80°C freezer for 4-6 hours prior to transfer to liquid nitrogen.

Cells were recovered by thawing rapidly at 37°C, before 5-10ml of pre-warmed growth medium was added. Cells were centrifuged at 1500RPM/210g for 5 minutes and then seeded to tissue culture flasks as required.

### 2.6.3 Carcinoma cell culture

Established urothelial cell carcinoma (UCC) lines EJ, RT112 and RT4 and colorectal carcinoma cell line HCT116, SW480 and SW480-CD40 were maintained in a 50:50 (v/v) mixture of Dulbecco's modified eagle medium (DMEM Sigma cat # D6546-6X500ML) and Roswell Park Memorial Institute 1640 (RPMI Sigma cat # R0883-6X500ML) (referred to as D:R), supplemented with 5% Fetal calf serum (FCS Biosera cat # S1810/500) and 1% L-Glutamine (Sigma cat #G7513-100ML). The latter media constitution will be abbreviated to DR/5%FCS/1%L-G. At all times cell lines were cultured in the aforementioned medium unless otherwise stated and incubated at 37°C in 5% $CO_2$.

For routine passaging, cells were harvested by washing with 0.1% (w/v) EDTA in phosphate buffered saline – calcium and magnesium free (PBS) (Invitrogen Cat# 14200-067) for 5 minutes and then addition of Trypsin-EDTA (Sigma Cat# T41474-20ml) in Calcium and Magnesium free Hanks-balanced salt solution (HBSS, Sigma Cat# H9394-6X500ML) until cells detached from the culture flask. Trypsin was inactivated by the re-addition of the respective serum-supplemented culture medium when cells were re-suspended.

### 2.6.4 Murine fibroblast (3T3) cell culture

The mouse fibroblastic cell line NIH3T3 has been previously stably transfected with two expression plasmids, one bearing the sequences coding for CD40L and Neomycin resistance gene (3T3-CD40L cells) and one with Neomycin resistance alone (3T3-Neo cells) as described in Bugajska et al. (2002). During routine culture, these 3T3 derivatives were maintained in D:R supplemented with 10% FCS, 1% L-Glutamine (DR:10%FCS/1%L-G) and 0.5µg/ml G418/Neomycin (Invivogen Cat# ant-gn-1; supplied by Autogen Bioclear) to ensure cells maintained transgene expression. At all times cell lines were cultured in the mentioned medium unless otherwise stated and incubated at 37℃ in 5% $CO_2$. 3T3 cells were harvested and passaged as carcinoma cells with the exemption of a two minute 0.1% (w/v) EDTA in PBS treatment as extended periods risked cell detachment.

## 2.7 Primary Urothelial Cell Culture

### 2.7.1 Tissue specimens

Specimens of human bladder, ureter and renal pelvis were provided by surgeons from Huddersfield Royal Infirmary. Tissue biopsies were taken for research purposes with fully informed consent from patients with no history of urothelial neoplasia and with the permission of the relevant Local Research Ethics Committee. Biopsies were collected in sterile 25ml polystyrene Universal tubes containing 15mls of sterile transport medium (Appendix II) and where possible were stored at 4℃ until processing.

### 2.7.2 Isolation of primary human urothelial cells

Primary urothelial cultures were established as previously described (Southgate et al., 1994; Southgate et al., 2002). Specimens were dissected in sterile Petri dishes (Nunc) using scissors and forceps to remove unwanted fat and connective tissue. Ureters were split longitudinally to allow access to the urothelium. Where possible a small cross-section was removed and fixed overnight in 10% (v/v) formalin in $PBS_c$ for routine histological analysis. The remaining tissue was incubated in 5ml of

stripper medium for 4 hours at 37℃ to dissociate the urothelium from the basement membrane. Urothelial sheets were detached from the underlying stroma using forceps and pelletted via centrifugation. A single cell suspension was achieved via incubation in 2ml (400U) of Collagenase IV (Appendix II) for 20 minutes at 37℃. Cells were then collected via centrifugation and counted prior to seeding into vacuum-gas plasma treated Primaria® flasks or Petri dishes (SLS). Normal human urothelial (NHU) primary cell cultures were established in Keratinocyte serum free medium (KSFM), supplemented with 50µg/ml bovine pituitary extract (BPE; Invitrogen) and 5ng/ml epidermal growth factor (rhEGF; Invitrogen) termed complete KSFM (KSFMc). For initial establishment of NHU cultures the KSFMc medium was also supplemented with 30ng/ml cholera toxin (Sigma).

### 2.7.3 Sub-culture of urothelial cell lines

Following initial isolation, NHU cells were maintained in KSFMc (without cholera toxin). At all times cells were cultured in the presence of KSFMc unless otherwise stated and were incubated at 37℃ in 5% $CO_2$. Urothelial cells were harvested by washing with 0.1% (w/v) EDTA in PBS for 5 minutes and then addition of Trypsin-EDTA until cells detached from the culture flask. Trypsin was inactivated by the re-addition of 10ml KSFMc containing 2mg Trypsin inhibitor (Sigma Cat# T6522-100mg). Cells were further removed from any traces of Trypsin and Trypsin inhibitor by centrifugation and re-suspension in a further 10ml of KSFMc. This technique was used for routine passage and cell NHU cells used in this study were only from passages 1-3.

### 2.7.4 Paramalignant cell culture

HU-hTERT cells were previously established by virus mediated over-expression of the catalytic subunit of Human Telomerase Reverse Transcriptase (hTERT) enzyme in NHU cells (Georgopoulos et al., 2011). These cells were cultured, harvested and passaged as for NHU cells (section 2.7.3). Cells used for any experiment were from passages 29-32.

## 2.8 Cell line transfections

### 2.8.1 Culture of Retropack™ PT67 Packaging Cell Line

The Retropack PT67 cell line (Clontech) is a NIH3T3 fibroblast derived cell line which has been genetically engineered to stably express the retroviral *gag*, *pol* and *env* genes. Once transfected with a retroviral vector, cells produce a replication-defective retrovirus with a broad (amphotrophic) mammalian host range. Cells were routinely cultured in DMEM supplemented with 10% (v/v) FCS and were passaged as for UCC cell lines (section 2.6.3). Cells were split at a ratio of between 1:5-1:15. Prior to transfection, cells were subjected to Hypoxanthine Aminopterin Thymidine (HAT; Invitrogen) medium re-selection as recommended by the supplier. PT67 cells were firstly cultured in normal growth medium supplemented with 100nM aminopterin for 5 days, and then 5 days in DMEM-HAT medium (30nM hypoxanthine, 1M aminopterin, 20mM thymidine), and then finally 5 days in DMEM-HT medium (30mM hypoxanthine, 20mM thymidine). Immediately after HAT re-selection, PT67 cells were either cryo-preserved (see section 2.6.2), or transfected.

### 2.8.2 Transfection of the packaging cell line PT67

All procedures involving transfected PT67 cells were carried out in a class II tissue culture hood (as described in section 2.6.1). The packaging cell line PT67 was maintained in DMEM (Sigma) supplemented with 10% FCS and 1% L-Glutamine until 60% confluent. Cells were then transfected using Effectene (Qiagen), a lipid-based transfection reagent according to the manufacturer's instructions. In brief, 5µg of endotoxin-free plasmid DNA was gently mixed with 150µl of buffer EC and 40µl of enhancer and incubated at ambient temperature for 5 minutes. 50µl of Effectene transfection reagent was added, gently mixed by pipetting for 10 seconds and incubated at ambient temperature for a further 10 minutes. To this, 1ml of complete growth medium (DMEM with 10% FBS and 1% L-glutamine) was added, pipetted up and down and then added drop-wise to the flask. A negative Control culture where the plasmid DNA was omitted was included in all experiments. Cultures were incubated for 48 hours, after which cells reached confluency. At confluency, the transfected PT67 cells and negative Control flask were harvested as with routine passaging and reseeded at a split ratio of 1:3 into complete medium supplemented

with 2ug/ml of Puromycin (Invivogen #ant-pr-1 supplied by Autogen Bioclear). A 100% stably transfected cell population was assumed in the test flask when all cells in the non-transfected negative Control flask had perished. Transfected PT67 cells were maintained under Puromycin selection pressure until viral particles were harvested.

### 2.8.3 Retroviral transduction

The infection efficiency of retroviruses can be employed to rapidly and stably express a transgene of interest within a population of mitotically active cells. Transduction is much more efficient than many transfection protocols, as it results in less cellular stress and subsequent cell death, and is thus the method of choice when using finite or infinite cell lines. It has been previously demonstrated that the transduction methods performed in our laboratory are >90% efficient (Crallan et al., 2006), as detailed below.

### 2.8.4 Retroviral transduction of Carcinoma cells

Stably transfected PT67 cells were grown to 100% confluency then the medium was changed to 10ml DR/5%FCS/1%L-G (replacing DR/10%/1%L-G that previously contained antibiotics) for 16 hours. Conditioned virus-containing antibiotic-free medium was then harvested and filtered through a 0.45µm Tuffryn filter (Acrodisc, VWR) to remove any cellular debris. Moreover, before use for infection, the virus-conditioned medium was supplemented with 8µg/ml of polybrene (Sigma) (see Appendix II). The previous day a 100% confluent T75 flask of EJ (p12-20) was split 1:20 into two separate T75 flasks, then the following day the medium was removed before one flask of EJ cells were treated a) with 8ml of polybrene and virus-containing conditioned medium or b) 8ml of DR/5%FCS/1%L-G to act as the negative control before re-incubation. Both transduced and non-transduced EJ carcinoma cells were then trypsinised collected by centrifugation and passaged at a split ratio of 1:10 into new T75 tissue culture flasks containing fresh culture medium and Puromycin at a concentration of 0.5µg/ml (concentration pre-determined by pre-titration experiments, see Figure 4-5. Transduced EJ and negative control EJ were

then observed under the microscope until all negative control cells had perished from the flask – see figure 4-6. A 100% stably transduced cell population was assumed at this point (generally 48-72 hours) and transduced cells were cultured in medium containing Puromycin concentration reduced to 0.25µg/ml in order to alleviate some antibiotic stress and allow adequate growth.

## 2.9 Molecular Biology

### 2.9.1 shRNA design

Short hairpin RNA (shRNA) sequences were designed using the Invitrogen siRNA design tool (http//rnaidesigner.invitrogen.com/rnaiexpress) and incorporating *BamHI* and *EcoR1* overhangs as well as an internal *MluI* restriction site to aid in selection of positive clones. A minimum of two shRNA oligos were created to improve the probability of a successful knockdown. Some of the designed shRNAs were based on published literature and some created using the online design tool from Invitrogen.

### 2.9.1 Cloning

Molecular cloning, transformation of competent *E.coli,* and purification of plasmid DNA was previously performed by Dr Nik Georgopoulos at the Leeds Institute of Molecular Medicine (LIMM), Cancer Research UK, St James Hospital (University of Leeds). A range of shRNAs were created using the designed oligonucleotides (supplied by Eurofins, former MWG Biotech) shown in Table 2-4.

| TARGET mRNA | Complete sequence (target) of Oligonucleotides (orientated 5' to 3') | Design source |
|---|---|---|
| MKK7 | GATCCGTAAGCTACTTGAACACAGCTTCAAGAGAGCTGTGTTCAAGTAGCTTATTTTTTACGCGTG' (MKK7siR1-for)<br>AATTCACGCGTAAAAAATAAGCTACTTGAACACAGCTCTCTTGAAGCTGTGTTCAAGTAGCTTACG (MKK7siR1-rev) | Deng et al., 2003 |
| MKK7 | GATCCGCAGGACAGTTTCCCTACAATTCAAGAGATTGTAGGGAAACTGTCCTGTTTTTTACGCGTG (MKK7siR2-for)<br>AATTCACGCGTAAAAAACAGGACAGTTTCCCTACAATCTCTTGAATTGTAGGGAAACTGTCCTGCG (MKK7siR2-rev) | Invitrogen design tool |
| TRAF3 | GATCCGAGTCAGGTTCCGATGATCTTCAAGAGAGATCATCGGAACCTGACTCTTTTTTACGCGTG (TRAF3siR1-for)<br>AATTCACGCGTAAAAAAGAGTCAGGTTCCGATGATCTCTCTTGAAGATCATCGGAACCTGACTCG (TRAF3siR1-rev) | Liao et al., 2004 |
| TRAF3 | GATCCGCCCACTGGAGAGATGAATTTCAAGAGAATTCATCTCTCCAGTGGGCTTTTTTACGCGTG (TRAF3siR2-for)<br>AATTCACGCGTAAAAAAGCCCACTGGAGAGATGAATTCTCTTGAAATTCATCTCTCCAGTGGGCG (TRAF3siR2-rev) | Invitrogen design tool |
| BAX | GATCCGCATGGAGCTGCAGAGGATGTTCAAGAGACATCCTCTGCAGCTCCATGTTTTTTACGCGTG (BaxsiR1-for)<br>AATTCACGCGTAAAAAACATGGAGCTGCAGAGGATGTCTCTTGAACATCCTCTGCAGCTCCATGCG (BaxsiR1-rev) | Ray and Almasan 2003 |
| BAX | GATCCGGTGCCGGAACTGATCAGATTCAAGAGATCTGATCAGTTCCGGCACCTTTTTTACGCGTG (BaxsiR2-for)<br>AATTCACGCGTAAAAAAGGTGCCGGAACTGATCAGATCTCTTGAATCTGATCAGTTCCGGCACCG (BaxsiR2-rev) | Bidere et al., 2003 |
| MKK4 | GATCCGTCCCAATCCTACAGGAGTTTTCAAGAGAAACTCCTGTAGGATTGGGATTTTTTACGCGTG (MKK4siR1-for)<br>AATTCACGCGTAAAAAATCCCAATCCTACAGGAGTTTCTCTTGAAAACTCCTGTAGGATTGGGACG (MKK4siR1-rev) | Invitrogen design tool |

| | | |
|---|---|---|
| MKK4 | GATCCGCTGTGAAAGCACTAAACCATTCAAGAGATGGTTTAGTGCTTTCACAGTTTTTTACGCGTG (MKK4siR2-for)<br><br>AATTCACGCGTAAAAAACTGTGAAAGCACTAAACCATCTCTTGAATGGTTTAGTGCTTTCACAGCG (MKK4siR2-rev) | Invitrogen design tool |
| BAK | GATCCGCCGACGCTATGACTCAGAGTTCAAGAGACTCTGAGTCATAGCGTCGGTTTTTTACGCGTG (BaksiR1-for)<br><br>AATTCACGCGTAAAAAACCGACGCTATGACTCAGAGTCTCTTGAACTCTGAGTCATAGCGTCGGCG (BaksiR1-rev) | Invitrogen design tool |
| BAK | GATCCGTGGTCCCATCCTGAACGTGTTCAAGAGACACGTTCAGGATGGGACCATTTTTTACGCGTG (BaksiR2-for)<br><br>AATTCACGCGTAAAAAATGGTCCCATCCTGAACGTGTCTCTTGAACACGTTCAGGATGGGACCACG (BaksiR2-rev) | Invitrogen design tool |
| ASK1 | GATCCGCCCTGCATTTTGGGAAACTTTCAAGAGAAGTTTCCCAAAATGCAGGGTTTTTTACGCGTG (ASK1siR1-for)<br><br>AATTCACGCGTAAAAAACCCTGCATTTTGGGAAACTTCTCTTGAAAGTTTCCCAAAATGCAGGGCG (ASK1siR1-rev) | Invitrogen design tool |
| ASK1 | GATCCGTTCGGCAGCGAGTAGATAATTCAAGAGATTATCTACTCGCTGCCGAATTTTTTACGCGTG (ASK1siR2-for)<br><br>AATTCACGCGTAAAAAATTCGGCAGCGAGTAGATAATCTCTTGAATTATCTACTCGCTGCCGAACG (ASK1siR2-rev) | Invitrogen design tool |

## Table 2-4 shRNA Oligonucleotides

The table shows the forward and reverse oligonucleotides for the construction of shRNA delivery vectors and expression by retroviral transduction using the pSIREN RetroQ system.

### 2.9.2 RNAi delivery plasmid

RNAi ready pSIREN RetroQ (Clontech) is a self-inactivating retroviral expression vector designed to express shRNAs via a U6 promoter. The vector encodes a 5' long terminal repeat (LTR) containing a cytomegalovirus type 1 (CMV) enhancer region and a mouse sarcoma virus (MSV) promoter to drive transcription of the RNA packaging signal $\Psi^+$, shRNA of interest and Puromycin resistance cassette in eukaryotic cells. When expressed in the packaging cell line PT67, the plasmid will produce infectious but replication-incompetent viral particles which lack the structural genes necessary for virus formation and can infect a wide host range but cannot replicate. Insertion of the target shRNA sequence is via *BamHI* and *EcoRI* restriction sites (Figure 2-1).

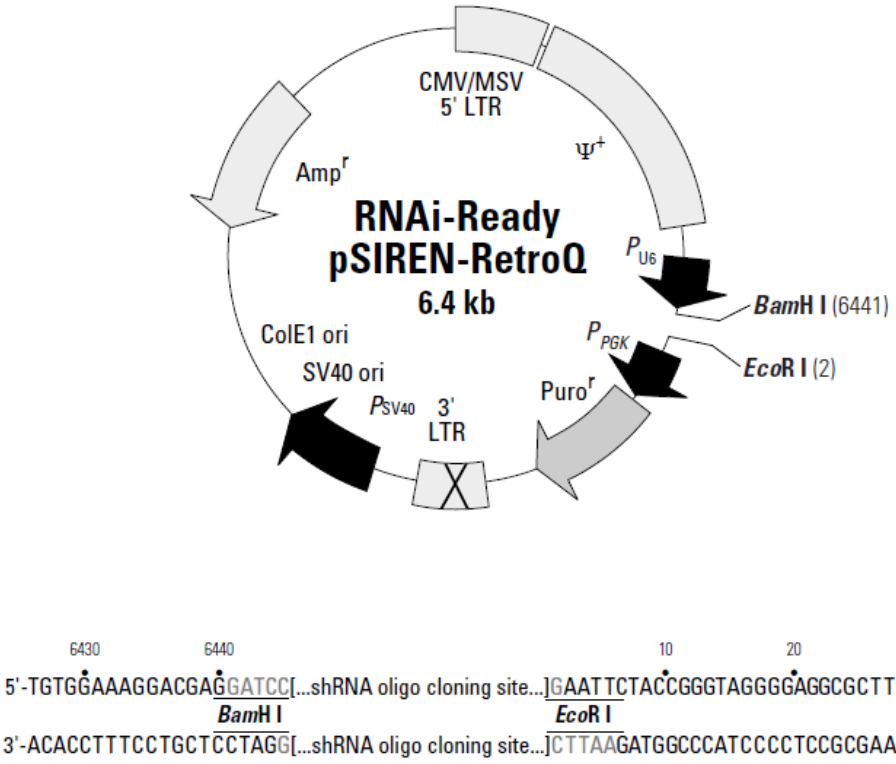


**Figure 2-1: pSIREN RetroQ plasmid vector**

pSIREN RetroQ plasmid is based on the Moloney mouse leukemia virus (MMLV) and can be used for targeted gene silencing using RNAi. Oligonucleotides encoding short-hairpin RNA sequences can be cloned between the *Bam*HI and *Eco*RI restriction enzyme sites. Plasmid is then propagated in competent E.*coli* bacteria using the ColE1 origin of replication ColE1$^{ORI}$) and successfully transformed cells are selected via expression of the ampicillin resistance gene (Amp$^r$). Upon transfection into the packaging cell line, PT67, the RNA packaging signal ($\Psi^+$), shRNA of interest and Puromycin resistance cassette (Puro$^r$) is transcribed via a 5' long terminal repeat (LTR) containing a cytomegalovirus type 1 (CMV) enhancer region and a mouse sarcoma virus (MSV) promoter. During reverse transcription of the retroviral RNA, the 3' LTR is copied and replaces the 5' LTR, resulting in inactivation of the 5' LTR CMV enhancer sequences. Vector is then packaged and the resulting retroviral particles can be utilised in a variety of mammalian cells. In target cells, expression of the short hairpin RNA and Puro$^r$ is driven via a U6 promoter, an RNA polymerase III-dependant promoter. Imaged reproduced from the Clontech pSIREN RetroQ manual PT3737-5.

## 2.10 Methods of CD40 ligation

CD40 receptor ligation for the experiments described in this study was carried out by either membrane CD40L or soluble agonist.

Delivery of membrane-presented CD40L (mCD40L) was achieved by co-culture of 3T3CD40L cells (mCD40L) with CD40-positive target epithelial cells. As a negative control, epithelial cells were co-cultured with equal numbers of 3T3Neo cells (Controls). mCD40L and Control cells were growth arrested by treatment with 0.5µg/ml of Mitomycin C (Sigma) for two hours in D:R before they were washed, harvested and seeded into 96 well plates at $10^4$ cells/well or 10cm$^2$ culture dishes at $3x10^6$/dish, for apoptosis detection assays and preparation of protein lysates, respectively. After mCD40L and Control cells attached to the tissue culture substrate (in most cases following overnight incubation), epithelial cells were added at a ratio of 0.8 or 0.9 epithelial cells to 1 fibroblast (as previously optimised in Bugajska et al., 2002). More specifically, $8x10^3$ epithelial cells were seeded into 3T3 cell-containing 96 well plates and $2.7x10^6$ cells were seeded into 10cm$^2$ culture dishes, respectively.

Receptor ligation by soluble CD40 agonists was performed by treatment of target cells (cultured at a density of $8x10^3$ cells per well) using the well characterised agonistic monoclonal antibody (mAb) G28-5 (Bugajska et al., 2002; Georgopoulos et al., 2006) at a final concentration of 10µg/ml (purified from cultured supernatant of the hybridoma line HB9110). For some experiments, the recombinant MegaCD40L™ preparation was also used (Enzo Life Sciences) at a final concentration of 0.1µg/ml.

## 2.11 Detection of cell viability, death (apoptosis) and reactive oxygen species (ROS) production

### 2.11.1 General

Previously published guidelines regarding the use and interpretation of assays for monitoring cell death (Galluzzi et al., 2009) have recommended that a minimum of two assays are utilised for the detection of cell apoptosis. The current study made use of a cell proliferation assay in addition to four apoptosis detection-specific

assays.caspase3/7 activation, DNA fragmentation and the loss of cell membrane integrity were all used as markers for apoptosis.

These assays were based on measurement of absorbance, fluorescence or luminescence. 96 well Nunc white, tissue treated culture plates (Fisher cat # TKT-186-010C) were used for luminescence and fluorescent based assays, 96 well Costar transparent tissue treated culture plates (Fisher Cat # TKT-186-010C) for absorbance, and 96 well ELISA microplate (Greiner bio one Cat # 655101) for ELISA. For most assays where epithelial cells were cultured with mCD40L and Control cells, 3T3-CD40L and 3T3-Neo background values were subtracted pair wise as appropriately, i.e. “mCD40L/EJ – mCD40L” and “Control/EJ – Control” readings. The exemption was DNA fragmentation as this was unnecessary due to the pre-labelling of target epithelial cells. Finally, in all experiments blank controls were included as appropriate.

### 2.11.2 Detection of cell viability using CellTiter 96® $AQ_{ueous}$ One Solution Cell Proliferation assay

The CellTiter 96® $AQ_{ueous}$ One Solution Cell Proliferation assay involves the use of the MTS tetrazolium (yellow) which is reduced to a formazan derivative (brown) by respiring cells. The observed change in colour is proportional to the total number of viable/proliferating cells. Epithelial cells were plated into 96 well plates with 6 replicate wells and then left to adhere overnight before the addition of culture medium containing pharmacological agonists or inhibitors. 20µl of CellTiter 96® $AQ_{ueous}$ One Solution was added to appropriate wells and plates were incubated at 37℃ in 5% $CO_2$ for a total of four hours. Total levels of formazan formation/cell viability were assessed using a FLUOstar OPTIMA (BMG Labtech) plate reader at a wavelength of 492nm and data was acquired using MARS software (BMG Labtech) and assessed using Microsoft Excel. Cell viability was calculated as percentage viability in comparison to controls using the following formula: (T/C)x100, where T= treated cells and C= controls cells.

### 2.11.3 Detection of apoptosis usingcaspase3/7 assays

The activation of Caspases 3/7 is a well established feature of cell apoptosis. Caspases 3 and 7 target a specific amino acid sequence located on many proteins which leads to overall cell demise by an organised apoptotic event. The activation of Caspases 3/7 was determined using the SensoLyte® Homogenous AFC Caspase-3/7 substrate (Anaspec Cat # 71114, supplied by Cambridge Bioscience), or thecaspase3/7-Glo substrate assay (Promega Cat # g8091).

#### 2.11.3.1 SensoLyte® Homogenous AFC Caspase-3/7 assay

The assay utilises the cleavage of the recognition sequence of caspase -3 and 7 that is Asp-Glu-Val-Asp (DEVD). The SensoLyte® Homogeneous AFC Capase-3/7 assay kit uses Ac-DEVD-AFC as the fluorogenic indicator for assaying caspase-3/7 activity. Upon caspase-3/7-mediated cleavage, Ac-DEVD-AFC generates the AFC fluorophore which has bright blue fluorescence and can be detected at Excitation/Emission=380nm/500nm. The degree of production of the strongly fluorescent fluorophore is relative to total levels of caspase-3/7 activation.

Epithelial cells were treated with membrane or soluble CD40 agonists in 96 well plates as described in section 2.10 before the addition of 50µl SensoLyte® Homogenous AFC Caspase-3/7 substrate. Fluorescence was measured using a FLUOstar OPTIMA (BMG Labtech) plate reader using Excitation/Emission 355nm/520nm filters, following calibration of the reader using the Gain function on the MARS software to ensure the measurements were taken within the dynamic range of the instrument. Plates were kept away from light and left at room temperature (RT) overnight after which fluorescence measurements were taken.. To account for background created by fibroblasts, these were cultured alone and their relative fluorescent units (RFU) subtracted from the representative co-culture in a pair wise fashion.

### 2.11.3.2 Caspase-Glo® 3/7 Assay

The assay utilises a proluminescent caspase-3/7 DEVD-aminoluciferin substrate and a thermostable luciferase in a reagent optimized for caspase-3/7 activity, luciferase activity and cell lysis. As the cells are lysed *in situ*, the luminescence can be detected immediately after substrate addition.

Epithelial cells were treated with membrane or soluble CD40 agonists as described in section 2.10 before the addition of 50µl caspase 3/7-Glo substrate. Luminescence was detected using a FLUOstar OPTIMA (BMG Labtech) plate reader, following calibration of the reader using the Gain function on the MARS software to ensure the measurements were taken within the dynamic range of the instrument. Plates were kept away from light and left at RT for 15 minutes before measurements were taken. Data was acquired using MARS software (BMG Labtech) and analysed by Microsoft Excel.

## 2.11.4 Detection of cell death using the CytoTox-Glo™ assay

The CytoTox-Glo assay is based on detection of the activity of a proprietary, specific protease normally present inside cells. During apoptosis, as the cell membrane is compromised the protease is released and it cleaves the AAF-Glo™ substrate thus generating a luminescence signal. The intensity of the luminescence signal indicates the degree of apoptotic cells in a population.

Epithelial cells were treated with membrane or soluble CD40 agonists as described in section 2.10 before the addition of 50µl CytoTox-Glo substrate. Luminescence was detected using a FLUOstar OPTIMA (BMG Labtech) plate reader, following calibration of the reader using the Gain function on the MARS software to ensure the measurements were taken within the dynamic range of the instrument. Plates were kept away from light and left at RT for 15 minutes before measurements were taken. Data was acquired using MARS software (BMG Labtech) and analysed by Microsoft Excel. In cases where the percentage of dead cells was calculated the detergent Digitonin was added to lyse all cells according to the manufacturer's recommendations and a further reading was taken 15 minutes initial readings taken. To calculate percentage cell death the equation used was: (Background-corrected

RLU before digitonin / background-corrected RLU after digitonin)x100, where RLU indicates relative luminescence units.

### 2.11.5 Detection of cell apoptosis using the DNA fragmentation ELISA

The fragmentation of DNA is a notable event during cell apoptosis and this assay uses 5-bromo-2'-deoxyuridine (BrdU) specific antibodies to detect BrdU-labelled fragments of DNA. Greater amounts of fragmented DNA labelled with BrdU represent a greater number of cells that have undergone apoptosis.

AS per manufactures instructions exponentially growing epithelial cells were loaded with the DNA labelling agent BrdU for 2 hours at a concentration of 10µM. Cells were then treated with mCD40L by co-culture as described in section 2.10. An ELISA plate was coated with an anti-DNA antibody and then blocked to remove any non-specific binding sites. After washing of the ELISA plate to remove any blocking buffer, supernatants from cell culture was added which may contain DNA fragments pulsed with BrdU. The labelled fragments of DNA stick to the plate via the anti-DNA antibody and then a secondary, enzyme-linked antibody that specifically recognises BrdU was added. Finally, an enzyme substrate was added which is converted into a blue colour by the secondary, enzyme-linked antibody. The increased amount of colour change is relative to the amount of secondary antibody bound to BrdU labelled fragments of DNA. Sulphuric acid was used to stop the reaction after sufficient colour change, and following this, a deeper colour of yellow represents a greater degree of cell apoptosis. The plates were used to measure absorbance at using a 455-10nm filter on a FLUOstar OPTIMA (BMG Labtech) plate reader. Data was acquired using MARS software and analysed by Microsoft Excel. No background controls were necessary as only epithelial cells were pulsed with the DNA labelling agent BrdU.

### 2.11.6 Detection of Reactive oxygen species using $H_2$DCFDA

6-carboxy-2',7'-dichlorodihydrofluorescein diacetate ($H_2$DCFDA) (Invitrogen Cat # c2938) is a cell permeable, chemically-reduced, acetylated form of fluorescein used as an indicator for reactive oxygen species (ROS) in cells. This non-fluorescent molecule is readily converted to a green-fluorescent form when the acetate groups are removed by intracellular esterases and ROS-associated oxidation within the cell.

As it is oxidation sensitive, $H_2$DCFDA was reconstituted in oxygen-free conditions (in a nitrogen environment) before aliquoting and storage at -80°C, as recommended by the manufacturer.

Epithelial cells were treated with membrane or soluble CD40 agonists as described in section 2.10. However when co-cultures were performed, 3T3 fibroblasts used in this instance were not growth arrested using Mitomycin C. Following CD40 ligation, cultures of agonist treated cells or co-cultures were first washed with PBS to remove any culture medium and were then treated with 1µM of $H_2$DCFDA in pre warmed (37°C) PBS for 30 minutes 37℃ in 5% $CO_2$. The reduced forms of the fluorescein lack any fluorescence until acetyl groups are removed by intracellular esterases and oxidation is occurring in the cell. When this occurs the charge of the molecules makes it much less likely to leave the cell and it also emits detectable fluorescence. Following treatment with $H_2$DCFDA for the indicated time periods, fluorescence was measured on a FLUOstar OPTIMA (BMG Labtech) plate reader at Excitation 485nm/Emission 520nm, following calibration of the reader using the Gain function on the MARS software to ensure the measurements were taken within the dynamic range of the instrument.

## 2.12 SDS-PAGE and Immunoblotting (Western Blotting)

### 2.12.1 General

Proteins from within a cell lysate can be gently extracted and maintained in buffers to ensure their integrity. Under denaturing conditions multiple proteins are size fractionated using SDS-PAGE, a form of gel electrophoresis. This electrophoresis utilises the electrophoretic mobility of proteins to run them down a gel and specific gel pores separate them by size and charge. Proteins separated by this method are then transferred toward a transfer membrane which has high binding affinity for them. Stably bound to a membrane, size fractionated and denatured proteins are detected using epitope specific primary antibodies. A near-infrared (NR) fluorophore conjugated secondary antibody raised against the primary antibody is then added to the membrane and the membrane is scanned using an infrared scanner.

.

### 2.12.2 Protein extraction

Co-cultures of mCD40L and Control cells with target epithelial cells were grown in 10cm$^2$ culture flasks and lysed *in situ*. In some cases (where stated) cultures were mainatined in the presence of pharmalogical agonist/antagonists as indicated. Culture medium was aspirated and cell sheets were washed 2x in ice-cold D-PBS to remove any excess proteins. 20µl of ice-cold 2x sodium dodecyl sulphate (SDS) buffer (Appendix II) containing 2mg/ml DTT and 0.2%(v/v) protease inhibitor cocktail set 3 (Calbiochem) was pipetted onto the cell monolayer and the cells were scraped using a cell scraper (Fisher Cat# FB55199) into lysate solution. The solution was then transferred to a chilled microcentrifuge tube kept on ice. Samples were sonicated using an ultrasonic probe (Sonics Vibra cell) for 10-second bursts until lysate resembled froth like consistency it was then cooled on ice for 30 minutes. The lysates were centrifuged at 10,000g, 4℃ for 30 minutes to pellet the insoluble material, before aliquoting the supernatant and storing at -20℃.

### 2.12.3 Protein Quantification

The protein concentration of each sample was determined using a Coomassie protein reagent assay kit (Pierce cat# PN23236). Samples were diluted 4:46 in $dH_2O$ and 10µl was aliquoted in quadruplicates into a transparent 96-well flat bottomed plate. A seven point standard curve of 0-1mg/ml (0, 25, 125, 250, 500, 750 100µg/ml) BSA (Pierce Cat# PN23208) was included on each plate. 200µl of ambient temperature Coomassie reagent was added to each well and mixed gently by pipetting. The absorbance was then measured using a FLUOstar OPTIMA (BMG Labtech) plate reader at Abs 595nm against a $dH_2O$ Control. MARS analysis software 2.0 (BMG Labtech) was used to plot a standard curve for the BSA and to estimate the protein concentration for each lysate.

### 2.12.4 SDS-Polyacrylamide gel Electrophoresis (SDS-PAGE)

20-40µg of protein lysate was made up to 13µl with $dH_2O$ then this was totalled to 20µl by the addition of 5µl 4x lithium dodecyl sulfate sample buffer (LDS; Invitrogen Cat# NP0007) and 2µl of 10x reducing agent (500mM Dithiothreitol) (Invitrogen Cat#NP0009). The sample was denatured by heating to 70°C for 10 minutes in a 70°C waterbath. 10-well NuPAGE™ Novex electrophoresis pre-cast gels (Invitrogen Cat# NP0321) were placed into an Xcell Surelock™ mini-cell upright electrophoresis tank (Invitrogen). 200ml and 600ml of 1x NuPAGE™ MES SDS running buffer (Invitrogen Cat# NP0002) was poured into the inner and outer chambers, respectively. 500µl of NuPAGE™ antioxidant (Invitrogen Cat # NP0005) was added to the inner chamber prior to loading of the samples. 5µl of All-Blue Precision Plus Protein™ standard (Bio-Rad #161-0373) was loaded alongside as a marker of protein size and the gel was run at 200V for 35 minutes.

### 2.12.5 Electrophoretic membrane transfer

Electrophoretically-seperated proteins were transferred onto Immobilon-FL™ polyvinylidine difluoride membrane (PVDF; Millipore) using an X*cell* II™ blot module (Invitrogen). PVDF membranes were dipped in methanol, rinsed in $dH_2O$ and then soaked in 0.5x "Towbin" transfer buffer with 20% (v/v) methanol (Appendix II) along with the required number of blotting pads and Whatman™ filter paper (Fisher). The gel membrane sandwich was assembled cathode to anode as follows; 2x blot pads, filter paper, gel, PVDF membrane, filter paper, 2x blot pads. The blot module was secured into the X*cell* SureLock™ Mini-Cell and filled with transfer buffer. The outer chamber was filled with ice-cold $dH_2O$ and the transfers were performed on ice at 25V for 2 hours.

### 2.12.6 Membrane immunolabelling and visualisation using the Li-Cor Odyssey system

To minimise non-specific binding, membranes were blocked in 50:50 (v/v) Odyssey blocking buffer (Li-Cor Cat# 927-4000):10mM TBS pH 7.6 at ambient temperature on a plate rocker for 1 hour. Membranes were then probed with 5-8ml of pre-titrated primary antibody diluted in TBS+0.1% (v/v) Tween-20. All primary antibody incubations were performed on a rocking platform overnight (O/N) at 4°C. Membranes were then washed 3 x 5 minutes in TBS+0.1% (v/v) Tween-20 prior to addition of 10ml appropriate infra red secondary antibodies (Table 2-2) for 1 hour at ambient temperature on a rocker. Membranes were washed as for primary antibody and then washed 1x for 5 minutes with TBS prior to visualization using an Odyssey™ Infra-red Imaging system (Li-Cor). Where available, a positive control lysate known to express the protein of interest was included. Equal loading of epithelial lysate was verified using an antibody raised against the house keeping gene, Cytokeratin 18. Densitometry was performed using Odyssey V3.1 software (Li-Cor) and protein expression was normalised relative to Cytokeratin 18.

## 2.13 Separation of subcellular fractions for Western Blotting

### 2.13.1 Nuclear fractionation

In order to determine the localisation of certain proteins in response to CD40 ligation, the nuclei of cells were isolated using the Fisher Nuclear extraction kit (Fisher cat# PN78833) as instructed by the manufacturer. Nuclear pellets from co-cultures carried out in $10cm^2$ dishes ($3x10^6$ 3T3 cells and $2.7x10^6$ epithelial cells) were lysed with the provided lysis buffer and were processed in the same manner as for normal cell lysates and immunoblotting (Section 2.12). The kit also allows the isolation of the Cytoplasmic proteins which are used to compare the localisation of proteins between the nucleus and cytoplasm. Nuclear fractions and cytoplasmic fractions of cell cultures were screened for the presence of CD40, which is cytoplasmic only, to validate separation of the two cellular compartments. The required primary and secondary antibodies were added and then membranes were scanned as normal for western blotting techniques.

### 2.13.2 Mitochondrial fractionation

Part of the intrinsic pathway that executes death involves the release of Cytochrome C from the mitochondrial matrix. In order to examine this phenomenon the mitochondria were isolated from co-cultures performed in $10cm^2$ dishes ($3x10^6$ 3T3 cells and $2.7x10^6$ epithelial cells) using Dounce homogenisation (Fisher 11582443) and centrifugation as instructed by the manufacturers of the Millipore mitochondrial isolation kit (Cat # MT1000). Mitochondrial pellets were then lysed as instructed and processed the same way as for normal cell lysate and Western Blotting. The kit also allows the isolation of the Cytoplasmic proteins which are used to compare the localisation of proteins. Mitochondrial fractions of cell cultures were screened for the presence of Bcl-2 a protein located in the mitochondrial membrane and Cytochrome c a protein found within the mitochondrial matrix. Cytoplasmic fractions were also tested for Cytochrome C to determine any release and also for the Cytoplasmic specific protein GAPDH. All antibodies for related proteins were supplied along with the kit along with recommended dilution factors. Appropriate primary and secondary antibodies were added and then membranes were scanned as normal for western blotting techniques.

## 2.14 Mycoplasma testing

*Mycoplasma spp.* contamination is a huge problem in eukaryotic cell culture and can lead to unreliable experimental results (Capes-Davis A., 2010). All cell lines were routinely tested for intracellular bacteria *Mycoplasma spp*. using the MycoProbe™ Mycoplasma detection assay (R&D systems Cat # CUL001B) which is designed for screening of cultured cells. This assay detects Mycoplasma 16S ribosomal RNA (rRNA) using a colorimetric signal amplification system with sensitivity comparable to PCR. The assay was performed as recommended by the manufacturer's instructions which involved sample preparation in 96 well plates, and an ELISA based detection of 16S Ribosomal RNA and signal detection at absorbance 492nm measured on a FLUOstar OPTIMA (BMG Labtech) plate reader. Results were compared to positive control samples that were included in the kit.

## 2.15 Statistical analysis

Data was presented graphically using Excel® (Microsoft) and as the mean of all replicates, with error bars representing ± the standard error of mean. Statistical analysis was performed using Minitab 15 statistical software. Two tailed, paired or unpaired t-tests were used to compare two sample means with levels of significance cited in the text. Comparisons were assumed to be biologically significant where $P<0.05$.

# 3.0 Optimisation of *in vitro* models and experimental techniques to investigate CD40-mediated apoptosis

## 3.1 Background rationale

It has been widely reported that CD40 engagement by CD40 agonists has the potential to regulate tumour cell growth (reviewed by (Tong and Stone, 2003, Eliopoulos and Young, 2004). However, it appears that the 'quality' of the CD40 signal is very important in the functional outcome of carcinoma cell CD40 ligation.

Although a number of studies have shown that soluble CD40 agonists can induce growth inhibition in carcinoma cells of various origins (as reviewed by (Vonderheide, 2007, Tong and Stone, 2003), these agonists are mainly growth inhibitory or weakly pro-apoptotic and only become significantly pro-apoptotic by pharmacological intervention (Hess and Engelmann, 1996, Afford et al., 2001, Ahmed-Choudhury et al., 2003, Bugajska et al., 2002). By contrast, CD40 ligation by cell-surface presented agonists and membrane CD40L (mCD40L) induces extensive apoptosis in carcinoma cells (Georgopoulos et al., 2006, Georgopoulos et al., 2007, Bugajska et al., 2002) whilst sparing their normal epithelial counterparts (Bugajska et al., 2002, Shaw et al., 2005). The necessity to deliver the signal in membrane, rather than soluble form for achievement of maximal pro-apoptotic capacity has also been supported by more recent work by Palmer, Young and colleagues (Elmetwali et al., 2010a, Elmetwali et al., 2010b).

In order to achieve CD40 ligation by membrane ligand (mCD40L) experimentally, target, epithelial cells are co-cultured with third-party cells engineered to express CD40L (detailed in Section 3.1.1). At the beginning of this project, and following the move of the Georgopoulos laboratory to Huddersfield University, a) it was essential to ensure the reproducibility of the co-culture system and b) the work aimed to establish and optimise a series of experimental techniques, for use with this co-culture system, that would permit accurate and reliable detection and quantification of mCD40L-mediated apoptosis based on 96-well plate format assays.

### 3.1.1 Co-culture model for CD40 ligation by mCD40L

For the ligation of CD40 on target cells, a membrane CD40 ligand signal was delivered by their co-culture with pharmacologically growth-arrested effector cells (See section 2.10). The effector cells are murine fibroblasts (NIH3T3) that have been genetically manipulated to express membrane CD40L (Bugajska et al., 2002) (Figure 3-1a). To avoid repetition and for simplicity, effector cells displaying CD40L on their membrane will be termed “mCD40L” cells throughout this study. To ensure that mCD40L cells retained CD40L expression (due to culture-related genetic drift) continuous culture in the presence of G418 antibiotic was performed, as a neomycin resistance gene was co-transfected as part of the CD40L gene expression construct. Homologous NIH3T3 cells with a gene cassette conferring G418 resistance only were used as negative (background) controls (Figure 3-1b) and therefore from this point will be termed “Control” cells throughout this study.

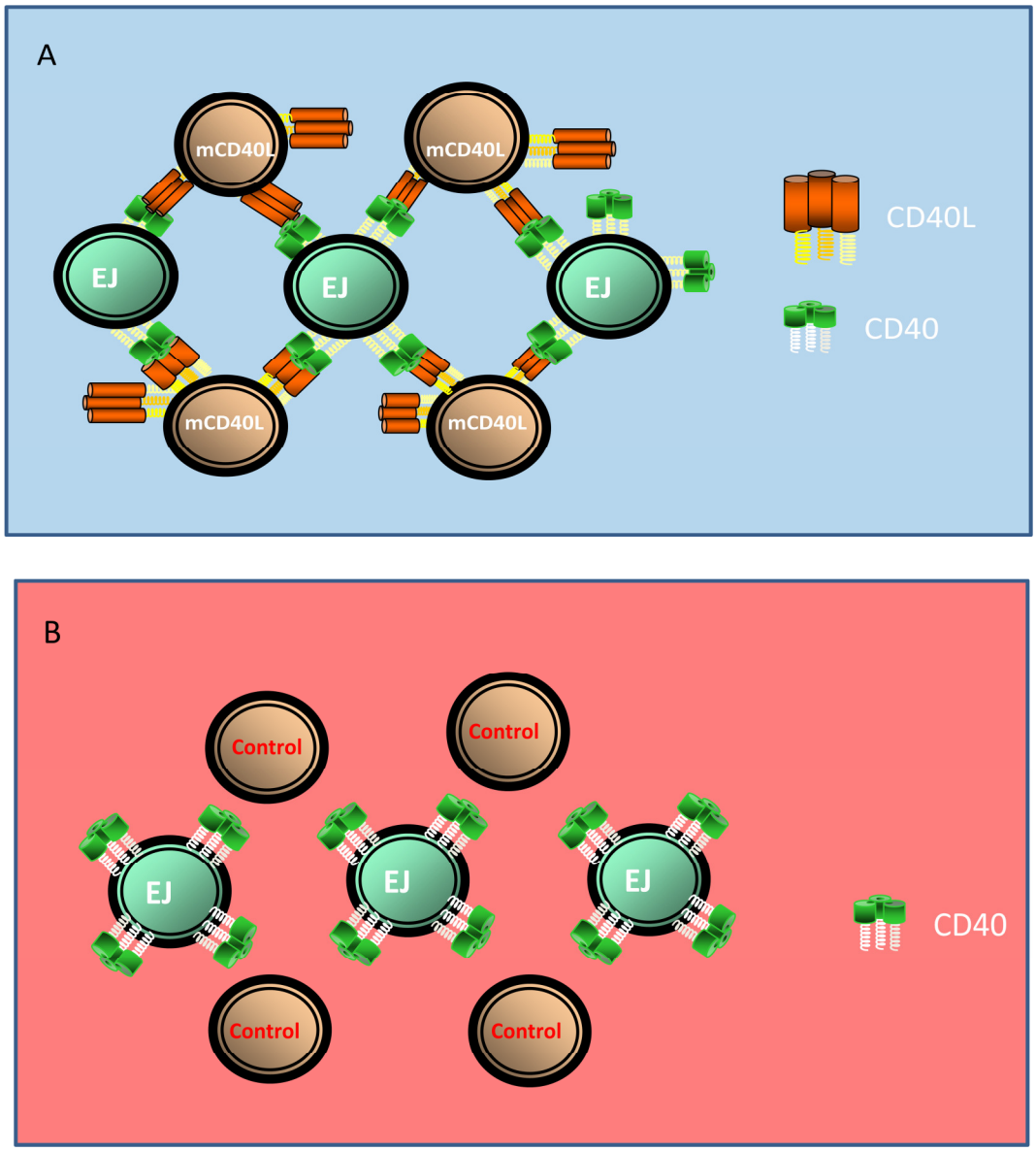


**Figure 3-1 An *in vitro* co-culture system for the delivery of membrane CD40L**

Schematic representation of the co-culture model used to investigate CD40-mediated apoptosis in this study. Target epithelial cells (the UCC line EJ is shown here) were co-cultured with previously growth-arrested, mitomycin C (MMC)-treated effector cells, which resulted in the direct cell-cell contact between effector and target cells. Co-cultures of target (EJ) cells with mCD40L expressing (mCD40L) 3T3 cells (**A**) and negative control (Control) third party cells (**B**) are presented.

## 3.2 Aims

The aims of this chapter were:

- To demonstrate the expression of CD40L in effector cells (mCD40L) and CD40 in the target cell lines employed in this study for use in the co-culture system.

- To establish and optimise a panel of cell death detection, 96-well-plate format-based assays for the *in vitro* detection of CD40-mediated apoptosis.

## 3.3 Results

### 3.3.1 Confirmation of protein expression in effector and target cells

Tumour cells are prone to genetic drift during *in vitro* culture (Kato et al., 1999), therefore the carcinoma cell line (EJ) used for investigation of CD40-mediated apoptosis in the majority of this study was screened by immunoblotting to ensure cells were CD40 positive. HCT116, a colorectal cell line that has endogenous CD40 expression, SW480-CD40 previously transduced with a retrovirus for *de novo* CD40 expression, and the original SW480 (CD40-negative) line (Georgopoulos et al., 2007) were all utilised to verify CD40 expression in EJ cells, as demonstrated in Figure 3-2. The 'bank' of EJ cells that was used throughout this study were routinely screened for CD40 expression and discarded within an appropriate number of passages (<10) in order to reduce the risk of CD40 reduction or loss. In addition to verifying receptor expression on target cells, effector mCD40L cells were also tested by immunoblotting to confirm CD40L expression. Although immunoblotting confirmed total CD40L-expression (Figure 3-3), surface CD40L expression was also confirmed by flow cytometry (not shown) as reported elsewhere (Bugajska et al., 2002).

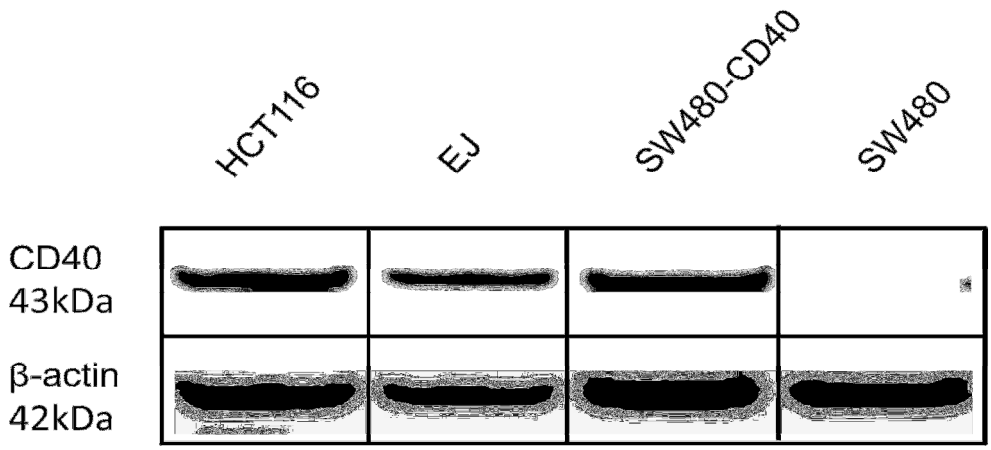


**Figure 3-2 Confirmation of CD40 expression in target cell line EJ**

Carcinoma cells lines were cultured in DR/5%FCS/1%L-G. 20µg of lysates were separated under denaturing conditions by SDS-PAGE using 4-12% (w/v) Bis-Tris gels and then immunoblotted onto a PVDF membrane. The PVDF membrane was probed overnight with an anti-CD40 antibody in TBS Tween 0.1% (1:500 dilution) and then probed with an anti-β-actin antibody in TBS Tween 0.1% (1:20000 dilution). The membrane was then incubated for one hour with goat anti-mouse IgG conjugated with Alexa 680 in TBS Tween 0.1% (1:10,000 dilution). Antibody binding was visualised at 700nm and 800nm using an Odyssey$^{TM}$ Infra-red Imaging system.

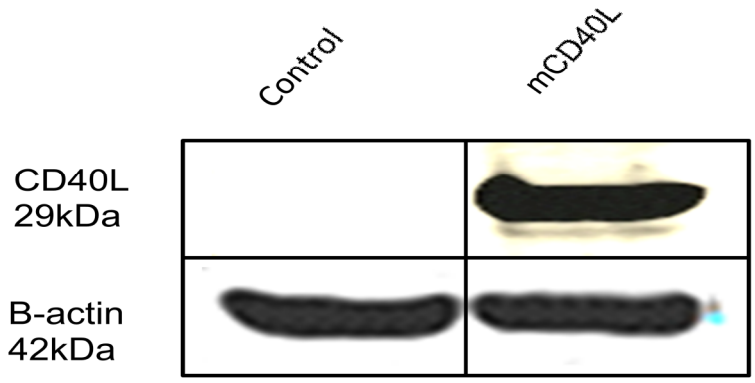


**Figure 3-3 Expression of CD40L in effector cells**

Effector mCD40L and Control cells were cultured in DR/10%FCS/1%L-G supplemented with 0.5µg/ml G418 antibiotic. 20µg of lysates were separated under denaturing conditions by SDS-PAGE using 4-12% (w/v) Bis-Tris gels and then immunoblotted onto a PVDF membrane. The PVDF membrane was probed overnight with an anti-CD40L in TBS Tween 0.1% (1:500 dilution) and then with an anti-β-actin antibody in TBS Tween 0.1% (1:20000 dilution). The membrane was then incubated for one hour with goat anti-mouse IgG Alexa 680 antibody in TBS Tween 0.1% (1:10,000 dilution). Antibody binding was visualised at 700nm and 800nm using an Odyssey$^{TM}$ Infra-red Imaging system.

## 3.3.2 The optimisation of apoptosis assays for detection of CD40-mediated cell death

### 3.3.2.1 Introduction

According to previously published guidelines regarding the use and interpretation of assays for monitoring cell death (Galluzzi et al., 2009), it is recommended that at least two independent assays are utilised for the detection of cell apoptosis.

Previous studies into CD40-mediated apoptosis by our group (Georgopoulos et al., 2007, Bugajska et al., 2002, Georgopoulos et al., 2006, Shaw et al., 2005, Hill et al., 2008a) generally used assays that a) involved use of radioactive precursors (such as the JAM test of DNA fragmentation, b) did not permit high-throughput 96-well plate-based analysis (Annexin V/PI) and were often very laborious, and c) were not very sensitive (thus had a short linear dynamic range). Therefore, one of the aims of this study was to employ assays that would address these issues and weaknesses. The apoptosis assays optimised for the detection of CD40-mediated cell death in this study were mainly the commercially available CytoTox-Glo cytotoxicity assay (Section 2.11.4) and the Sensolyte Homogenouscaspase3/7 assay (Section 2.11.3.1). The process of optimisation of these two assays for use in the co-culture system will be detailed below.

It should also be noted that a further two assays were investigated for their efficacy in this study. These were a) the DNA fragmentation ELISA assay (Roche Cat# 11585045001) (Section 2.11.5) and b) the Caspase-Glo-3/7 substrate assay (Promega Cat# g8091) (Section 2.11.3.2). Although the Caspase-Glo-3/7 gave similar results to the Sensolyte Homogenous Caspase-3/7 assay, it was less cost-effective, whilst the DNA fragmentation ELISA, though reliable, was particularly laborious and less sensitive in comparison to the other assays.

### 3.3.2.2 CytoTox-Glo Cytotoxicity assay for detection of apoptosis

The CytoTox-Glo assay is an advantageous assay as it involves the addition of a single reagent to cell cultures, requires no handling of radioactive substances, it permits high throughput analysis, is very sensitive and has a long dynamic range for functional studies, and results can be quickly generated for analysis only 15-minutes after substrate addition.

In brief this assay utilises a substrate (AAF-Glo) supplied to cells in culture but this substrate can only be cleaved by a specific intracellular protease. This proprietary protease is only capable of binding to its substrate when released from the cells due to membrane permeabilisation during apoptosis. Cleavage of the substrate *in situ* generates a luminescence signal (Figure 3-4) and the intensity of this signal is relative to the number of apoptotic cells in the population (Niles et al., 2007).

A series of initial experiments were performed based on the manufacturer's recommendations to ensure that measurement of death in carcinoma cells in the laboratory was accurate and reliable using recommended instrument specifications (CytoTox-Glo technical bulletin, Promega). The first series of experiments involved measurements of cell death in cultures that contained known numbers of dead cells (cells were treated as recommended by the manufacturer). The aim was to ensure that luminescence measurements (as 'relative luminescence units', or RLU) demonstrated a positive correlation with the number of total dead cell *in situ* and thus the assay was sensitively detecting dead cell numbers (Figure 3-5).

A second series of experiments involved the addition of both live and dead cells in the same cultures measured, in order to determine whether healthy, live cells created background luminescence (RLU). The results showed that live cell populations did not have an impact on overall RLU readings and thus the assay was suitable to discriminate between live and dead cell cultures *in situ* (Figure 3-6).

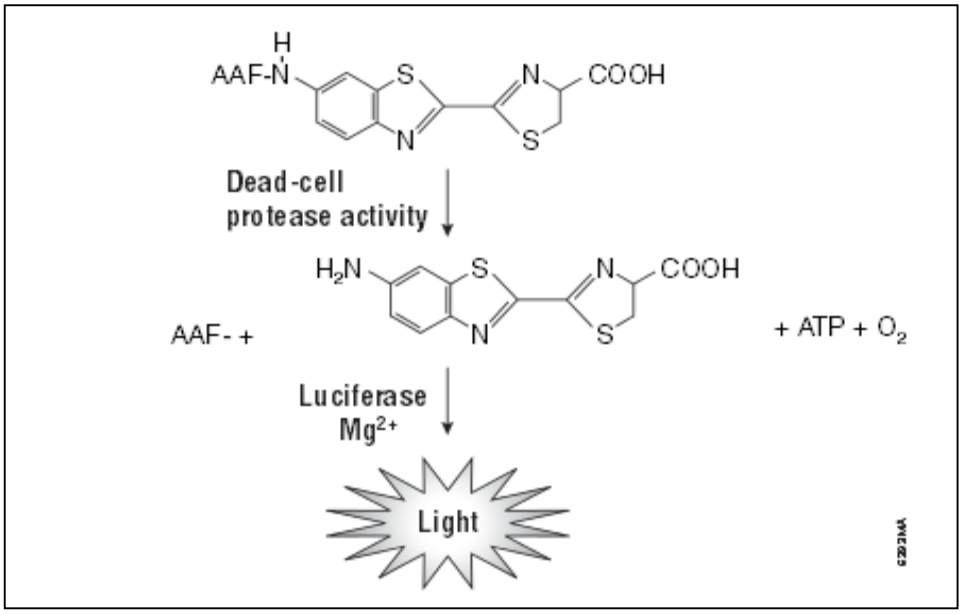


**Figure 3-4 The principle of the CytoTox-Glo™ assay**

The CytoTox-Glo™ assay uses a luminogenic peptide substrate (alanyl-alanyl-phenylalanyl-aminoluciferin; AAF-Glo™ Substrate) to measure “dead-cell protease activity”, which has been released from cells that have lost membrane integrity. The AAF-Glo™ Substrate cannot cross the intact membrane of live cells and does not generate any appreciable signal from the live-cell population. This assay relies on the properties of a proprietary thermostable luciferase (Ultra-Glo™ Recombinant Luciferase), which uses aminoluciferin as a substrate to generate a stable "glow-type" luminescent signal (CytoTox-Glo technical bulletin, Promega).

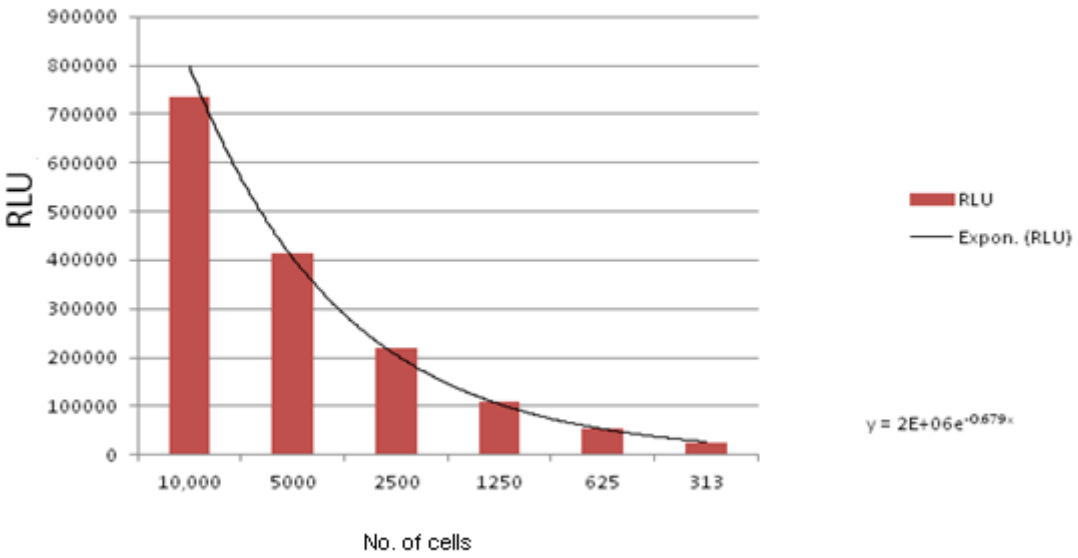


**Figure 3-5 Sensitivity of the CytoTox-Glo assay in detecting apoptosis in cultures with a defined number of dead cells**

EJ cells were seeded at the indicated densities in a 96-well non TC-treated white plate and cells were immediately lysed (using digitonin) whilst suspended in DR5%/FCS/1%L-G. 50µl of CytoTox-Glo assay reagent were added to each well and after 15 minutes luminescence (RLU) was measured (y-axis) reflecting total dead cell numbers (x-axis). Results are representative of single experiments which was repeated three times and each bar represents three technical replicates.

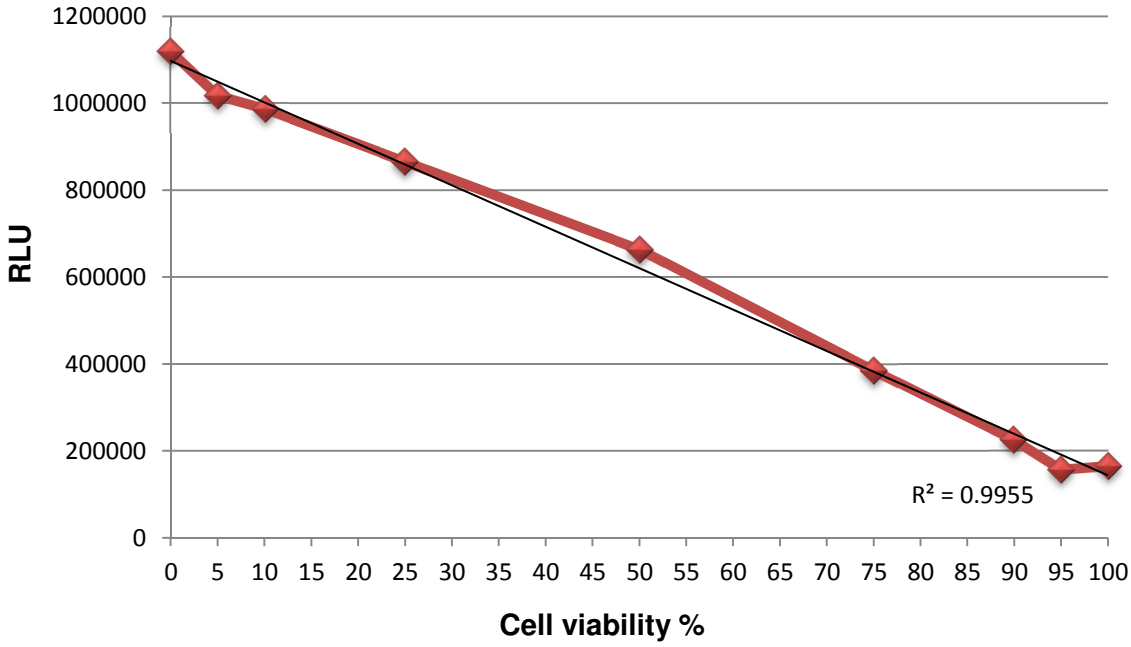


**Figure 3-6 Sensitivity of the CytoTox-Glo assay in detecting apoptosis in cultures with a mixture of defined numbers of live and dead cells**

Viable EJ cells were added in a DR/5%FCS/1%L-G suspension with a specific percentage of sonicated, non-viable cells in a non TC-treated 96 well plate. 50µl of CytoTox-Glo was added to each well and luminescence (RLU) measured reflecting total dead cell numbers. When dead cells and live cells were mixed together the assay could sensitively detect the percentage of dead cells. A correlation coefficient was used to calculate the accuracy of the best fit line ($R^2$ 0.9955). Results are representative of two independent experiments and each datum point represents 2-3 technical replicates.

## 3.3.3 Detection of mCD40L-induced apoptosis using the CytoTox-Glo assay

### 3.3.3.1 Initial assay results

Following initial preliminary experiments described above (Section 3.3.2.2), the CytoTox-Glo assay was tested for its ability to detect CD40-mediated apoptosis using the co-culture system. Co-cultures were carried out and the assay was performed as detailed in Section 2.10.

An important consideration for these experiments was that the CytoTox-Glo assay does not distinguish specifically between dead epithelial cells and effector (mCD40L and Control) cells during co-culture. In order to account for background RLU attributable to mCD40L and Control cells, in addition to experimental replicates that contained co-cultured cell populations, mCD40L and Control cultures alone were included, and their luminescence measured following substrate addition. Therefore, pair-wise subtraction of background readings was performed for each type of co-culture. For instance, as shown in a representative series of experiments in Figure 3-7, the background RLU from the third party cells (e.g. mCD40L - highlighted green, Figure 3-7a) was subtracted from the appropriate co-culture RLU (e.g. mCD40L/EJ - highlighted yellow, Figure 3-7a) giving background corrected RLU (highlighted blue, Figure 3-7b).

However, despite appropriate background correction, it was initially found that there were only minor differences between the RLU generated for co-cultures of mCD40L/EJ and Control/EJ, thus indicating no differences in apoptosis levels between control and mCD40L (Figure 3-8). This was in disagreement with previous findings in our laboratory using different apoptosis detection assays (e.g. Bugajska et al (2002) and Georgopoulos et al (2006) demonstrating that mCD40L/EJ co-cultures should show highly distinguishable levels of apoptosis compared with Control/EJ.

### 3.3.3.2 Further optimisation of CytoTox Glo assay for use in co-culture experiments

Whilst performing further explorative experiments, it became apparent that the CytoTox-Glo assay was extremely sensitive and that background RLU arising from low level spontaneous *in vitro* cell death of target (epithelial) cells was significantly interfering with assay sensitivity. To reduce such 'noise', it was ensured that target cell cultures were harvested only during their log phase of growth. This use of 'healthier' epithelial cells led to significant reductions in background RLU and allowed the cell apoptosis induced by mCD40L to be manifested (not shown).

Another important consideration related to the effector 3T3 cells (mCD40L and Controls). As these cells were treated with Mitomycin C to induce growth arrest, it was essential to ensure that this was efficient and they showed non-mitotic properties whilst remaining metabolically active. (See section 2.10). If this treatment was insufficient, it could result in the continued growth of effector cells and such culture overpopulation, increased levels of spontaneous death and interfered with the assay output. It was found that cell cycle arrest in combination with minimal cell toxicity was best achieved when mCD40L or Control cells were MMC treated during their log phase of growth and at approximately 50% confluency (data not shown, personal communication with Mr Albashir Mohamed). This optimisation meant that third party cells did not contribute too heavily 'Control' culture readings and thus led to a reduction in background 'noise' (not shown).

Collectively, incorporation of these changes and improvements in experimental methodologies, led to a dramatic improvement in the results obtained using this assay, in comparison to earlier findings (Figure 3-8). In fact, as shown in Figure 3-9, these changes allowed the assay to demonstrate a clear difference in luminescence between Control/EJ and mCD40L/EJ co-cultures, as was originally anticipated.

Previous studies investigating mCD40L mediated apoptosis in EJ cells (Georgopoulos et al., 2007, Georgopoulos et al., 2006, Bugajska et al., 2002) utilised, amongst other assays, Annexin V/PI and flow cytometry to demonstrate that maximal CD40-induced apoptosis occurred approximately 72 hours post CD40 ligation. Annexin V/PI is based on the detection of % cell apoptosis relying on the translocation of phosphatidylserine to the cell membrane, whereas CytoTox-Glo

relies on the exposure of substrate to a protease released during the loss of cell membrane integrity (Figure 3-4). Whilst both events (phosphatidylserine translocation and disruption of membrane integrity) are integral to apoptosis, it was important to determine the optimal time-point post CD40 ligation to perform CytoTox-Glo assays and whether perhaps an earlier time point might be more suitable. Results showed that, although differences could be detected 48 hours post-ligation (Figure 3-10), the optimal time point was 72 hours as then more consistent and dramatic differences were detected (Figure 3-11).

Finally, in addition to using the detection of luminescence using CytoTox-Glo as a surrogate marker of apoptosis, the assay may also be used to determine the percentage of apoptosis. When % cell death was calculated (as detailed in Section 2.11.4) it was found that in line with previous results by our group (e.g. (Georgopoulos et al., 2006) mCD40L results in approximately 75-80% cell death, which corresponds to a fold change of ~3-3.5 (Figure 3-12).

**A)**

| | RAW DATA | | | |
|---|---|---|---|---|
| Condition | **mCD40L/EJ** | **Control/EJ** | **mCD40L** | **Control** |
| RLU | 7711608 | 4118502 | 6573117 | 3085032 |
| | 7228411 | 3756440 | 6353735 | 2901318 |
| | 7017394 | 3598824 | 6328537 | 2876697 |
| | 6926750 | 3540456 | 6296610 | 2817687 |
| | 6820916 | 3512474 | 6013070 | 2792366 |
| **Average** | **7141016** | **3621225** | **6313014** | **2829238** |
| **SEM** | **263194** | **210831** | **126539** | **125111** |

**B)**

| | RAW DATA | |
|---|---|---|
| Condition | **mCD40L/EJ** | **NEO/EJ** |
| **RLU** | 1138491 | 1033470 |
| | 874676 | 855122 |
| | 688857 | 722127 |
| | 630140 | 722769 |
| | 807846 | 720108 |
| Average | *828002* | *791987* |
| **SEM** | *142865* | *101540* |

**Figure 3-7 CytoTox-Glo assay raw data before and after background correction**

$8x10^3$ EJ cells were co-cultured with $10^4$ MMC treated mCD40L or Control cells in DR/5%FCS/1%L-G in white 96-well plates as described in the Methods section. CytoTox-Glo substrate was added after 72 hours and luminescence was measured. EJ cell and 3T3 cell (mCD40L and Control) alone cultures were included as controls and for background correction, respectively. Raw data are shown from representative experiments for five technical replicates before (A) and after (B) background correction. Background corrected RLU raw data was generated using the following equations: (mCD40L/EJ RLU – mCD40L RLU) and (Control/EJ RLU – Control RLU).

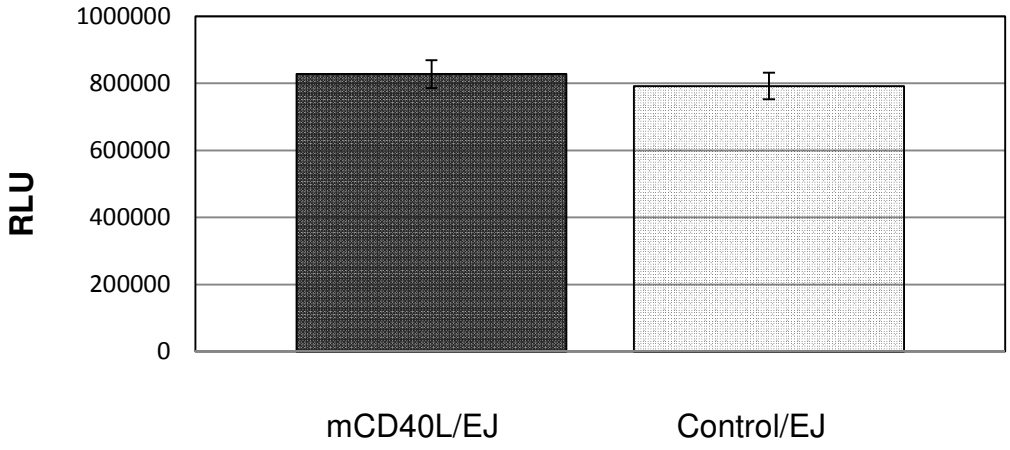


**Figure 3-8 mCD40L mediated apoptosis detection using CytoTox-Glo: before optimisation**

$8x10^3$ EJ were co-cultured with $10^4$ MMC treated mCD40L or Controls in DR/5%FCS/1%L-G in white 96-well plates. CytoTox-Glo substrate was added after 72 hours, luminescence was measured and background-corrected RLU deduced as described in Figure 3-7. Bars correspond to mean values of 5-6 technical replicates ± SEM.

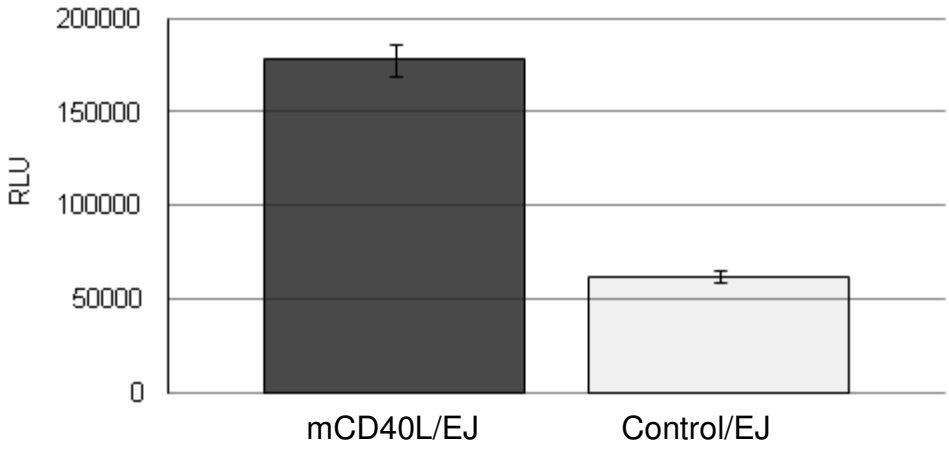


**Figure 3-9 mCD40L mediated apoptosis detection using CytoTox-Glo: after optimisation**

$8x10^3$ EJ were co-cultured with $10^4$ MMC treated mCD40L or Controls in DR/5%FCS/1%L-G in white 96-well plates. CytoTox-Glo substrate was added after 72 hours, luminescence was measured and background-corrected RLU readings deduced as described in Figure 3-7. Bars correspond to mean values of 5-6 technical replicates ± SEM.

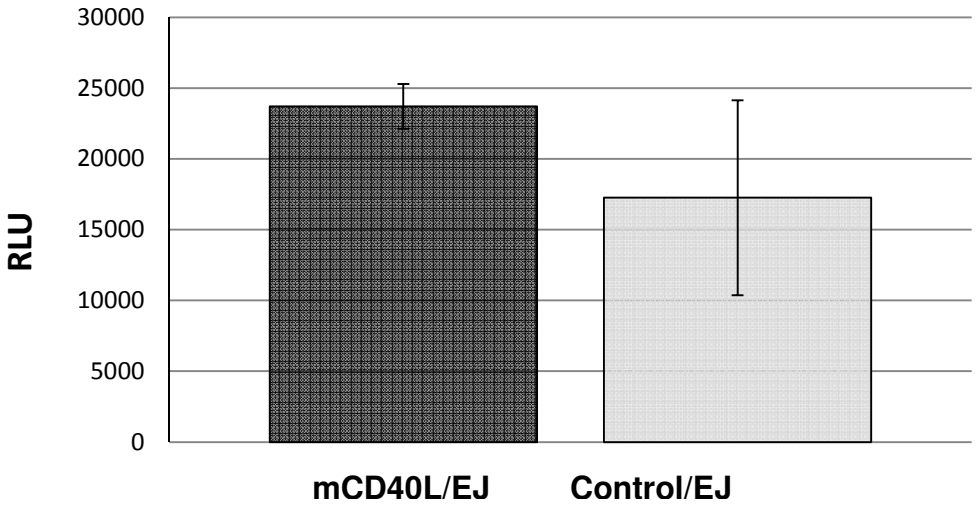


**Figure 3-10 mCD40L mediated apoptosis detection using CytoTox-Glo after 48 hours**

$8x10^3$ EJ were co-cultured with $10^4$ MMC treated mCD40L or Controls in DR/5%FCS/1%L-G in white 96-well plates. CytoTox-Glo substrate was added after 48 hours, luminescence was measured and background-corrected RLU readings deduced as described in Figure 3-7. Bars correspond to mean values of 5-6 technical replicates ± SEM.

**A)**

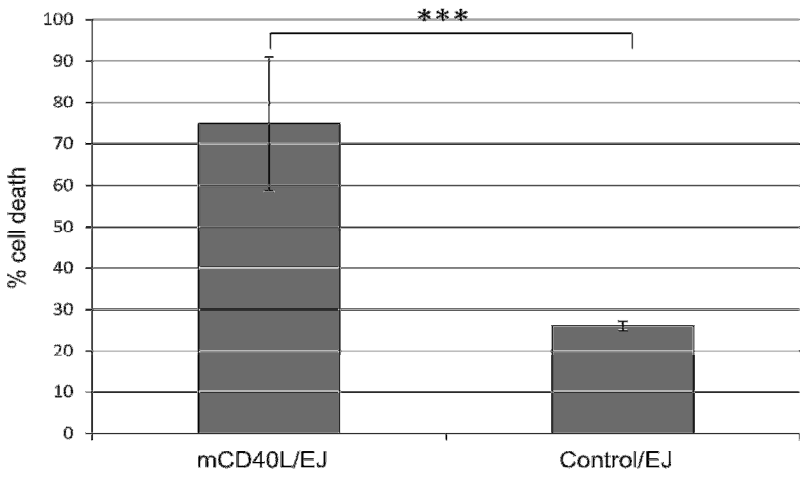


**B)**

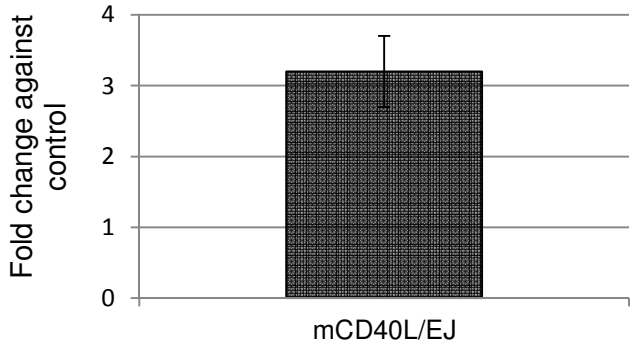


**Figure 3-11 Fully-optimised detection of CD40-mediated apoptosis after 72 hour co-cultures using the CytoTox-Glo assay**

$8x10^3$ EJ were co-cultured with $10^4$ MMC treated mCD40L or Controls in DR/5%FCS/1%L-G in white 96-well plates. CytoTox-Glo substrate was added after 72 hours, luminescence was measured and background-corrected RLU readings deduced as described in Figure 3-7.

**A)** Results are plotted as '% cell death' (calculated as detailed in Section 2.11.4), where each bar corresponds to the mean of 5-6 technical replicates. Error bars represent ±SEM. and *** denotes $p<0.01$.

**B)** Results are also presented as fold change (from raw RLU data used in A) by comparing mCD40L/EJ *versus* Control/EJ co-cultures (bar represents mean fold change ± SEM).

## 3.3.4 The principle of the SensoLytecaspase3/7 assay

### 3.3.4.1 Assay principle

The activation of caspase-3/7 is central to the execution phase of apoptosis and involves caspase-3/7-mediated cleavage of target intracellular proteins at the amino acid recognition sequence Asp-Glu-Val-Asp (DEVD) as described in detail in 2.11.3.1 the SensoLyte Homogenouscaspase3/7 substrate (Ac-DEVD-AMC) utilises the cleavage recognition sequence ofcaspase3/7 for the *in vitro* detection of active Caspases-3/7. Upon caspase-mediated cleavage, Ac-DEVD-AMC generates the AMC fluorophore which emits bright blue fluorescence upon excitation at the appropriate wavelength. The fluorescence signal emitted is proportional to caspase-3/7 activity after *in situ* lysis (Figure 3-12).

### 3.3.4.2 Detection of cell death using the SensoLytecaspase3/7 assay

For preliminary optimisation of thecaspasedetection assay, staurosporine was used as a positive control. Staurosporine is a DMSO soluble compound derived from *Streptomyces Staurosporeus* that inhibits a range of protein kinases essential for normal cell function. Staurosporine is often used as a positive control to induce apoptosis by the intrinsic pathway via MOMP and caspase-3/7 activation, as previously described by ourselves (Chopra et al., 2009) and others (Zhang et al., 2004b). As shown in EJ cells treated with staurosporine, the compound caused the activation of caspase-3/7 activity in a dose-dependent manner (Figure 3-13).

By utilising the experimental experience gained whilst establishing the CytoTox-Glo assay (Section 3.3.3), which involved a) appropriate calculations for background, 3T3 cell-related readings and b) the optimisation of target cell health and effector cell MMC treatment (Section 3.3.3.1 & 3.3.3.2), the equally sensitive Sensolyte assay was used for the detection of mCD40L mediated cell apoptosis. Detection of caspase-3/7 activity was measured at 48 hours post ligation, which was based on previous work in our laboratory for the detection of mCD40L-mediated induction of caspase-3/7 activity. Georgopoulos et al (2006) had previously shown using FAM

FLICA caspase detection assays and flow cytometry that Caspase-3 becomes active within 48 hours post CD40 ligation, which also coincided with the detection of DNA fragmentation (Georgopoulos et al., 2006), a direct downstream consequence of caspase activation during apoptosis.

Using the SensoLytecaspase3/7 assay, high degrees ofcaspase3/7 activation could be readily and sensitively detected in mCD40L/EJ co-cultures compared with Control/EJ ones, equating to a change of approximately 4-5 fold (Figure 3-14). Of note, when 24 and 72 hour time points were assessed, only little difference in caspase activation could be detected at these time points (data not shown). Not only this, a pancaspase inhibitor Z-VAD was used to confirm that CD40-mediated apoptosis is caspase dependant (not shown) as also reported by others (Georgopoulos et al., 2006).

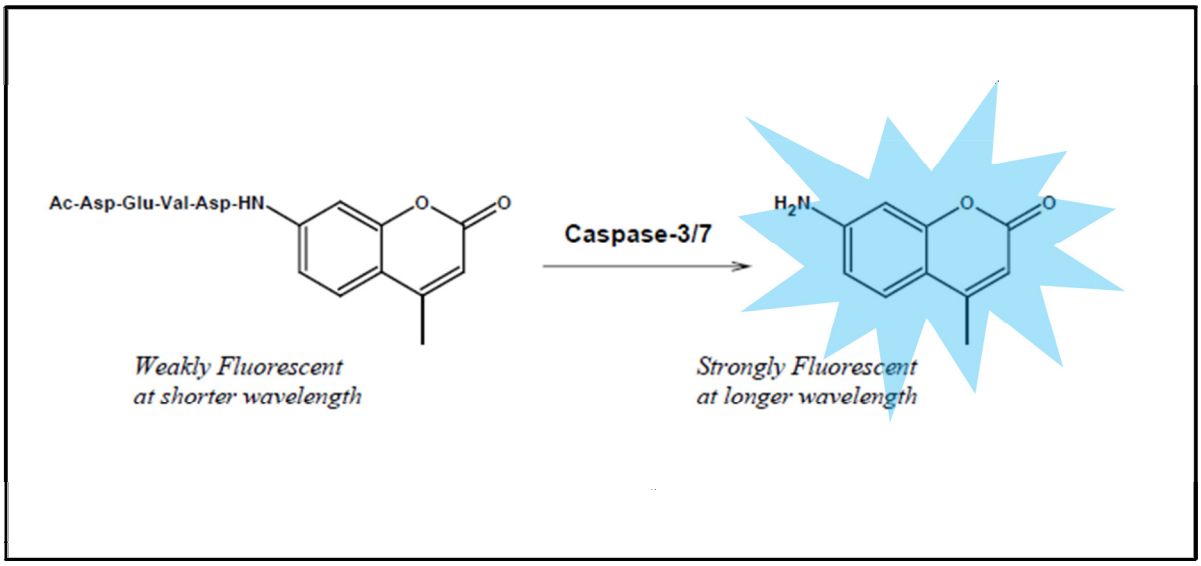


**Figure 3-12 The principle of the SensoLytecaspase3/7 assay**

Both caspases -3 and -7 have sequence specificity for the amino acid sequence Asp-Glu-Val-Asp (DEVD). Before caspase cleavage the substrate Ac-DEVD-AMC is a weakly fluorescent molecule. Caspases-3/7 recognises the sequence DEVD and cleaves it generating a bright blue fluorescent AMC fluorophore that is detectable at excitation 354nm and emission 442nm. Cells are lysed *in situ* by a lysis buffer mixed with the substrate releasing the internal enzymes from the cell.

Adapted from: http://www.anaspec.com/servePdf.asp?f=71118.pdf&t=datasheet

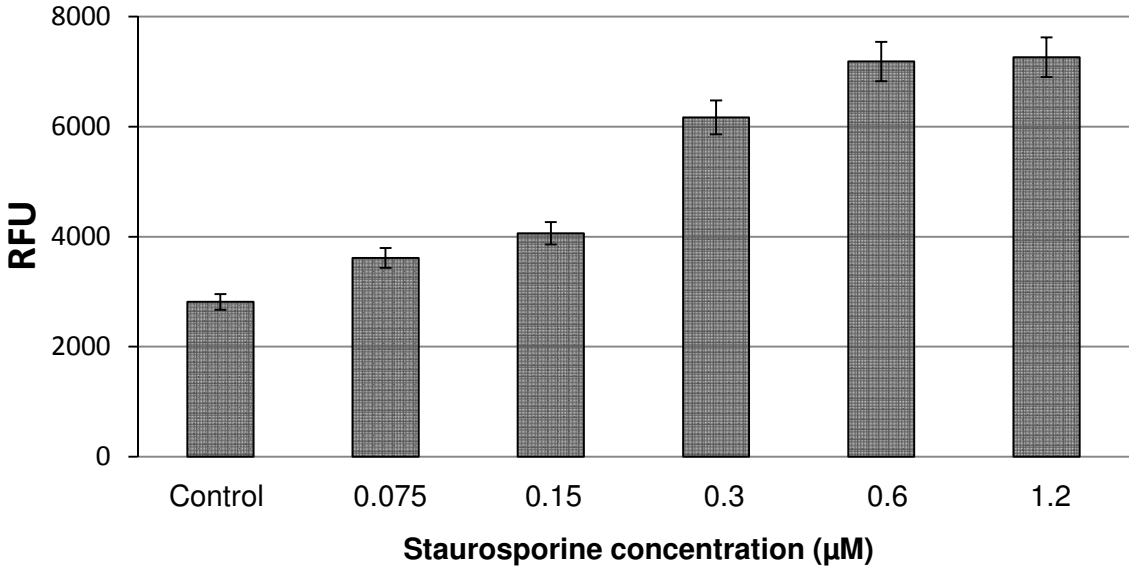


**Figure 3-13 caspase-3/7 activation by staurosporine treatment**

EJ were seeded at a density of $8x10^3$ cells per well in DR/5%FCS/1%L-G in white 96 well plates and subject to a range of staurosporine concentrations for 24 hours. Caspase-3/7 substrate was added after 24 hours and Relative Fluorescent Units (RFU) readings were assessed reflecting total levels of caspase-3/7 activation. Bars represent mean RFU values for 3-4 technical replicates ± SEM.

**A)**

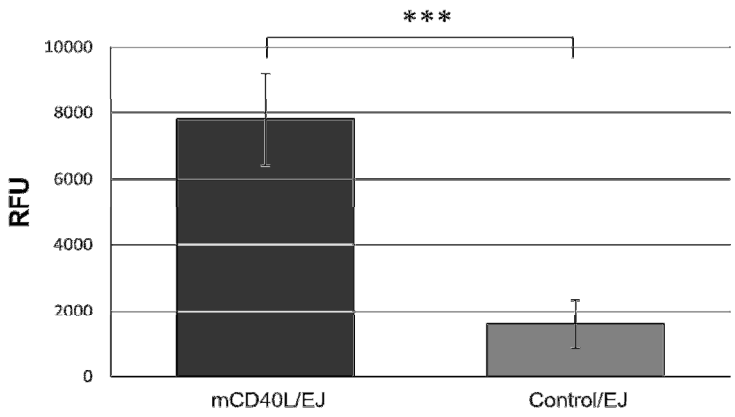


**B)**

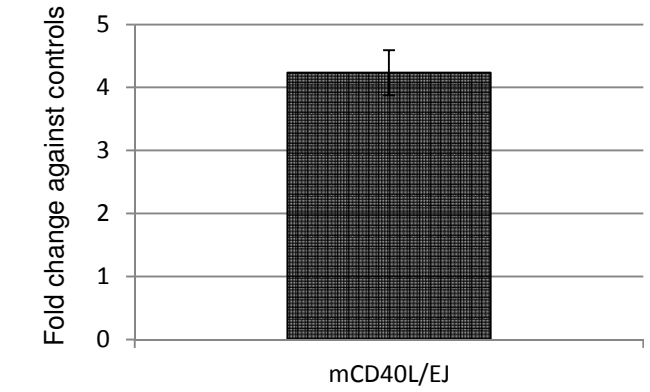


.

**Figure 3-14 Fully-optimised detection of CD40-induced caspase-3/7 activation after 48 hour co-cultures using the SensoLyte assay**

$8x10^3$ EJ were co-cultured with $10^4$ MMC treated mCD40L or Controls in DR/5%FCS/1%L-G in white 96-well plates. SensoLyte Caspase-3/7 reagent was added after 48 hours, fluorescence measured (as detailed in Section 2.11.3.1) and background-corrected RFU readings deduced by pair-wise subtraction of mCD40L and Control cell RFU from mCD40L/EJ and Control/EJ RFU readings. Bars (panel **A**) correspond to mean, background corrected RFU values for 5-6 technical replicates (error bars represent ± SEM). Results are also presented as 'fold change' (**B**) from raw RFU data (used in panel A) by comparing mCD40L/EJ *versus* Control/EJ co-cultures (bar represents mean fold change ± SEM). Stats: *** P<0.001, paired student t-test, mCD40L/EJ vs control/EJ.

## 3.4 Summary

The aim of this chapter was to confirm the fidelity of the co-culture system for the activation of CD40 in carcinoma cells *in vitro* and to establish a number of cell death and caspase-detection assays as biological readouts for mCD40L-mediated apoptosis detection.

In line with previous findings (Bugajska et al., 2002, Georgopoulos et al., 2006, Elmetwali et al., 2010b) the UCC line EJ was positive for CD40 expression by immunoblotting (a finding that was also confirmed by flow cytometry – not shown). As the cell line is well characterised in terms of its response to CD40 ligation, EJ will be used in subsequent chapters to systematically investigate the involvement of key intracellular signalling mediators of mCD40L-mediated apoptosis to improve our understanding of the mechanisms underlying carcinoma cell CD40-killing. Immunoblotting also confirmed that 3T3 CD40L/mCD40L cells expressed an abundant amount of CD40L (membrane localisation confirmed by flow cytometry – not shown). To ensure complete consistency during this work, the same 'banks' of both effector and target cells were used throughout in co-culture experiments.

Following a series of optimisation experiments detailed in previous sections, two main assays were established for the detection of CD40-mediated death using our *in vitro* co-culture system for mCD40L delivery. Following optimisation, the current study confirmed that mCD40L represents a molecule of high apoptotic potential in carcinoma cells (Bugajska et al., 2002, Georgopoulos et al., 2006, Elmetwali et al., 2010b). The two assays of choice were consistent, sensitive, reliable, cost effective, easy to perform and high throughput. The final feature was important as the main aim of the work was to identify key pro-apoptotic mediators and assess their involvement in CD40-killing by pharmacological or RNA interference-mediated inactivation; thus it was essential to establish assays that could allow a high number of conditions and treatments to be simultaneously and cost-effectively assessed.

In particular, the CytoTox-Glo assay was used both as a surrogate (luminescence based) marker for induction of cell death and could also be used to quantify % cell death in a way comparable to DNA fragmentation. It was based on indirectly quantifying death due to cell membrane integrity compromisation. Although

not measuring single cells to identify exact percentage of apoptotic/necrotic cells as would be possible with Annexin-V/PI assays, the assay detected maximal levels of death at the same time point (72 hours post ligation) as Annexin-V/PI assays routinely do (Bugajska et al., 2002), and was even more sensitive, cost effective and high throughput.

Finally, the Sensolyte Homogenous caspase-3/7 assay permitted detection of effector caspase activity as a biological readout of CD40-mediated apoptosis. An interesting observation made during optimisation of this assay was that no caspase activity was detected at 24 or 72 hours and maximal activation was observed at 48 hours, thus indicating that there was a specific time window within which caspase-3/7 activation takes place. Most importantly, the assay was equally sensitive and had all the useful features of CytoTox-Glo yet provided the ability to measure a different and independent feature of apoptosis, which is important to ensure accuracyaccording to published recommendations on the importance of utilising multiple assays when detecting apoptosis *in vitro* (Galluzzi et al., 2009).

Throughout this study the aforementioned assays were utilised to investigate the functional role of key downstream effectors involved in mCD40L-mediated apoptosis.

# 4.0 Investigation of the activation and functional involvement of key intracellular mediators of the CD40-mediated apoptosis signalling pathway

# 4.1 Tumour necrosis factor receptor associated factors (TRAFs)

## 4.1.1 General

TRAFs were first discovered for their ability to associate with the Tumour necrosis factor receptor 2 (TNF-RII) and were appropriately named Tumour necrosis factor Receptor Associated Factors (TRAFs). Functioning in association with CD40 the TRAFs relay signals controlling events such as apoptosis, cell survival, stress responses and inflammation with six TRAF proteins currently identified and well characterised (Bishop et al., 2007). TRAF molecules share a common feature which is a stretch of amino acids at their carboxyl terminus to allow TNFR binding and homo- or heterodimerisation, and a coiled configuration at the amino-terminal. The homologies shared between TRAFs 1-6 are shown in Figure 4-1.

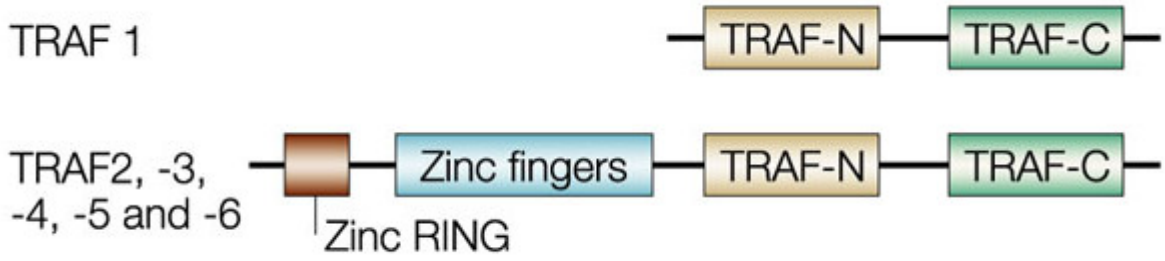


**Figure 4-1 The structure of TRAFs 1-6**

With the exemption of TRAF1, TRAFs 2-6 contain zinc finger domains necessary for DNA binding and protein interaction. Figure adopted from (Bishop, 2004).

The TRAFs associate with a number of TNFR superfamily of receptors, including CD40, where they bind in distinct regions post receptor ligation as illustrated in Figure 4-2.

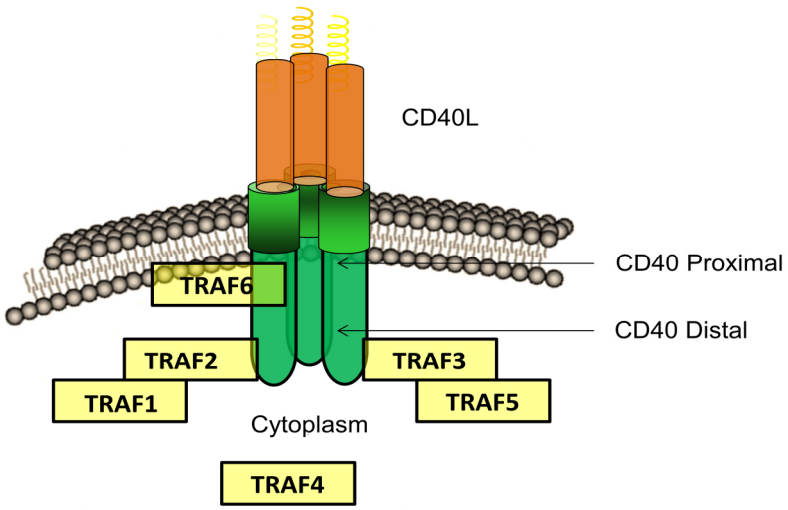


**Figure 4-2 The CD40 binding regions of the TRAF proteins**

The CD40 membrane proximal segment is used for TRAF6 association, and the receptor distal for the association of TRAF2 and 3. TRAF5 is indirectly bound to CD40 at distal region through the action of TRAF3, whereas TRAF2 recruits TRAF1 forming heterodimers. Diagram drawn based on information from (Pullen et al., 1998).

## 4.1.2 CD40-TRAF functions

TRAF3 was the first TRAF discovered through its capability to bind to mouse and human CD40, which subsequently sparked further interest in these molecules and lead to the discovery of TRAF -1, -2, -5 and -6 which are also involved in CD40 binding and signalling (Hu et al., 1999, Cheng et al., 1995, Hostager et al., 2000). The roles of CD40-TRAF interactions are highly context specific, and to add to this complexity it has been shown, using molecular studies that CD40 may alter its conformation depending on which TRAF occupies its cytoplasmic domain (Ni et al., 2000). For example, TRAF3 can outcompete TRAF2 for receptor occupancy during CD40 activation, whereas TRAF1 upregulation causes degradation of TRAF -2 and -

3. TRAF -1 and -2 are generally accepted to co-operate and relay CD40-mediated NF-κB signals (Xie et al., 2006). CD40-TRAF2 interactions may preferentially activate NF-κB and JNK, conversely TRAF2 is reported to be essential to induce CD40-mediated cell apoptosis through its interactions with RIP1 (Knox et al., 2011). There is limited information about CD40-TRAF5 interaction but studies *in vivo* suggest that it may be functional during B-cell adhesion, proliferation and co-stimulation (Nakano et al., 1999). TRAF6 is important for pro-survival JNK-signalling (Rowland et al., 2007), whereas others have reported that it may be necessary for CD40-induced apoptosis (Jundi et al., 2012, Eliopoulos et al., 2000a). Furthermore, in contradiction, other reports suggest its suppression is required in this for CD40-induced apoptosis (Elmetwali et al., 2010b). Despite the multifaceted nature of the TRAFs, there are more consistent reports on the role of TRAF3 in a CD40-mediated carcinoma cell apoptosis, particularly in UCC, and therefore, a more detailed focus on TRAF3 and its downstream effects will follow.

### 4.1.3 TRAF3-CD40 functions

Generally in epithelial cells TRAF3 relays growth inhibitory signals (Eliopoulos et al., 1996b) via downstream MAPK signalling (Baud and Karin, 2001, Ha and Lee, 2004) and as with other TNF members, emerging evidence suggests this is mediated by the production of ROS (Morgan and Liu, 2010, Kamata et al., 2005). The expression of a dominant negative TRAF3 blunts ROS production in response to sCD40L suggesting TRAF3 is a designated ROS inducer (Ha and Lee, 2004). TNF-α generates ROS through an interaction with the Nox-2 sub-unit p47phox (Dewas et al., 2003) and a previous report has provided evidence that TRAF3 may generate ROS via its interaction with Nox subunit p40phox, therefore implying ROS are a common mechanism for signal transduction (Ha and Lee, 2004). Independent of TRAF3, CD40 may also generate ROS via 5-lipooxygenase (Ha et al., 2011). The stabilisation of TRAF3 is essential for mCD40L-induced carcinoma cell apoptosis (Georgopoulos et al., 2006, Elmetwali et al., 2010b), however whether this is Nox and ROS dependent, as also reported in lymphotoxin mediated cell death (Chen et al., 2003), remains to be explored. In concert with other TRAFs, CD40-TRAF3 co-operations utilise MAPK signalling cascades to induce a range of cellular responses

(Xie, 2013, Bishop et al., 2007). The CD40-TRAF interaction and involvement of downstream MAPK signal transduction pathways is context specific, with a number of MAPK implicated in various CD40-mediated responses as discussed in section 4.2.

## 4.2 The three tiers of the MAPK signalling pathways

### 4.2.1 General

MAPKs are integral to eukaryotic cells for their co-ordinated and integrated responses to external stimuli such as hormones, growth factors, cytokines, G-coupled protein receptors, pathogen associated molecular patterns (PAMPs) and environmental stresses. The three tiers of MAPK signalling cascades are mitogen activated protein kinase kinase kinases (MAPKKKs), mitogen activated protein kinase kinases (MAPKKs) and mitogen activated protein kinases (MAPKs) (Kyriakis and Avruch, 2012). The MAPK signalling pathways implicated to TNFR are hugely extensive, thus only the signalling events linked to CD40 engagement, where applicable, are considered in this thesis.

### 4.2.2 MAPKKKs

#### 4.2.2.1 MEKs

MAPKKKs represent a diverse group of signalling molecules that activate downstream MAPKKs and include MEKK1-4, MLKs, TAK1, TAO, Tpl-1 plus ASK -1 and -2 (Kyriakis and Avruch, 2012). MEKK1 can activate MAPKKs MKK -4, -7 and MAPKs p38 and JNK during CD40 T-cell signalling (Matsuzawa et al., 2008). MEKK2 and -3 can activate MKK-3,-6 and MEK1/2 and MEKK4 can vary in their capacities to activate MKK4, MKK3 or MKK6 – the aforementioned interactions are summarised in Figure 4-3. There is no evidence that MEKK -2,-3 or -4 are relevant mediators of CD40 physiology.

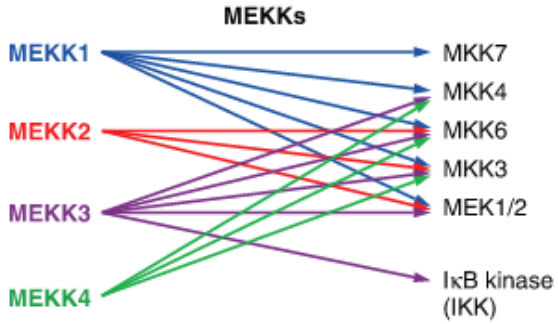


**Figure 4-3 The regulation of MAPKKs by MEKK1-4**

For an explanation of the activation interactions see text – section 4.2.2. Figure adopted from from (Kyriakis and Avruch, 2012).

### 4.2.2.2 Other MAPKKKs

MLKs can activate MKK-3,-4,-6 and -7 and in context of CD40 have been shown to regulate HIV-1 encephalitis neuroinflammation (Ramirez et al., 2010). TAK1 can activate MKK3, MKK6 and IKK (Kyriakis and Avruch, 2012) and in the context of CD40 activate JNK, IL-6 production (Arcipowski and Bishop, 2012) and B-cell proliferation also via JNK signalling (Sato et al., 2005). Thousand-and-one (TAO) kinases are reported to activate MKK3 and p38 (Kyriakis and Avruch., 2012), however no studies have been performed with regards to CD40 signalling. Tpl-2 can activate MEK1/2 and has been shown as essential for CD40-mediated ERK activation (Eliopoulos et al., 2002). ASK-1 and -2 can activate MKK-3,-4 and -6 but ASK2 is only expressed in skin and gut epithelium (Kyriakis and Avruch, 2012).

ASK1 has been the most prominently studied MAPKKK due to its regulation of apoptosis and interest has mounted in its biological inhibitor Thioredoxin (Trx). ASK1-Trx interaction is also known as the 'ASK1 signalosome' that acts as a redox switch responding to oxidative stress. ASK1 is further biologically inhibited by 14-3-3 protein and phosphatases PP5 and PP2A, which in concert with Trx are also released during oxidative stress (Goldman et al., 2004). The dissociation of Trx, 14-3-3, PP5 and PP2A during oxidative stress causes ASK1 oligomerization via an N-terminal coiled-coil domain, the recruitment of TRAF2 and -6 and ASK1

autophosphorylation (Soga et al., 2012). The over-expression of Trx prevents TNF-α mediated apoptosis (Zhang et al., 2004a) as does the over expression of Gluthathione S-transferase (GST), a redox protein also implicated as a biological inhibitor of ASK1 (Cho et al., 2001). Some studies report that TRAF2 and TRAF6 are essential for ASK1 activation in response to TNF-α (Hoeflich et al., 1999), however others have reported that TRAF3 is essential in Lymphotoxin-β mediated ASK1 activation (Chen et al., 2003). ASK1 regulates apoptosis via downstream MAPKKs MKK4/MKK7 and/or MKK3/MKK6 which further play a role in the regulation of JNK and p38 (Tobiume et al., 2001, Kim et al., 2005, Nishitoh et al., 1998). In light of the suggestion that CD40 engagement can generate ROS (Ha et al., 2004; Ha et al 2011) and that JNK is essential in CD40-mediated apoptosis (Georgopoulos et al., 2006; Elmetwali et al 2010) there is a strong possibility that ASK1 may regulate cell fate in this context, however this remains unexplored. A summary of MAPKK activation by remaining MAPKKKs is shown in Figure 1-14.

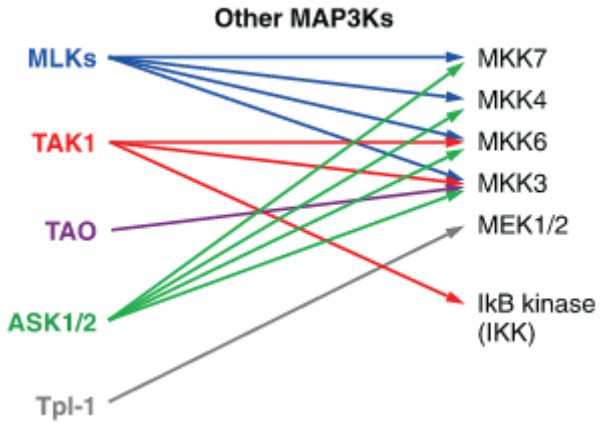


**Figure 4-4 The regulation of MAPKKs by other MAPKKKs (MAP3Ks)**

The diagram shows the activation interactions that are known to exist between MAPKKK (MAP3K) and MAPKK (MAP2Ks). Figure adopted from (Kyriakis and Avruch, 2012).

### 4.2.3 MAPKKs

MAPKKs operate through a signalling cascade that can involve a vast number of previously mentioned MAPKKKs (Symons et al., 2006, Kyriakis and Avruch, 2001) and include MKK-3, -4 and -6 -7, and MEK1/2. MKK3 preferentially activates p38 -α and -β, whereas MKK6 can equally activate all p38 isoforms. Neither MKK-3 or -6 are known to activate extracellular signal-regulated kinases (ERK) or JNK (Kyriakis and Avruch, 2012). CD40-mediated MKK3/6 and p38 activation have been shown to be important for IL-6 and IL-10 monocyte secretion during inflammation (Inoue et al., 2004). MEK1/2 specifically activates ERK (Kyriakis and Avruch, 2012) which has been shown as important for CD40-induced monocyte secretion of TNF-α and IL-1β (Suttles et al., 1999) and germinal centre formation by follicular dendritic cells (Park et al., 1999). MKK-4 and -7 activate JNK in response to external stimuli, however MKK4 additionally activates p38 (Kim et al., 2005, Haeusgen et al., 2011). MAPKKs typically involved in cell stress signalling are MKK -3, -4, -6 and -7 and murine MKK -4 and -7 genetic knockout models have shown that these are essential for normal liver development, effective immunity and the prevention of cancer (Haeusgen et al., 2011, Wang et al., 2007). No studies have yet confirmed a link between CD40-mediated MKK -4 or -7 JNK or p38 activation, despite reports of activation of JNK during CD40-mediated apoptosis (Georgopoulos et al., 2006, Elmetwali et al., 2010b). ASK1 regulates MKK4 activity by direct phosphorylation that in turn phosphorylates and activates either/or of the (SAPKs) JNK and p38 (Kim et al., 2005, Ichijo et al., 1997, Matsuura et al., 2002). There is no evidence to show that ASK1 acts directly on MKK7 and it is suggested that other proteins are needed to facilitate this process (Matsuura et al., 2002). MAPKKs are biologically inhibited by a family of dual-specificity MAPK phosphatises (DS-MKPs) (Camps et al., 2000, Farooq and Zhou, 2004) with a number of reports suggesting that these are directly affected by the redox status of the cell. In the presence of high ROS certain DSK-MPs may be inactivated (Torres and Forman, 2003). MKK4 is activated by ASK1 during oxidative stress but no data on MKK7 is available to date in this context (Liu et al., 2006). Although the activation of MAPKs by MAPKKs varies the general consensus is that MKK-4 and -7 activate JNK (Fleming et al., 2000), whereas MKK-3 and -6 activate p38 (Raingeaud et al., 1996) as illustrated in Figure 4-5.

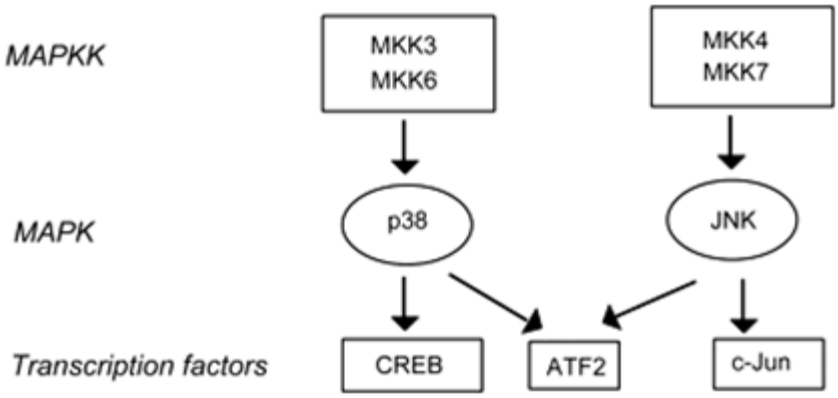


**4-5 JNK is commonly activated by MKK -4 & -7 and p38 by MKK -3 & -6**

JNK and p38 are part of the MAPK family of proteins. MAPK activity is controlled by MAPKKs and their activity by MAPKKKs. All members of the MAPK family are involved in a variety of cellular processes including migration, proliferation, differentiation, apoptosis and metabolism. Most report the phosphorylation of JNK in response to MKK4 or MKK7 activation with subsequent activation of c-Jun or ATF2 (Dhanasekaran and Johnson, 2007). p38 is activated by MKK3 and MKK6 and leads to activation of transcription factors CREB or ATF2. Figure adopted from (Wagner and Nebreda, 2009).

## 4.2.4 MAPKs

### 4.2.4.1 ERK and p38

The MAPKs include ERK, p38 and JNK all of which are activated by environmental stresses and inflammatory mediators. As previously mentioned ERK is regulated by MEK-1 and -2, with ERK activation occurring in response to Ras signalling, cytokines, PAMPS and low density lipoproteins (LDLs) (Kyriakis and Avruch, 2012). There are limited reports on the role of CD40 in ERK modulation, although it has been suggested that its activation occurs as a result of CD40-TRAF6 binding or via Ras signalling. The significance of this has not been investigated however, it was proposed that this pathway induces mitogenic signals (Kashiwada et al., 1998). The p38 MAPKs are activated by external stress and pro-inflammatory stimuli and consist of p38 –α, -β, -γ, and -δ (Wagner and Nebreda, 2009). The discovery of p38 came as an active mammalian phosphorylated kinase in response to osmotic and endotoxin cell stress, thus p38 is termed a stress activated protein kinase (SAPK) (Han et al., 1994). In some B-cell lines CD40 engagement can phosphorylate JNK, ERK1/2 and p38 depending on the degree of receptor ligation and this is important in the regulation of germinal centres (Batlle et al., 2009). CD40-p38 signalling is also used to stimulate IL-12 production dictating the action of macrophages against pathogens (Mathur et al., 2004). In addition to JNK, p38 is also activated in response to ROS in B-cells via a CD40-TRAF3 mediated mechanism (Ha and Lee, 2004).

### JNK 4.2.4.2

JNK is also a SAPK and was first discovered on H-Ras transfected oncogenic rat fibroblasts, UV-irradiated cervical carcinoma and TPA-treated T-cells when a kinase that phosphorylated the c-Jun transcription component was under investigation (Hibi et al., 1993). There are three JNK isoforms namely JNK -1, -2 and -3 and each is divided into α and β with all having similar substrate specificity (Kyriakis and Avruch, 2012). Many roles involved in homeostatic balance have been linked to JNK including diabetes, cardiac disease/function, liver function and the nervous system (Haeusgen et al., 2011). In line with p38, JNK also regulates a huge variety of cellular processes including proliferation, migration, apoptosis, cell survival

and metabolism (Dhanasekaran and Johnson, 2007). JNK may be activated by phosphorylation from active MKK4 and MKK7 via a conserved activation loop of the kinase domain and this leads to the phosphorylation of c-Jun, JunD and ATF2 components of the activator protein-1 complex (AP-1) (Dhanasekaran and Johnson, 2007). The constitutive activation of JNK is required for apoptosis, whereas transient levels drive a survival response (Lei et al., 2002, Kamata et al., 2005). High degrees of ROS induced by $H_20_2$ or UV radiation increase JNK activity (Tobiume et al., 2001) and some have reported JNK may co-operate in a feedback loop involving mitochondrial cell death (Chambers and LoGrasso, 2011). There are multiple reports linking the activation/phosphorylation of JNK with cellular stress and the proceeding events of apoptosis in normal and cancer cells (Bhogal et al., 2012, Kim et al., 2005, Liu et al., 2006), however due to the range of cell lines used and different functional experiments gaining a consensus remains difficult. CD40 also functions in synergy with other receptors (BCR and TLR7) to activate JNK, leading to the secretion of IL-6, which is important for humoral B-cell responses (Bush and Bishop, 2008). Recent reports have highlighted the significance of JNK in CD40-induced carcinoma apoptosis without any requirement for p38 or ERK activation (Eliopoulos et al., 2000a, Georgopoulos et al., 2006, Elmetwali et al., 2010b), therefore indicating that p38 or ERK are not important in this context. JNK activation has been suggested to induce apoptosis via the regulation of pro-apoptotic bcl-2 members during the intrinsic (mitochondrial) pathway of cell death (Georgopoulos et al., 2006). In the presence of ROS/oxidative stress, JNK phosphorylation causes activation of c-Jun which is part of the AP-1 transcriptional component (Biswas et al., 2006), therefore the two are closely interlinked and will often be referred to as JNK/AP-1 in this thesis.

## 4.3 Transcription factor AP-1

### 4.3.1 General

Activator protein-1 (AP1) is a mixture of dimers composed from members of the Jun family, basic leucine zippers associated with Fos or ATF family. The AP-1 complex recognises a DNA response element 5'-TGAG/CTCA known as the TPA responsive element (TRE) named due to its strong induction by the tumour promoter 12-O-tetradecanoylphorbol-13-acetate (TPA) (Eferl and Wagner, 2003). Mouse genetic knockout studies have provided some insight into the differential roles of each AP-1 dimer in development and cancer; however this has shed little light on its importance in immune regulation (Jochum et al., 2001).

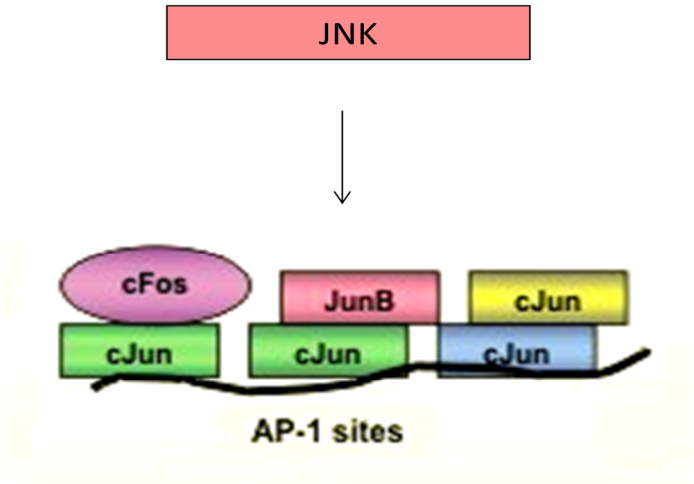


**Figure 4-6 The formation of AP-1 heterodimers in transcriptional activation**

The phosphorylation/activation of JNK leads to the activation of c-Jun or Jun-b transcription components which form heterodimers sometimes with c-Fos to become active transcription factors. Figure adopted from (Wagner and Nebreda, 2009).

### 4.3.2 Functions in apoptosis

It is well established that activation of JNK leads to an increase in AP-1 related component activity (Hibi et al., 1993, Liu et al., 2006, Kim et al., 2005, Elsby et al., 2003) and mitogens and genotoxic agents are commonly linked to AP-1 signalling through the prior activation of JNKs and downstream Jun and Fos (Ameyar et al., 2003, Hess et al., 2004), thus the focus here will remain on such related proteins. AP-1 transcriptionally regulates human breast adenocarcinoma vascular endothelial growth factor (VEGF) secretion in response to TNF-α and this facilitates the formation of tumours (Yin et al., 2009). AP-1 in erythroid cells can generate proliferative or apoptotic signals and this depends on the presence of c-Jun or jun-B proteins (Jacobs-Helber et al., 1998). In co-operation with TLR7 CD40 causes the increased level of active AP-1 components c-Jun and c-Fos in resting B-cells of mouse and human origin (Bush and Bishop, 2008). In human hepatocytes CD40 also causes an increase amount of AP-1 components c-Jun and Fos and this leads to apoptosis (Ahmed-Choudhury et al., 2003, Afford et al., 2001), however intrahepatic endothelial cells (IHEC) respond with an increase proliferation likely due to the overriding action of NF-κB (Ahmed-Choudhury et al., 2003).

As AP-1 is a transcription factor it can regulate the transcription of many other genes. Some have reported that after JNK activation AP-1 is used to regulate the activity of the pro-apoptotic protein Bax or Bak (Fan and Chambers, 2001, Lei et al., 2002). A study using human colon cancer cells has also shown, using a reporter construct utilising a Bax promoter region next to the luciferase gene, that AP-1 could be directly responsible for the transcriptional regulation of Bax (Mandal et al., 2001). A differential regulation may occur in leukaemia cell models as low levels of AP-1 activity drive increased activity of Myc and p53 which leads to an increased expression Bax followed by apoptosis (Park et al., 2004). In line with other proteins that are linked to MAPK signalling family, the role of AP-1 is dependent upon the composition of its dimers, the cell model explored and mode of activation, and it is suggested that understanding AP-1 components involved in cancer may offer a therapeutic avenue (Bitton-Worms et al., 2010). In UCC lines membrane-presented CD40L activates AP-1 and this is essential for apoptosis (Georgopoulos et al., 2006) however it remains to be investigated whether this modulates downstream regulation of pro-apoptotic Bcl-2 members.

## 4.4 Overall study rationale for CD40-mediated signal transduction pathway investigation

The signalling mechanisms that underlie mCD40L-CD40-mediated apoptosis in carcinoma cells are not yet fully resolved. Upon its agonistic engagement, the cytoplasmic domain of CD40 has the potential to bind TRAFs (as described above). TRAFs 1, 3 and 6, bind CD40 directly, TRAF2 via TRAF1, TRAF5 via TRAF3 with TRAF4 found only in the cytoplasm. Depending on the cell context the TRAFs orchestrate a diverse range of cell responses such as proliferation, differentiation or apoptosis (Bishop, 2004). It has been previously demonstrated in UCC lines that CD40 interaction with mCD40L, specifically elevates the expression of TRAF1, TRAF2 and TRAF3. The transient abrogation (via transient siRNA-mediated knockdown) of TRAF1 or TRAF2 has minor effects on the induction of apoptosis by mCD40L, conversely TRAF3 plays an essential role in this context (Georgopoulos et al., 2006). Others have also confirmed a pro-apoptotic role for TRAF3 in UCC lines but also suggested that it facilitates apoptosis by outcompeting TRAF6 for CD40 attachment and attenuating TRAF6-mediated survival signals (Elmetwali et al., 2010b). These results are in agreement with the original findings on the role of TRAF3 in relaying growth inhibitory, pro-apoptotic signals in a range of epithelial and carcinoma cell lines (Eliopoulos et al., 1996b), overall strongly suggesting that in some carcinomas TRAF3 may positively regulate cell death and recent findings in our laboratory have suggested an important role for TRAF3 in CD40-mediated colorectal carcinoma cell death (Mohamed and Georgopoulos, unpublished). By contrast, the importance of TRAF6 in regulation of UCC cell death is less clear, leaving the exact role for TRAF6 in CD40-mediated cell death yet to be fully established.

TRAF-mediated cell death is regulated by a group of MAPK signalling molecules namely MEKK1, p38, ERK and JNK (Grammer and Lipsky, 2001). MAPK signalling pathways are characterised by three tiers of control and share common features in their activation. As described above, MAPKKK are activated by phosphorylation at Ser/Thr residues in response to external stimuli, such as UV light and cytokines. MAPKKK activation leads to direct phosphorylation of MAPKKs and in turn these dual phosphorylate MAPKs to transcriptionally regulate cell responses (Cargnello and Roux, 2011). TRAF3 indirectly causes activation of MAPK JNK

(Dadgostar and Cheng, 2000), which generally displays a multifaceted nature regarding cell survival and apoptosis (Kennedy and Davis, 2003). Previous work by the Georgopoulos group (2006) provided evidence that JNK is essential for mCD40L induced cell death in UCC lines, which was supported more recently by Palmer and Young and colleagues (Elmetwali et al., 2010b). It was also demonstrated that CD40-induced apoptosis is regulated by AP-1 (Georgopoulos et al., 2006), with the AP-1 transcription factor being the main downstream target of JNK. JNK is often reported to be regulated by the MAPKKs MKK4 and/or MKK7 and this occurs in response to external stimuli which activate their relative upstream MAPKKK mediator (Lawler et al., 1998, Cargnello and Roux, 2011). ASK1 regulates lymphotoxin-mediated apoptosis (Chen et al., 2003) and in light of the structural homology shared between the lymphotoxin receptor and CD40 (neither has a death domain and both signal through TRAFs), there is a strong possibility that a CD40-ASK1 mechanism may also be involved in CD40-mediated apoptosis. There is therefore a requirement to identify the CD40-related machinery that forms the intracellular signalling axis leading to MAPKKK activation and downstream MAPKK regulation of JNK/AP-1 by intracellular mediators such as ASK1, MKK4 and MKK7.

It has been suggested that TRAF3-JNK signals may induce the expression of the pro-apoptotic Bcl-2 related members Bak and Bax (Georgopoulos et al., 2006) which, may in turn, promote MOMP during CD40-mediated apoptosis (Dhanasekaran and Reddy, 2008) and activate caspase-9 (Georgopoulos et al., 2006). A number of studies have provided direct evidence for association between JNK and intrinsic/mitochondrial cell death mediated by pro-apoptotic Bcl-2 members (Dhanasekaran and Reddy, 2008, Lei and Davis, 2003) but none have been in context of CD40-induced cell death. The association of TRAF3 and/or JNK in regulation of Bak/Bax therefore remains to be confirmed. Although elegantly performed and important in understanding apoptosis, the vast majority of the studies previously reported on the role of MKKs and JNK in induction of apoptosis by a variety of stress signals have almost exclusively involved over-expression of these intracellular mediators. However, it is essential to understand the role of these pro-apoptotic factors in a more ‘natural’ system based on their endogenous, non-engineered expression, which was a main aim of this work.

Based on our co-culture system to induce CD40-mCD40L engagement, the optimised apoptosis assays described in the previous chapter, stable RNAi by retrovirus-mediated shRNA over-expression and pharmacological inhibition of target molecules, this work aimed to a) provide a systematic investigation of the activation and precise functional role of key intracellular mediators of CD40-induced mediated cell death in UCC cell lines and b) identify novel signalling molecules that regulate the JNK-MAPK pathway to enhance our understanding of both CD40-mediated death and apoptosis in general.

## 4.5 Aims

The specific aims of this chapter were:

- To optimise immunoblotting techniques for accurate and sensitive detection of endogenous proteins linked to CD40-mediated apoptosis.

- To carry out retrovirus-mediated transduction of UCC lines and optimise the selection of carcinoma cells expressing virally-transduced shRNAs for RNAi-mediated protein knockdown.

- To use RNAi, immunoblotting and cell death assays to determine whether TRAF3 regulates a) JNK phosphorylation b) Bak and Bax expression c) CD40-mediated apoptosis.

- To use pharmalogical inhibitors to determine whether JNK/AP-1 regulates a) Bak and Bax expression and b) CD40-mediated apoptosis.

- To investigate for the first time whether MKK4 and/or MKK7 regulate a) JNK phosphorylation and b) CD40-mediated apoptosis, using RNAi, immunoblotting and cell death assays.

- To use RNAi, immunoblotting and cell death assays to determine for the first time whether ASK1 is activated following CD40 ligation and if, following activation, it regulates a) JNK phosphorylation and b) CD40-mediated apoptosis.

- To investigate the role of the intrinsic pathway of cell death via a) RNAi-mediated knockdown of Bak and Bax, immunoblotting and cell death assays, and b) changes in mitochondrial membrane permeability by cell fractionation.

## 4.6 Results

### 4.6.1 Optimisation of experimental methodologies for the detection of activation and functional inactivation of intracellular CD40-signalling pathway mediators

#### 4.6.1.1 Refinement of immunoblotting techniques for correct epithelial lysate loading and sensitive protein detection in co-cultures

The use of the co-culture system for the activation of CD40 in UCC cells poses some experimental constraints, not only in cell death detection assays (see optimisation experiments in Chapter 3), but also for immunoblotting purposes. An important consideration is that cell lysates obtained from co-cultures contain both effector cell (fibroblast) and target cell (epithelial) proteins (see section 2.11.2). Classical loading controls, such as the house-keeping proteins β-actin and GAPDH, are naturally present and detectable in both the aforementioned cell types, however expression of proteins such as cytokeratins are exclusive to epithelial cells (Moll et al., 1982). Thus expression of Cytokeratin-18 (CK18) has been previously used as a loading control for immunoblotting of co-culture derived lysates containing both epithelial and fibroblastic proteins (Bugajska et al., 2002, Georgopoulos et al., 2006).

Certain anti-CK18 antibody clones, such as the Zym5.2 (Invitrogen cat# 081213) were not epitope sensitive enough to detect CK18 in the target UCC cell line EJ, despite its detection in the well-differentiated UCC line RT4 and the colorectal carcinoma cell line HCT116 (Figure 4-7). An explanation for this is that EJ down regulate CK18 during their malignant progression as demonstrated in some breast carcinomas (Woelfle et al., 2004) and specifically for UCC lines including EJ (Moll et al., 1988). To overcome this problem, a laborious process of testing a number of commercially available CK18 antibodies was performed and an antibody clone was eventually identified that could efficiently detect EJ-CK18 expression. This clone, CY-90 (Sigma cat# C8541), was able to detect EJ-CK18 in protein lysates at concentrations as low as 10μg/ml and also confirmed that CK18 is epithelial lysate-

specific (Figure 4-8). The CY-90 anti-CK18 antibody was used throughout this study to demonstrate equal epithelial lysate loading obtained from co-cultures (i.e.mCD40L/EJ and Control/EJ).

### 4.6.1.2 Immunoblotting methodology: optimisation for intracellular signalling mediator detection

In the model UCC line EJ, which is used in the majority of this study, CD40 ligation causes a significant TRAF3 induction (Georgopoulos et al., 2006, Elmetwali et al., 2010b). Thus, the time-dependent detection of TRAF3 up-regulation was used to optimise immunoblotting-mediated, sensitive detection of CD40 signalling-related endogenous proteins. Preliminary experiments employed for TRAF3 detection showed weak sensitivity, thus a number of optimisation steps were followed including a) use of improved PVDF transfer membranes with better protein binding affinity and lower levels of auto-fluorescence, b) modifications in blocking buffer concentration during primary antibody incubation and dilution optimisation, c) testing different and selecting optimal primary polyclonal antibody batches and d) other practical considerations, such as transfer membrane exhaustion by stripping. As a result of these modifications, TRAF3 detection showed dramatically improved sensitivity, as is evident in representative results from experiments before and after optimisations shown in Figure 4-9. These improved immunoblotting procedures were applied for the detection of other intracellular signalling mediators in this chapter.

### 4.6.1.3 The selection of shRNA-expressing carcinoma cells

Short-hairpin RNAs (shRNAs) are a form of RNA interference (RNAi) and represent a tool for the expression of small interfering RNAs (siRNAs) in cells to specifically knockdown proteins of interest (Rao et al., 2009). A panel of retroviral shRNA expression vectors were prepared (Section 2.9.1) for the stable knockdown of proteins of interest for functional studies, including TRAF3 (below). Replication-incompetent retroviral particles were used to transduce the target UCC cell line EJ (as explained in section 2.8.4). For selection of stable shRNA EJ expressers,

puromycin antibiotic selection was used, as the viral expression cassette comprises a puromycin resistance gene (section 2.9.2).

The CellTiter 96® $AQ_{ueous}$ One Solution Cell Proliferation assay (section 2.11.2) was used to perform pre-titration experiments to determine adequately cytotoxic concentrations of puromycin for selection of antibiotic-resistant cell populations, following all viral transductions. This proliferation assay involves the use of MTS tetrazolium (yellow) which is reduced to a formazan derivative (brown) by respiring cells. The increased absorbance at 492nm occurs due to the colour change induced by viable cells as they produce electron coupling reagents such as NADH that reduce a formazan substrate (yellow-brown) (Figure 4-10). Following the combination of results from such pre-titration experiments (Figure 4-11) and routine phase contrast microscopic examination during antibiotic treatment, it was found that a concentration of 0.5µg/ml effectively perished non-transfected EJ, whilst allowing the continued proliferation of their virally-transduced counterparts. Figure 4-12 shows representative results for experiments involving EJ transduction with a retrovirus expressing TRAF3 shRNA (to be discussed in detail in subsequent sections). This methodology was used for the work described throughout this chapter to select cell populations with successful retroviral transduction.

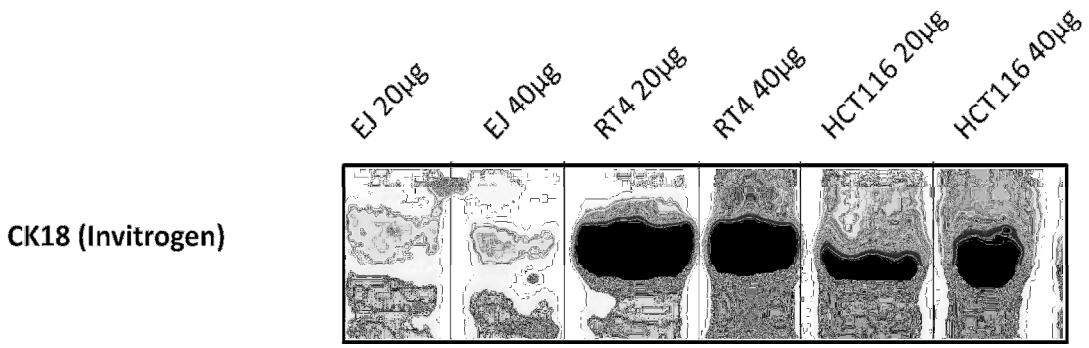


**Figure 4-7 Detection of CK18 expression in EJ cells using the Zym5.2 antibody**

Carcinoma cells lines were cultured to confluency in DR/5%FCS/1%L-G. 20 and 40µg of cell lysate (shown as 20µg and 40µg, respectively) were separated under denaturing conditions by SDS-PAGE using 4-12% (w/v) Bis-Tris gels and then immunoblotted onto a Immobilon-FL$^{TM}$ polyvinylidine difluoride membrane (PVDF membrane). The PVDF membrane was probed overnight with an anti-Cytokeratin-18 (CK18) antibody Invitrogen (Cat#081213) (1:2000). The membrane was then incubated for one hour with goat anti-mouse IgG conjugated with Alexa 680 in TBS Tween 0.1% (1:10,000 dilution). Antibody binding was visualised at 700nm and 800nm using an Odyssey$^{TM}$ Infra-red Imaging system.

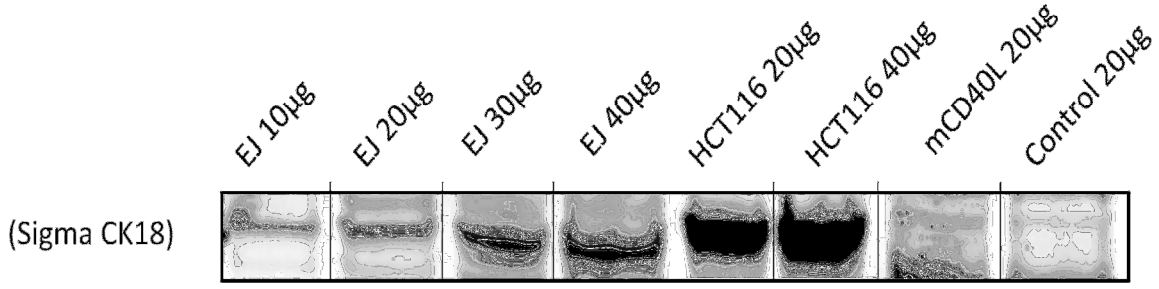


**Figure 4-8 Antibody clone CY-90 efficiently detects CK18 expression in carcinoma cells and shows epithelial lysate specificity**

Carcinoma cells lines (EJ & HCT116) were cultured to confluency in DR/5%FCS/1%L-G and 3T3 lines 3T3-Neo (Control) and 3T3-CD40L (mCD40L) were cultured to confluency in DR/10%FCS/1%L-G supplemented with G418 (0.5 µg/ml). 20 and 40µg of whole cell lysates were separated under denaturing conditions by SDS-PAGE using 4-12% (w/v) Bis-Tris gels and then immunoblotted onto a PVDF membrane. The PVDF membrane was probed overnight with an anti-CK18 antibody (Sigma Cat# C8541) (1:2000). The membrane was then incubated for one hour with goat anti-mouse IgG conjugated with Alexa 680 in TBS Tween 0.1% (1:10,000 dilution). Antibody binding was visualised at 700nm and 800nm using an Odyssey™ Infra-red Imaging system.

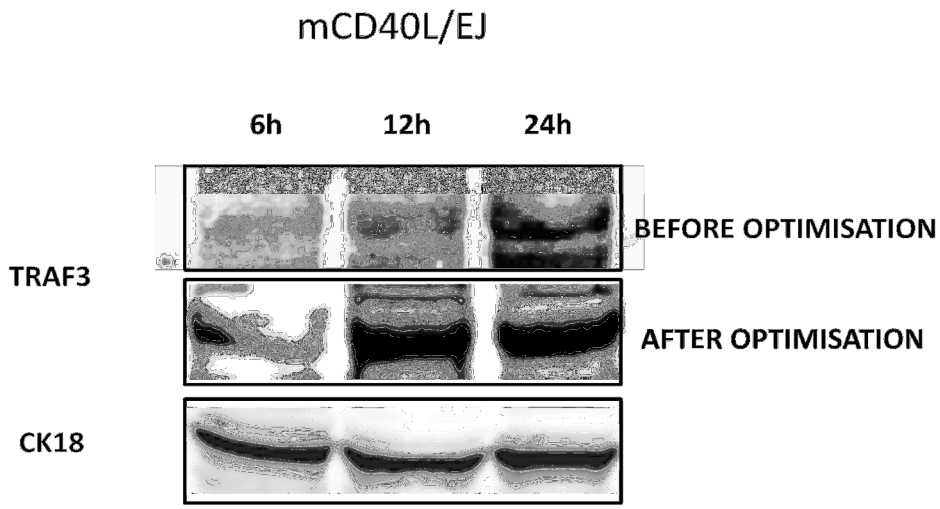


**Figure 4-9 Detection of mCD40L-mediated TRAF3 induction before and after immunoblotting optimisation**

$2.7x10^6$ EJ were co-cultured with $3x10^6$ MMC treated mCD40L or Controls in DR/5%FCS/1%L-G in $10cm^2$ culture dishes for 6, 12 and 24 hours prior to lyses with 2X SDS-lysis buffer. 20µg of lysates were separated under denaturing conditions by SDS-PAGE using 4-12% (w/v) Bis-Tris gels and then immunoblotted onto a PVDF membrane. The PVDF membrane was probed overnight with an anti-TRAF3 antibody in TBS Tween 0.1% (1:500 dilution) and then for an anti-CK18 antibody in TBS Tween 0.1% (1:2000 dilution). The membrane was incubated for one hour with goat anti-mouse IgG IRDye 800 (1:10,000 dilution) for the detection of TRAF3 and with goat anti-rabbit IgG Alexa 680 (1:10,000 dilution) for the detection of CK18. Antibody binding was visualised at 700nm and 800nm using an Odyssey™ Infra-red Imaging system.

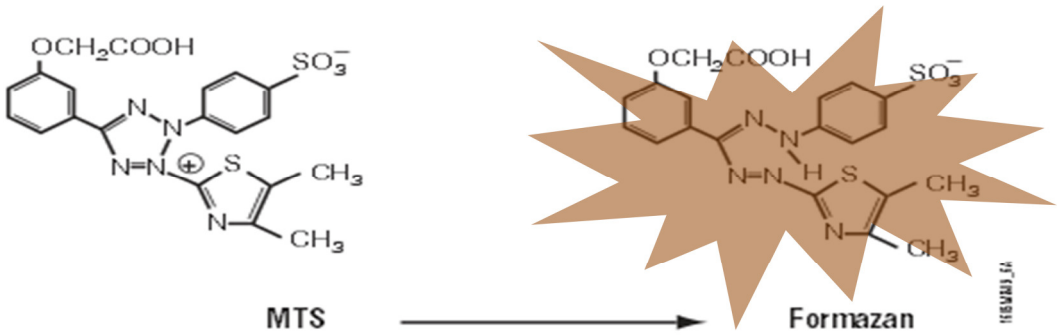


**Figure 4-10 The principle of the CellTiter 96® $AQ_{ueous}$ One Solution Cell Proliferation assay**

The CellTiter 96® $AQ_{ueous}$ One Solution Cell Proliferation assay is based on the notion that only viable cells have the ability to bioreduce the MTS tetrazolium compound into a coloured (brown) formazan product which is soluble in culture medium. The increased absorbance at 492nm is directly proportional to the number of viable cells as they produce electron coupling reagents such as NADH during respiration. Image adapted from

http://www.promega.co.uk/~/media/Files/Resources/Protocols/Technical%20Bulletins/0/CellTiter%2096%20AQueous%20One%20Solution%20Cell%20Proliferation%20Assay%20System%20Protocol.pdf

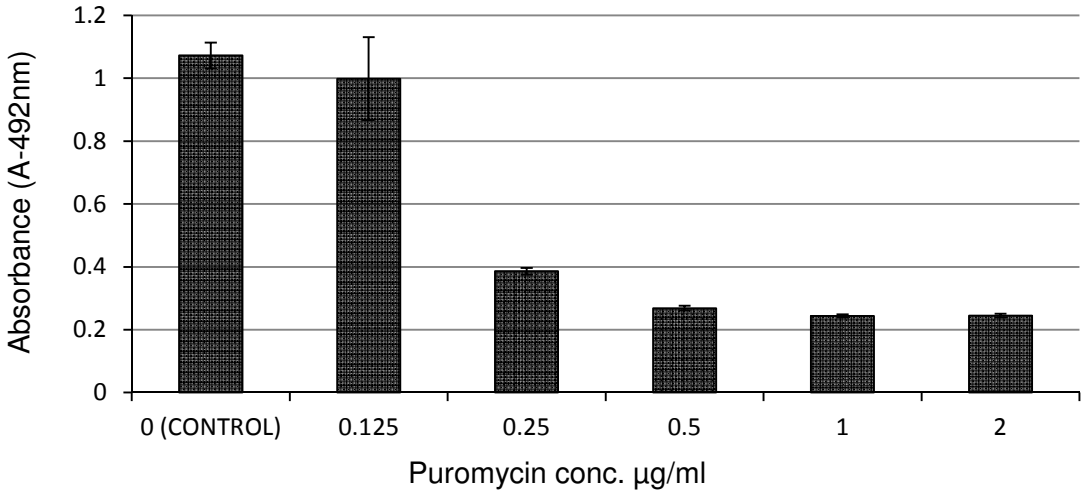


**Figure 4-11 EJ cell proliferation following treatment with a range of puromycin concentrations ('kill curve')**

$8x10^3$ EJ cells were seeded in in a transparent TC treated 96 well microplate and then treated with the indicated concentrations of puromycin antibiotic in DR/5%FCS/1%L-G for 48 hours. 20µl of CellTiter 96® $AQ_{ueous}$ One Solution was added to appropriate wells and plates were incubated at 37℃ in 5% $CO_2$ for a total of four hours. To assess cell viability, total levels of Formazan formation were measured using a FLUOstar OPTIMA (BMG Labtech) plate reader at a wavelength of 492nm. Bars correspond to mean absorbance values of 5-6 technical replicates ± SEM and results are representative of three independent experiments.

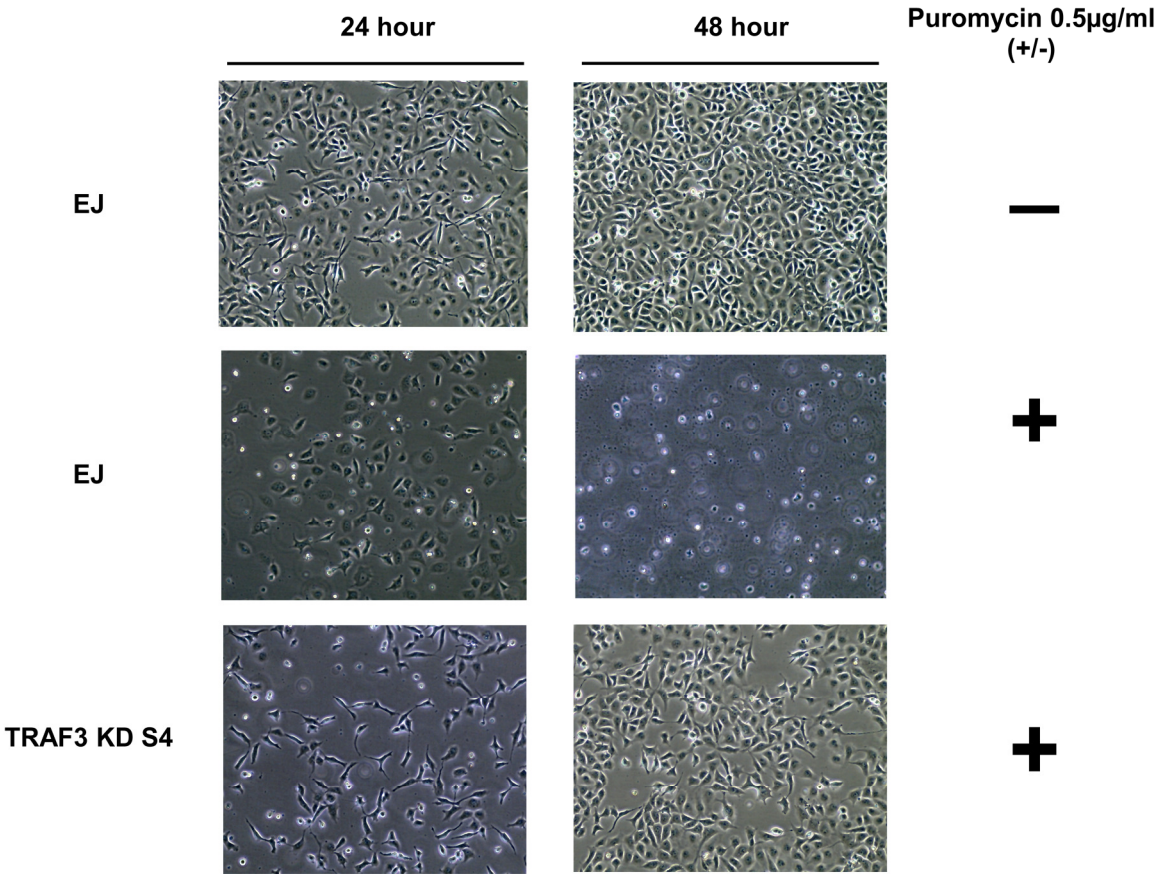


**Figure 4-12 Antibiotic selection of virally transduced carcinoma cells**

Transduced and non-transduced EJ cells were cultured in DR/5%FCS/1%L-G supplemented with 0.5µg/ml puromycin (the transduced cells shown here are cells in which an anti-TRAF3 shRNA is expressed, denoted TRAF3 KD S4 – see text for details). EJ were also cultured with DR/5%FCS/1%L-G alone to demonstrate their normal growth pattern (negative control). Note non-resistant EJ perish from the flask within 24-48 hours, however resistant cell populations continue to proliferate. Images are representative phase contrast micrographs (taken at 100x magnification).

### 4.6.2 The role of TRAF3 in CD40-mediated apoptosis

Using immunoblotting, the induction of TRAF3 was observed as early as 3 hours with further increases at 6 and 12 and maximal expression occurring 24 hours post CD40 ligation (Figure 4-13). Previous studies aiming to identify the role of TRAF3 in CD40-apoptosis (Elmetwali et al., 2010b, Georgopoulos et al., 2006) used 'exogenous', transient siRNA transfection to abrogate TRAF3 expression; however this only has a transient effect particularly in rapidly dividing cells (Rao et al., 2009). Retrovirus-mediated delivery of shRNAs for siRNA expression is by contrast stable and more efficacious and retrovirus-mediated transgene expression in urothelial cells can reach over 90% efficacy (Crallan et al., 2006). This high level of efficiency not only ensures shRNA expression but also negates clonal selection in antibiotic and allows maintenance of the heterogeneity of the original cell line, thus reducing the 'risks' associated with genetic drift during clonal selection.

EJ cells were thus transfected (as detailed in section 2.8.4.) using two independent shRNAs for knockdown of TRAF3 (shRNAs S4 and S6 as in Table 2-4) and cells were selected in puromycin as previously described (section 4.3.1.3). For the purposes of this thesis, EJ cell derivatives bearing the S4 shRNA will be termed TRAF3-KD-S4 and those bearing the S6 shRNA termed TRAF3-KD-S6. The ability of the designed shRNAs to knockdown TRAF3 protein expression was confirmed by immunoblotting (Figure 4-14) and densitometric analysis (Figure 4-15). TRAF3-KD-S4 cells were first used to confirm the role of TRAF3 in the induction of downstream JNK during CD40-mediated apoptosis. As shown in Figure 4-16 TRAF3 knockdown reduced the activation of JNK as evident by reduction in p-JNK levels, thus reciprocating previous reports (Elmetwali et al., 2010b, Georgopoulos et al., 2006).

As CD40 ligation by mCD40L induces apoptosis by activation of the intrinsic pathway (Georgopoulos et al., 2006), TRAF3-KD-S4 and TRAF-KD-S6 cells were used to explore whether TRAF3-mediated signalling drives expression of Bak and Bax proteins, of which their induction was reported previously (Bugajska et al., 2002). Results demonstrated exclusively that TRAF3-mediated signalling regulates the expression of pro-apoptotic regulators, as TRAF3 knockdown completely abrogated Bak and Bax expression subsequent to CD40 ligation (Figure 4-17).

The complete inhibition of CD40-mediated Bak and Bax protein induction by TRAF3 knockdown suggested that loss of TRAF3 interferes with the induction of apoptosis. This was confirmed using caspase activation-based apoptosis assays where TRAF3 knockdown led to a significant reduction ($P<0.001$) in caspase-3/7 activation during CD40 engagement. (Figure 4-18). The observations made were similar for both TRAF3 shRNA expressing lines.

### 4.7.3 Role of JNK/AP-1 in CD40-mediated apoptosis

Immunoblotting demonstrated that JNK phosphorylation occurs as early as 3 hours but most noticeably at 6 hours in response to CD40-mCD40L interaction (Figure 4-19). As CD40 ligation results in dramatic induction of Bak and Bax levels (Bugajska et al., 2002), it was hypothesised that the apoptosis induced by JNK/AP-1 is via their (Bak and Bax) expression. The regulation of the two pro-apoptotic mediators by JNK/AP-1 was confirmed for the first time by using immunoblotting and pre-titrated concentrations of the pharmacological inhibitors SP600125 and NDGA, which respectively, block JNK and AP-1 activity. Both inhibitors completely attenuated expression of Bak/Bax during CD40 engagement suggesting that these pro-apoptotic members are tightly regulated by JNK/AP1 (Figures 4-20 and 4-21). In line with these observations, inhibition of both JNK and AP-1 led to a significant reduction in apoptosis as determined by CytoTox-Glo death detection assays (Figure 4-22 & 4-23), which overall elegantly confirmed the key regulatory role of JNK/AP-1 in CD40-mediated cell death.

### 4.8.4 MKK4 and MKK7 regulation of CD40-mediated apoptosis

The regulation of the JNK by upstream MAPKKs MKK4 and MKK7 is well documented (Wagner and Nebreda, 2009). Therefore, this work aimed for the first time to examine whether MKK4 and/or MKK7 are involved in CD40 signalling and whether they are responsible for JNK activation.

MKK4 was activated in response to mCD40L as shown by phosphorylation at Ser257 (Figure 4-24); however it should be noted that this was a bit inconsistent between different experiments (not shown), most probably due to the particularly low levels of p-MKK4 levels detected. Despite the lack of significant p-MKK4 detection, immunoblotting using a phospho-MKK4 specific antibody showed that MKK4 phosphorylation occurred within 6 hours post CD40 ligation (Figure 4-24).

To establish a possible functional role for MKK4 in CD40 signalling and apoptosis, two independent EJ lines were established by retroviral transduction (section 2.8.4) for the expression of individual shRNAs for knockdown of MKK4, namely shRNAs S11 & S12 (see Table 2-4). EJ cell transduction and antibiotic (puromycin) selection were performed as previously described (section 4.3.1.3) and the cell lines established were MKK4-KD-S11 and MKK4-KD-S12, respectively. Although at the time this thesis was being written immunoblotting had not been used to demonstrate successful p-MKK4 knockdown, when the cell lines were functionally tested for JNK activation following CD40 ligation, it was observed that MKK4 knockdown led to marked attenuation of CD40-mediated JNK phosphorylation (Figure 4-25). In addition to a role for MKK4 in activating JNK, the functional importance of MKK4 in apoptosis was investigated using cell death assays. Both cell lines stably expressing anti-MKK4 shRNAs showed significant reduction ($P<0.001$) in caspase-3/7 activation (Figure 4-26) thus showing for the first time that MKK4 plays a positive role in CD40-mediated apoptosis.

In contrast to the MKK4-related findings, a phospho-MKK7 specific antibody was unable to demonstrate any clear, detectable induction in p-MKK7 expression over a number of experiments (Figure 4-27), although MKK7 expression levels observable were higher relatively to those of MKK4.

Even though the lack of induction of MKK7 suggested that this MAPKK may not be a functional molecule during CD40-mediated apoptosis, shRNA mediated RNAi was also used to further explore the role, if any, of MKK7 in CD40 signalling and apoptosis. As with MKK4 knockdown experiments, two independent EJ lines were prepared (section 2.8.4) expressing individual shRNAs for knockdown of MKK7, in particular shRNAs S11 & S12 (Table 2-4) and the cell lines established as previously described (section 4.3.1.3) were termed MKK7-KD-S1 and MKK7-KD-S2, respectively. Although at the time this thesis was being written immunoblotting had not been used to demonstrate successful p-MKK7 knockdown, expression of anti-MKK7 shRNAs did not affect the phosphorylation of JNK in response to mCD40L (Figure 4-28). Moreover, following CD40 ligation the MKK7-KD-S1 and MKK7-KD-S2 cell lines showed comparable levels of caspase-3/7 activation to those observed for control EJ cells (Figure 4-29). Collectively, these findings suggested that, unlike MKK4, the MKK7 MAPKK does not regulate JNK activation and mCD40L-induced apoptosis.

### 4.9.5 ASK1 regulation of CD40-mediated apoptosis

Having demonstrated a novel link between MKK4 and JNK activation as part of the signalling axis driving CD40/TRAF3-induced cell death, it was of interest to establish for the first time the missing link in the CD40/TRAF3 – MKK4/JNK signalling chain, i.e. identify which MAPKKK was responsible for the activation of MKK4. ASK1 was hypothesised as an ideal candidate, as it has been previously linked to TNF and Lymphotoxin ligand-associated cell responses (Matsuura et al., 2002, Kim et al., 2005, Chen et al., 2003) and its activation can lead to direct phosphorylation of MKK4 via a specific recognition sequence (Ichijo et al., 1997).

Using immunoblotting and a phospho-ASK1 antibody it was shown for the first time that CD40 ligation by mCD40L activated ASK1 as evidenced by specific, activatory phosphorylation at Thr845, which was observed approximately 3 hours post ligation (Figure 4-30). Although in some cases activation before the 3 hour time point was also observed (not shown), the levels of p-ASK1 returned to normal by 6 hours (Figure 4-30) and similar observations were made at 12 hours (not shown), and thus suggesting that ASK1 activation was a transient event.

The functional significance of p-ASK1 in the CD40 signalling pathway and overall in CD40 apoptosis, was investigated by RNAi. EJ cells were transduced with two independent shRNA expression vectors for targeted protein knockdown of ASK1 by expression of shRNAs S18 and S19 (Table 2-4). Cells were transduced and selected in antibiotic (section 4.3.1.3) and the stable S18 and S19 shRNA expressers termed ASK1-KD-S18 and ASK1-KD-S19, respectively, were established. The ability of the designed shRNAs to knockdown ASK1 protein expression was examined by immunoblotting. As shown in Figure 4-31, of the two transduced cell lines, ASK1-KD-S18 cells showed a marked attenuation of p-ASK1 induction in comparison to control cells at 3 hours post CD40 ligation (Figure 4-25), with little induction in p-ASK1. By contrast, ASK1-KD-S19 showed induction of p-ASK1 comparable to that observed in control cells, thus indicating that successful, efficient ASK1 knockdown was achieved in one but not the other cell line (presumably due to inherent differences of the two shRNAs in their capacity to down-regulate ASK1). For functional experiments (below), both cell lines were used, with more emphasis on the ASK1-KD-S18 line.

Following successful ASK1 knockdown, it was then investigated whether ASK1 may be functionally linked to JNK activation (phosphorylation). Immunoblotting demonstrated that ASK1 regulates the activation of JNK during mCD40L-induced signalling as ASK1-KD-S18 (and to a lesser extent ASK1-KD-S19) showed a markedly reduced JNK phosphorylation in comparison to control EJ cells that showed strong p-ASK1 up-regulation (Figure 4-32). On the other hand, a functional role for ASK1 in CD40-mediated apoptosis was supported by the fact that ASK1-KD-S18 cells demonstrated a significant reduction ($P<0.001$) in caspase-3/7 activation in comparison to control EJ cells following CD40 ligation (Figure 4-33). Due to the significance and the novelty of the findings, these observations were further corroborated using CytoTox-Glo assays (Figure 4-34), where it was shown that ASK1-KD-S18 (and to a lesser extent ASK1-KD-S19) showed dramatic loss of ability to undergo CD40-mediated apoptosis in comparison to control EJ cells, thus confirming the functional importance of ASK1 in JNK activation and subsequent apoptosis.

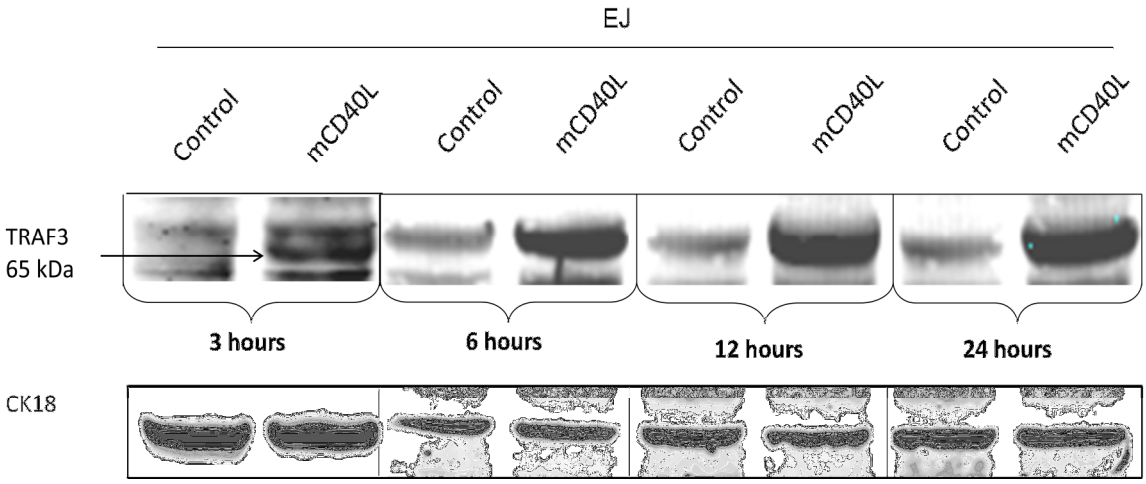


**Figure 4-13 The induction of TRAF3 expression in response to mCD40L**

$2.7x10^6$ EJ were co-cultured with $3x10^6$ MMC treated mCD40L and Controls for 3, 6, 12 and 24 hours in DR/5%FCS/1%L-G in $10cm^2$ culture dishes prior to lysis with 2X SDS-lysis buffer. 20µg of lysates were separated under denaturing conditions by SDS-PAGE using 4-12% (w/v) Bis-Tris gels and then immunoblotted onto a PVDF membrane. The PVDF membrane was probed overnight with an anti-TRAF3 antibody in TBS Tween 0.1% (1:500 dilution) and then with an anti-CK18 antibody in TBS Tween 0.1% (1:2000 dilution). The membrane was incubated for one hour with goat anti-mouse IgG IRDye 800 (1:10,000 dilution) for the detection of TRAF3 and with goat anti-rabbit IgG Alexa 680 (1:10,000) for the detection of CK18. Antibody binding was visualised at 700nm and 800nm using an Odyssey™ Infra-red Imaging system.

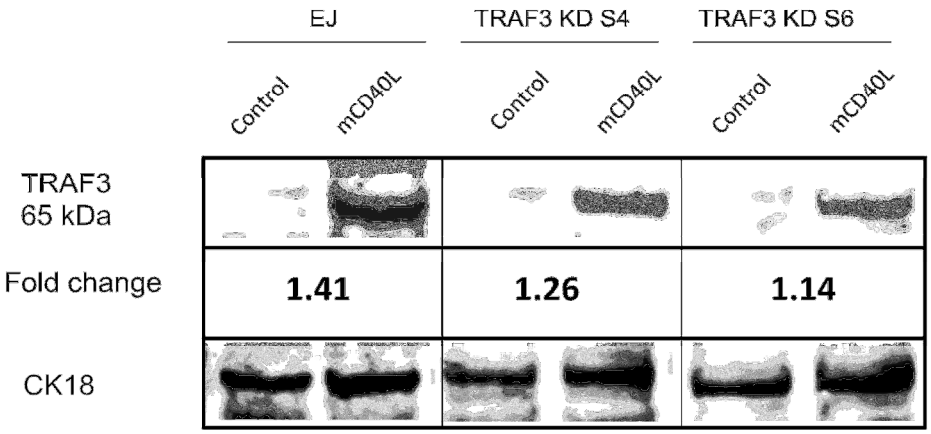


**Figure 4-14 shRNA mediated knockdown of TRAF3**

2.7x10$^6$ EJ, TRAF3-KD-S4 and TRAF3-KD-S6 cells were co-cultured with 3x10$^6$ MMC treated mCD40L and Controls for 24 hours in DR/5%FCS/1%L-G in 10cm$^2$ culture dishes prior to lysis with 2X SDS-lysis buffer. 20µg of lysates were separated under denaturing conditions by SDS-PAGE using 4-12% (w/v) Bis-Tris gels and then immunoblotted onto a PVDF membrane. The PVDF membrane was probed overnight with an anti-TRAF3 antibody (1:500 dilution) and then with an anti-CK18 antibody (1:2000 dilution). The membrane was incubated for one hour with goat anti-mouse IgG IRDye 800 (1:10,000 dilution) for the detection of TRAF3 and with goat anti-rabbit IgG Alexa 680 (1:10,000 dilution) for the detection of CK18. Antibody binding was visualised at 700nm and 800nm using an Odyssey$^{TM}$ Infra-red Imaging system.

| TRAF3 KD 24 hours | | | | | |
|---|---|---|---|---|---|
| **Co-culture** | **shRNA target** | **BC band intensity** | **CK18 BC band intensity** | **Normalised intensity** | **Fold change** |
| Control/EJ | N/A | 4278.27 | 3672.33 | 4278.27 | |
| mCD40L/EJ | N/A | 5772.70 | 3521.53 | 6019.70 | 1.4 |
| Control/EJ | TRAF3 S4 | 426.17 | 1718.16 | 426.17 | |
| mCD40L/EJ | TRAF3 S4 | 504.73 | 1785.19 | 485.78 | 1.14 |
| Control/EJ | TRAF3 S6 | 383.53 | 1492.54 | 383.53 | |
| mCD40L/EJ | TRAF3 S6 | 506.12 | 1566.88 | 482.11 | 1.26 |

**Figure 4-15 Densitometric analysis to calculate fold change in protein expression**

Densitometry was used to normalise data using Cytokeratin 18 as the loading Control. Readings represent band intensities values generated by the LiCor Odyssey analysis software. Data was normalised against densitometry values for Controls and then fold change was calculated by the following equation (mCD40L/EJ ÷ Control/EJ). BC - blank corrected. The table above is representative of values created from Figure 4-9.

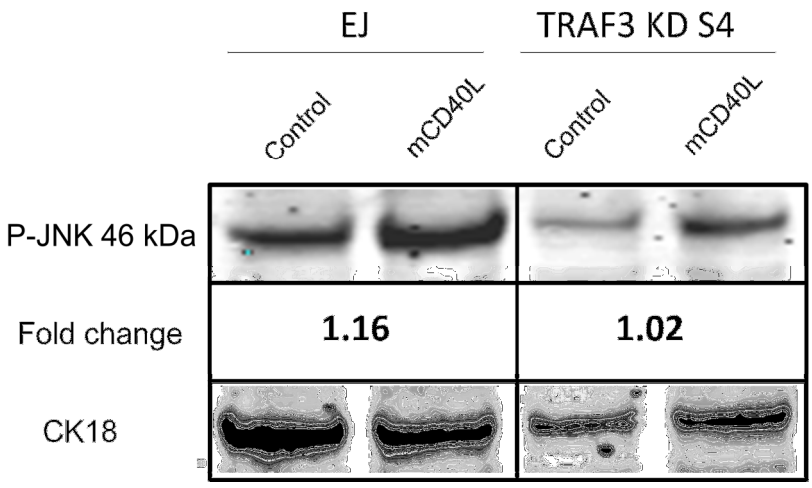


**Figure 4-16 The role of TRAF3 in the regulation of phospho-JNK expression during CD40-mediated apoptosis**

$2.7x10^6$ EJ and TRAF3-KD-S4 cells were co-cultured with $3x10^6$ MMC treated mCD40L and Controls for 6 hours in DR/5%FCS/1%L-G and $10cm^2$ culture dishes prior to lyses with 2X SDS-lysis buffer. 20-40µg of lysates were separated under denaturing conditions by SDS-PAGE using 4-12% (w/v) Bis-Tris gels and then immunoblotted onto a PVDF membrane. The PVDF membrane was probed overnight with an anti-phospho-JNK antibody (1:1000 dilution) and then with an anti-CK18 antibody (1:2000 dilution). The membrane was incubated for one hour with goat anti-rabbit IgG Alexa 680 (1:10,000 dilution) for the detection of p-JNK and CK18. Antibody binding was visualised at 700nm and 800nm using an Odyssey™ Infra-red Imaging system.

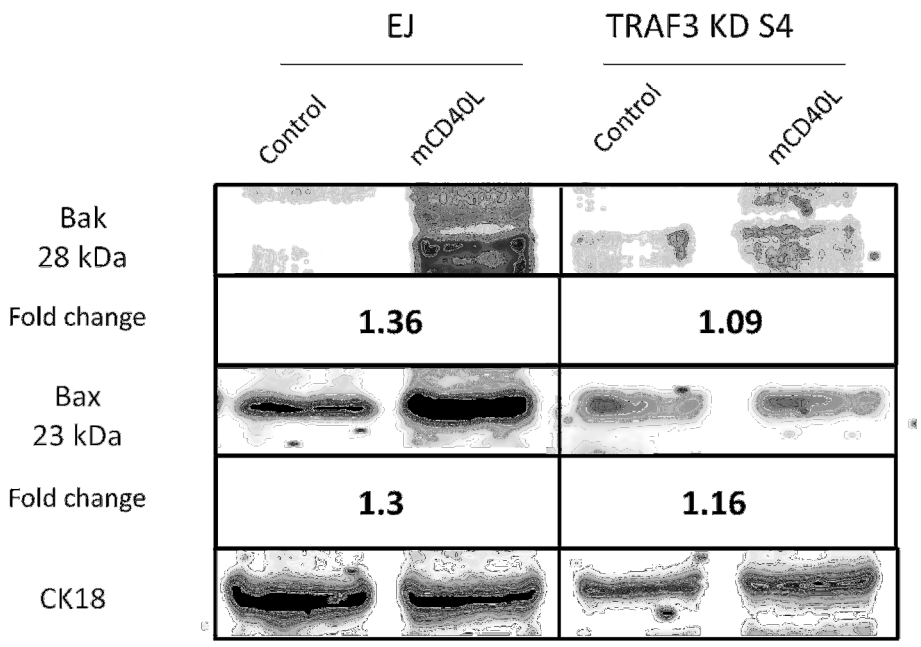


**Figure 4-17 Effect of TRAF3 down-regulation on Bak and Bax expression during CD40-mediated apoptosis**

$2.7x10^6$ EJ, TRAF3-KD-S4 and TRAF3-KD-S6 cells were co-cultured with $3x10^6$ MMC treated mCD40L and Controls for 24 hours in DR/5%FCS/1%L-G and $10cm^2$ culture dishes prior to lyses with 2X SDS-lysis buffer. 20-40µg of lysates were separated under denaturing conditions by SDS-PAGE using 4-12% (w/v) Bis-Tris gels and then immunoblotted onto a PVDF membrane. The PVDF membrane was probed overnight with an anti-Bak and an anti-Bax antibody (1:1000 dilution) and then with an anti-CK18 antibody (1:2000 dilution). The membrane was incubated for one hour with goat anti-mouse IgG IRDye 800 (1:10,000 dilution) for the detection of Bak. Goat anti-rabbit IgG Alexa 800 (1:10,000 dilution) was used for the detection of CK18 and BAX. Antibody binding was visualised at 700nm and 800nm using an Odyssey™ Infra-red Imaging system.

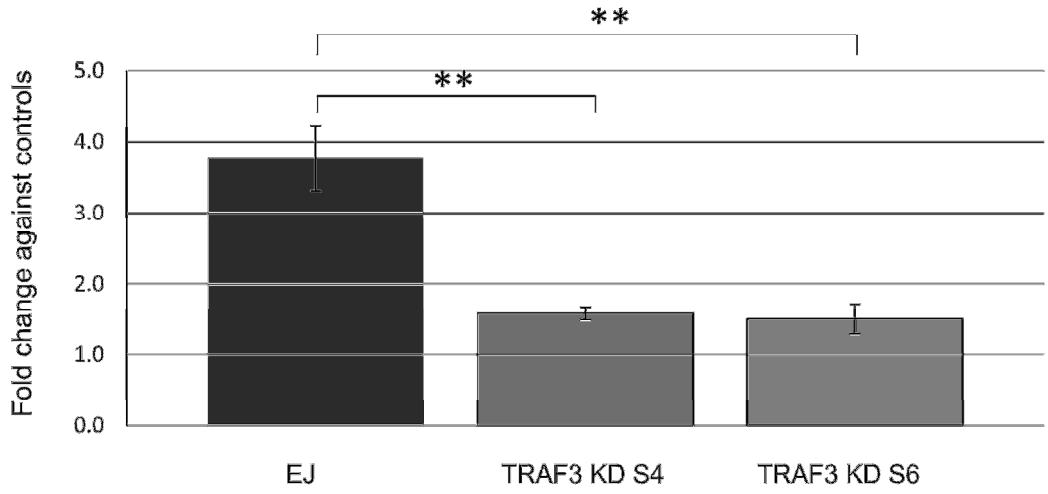


**Figure 4-18 Role of TRAF3 knockdown in caspase-3/7 activation during CD40-mediated apoptosis**

$8x10^3$ EJ, TRAF3-KD-S4 and TRAF3-KD-S6 were co-cultured with $10^4$ MMC treated mCD40L or Controls in DR/5%FCS/1%L-G in white 96-well plates. SensoLyte 3/7 reagent was added after 48 hours, fluorescence measured (as detailed in Section 2.11.3.1) and background-corrected RFU readings deduced by pair-wise subtraction of mCD40L and Control cell from the respective co-cultures. Bars represent mean RFU values for 5-6 technical replicates ± SEM, and results are representative of three independent experiments. Stats: ** $P<0.01$, paired student t-test, EJ Vs knockdown cells.

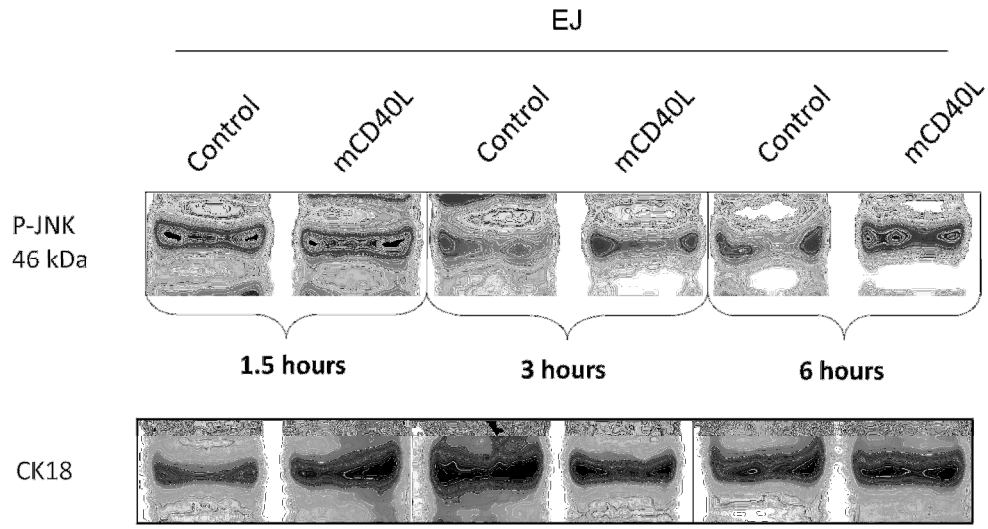


**Figure 4-19 JNK phosphorylation following CD40 ligation**

$2.7x10^6$ EJ were co-cultured with $2.7x10^6$ MMC treated mCD40L and Controls for 1.5, 3, and 6 hours in DR/5%FCS/1%L-G in $10cm^2$ culture dishes prior to lysis with 2X SDS-lysis buffer. 20µg of lysates were separated under denaturing conditions by SDS-PAGE using 4-12% (w/v) Bis-Tris gels and then immunoblotted onto a PVDF membrane. The PVDF membrane was probed overnight with an anti-phospho-JNK antibody (1:1000 dilution) and then with an anti-CK18 antibody (1:2000 dilution). The membrane was then incubated for one hour with goat anti-mouse IgG conjugated with Alexa 680 in TBS Tween 0.1% for both p-JNK and CK18 (1:10,000 dilution). Antibody binding was visualised at 700nm and 800nm using an Odyssey™ Infra-red Imaging system.

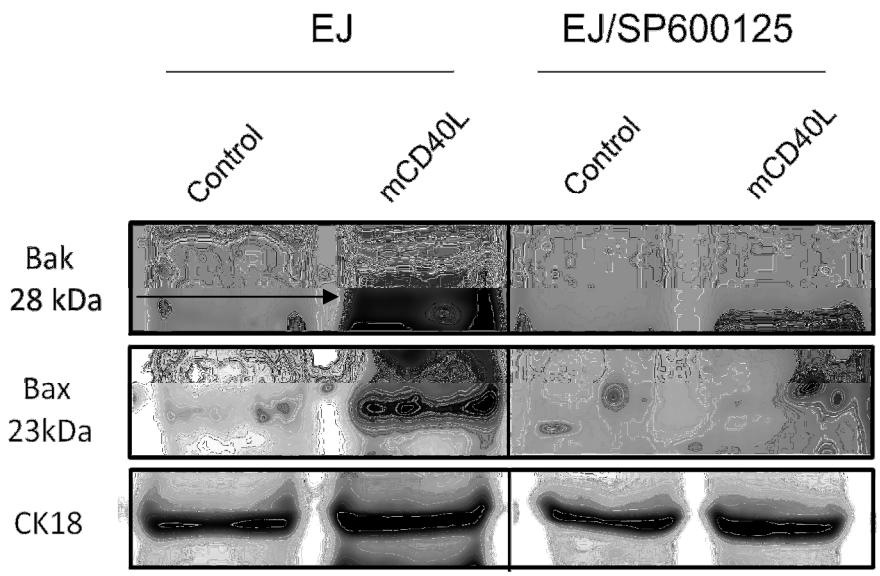


**Figure 4-20 JNK-mediated regulation of Bak and Bax during CD40-mediated apoptosis**

$2.7x10^6$ EJ cells were co-cultured with $3x10^6$ MMC treated mCD40L and Controls for 24 hours in DR/5%FCS/1%L-G ± 25µM SP600125 in $10cm^2$ culture dishes prior to lysis with 2X SDS-lysis buffer. 20-µg of lysates were separated under denaturing conditions by SDS-PAGE using 4-12% (w/v) Bis-Tris gels and then immunoblotted onto a PVDF membrane. The PVDF membrane was probed overnight with an anti-Bak and anti-Bax antibody (1:1000 dilution) and then with an anti-CK18 antibody (1:2000 dilution). The membrane was incubated for one hour with goat anti-mouse IRDye Alexa 800 (1:10,000 dilution) for the detection of Bak and with goat anti-rabbit IgG Alexa 680 (1:10,000 dilution) for the detection of CK18 and Bax. Antibody binding was visualised at 700nm and 800nm using an Odyssey™ Infra-red Imaging system.

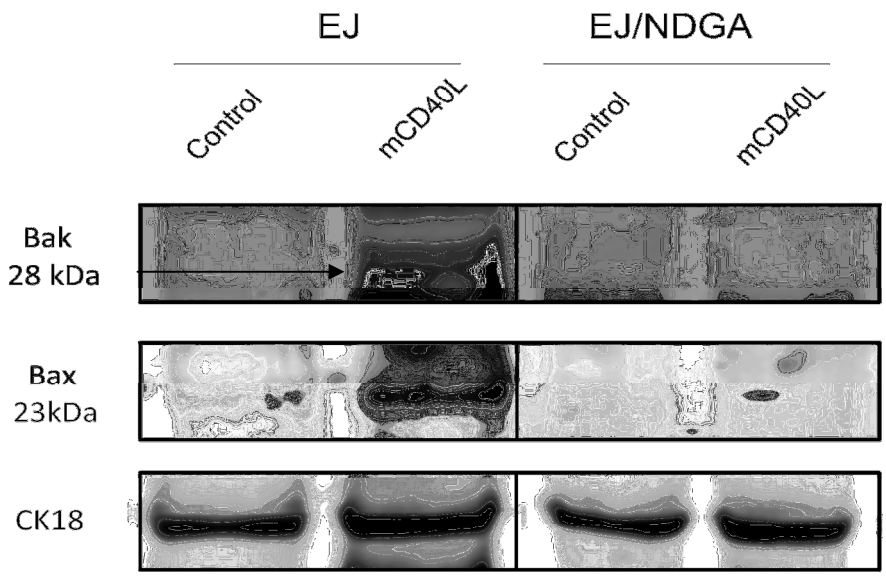


**Figure 4-21 Regulation of Bak and Bax by AP-1 in response to mCD40L**

$2.7x10^6$ EJ cells were co-cultured with $3x10^6$ MMC treated mCD40L and Controls for 24 hours in DR/5%FCS/1%L-G ± 10µM NDGA in $10cm^2$ culture dishes prior to lysis with 2X SDS-lysis buffer. 20µg of lysates were separated under denaturing conditions by SDS-PAGE using 4-12% (w/v) Bis-Tris gels and then immunoblotted onto a PVDF membrane. The PVDF membrane was probed overnight with an anti-Bak and anti-Bax antibody (1:1000 dilution) and then with an anti-CK18 antibody (1:2000 dilution). The membrane was incubated for one hour with goat anti-mouse IgG IRDye 800 (1:10,000 dilution) for the detection of Bak and with goat anti-rabbit IgG Alexa 680 (1:10,000 dilution) for the detection of CK18 and Bax. Antibody binding was visualised at 700nm and 800nm using an Odyssey™ Infra-red Imaging system.

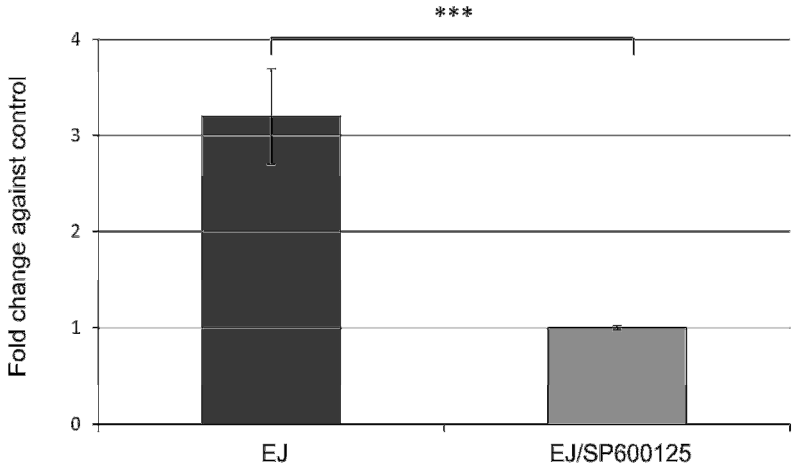


### 4-22 JNK regulation of CD40-mediated apoptosis

$8x10^3$ EJ were co-cultured with $10^4$ MMC treated mCD40L or Controls in DR/5%FCS/1%L-G ± 25µM SP600125 in white 96-well plates. CytoTox-Glo substrate was added after 72 hours, luminescence was measured and background-corrected RLU readings deduced as described in Figure 3-7. Bars correspond to mean values of 5-6 technical replicates ± SEM and results are representative of three independent experiments. Stats: *** P<0.001, paired student t-test, EJ vs EJ/SP600125.

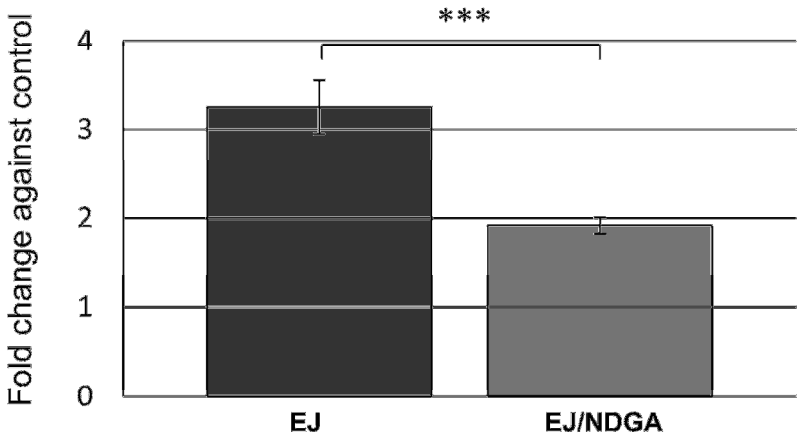


**Figure 4-23 Regulation of apoptosis by AP-1 in response to mCD40L**

$8x10^3$ EJ were co-cultured with $10^4$ MMC treated mCD40L or Controls in DR/5%FCS/1%L-G ± 10µM NDGA in white 96-well plates. CytoTox-Glo substrate was added after 72 hours, luminescence was measured and background-corrected RLU readings deduced as described in Figure 3-7. Bars correspond to mean values of 5-6 technical replicates ± SEM and results are representative of three independent experiments. Stats: *** P<0.001, paired student t-test, EJ vs EJ/NDGA.

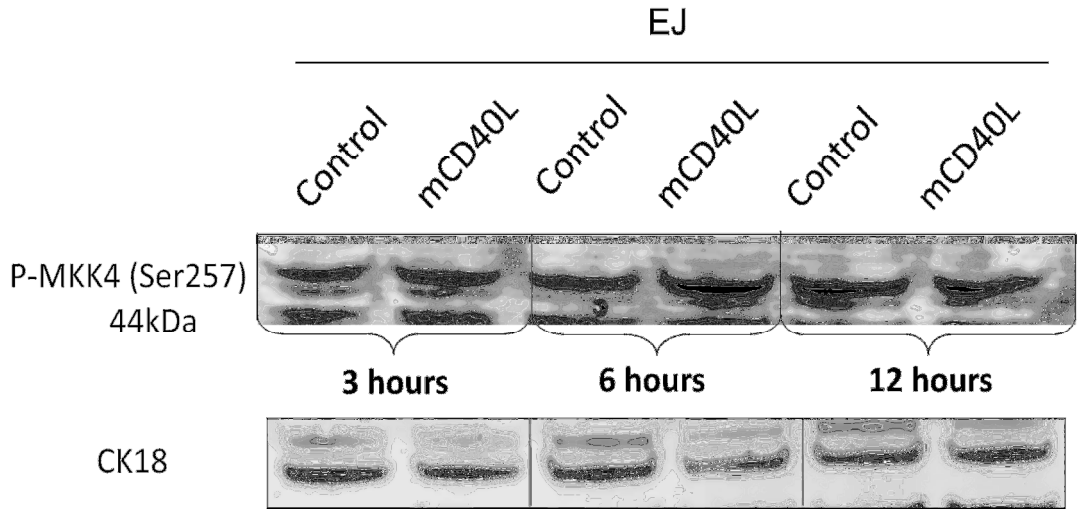


**Figure 4-24 The activation of MKK4 in response to mCD40L**

$2.7x10^6$ EJ were co-cultured with $3x10^6$ MMC treated mCD40L and Controls for 3, 6 and 12 hours in DR/5%FCS/1%L-G within $10cm^2$ culture dishes prior to lyses with 2X SDS-lysis buffer. 20-40µg of lysates were separated under denaturing conditions by SDS-PAGE using 4-12% (w/v) Bis-Tris gels and then immunoblotted onto a PVDF membrane. The PVDF membrane was probed overnight with an anti-phospho-MKK4 (Ser257) antibody (1:1000 dilution) and then with an anti-CK18 antibody (1:2000 dilution). The membrane was incubated for one hour with goat anti-mouse IgG IRDye 800 (1:10,000 dilution) for the detection of phospho-MKK4 and with goat anti-rabbit IgG Alexa 680 (1:10,000 dilution) for the detection of CK18. Antibody binding was visualised at 700nm and 800nm using an Odyssey™ Infra-red Imaging system.

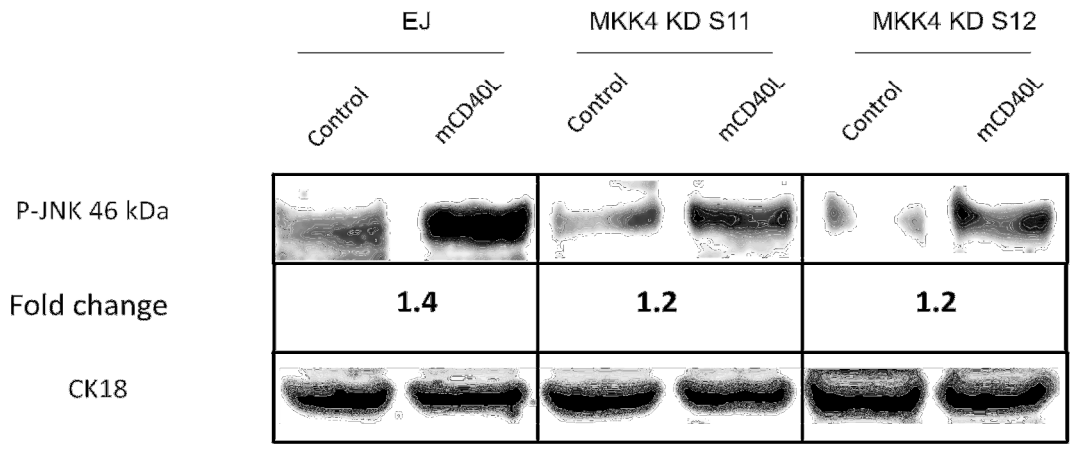


**Figure 4-25 Effect of MKK4 knockdown on phospho-JNK during CD40-mediated apoptosis**

$2.7x10^6$ EJ, MKK4-KD-S11 and MKK4-KD-S12 cells were co-cultured with $3x10^6$ MMC treated mCD40L and Controls for 6 hours in DR/5%FCS/1%L-G in $10cm^2$ culture dishes prior to lysis with 2X SDS-lysis buffer. 40µg of lysates were separated under denaturing conditions by SDS-PAGE using 4-12% (w/v) Bis-Tris gels and then immunoblotted onto a PVDF membrane. The PVDF membrane was probed overnight with an anti-phospho-MKK4 antibody (1:1000 dilution) and then with an anti-CK18 antibody (1:2000 dilution). The membrane was incubated for one hour with goat anti-mouse IgG IRDye 800 (1:10,000 dilution) for the detection of phospho-MKK4 and with goat anti-rabbit IgG Alexa 680 (1:10,000 dilution) for the detection of CK18. Antibody binding was visualised at 700nm and 800nm using an Odyssey™ Infra-red Imaging system.

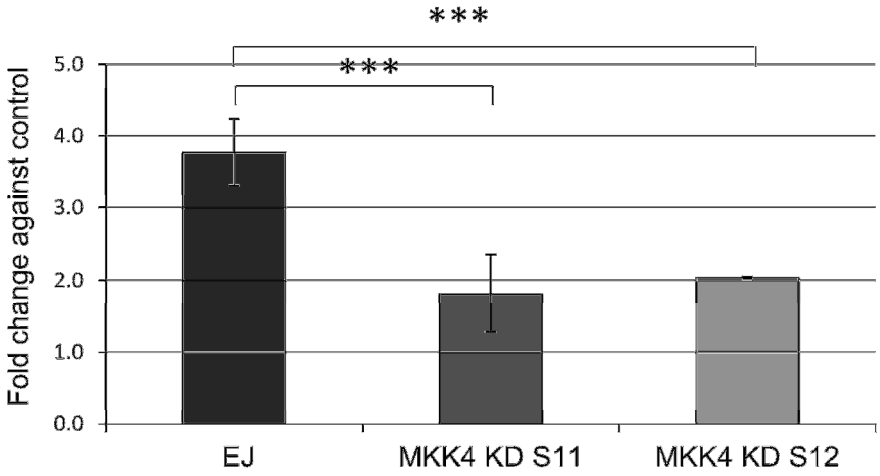


**Figure 4-26 Effect of MKK4 knockdown on caspase-3/7 activation during CD40-mediated apoptosis**

$8x10^3$ EJ, MKK4-KD-S11 and MKK4-KD-S12 were co-cultured with $10^4$ MMC treated mCD40L or Controls in DR/5%FCS/1%L-G in white 96-well plates. SensoLyte 3/7 reagent was added after 48 hours, fluorescence measured (as detailed in Section 2.11.3.1) and background-corrected RFU readings deduced by pair-wise subtraction of mCD40L and Control cell from the respective co-culture. Bars represent mean RFU values for 5-6 technical replicates ± SEM and results are representative of three independent experiments. Stats: *** P<0.001, paired student t-test for EJ Vs knockdown cells.

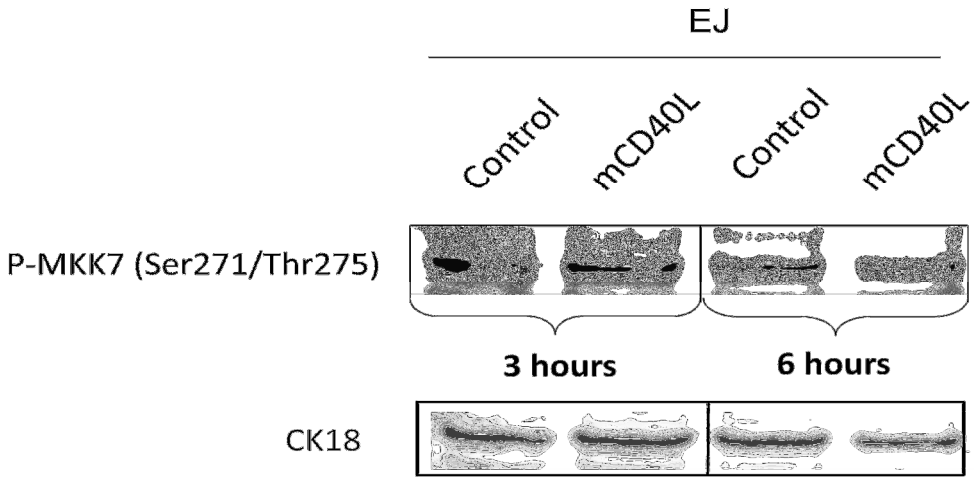


**Figure 4-27 Detection of MKK7 kinase during mCD40L signalling**

$2.7x10^6$ EJ were co-cultured with $3x10^6$ MMC treated mCD40L and Controls for 3 and 6 in DR/5%FCS/1%L-G in $10cm^2$ culture dishes hours prior to lysis with 2X SDS-lysis buffer. 20µg of lysates were separated under denaturing conditions by SDS-PAGE using 4-12% (w/v) Bis-Tris gels and then immunoblotted onto a PVDF membrane. The PVDF membrane was probed overnight with an anti-phospho-MKK7 (Ser271/Thr275) antibody (1:1000 dilution) and then with an anti-CK18 antibody (1:2000 dilution). The membrane was incubated for one hour with goat anti-mouse IgG IRDye 800 (1:10,000 dilution) for the detection of phospho-MKK7 and with goat anti-rabbit IgG Alexa 680 (1:10,000 dilution) for the detection of CK18. Antibody binding was visualised at 700nm and 800nm using an Odyssey™ Infra-red Imaging system.

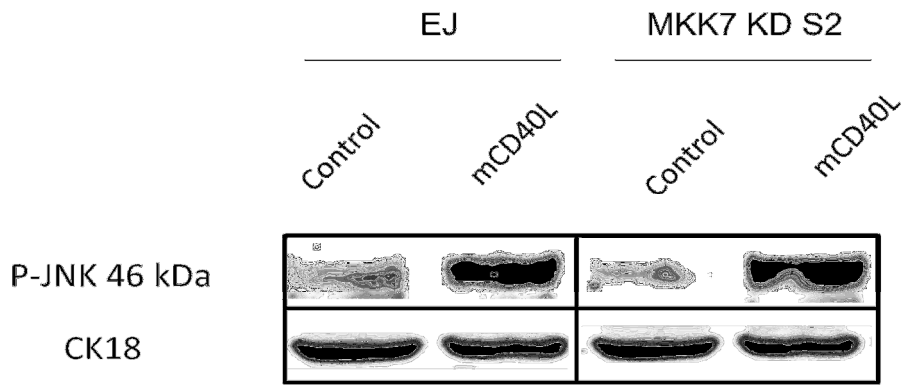


**Figure 4-28 Effect of MKK7 knockdown on phospho-JNK expression during CD40-mediated signalling**

$2.7x10^6$ EJ and MKK7-KD-S2 cells were co-cultured with $3x10^6$ MMC treated mCD40L and Controls for 6 hours in DR/5%FCS/1%L-G in $10cm^2$ culture dishes prior to lysis with 2X SDS-lysis buffer. 20µg of lysates were separated under denaturing conditions by SDS-PAGE using 4-12% (w/v) Bis-Tris gels and then immunoblotted onto a PVDF membrane. The PVDF membrane was probed overnight with an anti-phospho-MKK7 antibody (1:1000 dilution) and then with an anti-CK18 antibody (1:2000 dilution). The membrane was incubated for one hour with goat anti-mouse IgG IRDye 800 (1:10,000 dilution) for the detection of phospho-MKK7 and with goat anti-rabbit IgG Alexa 680 (1:10,000 dilution) for the detection of CK18. Antibody binding was visualised at 700nm and 800nm using an Odyssey™ Infra-red Imaging system.

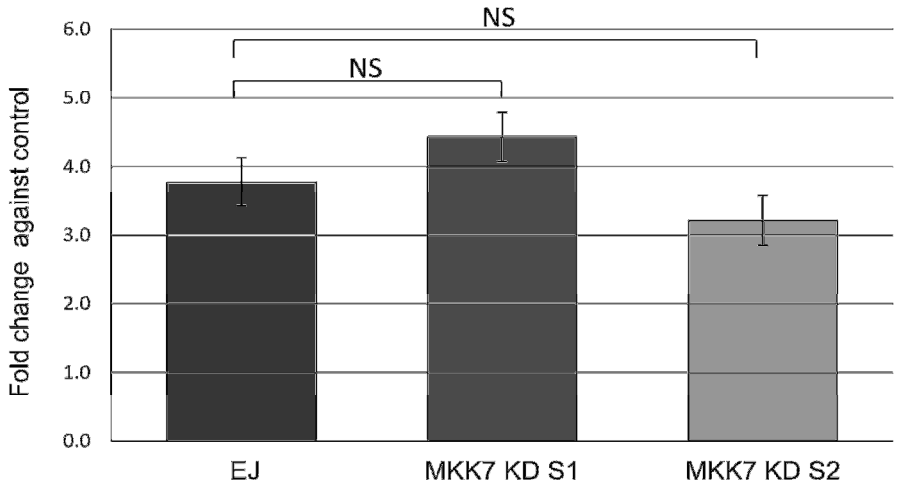


**Figure 4-29 Effect of MKK7 knockdown on caspase-3/7 activation during CD40-mediated apoptosis**

$8x10^3$ EJ, MKK7-KD-S1 and MKK7-KD-S2 were co-cultured with $10^4$ MMC treated mCD40L or Controls in DR/5%FCS/1%L-G in white 96-well plates. SensoLyte 3/7 reagent was added after 48 hours, fluorescence measured (as detailed in Section 2.11.3.1) and background-corrected RFU readings deduced by pair-wise subtraction of mCD40L and Control cell from the respective co-culture. Bars represent mean RFU values for 5-6 technical replicates ± SEM and results are representative of three independent experiments. Stats: NS – non-significant, paired student t-test, EJ Vs knockdown cells.

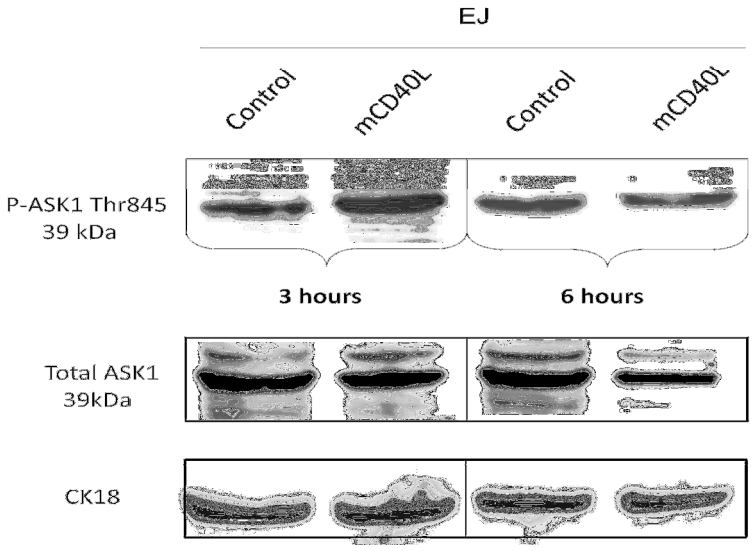


**Figure 4-30 Activation of ASK1 evident by activatory Thr845 phosphorylation in response to mCD40L**

2.7x10$^6$ EJ were co-cultured with 3x10$^6$MMC treated mCD40L and Controls for 3 and 6 hours in DR/5%FCS/1%L-G in 10cm$^2$ culture dishes prior to lysis with 2X SDS-lysis buffer. 20µg of lysates were separated under denaturing conditions by SDS-PAGE using 4-12% (w/v) Bis-Tris gels and then immunoblotted onto a PVDF membrane. The PVDF membrane was probed overnight with an anti-phospho-ASK1 (Thr845) antibody (1:1000 dilution) and then with an anti-CK18 antibody (1:2000 dilution). The membrane was incubated for one hour with goat anti-mouse IgG IRDye 800 (1:10,000 dilution) for the detection of phospho-ASK1 and with goat anti-rabbit IgG Alexa 680 (1:10,000 dilution) for the detection of CK18. Antibody binding was visualised at 700nm and 800nm using an Odyssey$^{TM}$ Infra-red Imaging system.

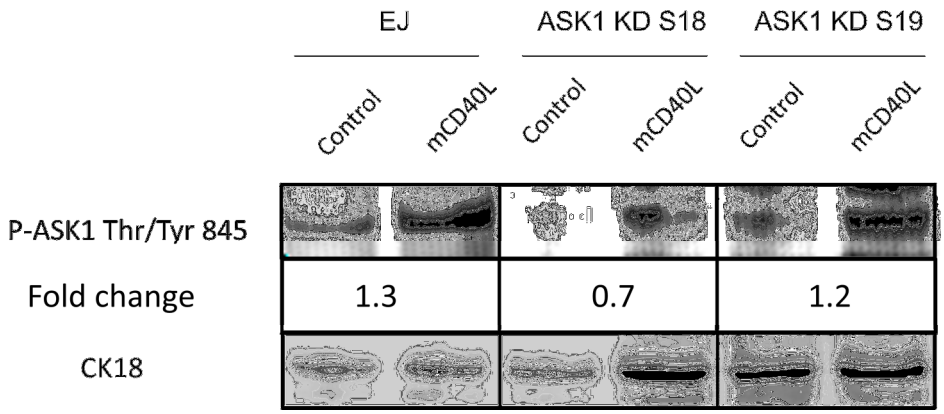


**Figure 4-31 shRNA-mediated ASK1 protein knockdown during CD40-mediated apoptosis**

$2.7x10^6$ EJ, ASK1-KD-S18 and ASK1-KD-S19 cells were co-cultured with $3x10^6$ MMC treated mCD40L and Controls for 3 hours in DR/5%FCS/1%L-G in $10cm^2$ culture dishes prior to lysis with 2X SDS-lysis buffer. 20µg of lysates were separated under denaturing conditions by SDS-PAGE using 4-12% (w/v) Bis-Tris gels and then immunoblotted onto a PVDF membrane. The PVDF membrane was probed overnight with an anti-phospho-ASK1 antibody (1:1000 dilution) and then with an anti-CK18 antibody (1:2000 dilution). The membrane was incubated for one hour with goat anti-mouse IgG IRDye 800 (1:10,000 dilution) for the detection of phospho-ASK1 and with goat anti-rabbit IgG Alexa 680 (1:10,000 dilution) for the detection of CK18. Antibody binding was visualised at 700nm and 800nm using an Odyssey™ Infra-red Imaging system.

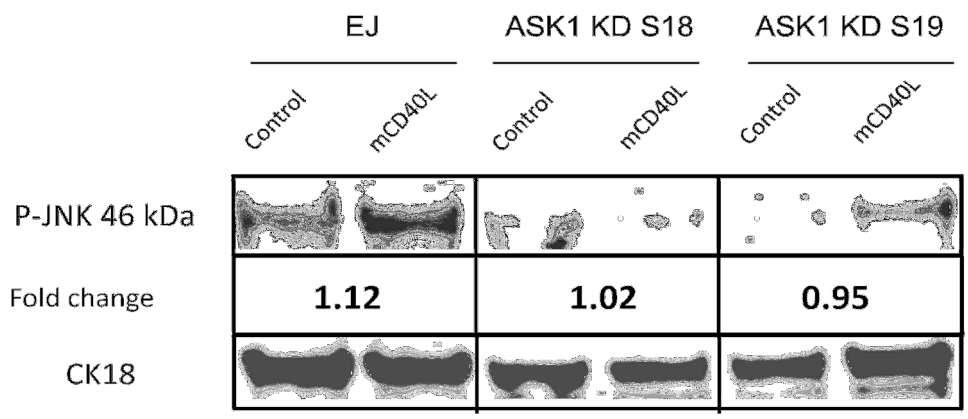


**Figure 4-32 Effect of ASK1 knockdown on phospho-JNK activation during CD40 signalling**

$2.7x10^6$ EJ, ASK1-KD-S18 and ASK1-KD-S19 cells were co-cultured with $3x10^6$ MMC treated mCD40L and Controls for 6 hours in DR/5%FCS/1%L-G in $10cm^2$ culture dishes prior to lysis with 2X SDS-lysis buffer. 40µg of lysates were separated under denaturing conditions by SDS-PAGE using 4-12% (w/v) Bis-Tris gels and then immunoblotted onto a PVDF membrane. The PVDF membrane was probed overnight with an anti-phospho-JNK antibody (1:1000 dilution) and then with an anti-CK18 antibody (1:2000 dilution). The membrane was incubated for one hour with goat anti-mouse IgG IRDye 800 (1:10,000 dilution) for the detection of phospho-JNK and with goat anti-rabbit IgG Alexa 680 (1:10,000 dilution) for the detection of CK18. Antibody binding was visualised at 700nm and 800nm using an Odyssey™ Infra-red Imaging system.

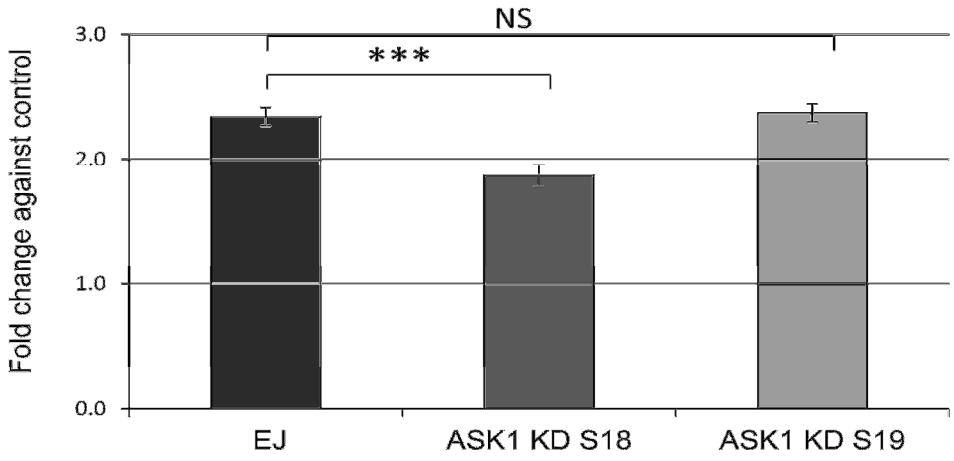


**Figure 4-33 Effect of ASK1 knockdown on caspase-3/7 activation during CD40-mediated apoptosis**

$8x10^3$ EJ, ASK1-KD-S18 and ASK1-KD-S18 were co-cultured with $10^4$ MMC treated mCD40L or Controls in DR/5%FCS/1%L-G in white 96-well plates. SensoLyte 3/7 reagent was added after 48 hours, fluorescence measured (as detailed in Section 2.11.3.1) and background-corrected RFU readings deduced by pair-wise subtraction of mCD40L and Control cell from the respective co-culture. Bars represent mean RFU values for 5-6 technical replicates ± SEM and results are representative of three independent experiments. Stats: NS – non-significant *** $P<0.001$, paired student t-test for EJ vs knockdown cells.

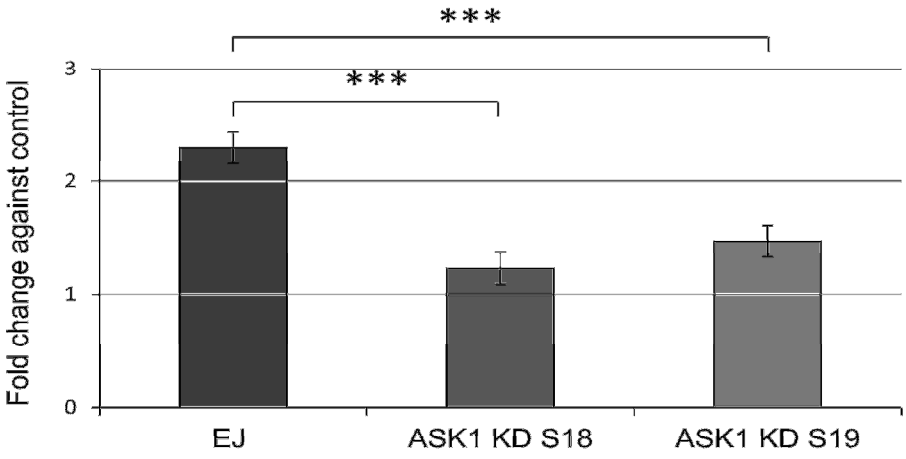


**Figure 4-34 Effect of ASK1 knockdown on CD40-mediated apoptosis**

$8x10^3$ EJ, ASK1-KD-S18 and ASK1-KD-S19 were co-cultured with $10^4$ MMC treated mCD40L or Controls in DR/5%FCS/1%L-G in white 96-well plates. CytoTox-Glo substrate was added after 72 hours, luminescence was measured and background-corrected RLU readings deduced as described in Figure 3-7. Bars correspond to mean values of 5-6 technical replicates ± SEM and results are representative of three independent experiments. Stats: *** P<0.001, paired student t-test, EJ vs knockdown cells.

### 4.3.6 Intrinsic (mitochondrial) pathway regulation and functional involvement during CD40-mediated apoptosis

Previous studies by Georgopoulos and colleagues have demonstrated that CD40 engagement by mCD40L induces expression of the pro-apoptotic molecules Bak and Bax, whilst down-regulating anti-apoptotic Bcl-2 protein (Bugajska et al., 2002). In agreement with these studies it was shown in the UCC line EJ that CD40 engagement caused the induction of Bak (Figure 4-35) and Bax (Figure 4-36) expression 24 hours post receptor ligation. No induction of these pro-apoptotic mediators was observed at 12 hours or earlier and was the same for 36 and 48 hours (not shown).

The significance of Bak/Bax expression in CD40-mediated apoptosis was investigated through shRNA mediated RNAi. EJ cells were transduced (section 2.8.4) with shRNAs specific for Bak (shRNAs S9 and S10) and Bax (shRNAs S14 and S15) (see Table 2-4), and EJ transductants were established as previously described (section 5.3.1). These EJ derivatives were termed Bak-KD-S14, Bak-KD-S15, Bax-KD-S9 and Bax-KD-S10 cells, respectively. The ability of the shRNAs to knockdown the expression of Bak and Bax was confirmed by immunoblotting as shown in Figures 4-37 and 4-38. An interesting observation during the preparation of the Bak and particularly Bax knockdown cells lines was that following initial selection in antibiotic and establishment in culture, the functional knockout cells demonstrated increased growth rates in comparison to control cells (not shown), thus providing additional confirmation of successful shRNA-mediated knockdown. The increased growth rates appeared to be due to attenuation of spontaneous, culture stress-related apoptosis *in vitro* (not shown).

Experiments were also performed to examine whether the induction of Bak/Bax was of functional importance in CD40 killing. It was found that Bak and more prominently Bax played an important role in apoptosis induction, as Bak knockdown attenuated (Figure 4-39) and Bax inactivation completely abolished (Figure 4-40) the activation of caspases-3/7 during CD40-mediated apoptosis. These findings suggested that Bax (and to a lesser extent Bak) plays a critical role during the intrinsic pathway of CD40-mediated apoptosis.

It is well established that Bak and Bax regulate apoptotic cell death by facilitating MOMP, subsequent cytochrome c release and activation of caspase-9 during the intrinsic pathway (Kroemer et al., 2007). Previous studies have demonstrated that caspase-9 activation is essential for CD40-mediated apoptosis (Georgopoulos et al., 2006), however no evidence was provided for cytochrome c release. To formally demonstrate MOMP activation, cell fractionation was used to cellular organelles from different cellular compartments, in particular mitochondrial fractions, which were compared to cytoplasmic lysates. This cellular fractionation approach followed by lysis and immunoblotting was used to investigate changes in mitochondrial permeability during CD40-mediated apoptosis. Having confirmed the integrity of each fraction by confirming fraction-specific expression of Bcl-2 (mitochondrial fraction) and GAPDH (cytoplasmic fraction), it was shown that cytochrome c was released to the cytoplasm of cells undergoing mCD40L-induced apoptosis (Figure 4-41). Although used as a marker for the mitochondrial fraction, it was also interesting to observe a decrease in Bcl-2 in apoptotic cells which is in agreement with previous reports (Bugajska et al., 2002), thus indicating that the reduced Bcl-2 level was not indicative of lack of equal gel loading, but an active down-regulation of Bcl-2.

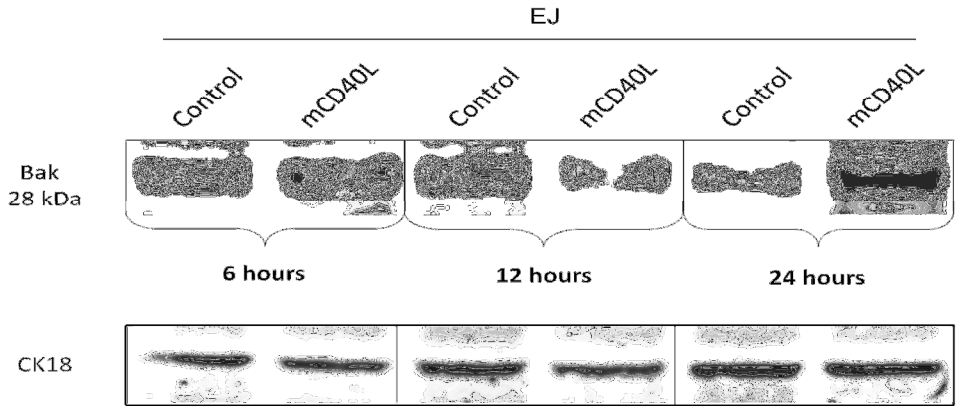


**Figure 4-35 The induction of Bak expression in response to mCD40L**

$2.7x10^6$ EJ were co-cultured with $3x10^6$ MMC treated mCD40L and Controls for 6, 12, and 24 hours in DR/5%FCS/1%L-G in $10cm^2$ culture dishes prior to lysis with 2X SDS-lysis buffer. 20µg of lysates were separated under denaturing conditions by SDS-PAGE using 4-12% (w/v) Bis-Tris gels and then immunoblotted onto a PVDF membrane. The PVDF membrane was probed overnight with an anti-Bak antibody (1:1000 dilution) and then with an anti-CK18 antibody (1:2000 dilution). The membrane was incubated for one hour with goat anti-mouse IgG IRDye 800 (1:10,000 dilution) for the detection of Bak and with goat anti-rabbit IgG Alexa 680 (1:10,000 dilution) for the detection of CK18. Antibody binding was visualised at 700nm and 800nm using an Odyssey™ Infra-red Imaging system.

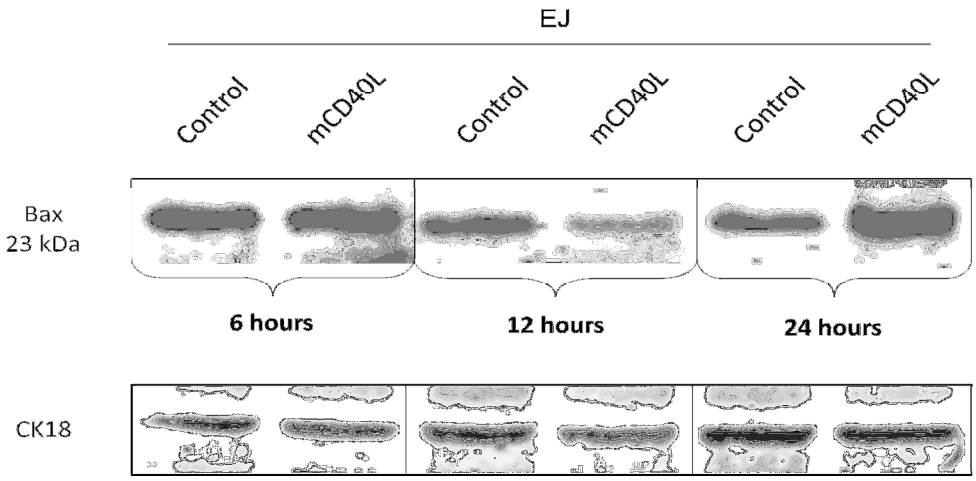


**Figure 4-36 The induction of Bax expression in response to mCD40L**

$2.7x10^6$ EJ were co-cultured with $3x10^6$ MMC treated mCD40L and Controls for 6, 12, and 24 hours in DR/5%FCS/1%L-G in $10cm^2$ culture dishes prior to lysis with 2X SDS-lysis buffer. 20µg of lysates were separated under denaturing conditions by SDS-PAGE using 4-12% (w/v) Bis-Tris gels and then immunoblotted onto a PVDF membrane. The PVDF membrane was probed overnight with an anti-Bax antibody (1:1000 dilution) and then with an anti-CK18 antibody (1:2000 dilution). The membrane was then incubated for one hour with goat anti-mouse IgG conjugated with Alexa 680 in TBS Tween 0.1% (1:10,000 dilution). Antibody binding was visualised at 700nm and 800nm using an Odyssey™ Infra-red Imaging system.

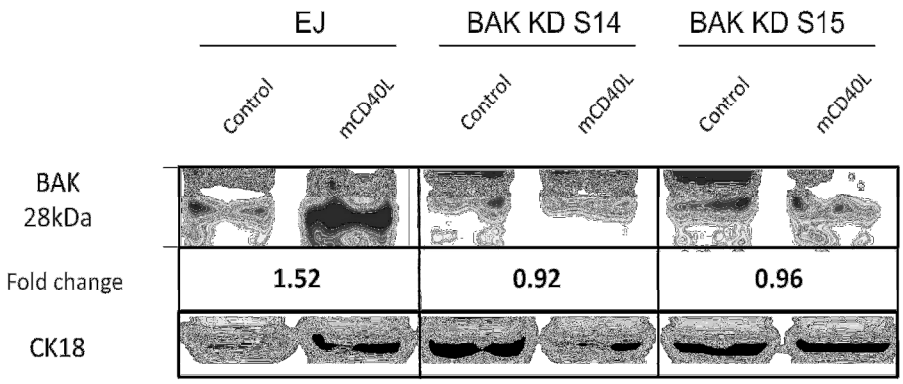


**Figure 4-37 shRNA mediated Bak protein knockdown during CD40-mediated apoptosis**

$2.7x10^6$ EJ, Bak-KD-S14 and Bak-KD-S15 cells were co-cultured with $3x10^6$ MMC treated mCD40L and Controls for 24 hours in DR/5%FCS/1%L-G in $10cm^2$ culture dishes prior to lysis with 2X SDS-lysis buffer. 20-40µg of lysates were separated under denaturing conditions by SDS-PAGE using 4-12% (w/v) Bis-Tris gels and then immunoblotted onto a PVDF membrane. The PVDF membrane was probed overnight with an anti-Bak antibody (1:1000 dilution) and then with an anti-CK18 antibody (1:2000 dilution). The membrane was incubated for one hour with goat anti-mouse IgG IRDye 800 (1:10,000 dilution) for the detection of Bak and with goat anti-rabbit IgG Alexa 680 (1:10,000 dilution) for the detection of CK18. Antibody binding was visualised at 700nm and 800nm using an Odyssey™ Infra-red Imaging system.

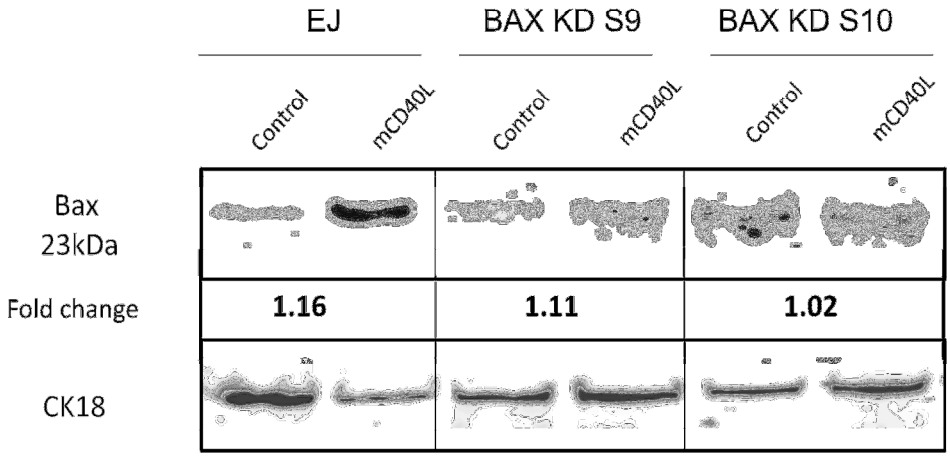


**Figure 4-38 shRNA-mediated Bax protein knockdowns during CD40-mediated apoptosis**

$2.7x10^6$ EJ, Bax-KD-S9 and Bax-KD-S10 cells were co-cultured with $3x10^6$ MMC treated mCD40L and Controls for 24 hours in DR/5%FCS/1%L-G in $10cm^2$ culture dishes prior to lysis with 2X SDS-lysis buffer. 20µg of lysates were separated under denaturing conditions by SDS-PAGE using 4-12% (w/v) Bis-Tris gels and then immunoblotted onto a PVDF membrane. The PVDF membrane was probed overnight with an anti-Bax antibody (1:1000 dilution) and then with an anti-CK18 antibody (1:2000 dilution). The membrane was incubated for one hour with goat anti-mouse IgG Alexa 680 (1:10,000 dilution). Antibody binding was visualised at 700nm using an Odyssey™ Infra-red Imaging system.

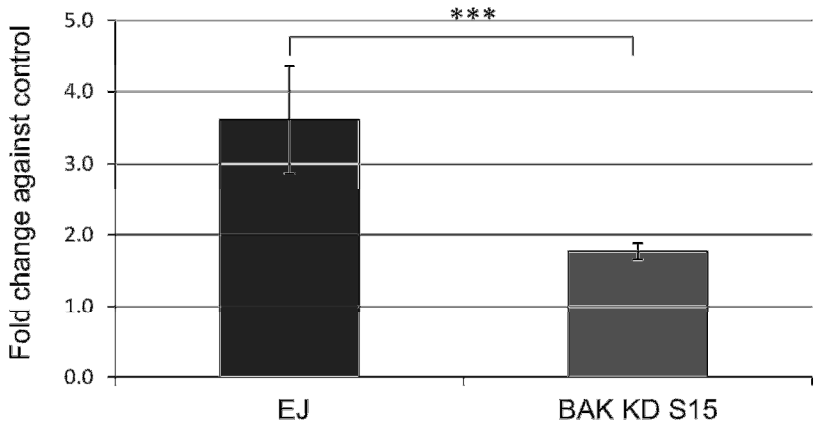


**Figure 4-39 Effect of Bak knockdown on caspase-3/7 activation during CD40-mediated apoptosis**

$8x10^3$ EJ, Bak-KD-S15 were co-cultured with $10^4$ MMC treated mCD40L or Controls in DR/5%FCS/1%L-G in white 96-well plates. SensoLyte 3/7 reagent was added after 48 hours, fluorescence measured (as detailed in Section 2.11.3.1) and background-corrected RFU readings deduced by pair-wise subtraction of mCD40L and Control cell from the respective co-culture. Bars represent mean RFU values for 5-6 technical replicates ± SEM and results are representative of three independent experiments. Stats: *** $P<0.001$, paired student t-test for EJ vs knockdown cells.

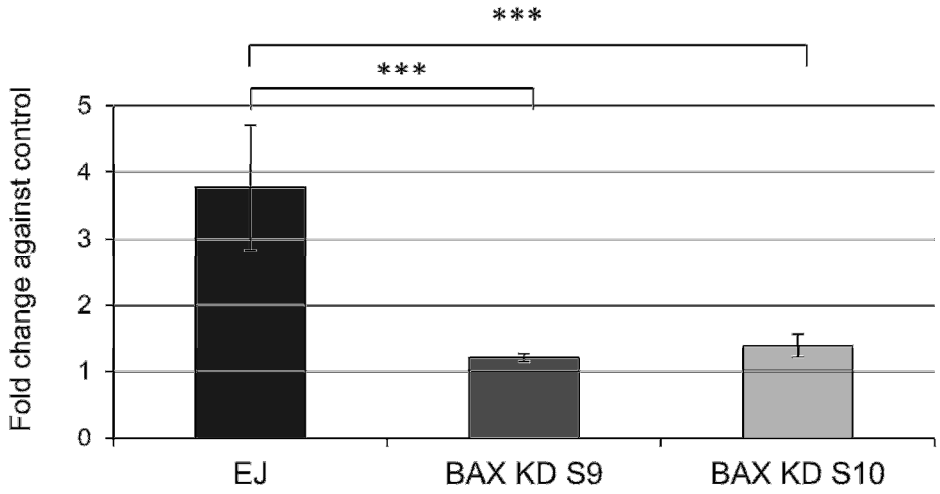


**Figure 4-40 Effect of Bax knockdown on caspase-3/7 activation during CD40-mediated apoptosis**

$8x10^3$ EJ, Bax-KD-S9 and Bax-KD-S10 were co-cultured with $10^4$ MMC treated mCD40L or Controls in DR/5%FCS/1%L-G in white 96-well plates. SensoLyte 3/7 reagent was added after 48 hours, fluorescence measured (as detailed in Section 2.11.3.1) and background-corrected RFU readings deduced by pair-wise subtraction of mCD40L and Control cell from the respective co-culture. Bars represent mean RFU values for 5-6 technical replicates ± SEM and results are representative of three independent experiments. Stats: *** $P<0.001$, paired student t-test for EJ vs knockdown cells.

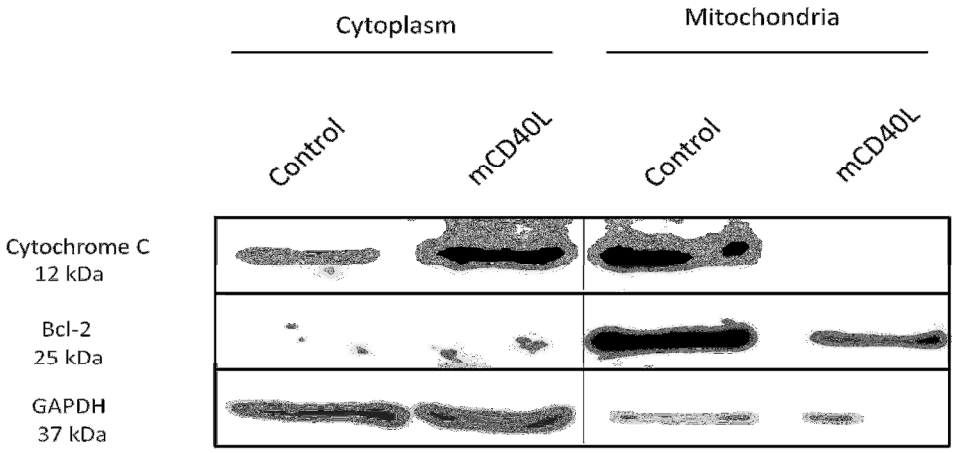


**Figure 4-41 Induction of MOMP by mCD40L**

$2.7x10^6$ EJ cells were co-cultured with $3x10^6$ MMC treated mCD40L and Controls for 24 hours in DR/5%FCS/1%L-G in $10cm^2$ culture before cells were harvested by trypsinisation and processed accordingly to the manufacturers protocol for the Merck mitochondrial isolation kit (section 2.13.2). 20µg of mitochondrial and cytoplasmic lysate was separated under denaturing conditions by SDS-PAGE using 4-12% (w/v) Bis-Tris gels and then immunoblotted onto a PVDF membrane. The PVDF membrane was probed overnight with an anti-Cytochrome C (1:500), anti-GAPDH antibody (1:1000 dilution) and anti-Bcl-2 antibody (1:500). The membrane was incubated for one hour with goat anti-mouse IgG Alexa 680 (1:10,000 dilution). Antibody binding was visualised at 700nm using an Odyssey™ Infra-red Imaging system.

## 4.4 Summary

The first part of the work described in this chapter involved an extensive process in optimisation of immunoblotting techniques to overcome practical constraints imposed by use of the co-culture experimental system. In addition to using human-specific antibody reagents, it was essential to ensure sensitive and accurate detection in proteins of interest to determine their functional role in CD40-signalling. Based on successful optimisation, the largest part of the work described in this chapter permitted for the first time the systematic characterisation of the CD40 apoptotic pathway. The work allowed the confirmation of regulation of signalling components previously implicated in apoptosis and also revealed for the first time their precise mechanisms of action. More importantly, the work led to the identification of novel intracellular mediators and their critical and functional role in CD40-mediated apoptosis.

It was confirmed, in line with previous reports in our laboratory, that mCD40L-CD40 interaction caused a) rapid stabilisation of TRAF3 b) phosphorylation of JNK and c) expression of the pro-apoptotic mediators Bak and Bax (Bugajska et al., 2002, Georgopoulos et al., 2006). Activation of Bak/Bax was shown for the first time to mediate MOMP and cytochrome c release, which is in line with previous observations for an important role for caspase-9 in CD40-mediated apoptosis (Georgopoulos et al., 2006).

Before the work by Georgopoulos and colleagues (2006), the downstream signalling events mediated by mCD40L-CD40 interactions in carcinoma cells were largely unknown. TRAF3 and JNK/AP-1 appeared to be induced and play a role in the regulation of cell death mediated by mCD40L, findings subsequently confirmed by Young and colleagues (Elmetwali et al., 2010b). This study provided for the first time unequivocal evidence for a key role for TRAF3 in mediating CD40-induced apoptosis and this was dependent on its ability to regulate the activation of JNK/AP-1. Exclusively, this study also shows that TRAF3 and JNK/AP-1 regulate the expression of the pro-apoptotic Bcl-2 members Bak/Bax formally now confirming hypotheses previously made elsewhere (Bugajska et al., 2002, Georgopoulos et al., 2006). Having shown that Bak and Bax were induced by CD40 ligation in a TRAF3- and JNK-dependent manner, further Bak and Bax knockdown experiments

suggested a more significant role for Bax (and to a lesser extent for Bak) in apoptosis. Collectively, these findings formally established the critical role of activation of the intrinsic apoptotic pathway in CD40-mediated killing, at least in bladder carcinoma (UCC) cells.

More importantly, the work led to novel observations with regards to the involvement of more proximal intracellular signalling components before activation of distal mediators such as JNK/AP-1. JNK activation is often regulated by MKK4 and/or MKK7 following their activation by ASK1 (Wagner and Nebreda, 2009, Cargnello and Roux, 2011). Expression studies and RNAi experiments on MKK4 revealed that it was induced following CD40 ligation and it directly regulated the phosphorylation of JNK and apoptosis. By contrast, MKK7 did not appear to be induced by CD40 ligation, nor did its loss by RNAi (using shRNA sequences based on previously published siRNAs) affect cell death. This suggested a TRAF3-MKK4-JNK signalling pathway being critical in apoptosis.

The missing link in the CD40 apoptotic signalling axis was the MAPKKK that would be responsible for linking TRAF3 and MKK4/JNK was identified to be the ASK1 kinase, which has previously been implicated in TNF-α (Nishitoh et al., 1998) and Lymphotoxin-mediated apoptosis in some carcinoma cells (Chen et al., 2003). ASK1 was shown for the first time to be highly induced soon after CD40 ligation in a transient manner and RNAi demonstrated that ASK1 was responsible for downstream regulation of the activation of JNK, most likely through MKK4, and was critical in the control of mCD40L-induced apoptosis.

The mCD40L-mediated regulation and functional involvement of ASK1 in CD40-apoptosis was not only an exciting observation unravelling the early events in CD40 signalling in carcinoma cells, but also, because of its implication in ROS-mediated apoptotic responses, provided further clues as to the precise molecular nature of the intracellular mechanisms driving mCD40L-mediated apoptosis. This was the subject of the work described in the following chapter which explored the key mechanisms in ASK1 activation.

# 5.0 Reactive oxygen species and CD40-mediated apoptosis: unravelling the molecular basis of the tumour specificity of CD40 ligation and designing a novel combinatorial CD40 agonist-based anticancer therapy

## 5.1 NADPH oxidases

The NADPH oxidase (Nox) protein family comprises several isoforms, namely NOX -1,-2,-3,-4,-5, DUOX -1 and -2, with each member composed of differential sub-units. Nox transfers electrons from NADPH to oxygen ($O_2$) with subsequent generation of the ROS molecules superoxide anion ($O_2^{\bullet-}$) and Hydrogen Peroxide ($H_20_2$) (Paletta-Silva et al., 2013). Due to their ability to dictate ROS production, which is a well-characterised mutagen, Nox members are linked to the progression of cancers and ageing (Paletta-Silva et al., 2013, Jiang et al., 2011). Additionally Nox-ROS mediated mechanisms may activate stress-responsive MAPKs to regulate ROS-regulated responses such as apoptosis and proliferation, as illustrated in Figure 5-1 (Griendling and Ushio-Fukai, 2000). Cellular exposure to cytotoxic compounds, such as Cisplatin, generates ROS through Nox which activates apoptotic pathways and kills tumour cells (Kim et al., 2010, Benhar et al., 2001).

Emerging evidence has shown that the TNFR superfamily may also utilise Nox via the aforementioned mechanisms to induce ROS mediated cell death (Kim et al., 2007, Gustafson et al., 2012, Bhogal et al., 2012). CD40 has been reported to generate ROS via Nox and TRAF3 as shown in B-cells (Ha and Lee, 2004). The ability of CD40 to induce Nox mediated cell death appears dependent on the redox status of the cell, as shown in hepatocyte ischemia reperfusion of blood platelets expressing CD40 ligands. Bhogal et al show that an already heightened state of oxidative stress, due to the re-entry of oxygenated blood, in addition to CD40 ligation, pushes ROS levels past a cytotoxic threshold thus inducing apoptosis and necrosis (Bhogal et al., 2012). It has been proposed that further understanding of the mechanisms that underlie Nox-mediated ROS generation may allow the lethal induction of tumour-specific oxidative stress, as malignant cells are already under oxidative stress (Paletta-Silva et al., 2013).

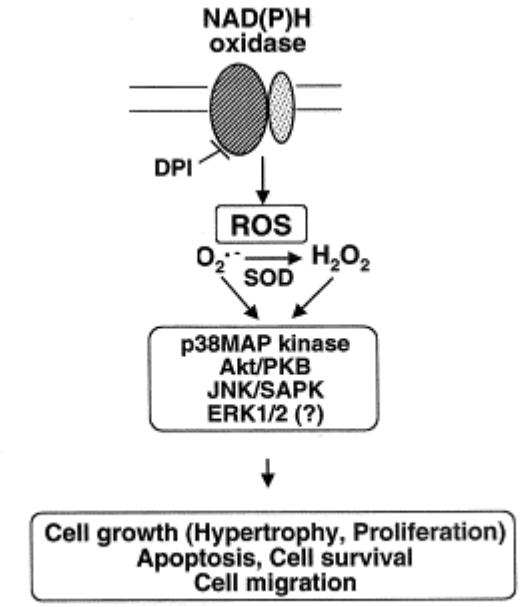


**Figure 5-1 The roles of Nox and ROS in stress signalling**

NADPH oxidase is used to generate ROS but may be pharmacologically inhibited by DPI. The generation of ROS (see section 5.2 activates stress responsive MAPK signalling pathways which lead to the cellular response as stated. Figure adopted from (Griendling and Ushio-Fukai, 2000).

## 5.2 Reactive oxygen species (ROS)

### 5.2.1 Mechanisms of ROS generation and their role as signalling molecules

Nox generates ROS by electron transfer from NADPH to $O_2$ via an FAD heme group, which produces $O_2^{\bullet-}$. ROS include the $O_2^{\bullet-}$, $OH^{\bullet-}$ and $H_20_2$ molecules and the mitochondrion is the major source of ROS production, generating $O_2^{\bullet-}$ from its uptake of $O_2$. $O_2^{\bullet-}$ is converted to $H_20_2$ by superoxide dismutase (SOD) and $H_20_2$ can form water or $OH^{\bullet-}$ depending on whether it reacts with metal ions or is instantly modified to $H_2O$ by gluthathione peroxidise catalase, as illustrated in Figure 5-2 (Winterbourn, 2008, Paletta-Silva et al., 2013, Terada, 2006).

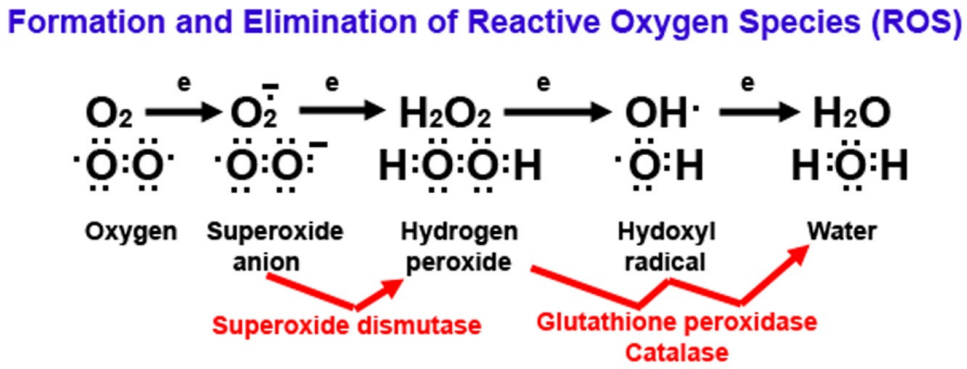


**Figure 5-2 The formation and elimination of ROS**

The acceptance of an electron by oxygen produces the highly reactive superoxide anion. Superoxide anion is converted to hydrogen peroxide by superoxide dismutase (SOD). Hydrogen peroxide may accept electrons to form hydroxyl radicals which are turned into water by Gluthathione peroxidise catalase. Figure adopted from (Terada, 2006).

ROS represent important and ubiquitous secondary messengers additionally their intracellular concentration appears to dictate stress survival or apoptotic responses. Accumulating evidence suggests that low levels of ROS are utilised within the cell as signalling intermediates for normal homeostasis (often proliferation), intermediate levels (although connected to proliferation) may induce a stress response, causing cells to adapt via the expression of anti-oxidants, whereas high levels of ROS at a pro-apoptotic threshold, directly damage cellular structural components and actively induce pathways of apoptosis – see Figure 5-3 (Sena and Chandel, 2012, Terada, 2006, Jiang et al., 2011).

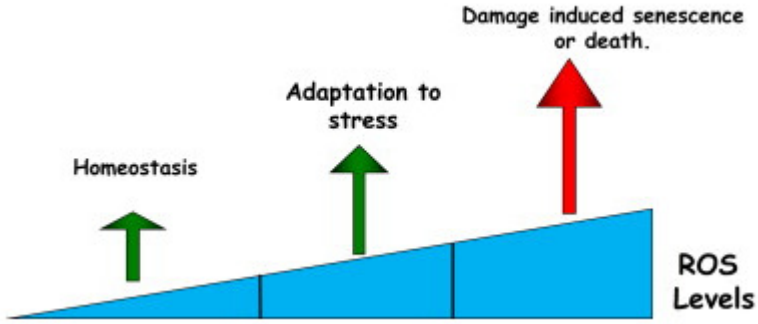


**Figure 5-3 Balance shifts in ROS alter cellular homeostasis**

The production of low ROS is normal during cell homeostasis whereas raised amounts cause cellular adaptation such as increased anti-oxidant expression via NF-kB and Ref-1 pathways. High levels of ROS/oxidative stress activate pathways of apoptosis or cell senescence via p38 or JNK (Taken from Terada, 2006).

## 5.2.2 ROS and malignant transformation

The rapid division rate of tumour cells following oncogene activation and tumour suppressor mutation appears to positively regulate tumour progression via ROS-related mechanisms (Dang, 2012). Studies show that the de novo activation of the oncogenes epidermal growth factor receptor (EGFR), HER-1 and -2 receptor (Trachootham et al., 2006) and H-Ras increase the *in vitro* rate of tumour cell proliferation alongside intrinsic ROS concentrations (Choudhary et al., 2011, Choudhary and Wang, 2009, Choudhary et al., 2010). Furthermore, the over-expression of leukotrine B4 receptor 2 (LTB4R2) gene increases NOX -1 and -4 expression, and causes higher levels of oxidative stress *in vitro* and *in vivo* (Kim et

al., 2009, Shimada et al., 2009). In concert with these findings, the *in vivo* silencing of ROS promoting genes NOX-1 and alkylated DNA repair protein alkB homolog 8 (ALKBH8) reduce oxidative stress (Shimada et al., 2009). Another gene mutated and implicated in bladder cancer is mitochondrial cytochrome B gene (MT-CYB). MT-CYB increases oxidative stress, NF-κB activation, Cyclin-D1 and type IV collagenase, which support the highly malignant properties of tumour cells *in vivo* (Dasgupta et al., 2008). Therefore, there is a strong link between oncogene activation and the production of oxidative stress in epithelial cell models. The significance of tumour suppressors is discussed in detail in Chapter 6.

The increased energy demands required for excessive cell division following oncogene activation cause the mitochondria to produce ROS as natural by-products, which leads to oxidative stress (Trachootham et al., 2006, Trachootham et al., 2009, Chung et al., 2009). The excess ROS causes more DNA damage (mutations) and also activates cell survival and proliferation pathways via NF-κB and Ref-1, which chronically promote carcinogenesis (Weinberg et al., 2010, Angkeow et al., 2002, Li et al., 2009). In addition, it has also been suggested that oxidative stress may leave the cell in the form of $H_20_2$ and advantageously modify the tumour microenvironment for continued growth (Schmielau and Finn, 2001). Therefore, unmanaged ROS production, may promote many properties that hallmark cancer progression.

Nonetheless, despite the proliferative advantage offered by ROS-mediated signalling, the raised oxidative stress in response to hyperproliferative signalling comes at the cell's detriment, as it becomes 'pushed' towards a ROS-associated pro-apoptotic threshold. In fact, it has been shown that *de novo* oncogene expression sensitises non-transformed cells to cisplatin or $H_20_2$ and that this is due to an increased sensitisation of JNK by ROS level augmentation (Benhar et al., 2001, Trachootham et al., 2006). Additionally oncogenic transformation sensitises carcinomas to histone deacetylase inhibitors (HDACIs) (Choudhary and Wang, 2007) a promising new set of drugs for cancer treatment that utilise oxidative stress mediated apoptosis (Marks and Xu, 2009). As they adapt to the higher metabolic needs, cancer cells must manage their intrinsic ROS concentrations by over-expression of antioxidants in order to prevent cell death. This has been well demonstrated by the toxicity of β-phenylethyl isothiocyanate (PITC), a chemical

which disrupts the cell's core antioxidant protein Glutathione (GSH). The pharmalogical inhibitor PITC in combination with cisplatin has shown to be more selective for aggressive tumours over cisplatin alone as the tumour cell is so dependent on the removal of metabolic ROS through intrinsic GSH antioxidant defence (Trachootham et al., 2006). The differences in ROS between normal cells and malignant cells arising during carcinogenesis are now an attractive area of research and are being increasingly recognised as an effective way to target the unavoidable biochemical changes that tumour cells require for progression (Wang and Choudhary, 2011).

## 5.3 Cancer cell antioxidant defence against ROS

### 5.3.1 General

It is well documented that tumour cells over time develop resistance to chemotherapeutic drugs as they modify their environment (Shannon et al., 2003). Since ROS mediated oxidative stress is fundamental to cancer progression, tumour cells adapt by heightening expression of the antioxidant protein families Gluthathione (GSH) and Thioredexin (Trx), thus maintaining intracellular ROS concentrations below critical pro-apoptotic thresholds that may 'push' them towards cell death (Raffel et al., 2003, Godwin et al., 1992). Such over-expression protects cancer cells from the activation of oxidative stress responsive ASK1, the sustained activation of JNK (Liu and Min, 2002, Dorion et al., 2002), and the opening of PTP pores in the mitochondria, all of which can trigger apoptotic death (Damdimopoulos et al., 2002). Additionally, Trx and GSH are found in the mitochondria, where they balance mitochondrial levels of oxidative stress and prevent cell apoptosis along with antioxidant enzymes such as cytochrome c (Aon et al., 2012). The complex roles of Trx and GSH in the management of oxidative stress and ROS-induced cell apoptosis and consequently their influence on cancer progression are becoming increasingly understood.

### 5.3.2 Glutathione (GSH)

GSH is catalysed by the conjugation of GSTps, both of which are reported as over-expressed in many malignancies (Pljesa-Ercegovac et al., 2011). The increased expression of GSH and GSTp serves to protect cancer cells from ROS inducing agents such as chemotherapy, radiotherapy and oxidative stress-inducing cancer drugs (Kato et al., 2000). As a result, targeting the GSH system for depletion may allow the selective targeting of tumour cells by ROS induced cell death as they are already sensitised to oxidative stress compared with their normal counterparts (Estrela et al., 2006, Trachootham et al., 2006). Since GSTp is a biological inhibitor of JNK and ASK1 (Simic et al., 2009) there have been suggestions that GSH depletion may sensitise tumour cells to TNFR mediated apoptosis (Estrela et al., 2006), however no clinical trials have yet been reported utilising this mechanism.

GSH depletion in combination with tumour-apoptotic promoting molecules are suggested to represent the next generation of cancer therapies (Ortega et al., 2011).

JNK activation depends on its release by its biological inhibitor protein GSTp after ROS causes disulphide bond formation and dimerization as illustrated in Figure 5-4 (Adler et al., 1999). *In vivo* studies have shown that genetic knockout of GSTp attenuates JNK activation and in line with this, mice lacking GSTp entail constitutive activation of JNK (and subsequently AP-1), which causes the increased transcription of antioxidant enzymes in order to defend the cell from oxidative stress (Elsby et al., 2003). As the increased expression of GSTp is has been observed in carcinomas of the bladder (UCC), it has been suggested that it may prevent the activation of apoptotic pathways and make tumours highly resistant to chemotherapeutic drugs (Simic et al., 2009). In addition, bladder cancers may over-express superoxide dismutase (SOD) an enzyme which converts superoxide anion to hydrogen peroxide (Hempel et al., 2009).

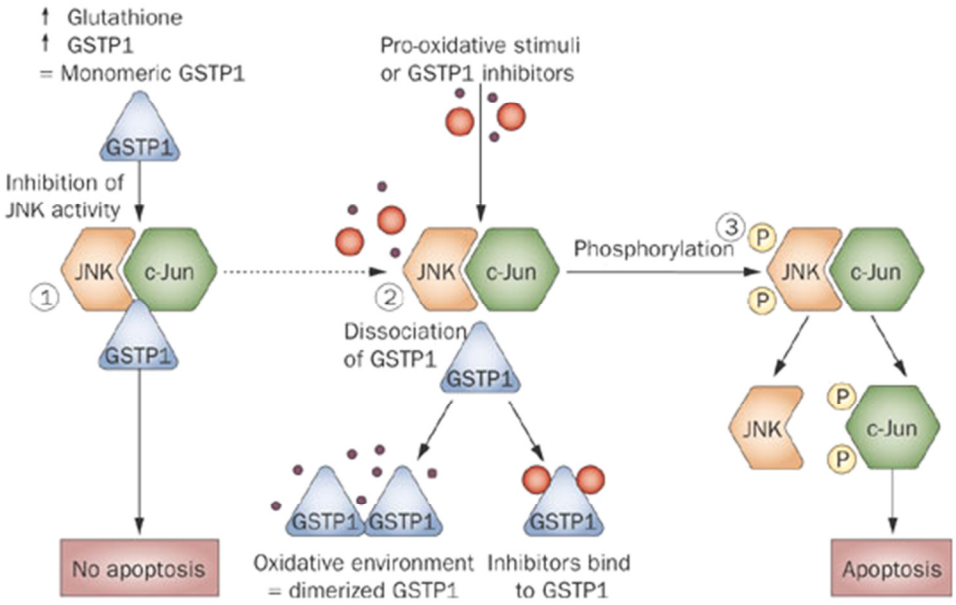


**Figure 5-4 The regulation of JNK by GSTp**

Monomeric GSTp inhibits JNK activity and thus the activation of c-Jun. Increased oxidative stress/high ROS causes GSTp to dimerize and dissociate from JNK allowing it to activate c-Jun and induce cellular apoptosis (for more explanation see 5.3.2). Figure adopted from (Simic et al., 2009).

### 5.3.3 Thioredoxin (Trx)

The human Thioredoxin (Trx) system consists of both Trx and Trx reductase which act as antioxidants to control cellular redox reactions. Reports have shown that Trx translocates from the cytoplasm to the nucleus during oxidative stress to facilitate activation of transcription factors NF-κB, AP-1 and p53 (Hirota et al., 1999, Ueno et al., 1999). Oxidative stress, like many other external stresses, leads to the activation of ROS sensitive MAPK signalling pathways which orchestrate the apoptotic response (Apel and Hirt, 2004) and the most prominent target implicated is mitogen activated protein kinase-kinase-kinase (MAPKKK) apoptosis signalling kinase-1 (ASK1). Reduced Trx is oxidised by ROS/oxidative stress, binds to the N-terminus of ASK1 and following this ASK1 homo-oligomerises and autophosphorylates at Thr845 as illustrated in Figure 5-5 (Liu and Min, 2002).

Clinically the over-expression of Trx in colon tumours has been linked to more aggressive tumours, decreased sensitivity to chemotherapy and overall decreased survival rates (Raffel et al., 2003). Tumours metastasising to the liver have shown an increased expression of Trx. This decreases patient prognosis as it drives the production of VEGF and Ref-1 which are involved in angiogenesis and cell survival (Noike et al., 2008). A phase I clinical trial has shown that cancer patients have Trx blood plasma levels, which are elevated by up to as much as seven fold and this is again correlated with increased production of VEGF. Thus, inhibition of Trx via the use of novel Trx inhibitors, such as PX-12, has been proposed as a cancer therapeutic agent acting to decrease Trx and VEGF in cancer patients (Baker et al., 2006). A phase I study revealed some intolerance in response to intravenous infusions of PX-12 however there were promising reports of increased survival rates (Ramanathan et al., 2009). The intolerances were slightly reduced with greater lengths of infusion time however, the overall conclusion is that PX-12 therapy could lead to pneumonitis (Ramanathan et al., 2011). It has been suggested that future studies should focus on next generation Trx inhibitors if these were to be used as mono-therapies.

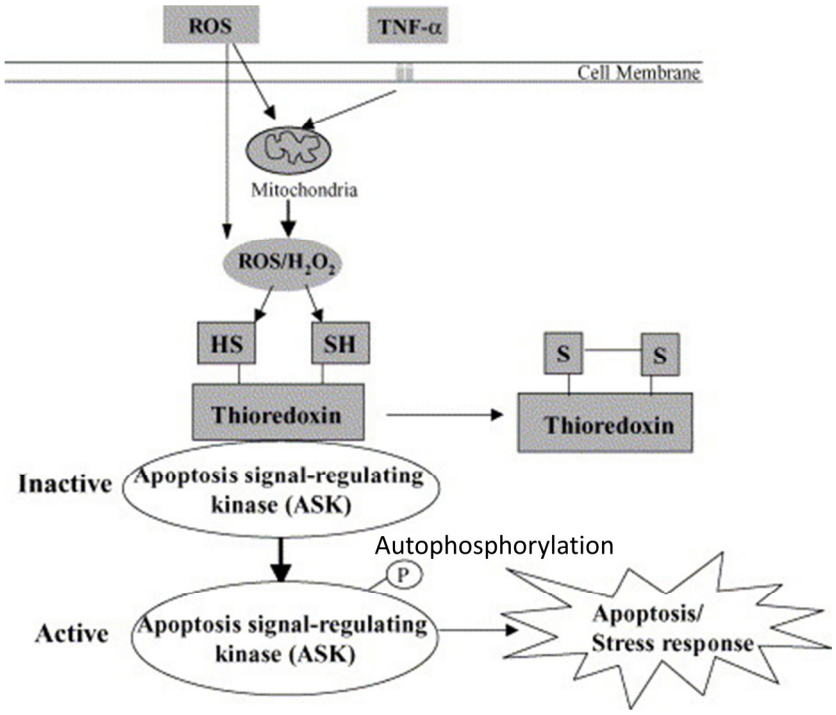


**Figure 5-5 The regulation of ASK1 by thioredoxin**

Under oxidative stress ROS oxidises thioredoxin causing its release from ASK1. ASK1 is autophosphorylated and drives apoptosis or cell stress responses. Figure adopted from (Biswas et al., 2006).

## 5.4 Rationale for the study of ROS and antioxidant defence in CD40 signalling

As detailed above, ROS are natural by-products of mitochondrial oxidative metabolism but also act as a secondary messengers to homeostatically balance cell proliferation and survival (Terada, 2006, Ray et al., 2012). ROS are raised in response to external stress signals such as cytokines, bacterial invasion and xenobiotics in order to alarm the cell there is a need to adapt (Jiang et al., 2011). In circumstances where ROS are not controlled by antioxidants, a cellular state occurs known as 'oxidative stress'. Oxidative stress causes macromolecular damage (Sharma et al., 2004), whilst its chronic persistence is implicated in malignant transformation as it causes DNA damage and thus an increased rate of oncogene and/or tumour suppressor mutations (Valko et al., 2004). The regulatory importance of oxidative stress is clinically manifested by an increased risk of cancers by mutations in the cellular antioxidants GSH and Trx. Yet, paradoxically, numerous cancers over-express antioxidants to defend against oxidative stress occurring from their abnormally high energy production demands (Halliwell, 2007). It has therefore been hypothesised that tumour cells utilise sustained oxidative stress to activate cell proliferation pathways.

However, it is equally well-established that ROS activation plays an important role in pro-apoptotic responses (Circu and Aw, 2010, Biswas et al., 2006) and primarily (although not exclusively) those involving mitochondrial pathways. Thus, collectively, ROS activation represents a 'double-edged sword' (Pan et al., 2009) offering increased proliferation capacity at early stages of malignant transformation yet increasing sensitivity to pro-apoptotic signals. As a consequence of this, it has been suggested that tumour cells may be selectively pushed over a pro-apoptotic 'ROS threshold' in comparison to their normal cell counterparts (Wang and Choudhary, 2011, Raj et al., 2011). Although there are multiple factors to consider in cellular redox management, there is a general consensus that a) low levels of ROS are standard for cell homeostasis, b) raised ROS levels activate stress-responsive cell signalling pathways such as NF-κB and JNK, and c) high ROS/oxidative stress activates intrinsic pathways of cell apoptosis (D'Autreaux and Toledano, 2007, Terada, 2006).

Many members of the TNFR superfamily utilise ROS to regulate cell survival and apoptosis by activating oxidative stress responsive MAPK signalling pathways (Shen and Pervaiz, 2006). The production of ROS is often a consequence of receptor-TRAF interaction with NADPH oxidases (Li et al., 2005, Ha and Lee, 2004, Chandel et al., 2001), which play a designated role in ROS generation (Jiang et al., 2011). Recent, yet limited, evidence suggests that CD40 generates ROS through the 5-lipoxygenase pathway (Ha et al., 2011), whilst TRAF3-NADPH oxidase interactions have previously been implicated (Ha and Lee, 2004). B-cell studies show that low levels of CD40 cross-linking generates low levels of ROS and activates NF-κB whereas high receptor cross-linking generates high oxidative stress, inducing the activation of JNK (Lee and Lee, 2002). Oxidative stress is implicated in the positive regulation of apoptotic pathways as it directly modifies stress responsive proteins (Circu and Aw, 2010). As detailed above, oxidative stress causes the activation of ASK1 via Thioredoxin release and autophosphorylation (Liu and Min, 2002) and the activation of MAPKs via their release from dual-specificity MAPK phosphatases (DS-MKPs) (Bermudez et al., 2010). In parallel, oxidative stress allows the activation of JNK through GSTp release (Simic et al., 2009) and enhances AP-1 formation (Biswas et al., 2006), and there is evidence suggesting that pro-apoptotic members of the Bcl-2 family, such as Bak/Bax are also modified by oxidative stress (Tomiyama et al., 2006, Steckley et al., 2007), as are the enzymatic mediators of cell death, the caspases (Circu and Aw, 2010). In light of this evidence, and results from Chapter 4 implicating a crucial role for ASK-1 in apoptosis, it was hypothesised that ROS-related oxidative stress may have a major influence on CD40-mediated cell death.

To date, there has not been a detailed investigation into the role of CD40-mediated ROS induction in the context of apoptosis in the fate of cells of an epithelial origin. For this purpose, the co-culture system (Figure 3-1) combined with optimised apoptosis assay and immunoblotting techniques were utilised to systematically investigate the possible induction of ROS by mCD40L and to unravel the precise role of ROS generation in the functional outcome of CD40 ligation. In addition, the agonistic monoclonal antibody G28-5 was used (Pound et al., 1999) to compare ROS generation by soluble and membrane CD40 agonists. Equally important, to accomplish an in depth investigation into the influence of ROS on CD40 mediated

killing in malignant versus normal epithelial cells as well as provide evidence as to whether ROS may provide clues as to the tumour-specific capability of CD40 ligation, we utilised our well-established and characterised urothelial system comprising UCC lines EJ, RT112 and RT4 as well as their normal urothelial cell counterparts (Crallan et al., 2006). EJ represents an anaplastic, highly-malignant (invasive) and rapidly proliferative cell line, RT112 a moderately-differentiated, minimally-invasive and moderately-proliferative cell line, whilst RT4 is a highly-differentiated, non-invasive line of lower proliferative capacity. These UCC cell lines retain the characteristics of their respective originating tumour (Masters et al., 1986) and their behaviour has also been re-capitulated using organotypic culture systems (Booth et al., 1997) thus making an ideal model to study ROS with regards to malignant transformation. Uniquely, our laboratory can also utilise a system for the culture of Normal Human Urothelial (NHU) cells from surgical specimens (Southgate et al., 2002) for the *in vitro* comparison of malignant and non-malignant urothelial cells.

## 5.5 Aims

The specific aims of this chapter are:

- To determine, using pharmacological antagonists and cell death assays, whether ROS is a mediator of the CD40 death signalling pathway.

- To use immunoblotting and cell death assays in the presence of pharmacological inhibitors to determine whether NADPH oxidases may be critical regulators of ROS production and CD40-induced apoptosis.

- To use an optimised ROS detection system to determine whether ROS production is a consequence of CD40 engagement in epithelial cell based models.

- To induce oxidative stress in normal, benign, moderately differentiated and anaplastic UCC cell lines and determine their resistance to ROS using cell viability assays.

- To investigate the importance of the ASK-1 and Trx signalling axis (using shRNA mediate interference and pharmacological inhibition) in CD40-mediated apoptosis and determine whether this ROS-modulating pathway provides a mechanistic explanation for the difference in the pro-apoptotic potential for soluble versus membrane CD40 agonists.

- To determine, using pharmacological inhibition of Trx, stably transduced ASK1 shRNA expressing tumour cells and apoptosis assays, whether combinatorial Trx-ASK1 targeting holds therapeutic potential.

- To examine the significance of Glutathione in CD40-mediated apoptosis by its pharmacological inhibition and cell death assays.

## 5.6 Results

### 5.6.1 The role of ROS in CD40-mediated cell death

It was first determined whether ROS-mediated oxidative stress is central to mCD40L-induced cell death. The UCC cell line EJ was co-cultured to achieve mCD40L-CD40 ligation (Figure 3-1) in the presence of the antioxidant/ROS scavenger N-acetyl L-cysteine (NAC), following pre-titration experiments using the CellTiter 96® $AQ_{ueous}$ One Solution Cell Proliferation assay to determine an effective dose (see section 2.11.2 – data not shown). The addition of 30mM NAC during co-culture completely significantly ($p<0.001$) abrogated mCD40L induced cell death as determined by CytoTox-Glo and to a lesser extent caspase-3/7 activation assays (Figures 5-6 and 5-7). To also determine whether oxidative stress is important during early stages of CD40 signalling, or whether a sustained ROS activation is equally essential, CD40 ligation was allowed to proceed for 24 hours after mCD40L-CD40 ligation prior to NAC addition. Results from CytoTox-Glo death detection assays revealed that ROS induced cell apoptosis is reversible when oxidative stress is abrogated up to 24-hours post CD40-mCD40L interaction (Figure 5-7). Moreover mCD40L induced cell death is significantly ($p<0.001$) abolished to the extent seen when NAC is added immediately upon CD40 ligation. These data showed for the first time not only that ROS mediate mCD40L-CD40-mediated apoptosis, but also that oxidative stress requires a sustained period in order to mediate its effect. Although time did not permit the investigation of NAC added at or after 48 hours, it would be interesting to determine at which point over the 72 hour period cell death can be reversed and whether all events (i.e. JNK, Bak/Bax etc) leading to cell apoptosis, require prolonged oxidative stress for their apoptotic potential to be manifested.

### 5.6.2 The role of NADPH oxidase in CD40-mediated cell death

Since it has been shown in B-cells that CD40 generates ROS via TRAF3 and Nox (Ha and Lee, 2004) it was hypothesised that this may also occur in epithelial (carcinoma) cells. It was also hypothesised that attenuation of Nox activity would prevent the production of ROS and hence prevent mCD40L-CD40-mediated cell apoptosis. Following pre-titration experiments using the Cell Titer 96® $AQ_{ueous}$ One Solution Cell Proliferation assay to determine an effective dose (section 2.11.2) (data not shown), the highly specific Nox inhibitor DPI was added during mCD40L-CD40 ligation by means of the co-culture method (Figure 3-1). The addition of DPI completely abrogated mCD40L-CD40-induced cell death in comparison to the control, as determined by CytoTox-Glo death detection assays (Figure 5-8). In addition to a significant reduction in apoptosis ($p<0.001$), DPI prevented the expression of pro-apoptotic Bak, as determined by immunoblotting (Figure 5-9). These data suggest for the first time that CD40-mediated death by membrane ligand in carcinoma cells is dependent on ROS induction by Nox.

Immunoblotting was used to further determine whether ROS production may be linked to the association of TRAF3 with the specific Nox subunit p40-phox as observed by others (Ha and Lee, 2004). Results implied that CD40 engagement generates ROS through p40-phox as this was phosphorylated by 3 and more prominently, 6 hours post mCD40L-CD40 ligation, however no changes were seen in the control (Figure 5-10). Although strictly no direct interaction of TRAF3 and p40-phox was demonstrated here, the results strongly imply that the same mechanism for ROS production by CD40/TRAF3/Nox may occur in both B and carcinoma cells (Ha and Lee, 2004).

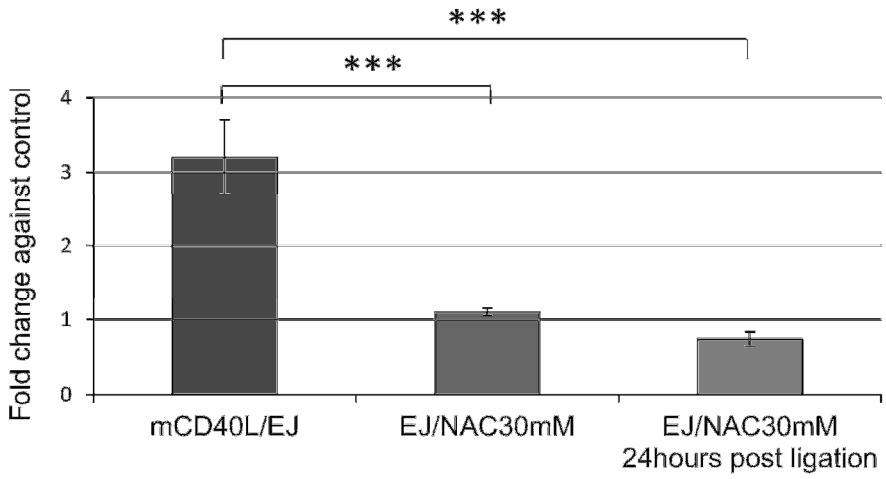


**Figure 5-6 Antioxidants abrogate mCD40L induced cell death**

$8x10^3$ EJ were co-cultured with $10^4$ MMC treated mCD40L or Controls in DR/5%FCS/1%L-G ± 30mM NAC in white 96-well plates. CytoTox-Glo substrate was added after 72 hours (unless otherwise stated), luminescence was measured and background-corrected RLU readings deduced as described in Figure 3-7. Bars correspond to mean values of 5-6 technical replicates ± SEM and results are representative of three independent experiments. Stats: *** $p<0.001$, paired student t-test, EJ vs EJ/NAC.

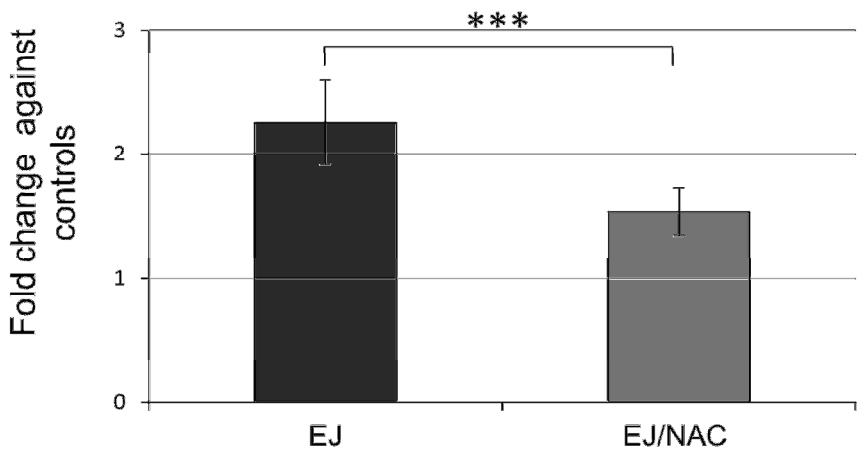


**Figure 5-7 Antioxidants attenuate mCD40L-induced caspase-3/7 activation**

$8x10^3$ EJ were co-cultured with $10^4$ MMC treated mCD40L or Controls in DR/5%FCS/1%L-G ± 30mM NAC in white 96-well plates. SensoLyte 3/7 reagent was added after 48 hours, fluorescence measured (as detailed in Section 2.11.3.1) and background-corrected RFU readings deduced by pair-wise subtraction of mCD40L and Control cell from the respective co-culture. Bars represent mean RFU values for 5-6 technical replicates ± SEM and results are representative of three independent experiments. Stats: *** $p<0.001$, paired student t-test EJ vs EJ/NAC.

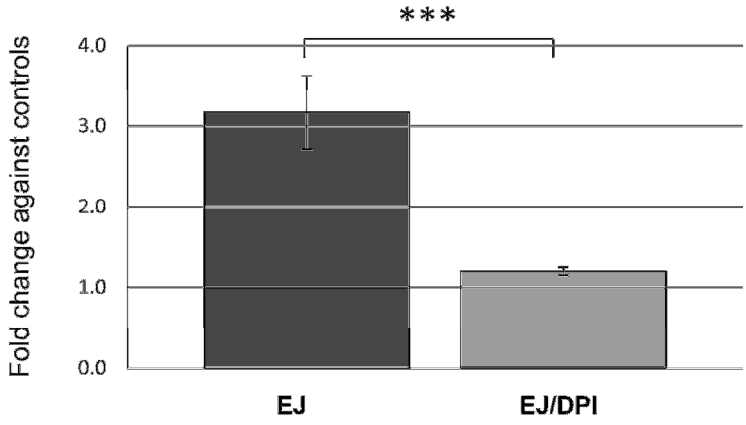


**Figure 5-8 Nox inhibition attenuates CD40-mediated apoptosis**

$8x10^3$ EJ were co-cultured with $10^4$ MMC treated mCD40L or Controls in DR/5%FCS/1%L-G ± 2.5µM DPI in white 96-well plates. CytoTox-Glo substrate was added after 72 hours, luminescence was measured and background-corrected RLU readings deduced as described in Figure 3-7. Bars correspond to mean values of 5-6 technical replicates ± SEM and results are representative of three independent experiments. Stats: *** $p<0.001$, paired student t-test, EJ vs EJ/DPI.

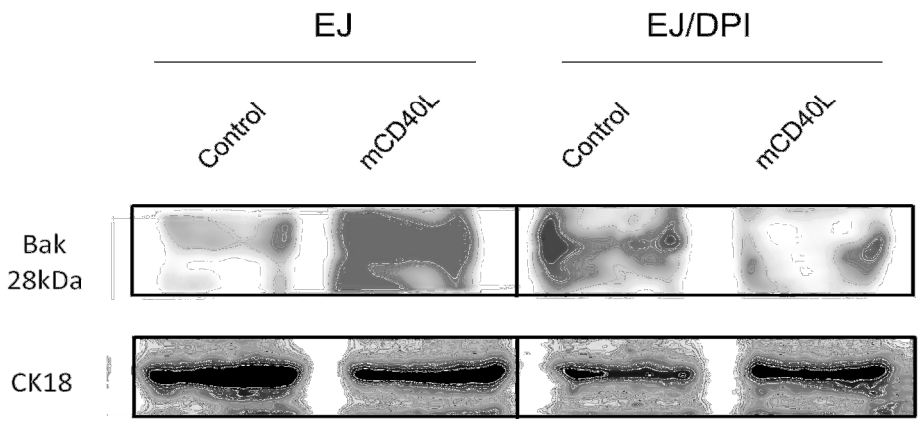


**Figures 5-9 Nox inhibition prevents mCD40L-mediated Bak induction**

$2.7x10^6$ EJ were co-cultured with $3x10^6$ MMC treated mCD40L and Controls for 24 hours in DR/5%FCS/1%L-G ± 2.5 µm DPI and $10cm^2$ culture dishes hours prior to lysis with 2X SDS-lysis buffer. 20µg of lysates were separated under denaturing conditions by SDS-PAGE using 4-12% (w/v) Bis-Tris gels and then immunoblotted onto a PVDF membrane. The PVDF membrane was probed overnight with an anti-Bak antibody (1:500 dilution) and then with an anti-CK18 antibody (1:2000 dilution). The membrane was incubated for one hour with goat anti-mouse IgG Alexa 680 (1:10,000 dilution) for the detection of CK18 and with goat anti-rabbit IgG IRDye 800 (1:10,000 dilution) for the detection of Bak. Antibody binding was visualised at 700nm and 800nm using an Odyssey™ Infra-red Imaging system.

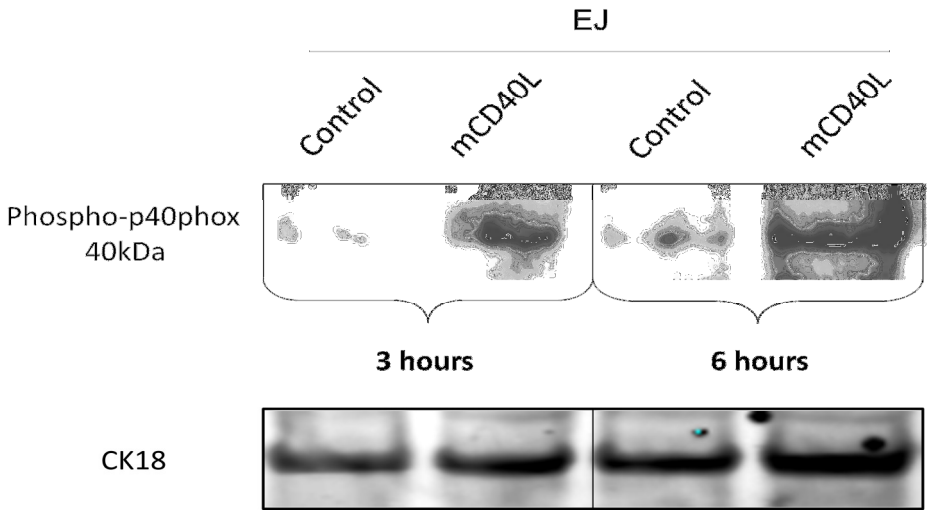


**Figure 5-10 mCD40L-induced p40phox phosphorylation**

$2.7x10^6$ EJ were co-cultured with $3x10^6$ MMC treated mCD40L and Controls for 3 and 6 in DR/5%FCS/1%L-G and $10cm^2$ culture dishes hours prior to lysis with 2X SDS-lysis buffer. 20µg of lysates were separated under denaturing conditions by SDS-PAGE using 4-12% (w/v) Bis-Tris gels and then immunoblotted onto a PVDF membrane. The PVDF membrane was probed overnight with an anti-p40phox antibody (1:500 dilution) and then with an anti-CK18 antibody (1:2000 dilution). The membrane was incubated for one hour with goat anti-mouse IgG Alexa 680 (1:10,000 dilution) for the detection of CK18 and with goat anti-rabbit IgG IRDye 800 (1:10,000 dilution) for the detection of phospho-p40phox. Antibody binding was visualised at 700nm and 800nm using an Odyssey™ Infra-red Imaging system.

### 5.6.3 The optimisation of ROS detection in epithelial cell models

This study as mentioned aimed to provide detailed and functional evidence that mCD40L-CD40-induced apoptosis is dependent on the production of ROS via Nox. To investigate the significance of ROS production in carcinoma cell death the ROS fluorescent marker 6-carboxy-2',7'-dichlorodihydrofluorescein diacetate ($H_2$DCFDA) was used. $H_2$DCFDA is a non fluorescent molecule, however it fluoresces green when oxidised by intracellular ROS (Figure 5-11) and thus the level of fluorescence is relative to the oxidative state of the cells (see section 2.11.6). In initial experiments the three UCC lines RT4, RT112 and EJ were used to determine the concentration of $H_2$DCFDA that would sensitively determine levels of intracellular ROS and discriminate between the different cell lines (as a high reagent excess resulted in misleadingly high fluorescence levels in all cell lines). By accounting for fluorescence background arising from differences in cell line dependent metabolism and division rate (which affects confluency) relative fluorescent values derived from treatment with $H_2$DCFDA were optimised based on natural 'autofluorescence' of the three cell lines (Figure 5-12). During a long series of pre-titration experiments for the optimisation of conditions including a) $H_2$DCFDA concentration, b) incubation periods and c) ROS agonists as positive controls (Staurosporine) (data not shown), it was found that the concentration of 1µM $H_2$DCFDA sensitively and consistently discriminated between intracellular concentrations of ROS (Figure 5-13); these optimised methods for ROS detection were applied for all experiments.

Georgopoulos and colleagues have previously determined the proliferation rate of cell lines EJ, RT112 and RT4 and have shown that EJ have the greatest mitotic rate in comparison to RT112 and RT4 (not shown). In line with previous reports on ROS levels and proliferative capacity (Gupta et al., 1999, Benhar et al., 2001) results in this study showed that cell lines demonstrating higher proliferation rates *in vitro* namely EJ, show a significantly greater ($p<0.001$) production of intracellular ROS over less proliferative cell lines such as RT112 and RT4 (Figure 5-13). It is of note that all cells were cultured in the same culture media and thus the levels of ROS detected were specific to the cell genotype and not to any other variables. This showed for the first time in bladder carcinoma cell lines that the degree of malignant transformation is reflected by the basal rate of ROS production during normal metabolism, in agreement with previous reports (Raj et al., 2011).

### 5.6.4 The induction of ROS by CD40 agonists

This study further determined whether the optimised system for ROS detection could be used to demonstrate ROS induction as a consequence of mCD40L-CD40 engagement, as reported by others (Bhogal et al., 2012, Ha and Lee, 2004, Ha et al., 2011). Target cells EJ were first screened for ROS elevation using the co-culture methods for CD40-mCD40L interaction (section 3.1.1) following fluorescence (RFU) 3T3 cell-associated background correction, as described previously for cell death assays (section 3.3.3.1). The results showed 3-hours post CD40 ligation that mCD40L treated cells have a significantly greater ($p<0.05$) degree of ROS production compared with the controls (Figure 5-14). The earlier time point of 1 hour was investigated, but the results demonstrated no differences at later time points of 4 and 5 hours RFU values were higher in mCD40L-co-cultured EJ cells but the results did not reach statistical significance (not shown). Since this was such a novel finding in the context of CD40 signalling, RT4 another CD40-positive cell line (Bugajska et al., 2002) was for confirmation of CD40-ROS induction, producing comparable results (Figure 5-15).

To further support these observations, the monoclonal antibody (mAb) G28-5, an efficient CD40 agonist in B cells (Pound et al., 1999) was also used to treat carcinoma cells at a concentration of 10µg/ml that was previously optimised for maximal CD40 ligation (Pound et al., 1999). The aim was to test whether the degree of CD40 ligation determines the extent of ROS generation. Unlike mCD40L, G28-5-mediated CD40 ligation caused a very modest increase in detectable ROS compared with control-untreated EJ (Figure 5-16). Thus, for the first time, this study has shown that CD40 ligation causes a rapid increase in production of ROS and this is determined by the 'quality' of the CD40 signal. It was interesting to observe that ASK1 phosphorylation in response to mCD40L-CD40 ligation also occurred at 3-hours which is the point when maximal ROS elevation could be detected – refer back to Figure 4-30.

To further support these findings and provide a mechanistic basis for the results, another series of experiments were performed whereby a variety of conditions and pharmacological inhibition tests were performed at the same time. This was particularly critical due to the nature of the ROS detection assay and in

order to provide a 'fair' and reliable comparison between culture vs co-culture and controls vs drug treated cells. Conditions included a) CD40 co-cultures at 3 hours b) CD40 co-cultures supplemented with NAC at 3 hours c) CD40 co-cultures supplemented with DPI at 3 hours and d) individual culture of EJ supplemented with G28-5 mAb at 1 hour. These findings confirmed that the greatest ROS induction was achieved using mCD40L compared with the soluble agonist G28-5 and more importantly that mCD40L-mediated ROS generation is completely attenuated by DPI and NAC as shown in Figure 5-17. Therefore, implying that mCD40L induced cell death is underpinned by its higher capacity to elevate ROS (than that of soluble agonists) and thus explains why the soluble CD40 agonists do not show apoptotic capacity - as previously reported (Bugajska et al., 2002). Furthermore, and highly importantly, the results demonstrated that the ability of DPI and NAC to prevent mCD40L-induced apoptosis is linked to their ability to prevent the induction of ROS and thus oxidative stress.

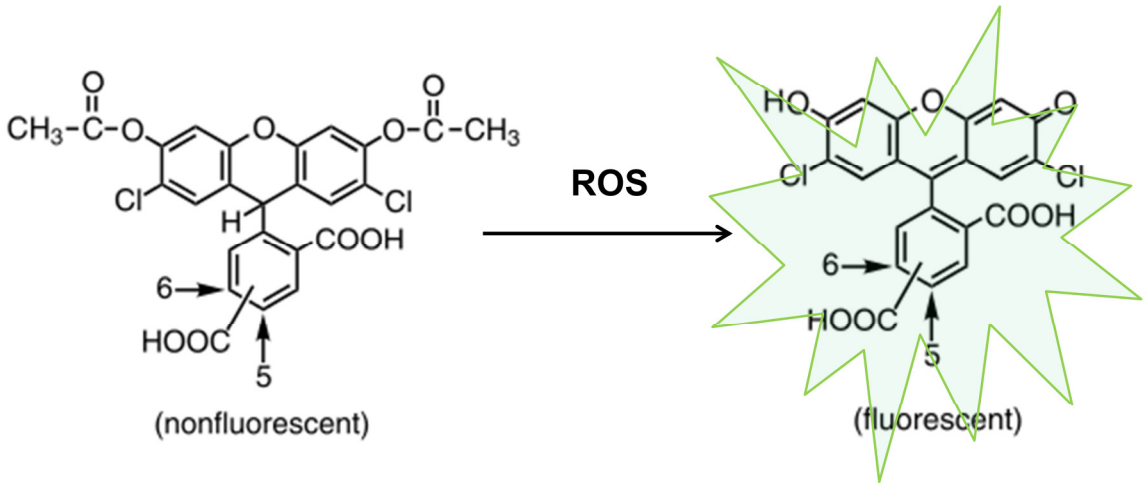


**Figure 5-11 The principle of ROS detection using $H_2$DCFDA**

6-carboxy-2',7'-dichlorodihydrofluorescein diacetate ($H_2$DCFDA) is a derivative of reduced fluorescein that has cell permeability. The reduced forms of fluorescein lack any fluorescence until acetyl groups are removed by intracellular esterase(s) and oxidation is occurring within the cells. When this occurs the charge of the molecules makes it much less likely to leave the cell and also emits detectable fluorescence. The levels of fluorescence intensity deduced are therefore an indication of the intracellular concentration of ROS.

Adapted from http://tools.invitrogen.com/content/sfs/manuals/mp36103.pdf

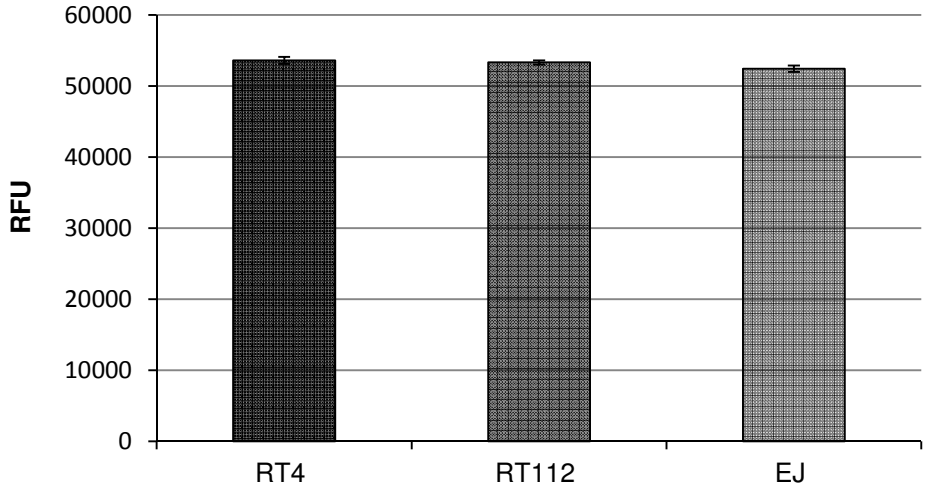


**Figure 5-12 Optimisation experiments for measurement of ROS activation in carcinoma cells (measurement of auto-fluorescence)**

$8x10^3$ RT4, RT112 and EJ were plated for 24 hours in DR/5%FCS/1%L-G in white 96-well plates. The next day all lines were assessed for their relative autofluorescence at Excitation 485nm/Emission 520nm in the presence of PBS. Bars represent mean RFU values for 11-12 technical replicates ± SEM and results are representative of three independent experiments.

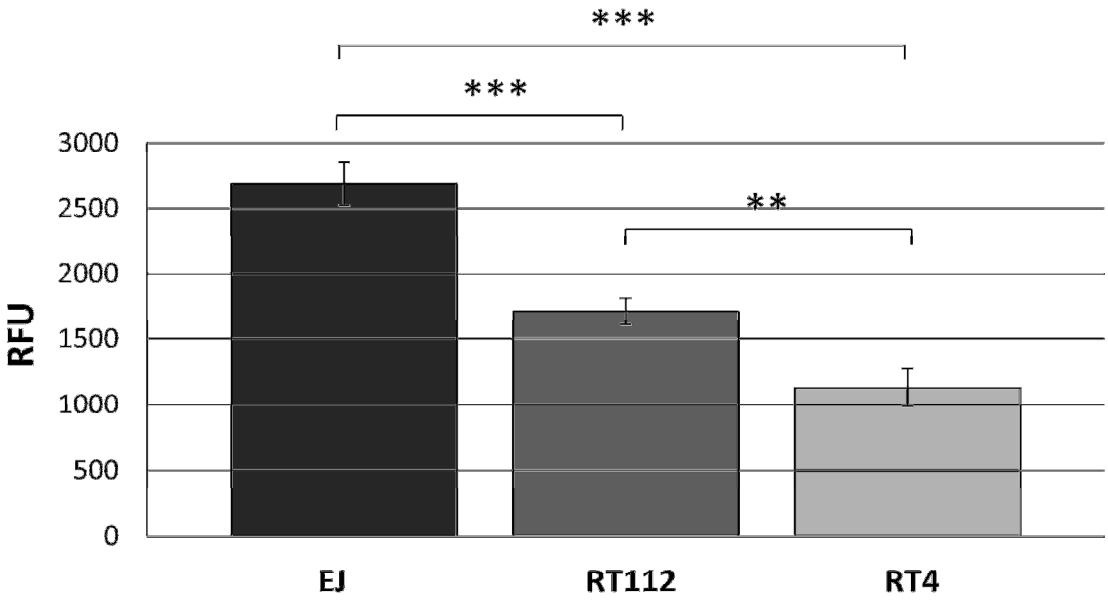


**Figure 5-13 Basal ROS production relative to tumour grade**

$8x10^3$ RT4, RT112 and EJ were plated for 24 hours in DR/5%FCS/1%L-G in white 96-well plates. Cells were first washed with PBS to remove any culture medium and were then treated with 1µM of $H_2$DCFDA in pre-warmed (37°C) PBS for 30 minutes 37℃ in 5% $CO_2$. Cells were background corrected by subtraction of the relative autofluorescence (Figure 5-7). Bars represent mean RFU values for 24 technical replicates ± SEM and results are representative of three independent experiments. Stats: ** $p<0.01$, *** $p<0.001$ unpaired student t-test for EJ vs RT4, EJ vs RT112 and RT112 vs RT4.

**A)**

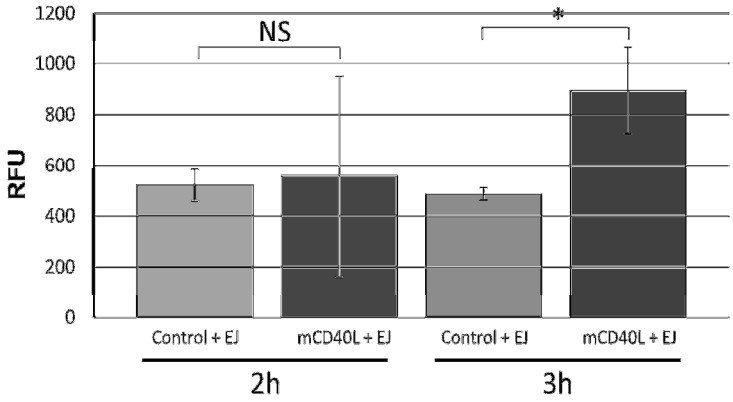


**B)**

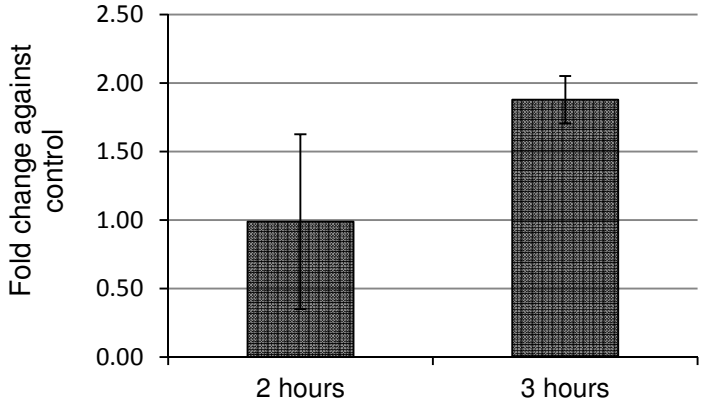


**Figure 5-14 mCD40L-mediated ROS induction in EJ cells**

$8x10^3$ EJ were co-cultured with $10^4$ mCD40L or Controls in DR/5%FCS/1%L-G in white 96-well plates. Cells were first washed with PBS to remove any culture medium and were then treated with 1µM of $H_2$DCFDA in pre warmed (37°C) PBS for 30 minutes 37℃ in 5% $CO_2$. Background-corrected RFU readings deduced by pair-wise subtraction of mCD40L and Control cells from the respective co-culture. Data is presented as A) mean RFU values and B) Fold change against controls for 5-6 technical replicates ± SEM and results are representative of three independent experiments. Stats: NS – non-significant * $p<0.05$, paired student t-test mCD40L/EJ vs Control/EJ.

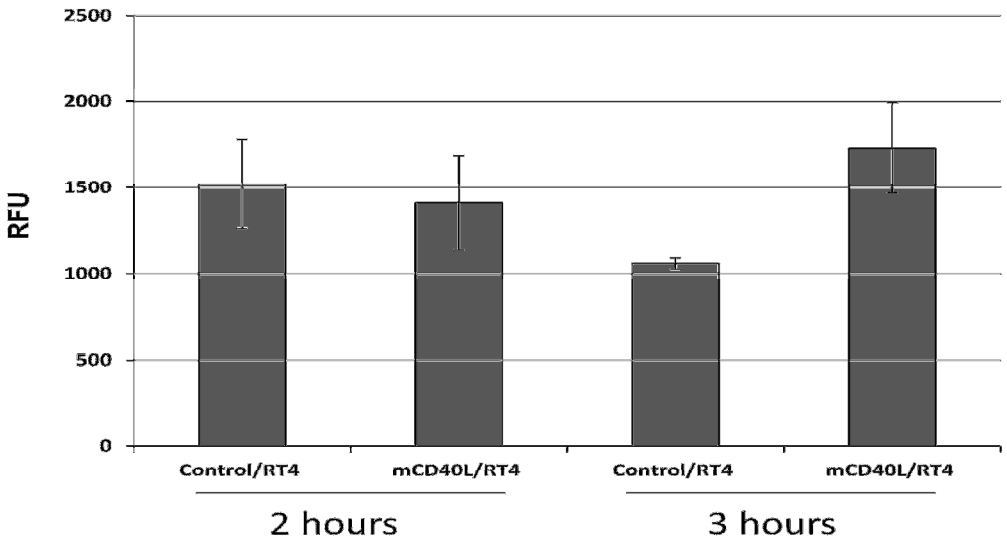


**Figure 5-15 mCD40L mediated ROS induction in RT4 cells**

$8x10^3$ RT4 were co-cultured with $10^4$ mCD40L or Controls in DR/5%FCS/1%L-G in white 96-well plates. Cells were first washed with PBS to remove any culture medium and were then treated with 1µM of $H_2$DCFDA in pre warmed (37℃) PBS for 30 minutes 37℃ in 5% $CO_2$. Background-corrected RFU readings deduced by pair-wise subtraction of mCD40L and Control cells from the respective co-culture. Bars represent mean RFU values for 5-6 technical replicates ± SEM and results are representative of three independent experiments.

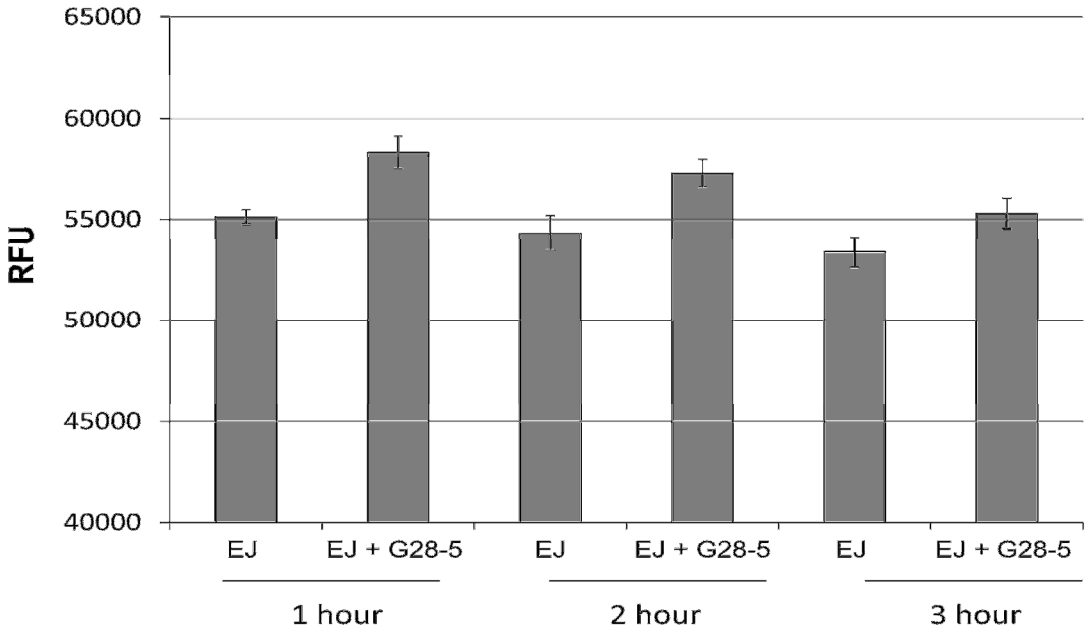


**Figure 5-16 Soluble CD40 agonist mediated ROS induction**

$8x10^3$ EJ were cultured in DR/5%FCS/1%L-G and white 96-well plates ± G28-5 (10µg/ml). Cells were first washed with PBS to remove any culture medium and were then treated with 1µM of $H_2$DCFDA in pre warmed (37°C) PBS for 30 minutes 37℃ in 5% $CO_2$. Bars represent mean background-corrected RFU values for 5-6 technical replicates ± SEM and results are representative of three independent experiments. The y-axis minimal value has been set at 40,000 RFU for easier comparison of maximal readings for different conditions.

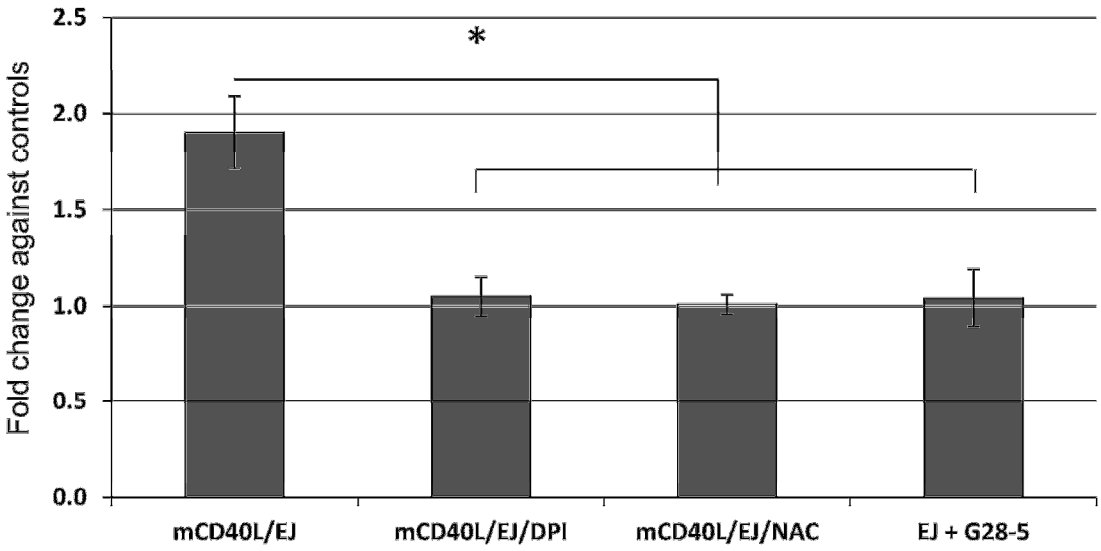


**Figure 5-17 DPI and NAC attenuate CD40-mediated ROS generation**

$8x10^3$ EJ were co-cultured with $10^4$ mCD40L or Controls in ± NAC or DPI. $8x10^3$ and EJ were cultured alone all in DR/5%FCS/1%L-G and white 96-well plates. Cells alone were subject to 10µg/ml G28-5 treatment. Cells were first washed with PBS to remove any culture medium and were then treated with 1µM of $H_2$DCFDA in pre-warmed (37°C) PBS for 30 minutes 37℃ in 5% $CO_2$. Co-cultures were background corrected by pair-wise subtraction of mCD40L and Control cells from the respective co-culture, EJ were background corrected by their relative autofluorescence. Results are presented as fold change (from generated RFU) by comparing T/EJ versus C/EJ) where T= treated cells and C= controls cells. Bars represent mean RFU values for 5-6 technical replicates ± SEM and results are representative of three independent experiments. Stats:, * $p<0.05$ paired student t-test.

### 5.6.5 The susceptibility of bladder tumour cells lines to exogenous ROS

A study by Bugajska et al (2002) used the established UCC model EJ, RT112 and RT4 to show that the susceptibility of carcinoma cells to CD40-mediated apoptosis correlates with malignant phenotype. By contrast, normal urothelial cells (NHU) are resilient to mCD40L-induced cytotoxicity but become susceptible when malignantly transformed *de novo* by engineered introduction of genetic alterations observed in malignant transformation (Shaw et al., 2005). Based often on similar approaches, for instance engineered introduction of oncogenes, recent studies have provided increasing evidence that the degree of cell malignancy correlates with increased ROS production and that this makes such cells potentially selectively sensitive to further ROS insults (Benhar et al., 2001, Trachootham et al., 2006, Trachootham et al., 2009, Raj et al., 2011).

On the basis of this and results in this chapter, demonstrating that each UCC line has various intracellular concentrations of basal ROS, the three UCC lines that represent different degrees/stages of malignancy were used to investigate their relative susceptibility to oxidative stress. To stimulate a ROS-mediated oxidative stress in EJ, RT112 and RT4 cells hydrogen peroxide ($H_2O_2$) was utilised. $H_2O_2$ is culture media soluble and is a natural source of ROS within cells produced during respiration, albeit at low levels under physiological conditions. The cells contain catalases and other enzymes that detoxify $H_2O_2$, however at a specific threshold it induces apoptosis or necrosis (Kahl et al., 2004). Initial experiments involved the pre-titration of $H_2O_2$ using the CellTiter 96® $AQ_{ueous}$ One Solution Cell Proliferation assay, in order to optimise an effective range of concentrations. The results showed that there are marked differences between the more malignant UCC cell line EJ, compared with the less anaplastic lines (RT112 and RT4) in terms of their capability to manage oxidative stress (Figure 5-18), which is in agreement with previous reports (Benhar et al., 2001). Strikingly, EJ had lost the ability to proliferate at concentrations where RT112 and RT4 remained 100% viable suggesting that malignant cells are selectively far more sensitive to oxidative stress. In addition at $H_2O_2$ concentrations where EJ had perished, RT112 and RT4 lines still retained around 40-50% viability. Further to this, it was interesting to observe that although at lower ROS insults RT112 were more resistant than RT4, when exposed to higher

$H_2O_2$ concentrations RT112 showed increased vulnerability. This confirms the clear correlation of susceptibility to ROS and degree of anaplasty and suggests that tumours are 'wired' for differential responses to oxidative stress.

In correlating these findings with previous observations that mCD40L-CD40 engagement kills UCC cells whilst sparing their normal counterparts (Shaw et al., 2005, Bugajska et al., 2002) (also see Chapter 6), it was hypothesised that this resistance to CD40 ligation may be due to their ability to withstand ROS/oxidative stress insults. To explore this, normal urothelial cells (NHU) were subjected to a range of $H_2O_2$ concentrations previously shown to be dose-dependently toxic to EJ cells, and they were then assessed for their relative viability as described above. It is of note that EJ and NHU were both treated with $H_2O_2$ in KSFMc culture medium to remove the variable that different culture medium (i.e. DR/5%FCS/1%L-G) may contain different antioxidant activities. As evident in Figure 5-19, NHU cells were able to withstand ROS insults at doses 4-fold greater than EJ cells; in fact at a concentration of up to 3200µM where EJ were completely killed, NHUs remained 100% viable. These findings provide indirect evidence that the resistance of NHUs to CD40-mediated apoptosis may be linked to their ability to withstand ROS-associated cytotoxicity that leads to lethal oxidative stress in their malignant counterparts. Interestingly, not only were NHU cells resistant to oxidative stress, but instead at lower doses, $H_2O_2$ caused an increase rather than a decrease in cell biomass/number.

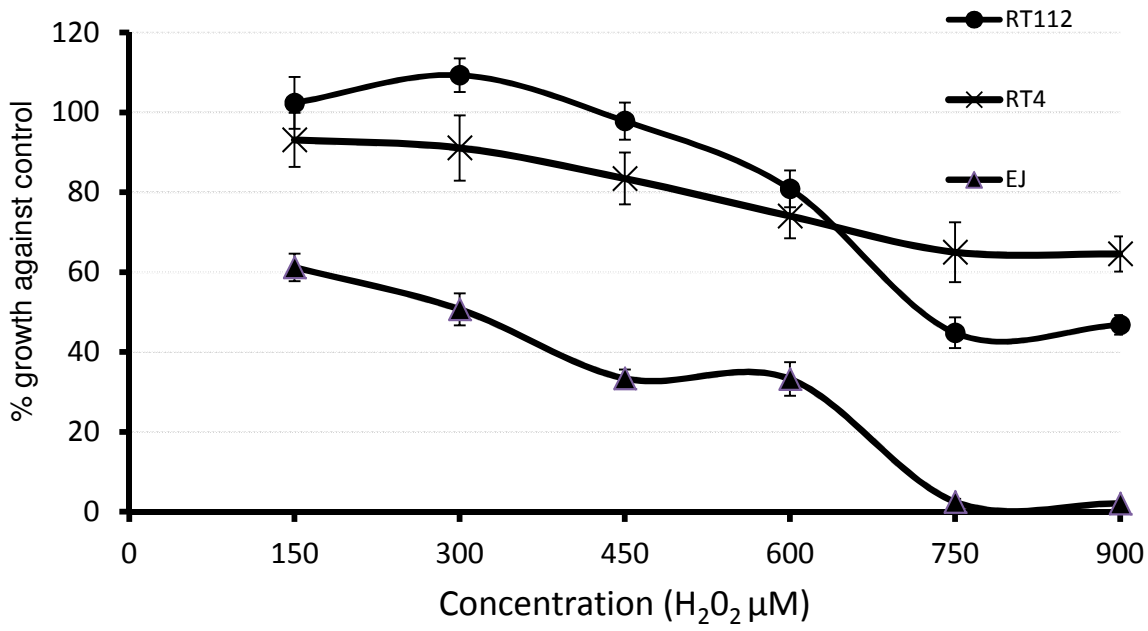


**Figure 5-18 $H_2O_2$ susceptibility of UCC cell lines**

$8x10^3$ RT4, RT112 and EJ were seeded and allowed to adhere for 24 hours in DR/5%FCS/1%L-G in transparent 96-well plates and subject to a range of $H_2O_2$ concentrations for 24 hours. 20µl of CellTiter 96® $AQ_{ueous}$ One Solution was added to appropriate wells and plates were incubated at 37℃ in 5% $CO_2$ for a total of 24 hours prior to the measurement of absorbance (Abs) at 492nm. Cell viability was calculated as percentage viability in comparison to controls using the following formula: (T/C) x100, where T= treated cells and C= controls cells. Bars represent mean Abs values for 5-6 technical replicates ± SEM and results are representative of three independent experiments.

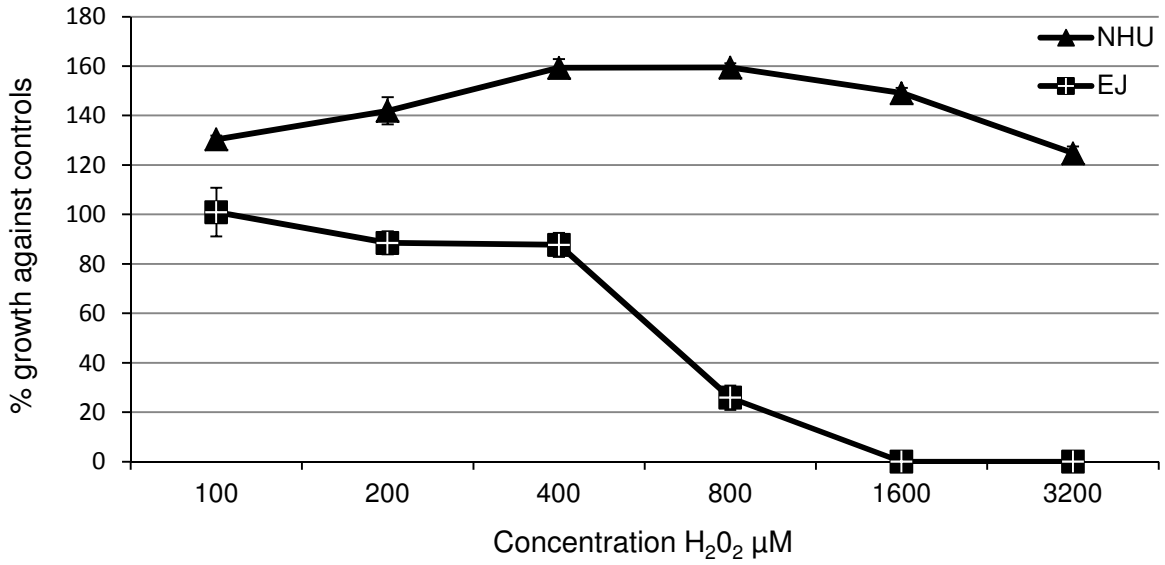


**Figure 5-19 Susceptibility of normal (NHU) and malignant (EJ) urothelial cells to $H_20_2$ cytotoxicity**

$8x10^3$ NHU and EJ were seeded for 24 hours in KSFMc in transparent 96-well plates before being subjected to a range of $H_2O_2$ concentrations for 24 hours. 20µl of CellTiter 96® $AQ_{ueous}$ One Solution was added to appropriate wells and plates were incubated at 37°C in 5% $CO_2$ for a total of 24 hours prior to the measurement of Abs. Cell viability was calculated as percentage viability in comparison to controls using the following formula: (T/C) x100, where T= treated cells and C= controls cells. Bars represent mean Abs values for 5-6 technical replicates ± SEM and results are representative of three independent experiments.

### 5.6.6 ASK1 and Thioredoxin (Trx) in CD40-mediated apoptosis: pharmacological inhibition of Trx transforms soluble CD40 agonist to a potent pro-apoptotic signal *in vitro*

In Chapter 4, it was shown that CD40-mediated apoptosis is dependent on the activation of ASK1. ASK1 is regulated by Trx which under physiological ROS levels physically binds ASK1 and inhibits its autophosphorylation and thus activation. During oxidative stress, Trx scavenges ROS, however in doing so it releases ASK1 which undergoes activation via autophosphorylation at Thr845 (Soga et al., 2012).

Based on the findings shown in this and the previous chapter, it was hypothesised that pharmacological inhibition of Trx may allow more constitutive signalling of ASK1, which would facilitate CD40-mediated apoptosis possibly via MKK4-JNK. To investigate this, EJ were subject to mCD40L-CD40 ligation using the co-culture method (Figure 3-1) in the presence of the most specific commercially available pharmacological inhibitor of Trx, PX-12. The inhibitor was added at near sub-cytotoxic concentrations as determined by pre-titration experiments using the CellTiter 96® $AQ_{ueous}$ One Solution Cell Proliferation assay (data not shown). It was found that Trx inhibition could not significantly enhance the potency of the membrane ligand in the activation of caspases-3/7 after 24 or 48-hours post-ligation as shown in Figure 5-20a and 5-20b. In addition Trx inhibition did not further enhance total levels of mCD40L-induced apoptosis as determined by CytoTox-Glo death detection assays shown in Figure 5-21. These findings suggested that mCD40L is a strong pro-apoptotic signal that achieves maximal ROS elevation and hence ASK1 activity in carcinoma cells, implying that it results in maximal Trx/ROS-'occupancy' for rapid release of ASK1 within less than 3 hours post-ligation. To support this theory, immunoblotting was used to examine the expression of Trx over a CD40-mCD40L 24 hour time window. Strikingly, it was found that Trx expression appeared to be abrogated by mCD40L-CD40 ligation beginning with low expression at 3 hours with a further gradual decrease over 6, 12, and 24 hour intervals. Even more interesting was the gradual increased expression of Trx in the Controls (Figure 5-22) suggesting that during *in vitro* cell culture, tumour cells progressively increase Trx possibly as a cyto-protective mechanism against culture related stress. In support of this result, it has been observed that Trx inhibition growth inhibits carcinoma cells *in vivo* (Welsh

et al., 2003) suggesting appropriate levels of Trx expression are necessary for continued cell proliferation.

As the present work strongly implied a ROS-driven apoptotic pathway was triggered by mCD40L and suggested that the weakly pro-apoptotic nature of soluble agonists was due to its inability to efficiently trigger adequate ROS levels to 'occupy' Trx and release ASK1, it was further hypothesised, that pharmacological Trx inhibition may sensitise cells to soluble CD40 agonist-mediated cell apoptosis. This likely due to a combined effect on ASK1 activation and the overall cellular redox status. Strikingly, although neither inhibitor or soluble agonist alone had little significant apoptotic activity, it was found that the Trx inhibitor PX-12 could act in synergy with the soluble CD40 agonist G28-5 (10µg/ml) to significantly increase cell death ($p<0.01$) as determined by CytoTox-Glo (Figure 5-23) and caspase-3/7 apoptosis assays (Figure 5-24). Visual observations on cell morphology using phase contrast microscopy implied also that a) G28-5 was non-toxic to EJ cells, b) PX-12 was largely growth inhibitory and c) combination of PX-12 and G28-5 (PX-12/G28-5) was visibly pro-apoptotic (Figure 5-25). This suggested that tumour cells can be sensitised to previously weakly apoptotic soluble CD40 agonists by pharmacological intervention of redox sensitive pathways. Moreover, the level of apoptosis observed with the PX-12/G28-5 combinatorial treatment was equivalent to that obtained in co-cultures indicates that the combination of soluble agonist plus Trx inhibitor is functionally equivalent (at least in terms of pro-apoptotic potential) to mCD40L alone.

As it was hypothesised that Trx inhibition sensitised EJ to soluble CD40 agonist-generated ROS oxidative stress, it was determined whether NAC could prevent PX-12/G28-5 mediated apoptosis. The PX-12/G28-5 combination treatment was added to UCC cell line EJ in the presence of 15mM NAC and assessed for toxicity using CytoTox-Glo cell death detection assays. As shown in Figure 5-26, the toxicity of PX-12/G28-5 is completely attenuated by NAC to that equal of the controls thus demonstrating death is ROS/oxidative stress mediated. With regards to the suggestion that Trx inhibition may facilitate apoptosis via the autophosphorylation of ASK1 at Thr845, ASK1-KD-S18 cells (see section 4.3.5) were also assessed for their sensitivity to PX-12/G28-5 induced cell toxicity. As determined by CytoTox-Glo, RNAi mediated knockdown of ASK1 completely abrogated cell death in response to PX-12/G28-5 down to levels observed in the control (Figure 5-27) and also significantly

($P<0.001$) abrogated caspase-3/7 activity EJ, compared to PX-12/G28-5-treated untransduced EJ (Figure 5-28). Collectively these results strongly support the notion that PX-12/G28-5 combinatorial treatment functionally mimics mCD40L and is likely to utilise the same ROS/oxidative stress/ASK1-dependent pathway of apoptosis as mCD40L.

To support the universality of the findings, sub-cytotoxic concentrations of PX-12 were also applied to a CD40 positive colorectal carcinoma (CRC) cell line HCT116, which are highly susceptible to CD40 ligation and undergo rapid apoptosis within less than 12 hours post-ligation (Mohamed, Dunnill and Georgopoulos, manuscript in preparation). In line with bladder carcinoma cells, the PX-12/G28-5 combinatorial treatment also showed significant ($p<0.01$) cell toxicity in CRCs compared with G28-5 or PX-12 alone (Figure 5-29) as determined by CytoTox-Glo cell death detection assays. It was interesting to observe that CRC cells required a concentration that was between 20-40x lower than required in the UCC cell line EJ to bring them to a sub-cytotoxic threshold (data not shown). It should be noted that in these assays the fold change in Cytotox-Glo readings appeared moderate in comparison with the observations with UCC cells. Although this is currently under investigation, it appeared the PX-12/G28-5 combinatorial treatment was so much more efficient at inducing CRC cell death that a more necrotic (rather than apoptotic) response was observed, hence the more modest fold-change values observed in the Cytotox-Glo apoptosis assays.

Finally the carcinoma cell-specificity of PX-12/G28-5 combinatorial treatment was tested by utilising normal human urothelial (NHU) cells. NHU cells obtained from surgical specimens are CD40 positive (Bugajska et al., 2002) and thus were used to determine the tumour cell specificity of PX-12/G28-5 induced cell apoptosis. As shown in Figure 5-30 the combinatorial treatment was specifically toxic to EJ cells and not to its normal NHU cell counterparts. Based on previous findings that PX-12/G28-5 mediated cell death is ROS-driven and that NHU are highly resilient to oxidative stress, it can be hypothesised that the lack of toxicity was due to the ability of normal cells to withstand ROS insults. Collectively, these results indicate that the PX-12/G28-5 combinatorial treatment appears to be qualitatively (tumour-specific) and quantitatively equivalent to mCD40L.

A)

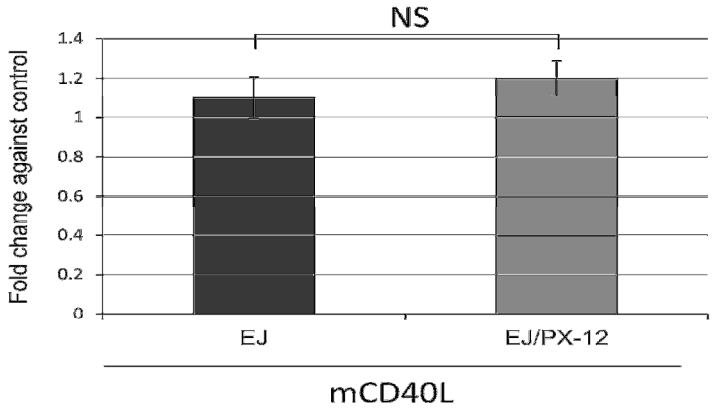


B)

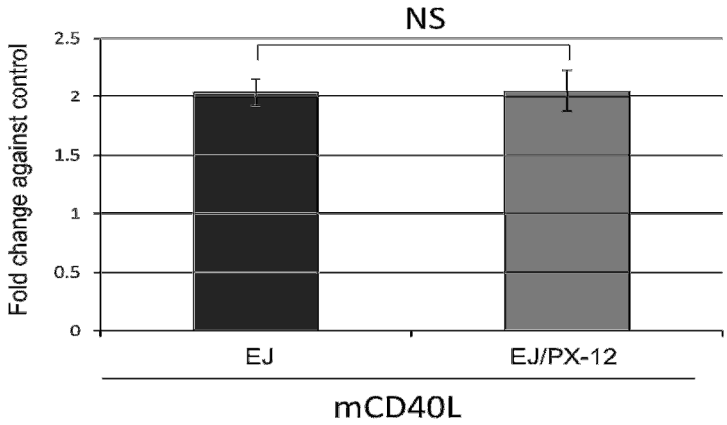


**Figure 5-20 Pharmacological Trx inhibition does not enhance mCD40L-induced caspase-3/7 activation**

$8x10^3$ EJ were co-cultured with $10^4$ MMC treated mCD40L or Controls in DR/5%FCS/1%L-G in white 96-well plates ± 2µM PX-12. SensoLyte 3/7 reagent was added after A) 24 hours or B) 48 hours, fluorescence measured and background-corrected RFU readings deduced by pair-wise subtraction of mCD40L and Control cell RFU from mCD40L/EJ and Control/EJ RFU readings. Bars correspond to mean values of 5-6 technical replicates ± SEM. Stats: NS – non-significant, paired student t-test, EJ/PX-12 vs EJ.

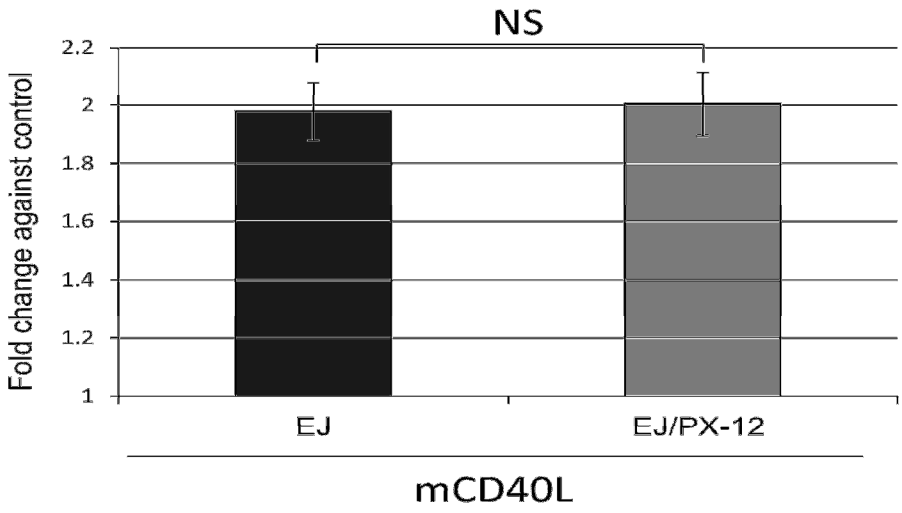


**Figure 5-21 Trx inhibition does not enhance mCD40L-induced cell apoptosis**

$8x10^3$ EJ were co-cultured with $10^4$ MMC treated mCD40L or Controls in DR/5%FCS/1%L-G in white 96-well plates ± 2µM PX-12. CytoTox-Glo substrate was added after 72 hours, luminescence was measured and background-corrected RLU deduced as described in Figure 3-7. Bars correspond to mean values of 5-6 technical replicates ± SEM. Stats: NS – non-significant, paired student t-test, EJ/PX-12 vs EJ.

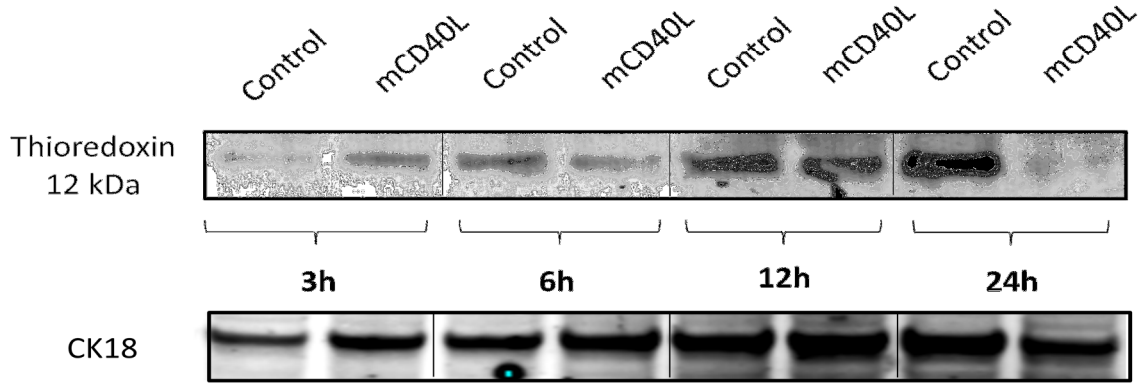


**Figure 5-22 Progressive reduction of Trx expression following CD40 ligation**

$2.7x10^6$ EJ were co-cultured with $3x10^6$ MMC treated mCD40L and Controls for 3, 6, 12 and 24 hours in DR/5%FCS/1%L-G in $10cm^2$ culture dishes prior to lysis with 2X SDS-lysis buffer. 20µg of lysates were separated under denaturing conditions by SDS-PAGE using 4-12% (w/v) Bis-Tris gels and then immunoblotted onto a PVDF membrane. The PVDF membrane was probed overnight with an anti-Trx antibody in TBS Tween 0.1% (1:500 dilution) and then with an anti-CK18 antibody in TBS Tween 0.1% (1:2000 dilution). The membrane was incubated for one hour with goat anti-mouse IgG IRDye 800 (1:10,000 dilution) for the detection of Trx and with goat anti-rabbit IgG Alexa 680 (1:10,000) for the detection of CK18. Antibody binding was visualised at 700nm and 800nm using an Odyssey™ Infra-red Imaging system.

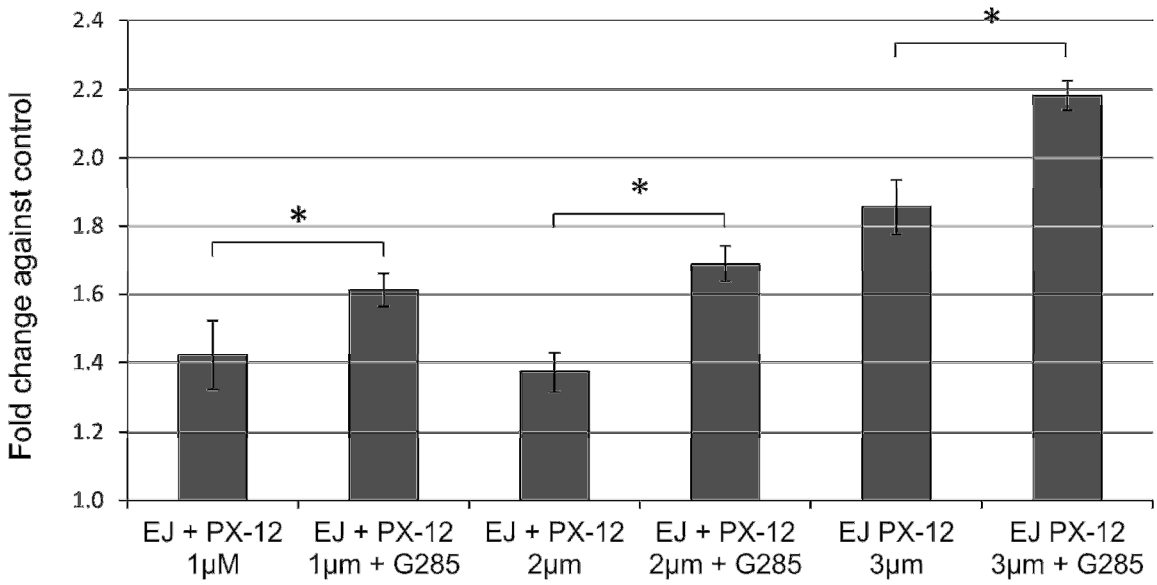


**Figure 5-23 Trx inhibition sensitises UCC cells to soluble CD40 agonists**

EJ were seeded at a density of $8x10^3$ in DR/5%FCS/1%L-G in white 96-well plates. PX-12 was added at various concentrations (see graph) for one hour before the addition of G28-5 (10μg/ml). CytoTox-Glo substrate was added after 48 hours and RLU was assessed reflecting total levels of cell death. Results are presented as fold change (from generated RLU) by comparing T/EJ versus C/EJ, where T/EJ= treatment of EJ with agonists (PX-12 & G28-5) and C/EJ = control EJ. Bars correspond to mean values of 5-6 technical replicates ± SEM and results are representative of three independent experiments. Stats: * $p<0.05$, paired student t-test, T/EJ vs C/EJ).

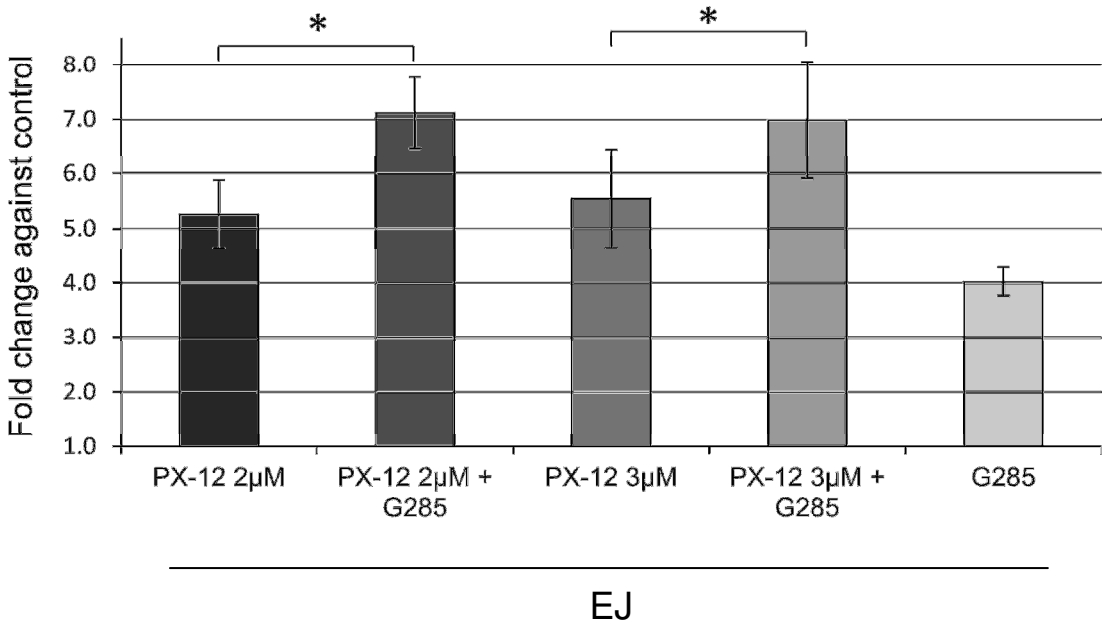


**Figure 5-24 Trx inhibition in combination with soluble CD40 agonist induces-caspase-3/7 activation**

EJ were seeded at a density of $8x10^3$ in DR/5%FCS/1%L-G in white 96-well plates. PX-12 was added at various concentrations (see graph) for one hour before the addition of G28-5 (10μg/ml). SensoLyte 3/7 reagent was added after 24 hours and RFU was assessed reflecting total levels of cell death. Results are presented as fold change (from generated RFU) by comparing T/EJ versus C/EJ, where T/EJ= treatment of EJ with agonists (PX-12 & G28-5) and C/EJ = control EJ. Bars correspond to mean values of 5-6 technical replicates ± SEM and results are representative of three independent experiments. Stats: * $p<0.05$, paired student t-test, T/EJ vs C/EJ).

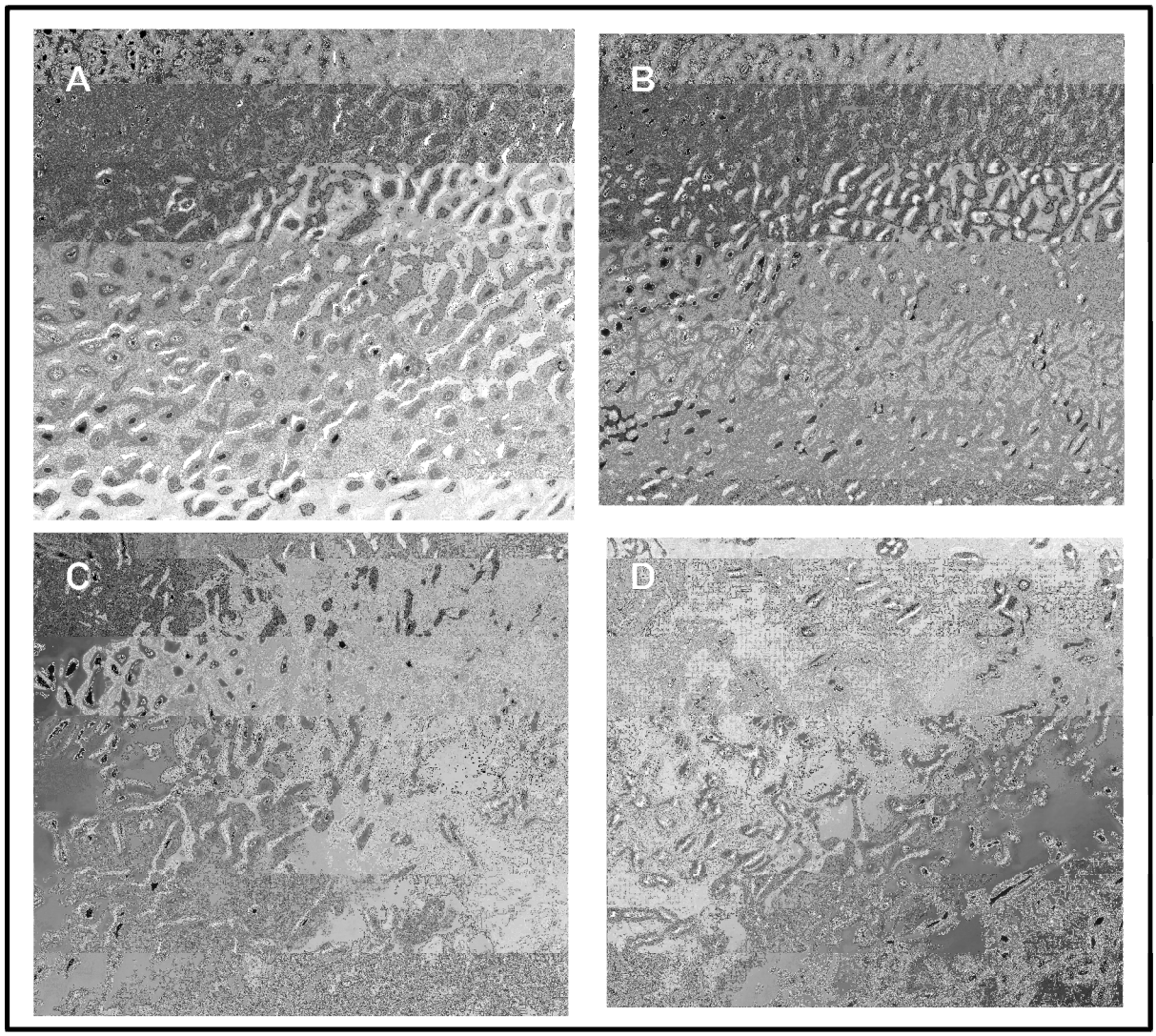


**Figure 5-25 Phase contrast microscopy of cells treated with Trx/soluble agonist combination in 96-well plates**

EJ were seeded at a density of $8x10^3$ in: DR/5%FCS/1%L-G and treated with:

A) Medium alone (control)
B) G28-5 mAb (10µg/ml)
C) 2µM PX-12
D) 2µM PX-12 + G28-5 mAb (10µg/ml)

Images were taken using an inverted microscope (x100 magnification) after 48 hours of treatment.

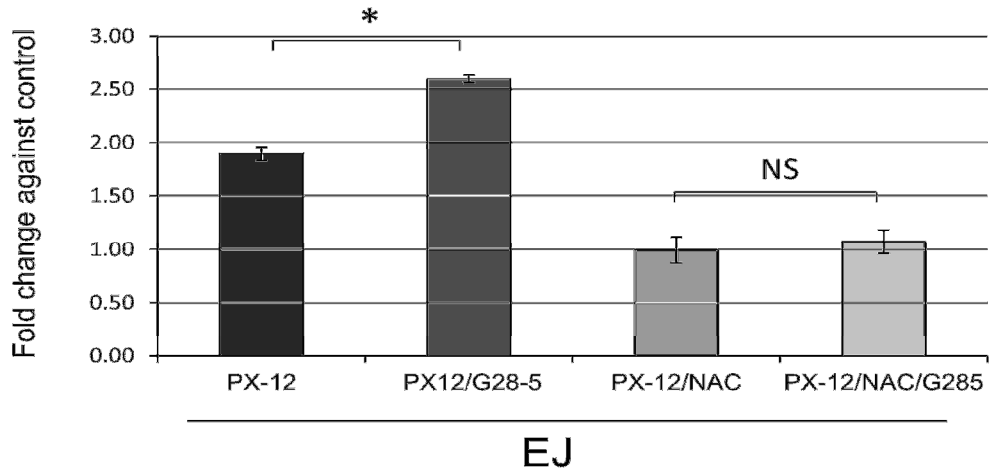


**Figure 5-26 Antioxidants prevent PX-12/G28-5-mediated apoptosis**

EJ were seeded at a density of $8x10^3$ in DR/5%FCS/1%L-G in white 96-well plates. PX-12 was added at 2µm for one hour before the addition of G28-5 (10µg/ml) plus NAC (15mM). CytoTox-Glo substrate was added after 48 hours and RLU was assessed reflecting total levels of cell death. Results are presented as fold change (from generated RLU) by comparing T/EJ versus C/EJ, where T/EJ = treatment of EJ with drugs (PX-12, G28-5 & NAC) and C/EJ = control EJ. Bars correspond to mean values of 5-6 technical replicates ± SEM and results are representative of three independent experiments. Stats: NS – non-significant * $p<0.05$, paired student t-test, T/EJ vs C/EJ).

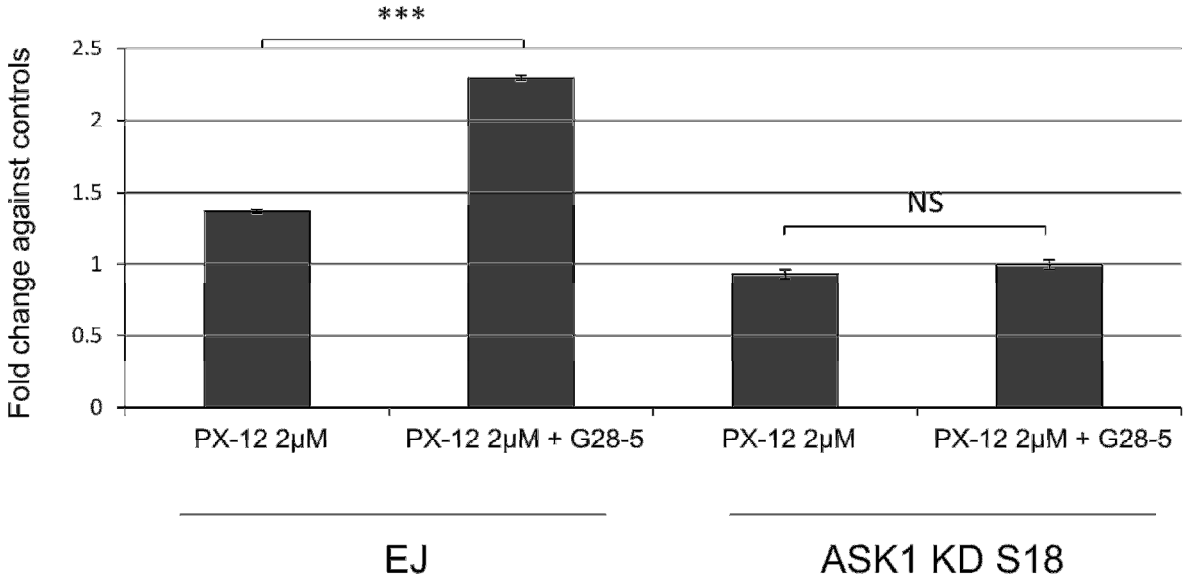


**Figure 5-27 ASK1 regulates PX-12/G28-5-mediated apoptosis**

EJ and ASK1-KD-S18 cells were seeded at a density of $8x10^3$ in DR/5%FCS/1%L-G in white 96-well plates. PX-12 was added at 2µm for one hour before the addition of G28-5 (10µg/ml) CytoTox-Glo substrate was added after 24 hours and RLU was assessed reflecting total levels of cell death. Results are presented as fold change (from generated RLU) comparing T/EJ *versus* C/EJ or T/ASK1-KD-S18 *versus* C/ASK1-KD-S18, where T/EJ= treatment of EJ with drugs (PX-12 & G28-5) and C/EJ = control EJ or T/ASK1-KD-S18 = treatment of ASK1-KD-S18 with drugs (PX-12 & G28-5) and C/ASK1-KD-S18 = Control ASK1-KD-S18. Bars correspond to mean values of 5-6 technical replicates ± SEM and results are representative of three independent experiments. Stats: NS - non-significant *** $p<0.001$, paired student t-test, T/EJ vs C/EJ and T/ASK1-KD-S18 vs C/ASK1-KD-S18.

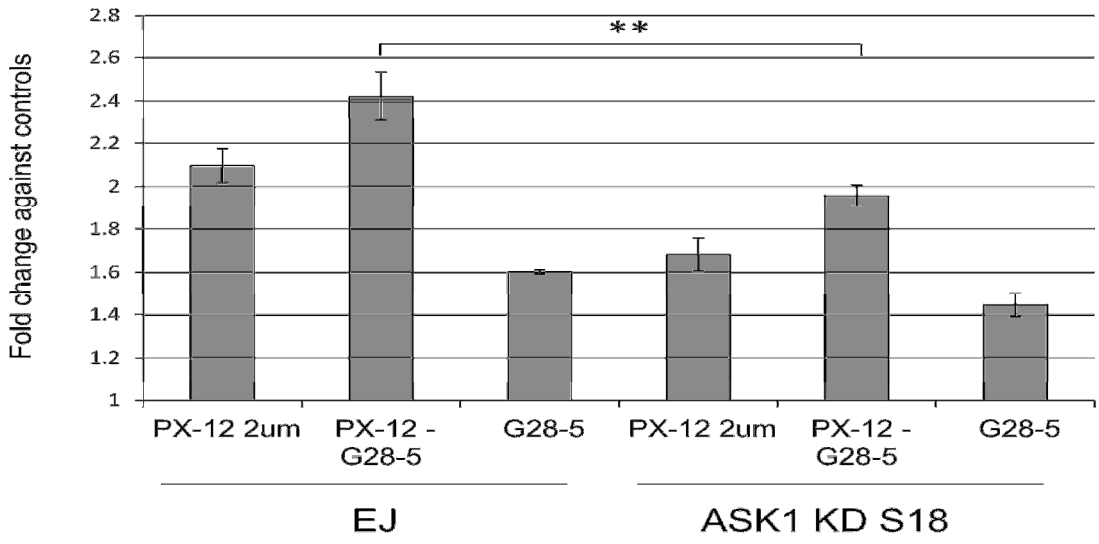


**Figure 5-28 ASK1 regulates PX-12/G28-5 mediated caspase-3/7 activation**

EJ and ASK1-KD-S18 cells were seeded at a density of $8x10^3$ in DR/5%FCS/1%L-G. PX-12 was added at 2µM for one hour before the addition of G28-5 (10µg/ml). SensoLyte 3/7 reagent was added after 24 hours and RFU was assessed reflecting total levels of cell death. Results are presented as fold change (from generated RFU) comparing T/EJ *versus* C/EJ or T/ASK1-KD-S18 *versus* C/ASK1-KD-S18, where T/EJ= treatment of EJ with drugs (PX-12 & G28-5) and C/EJ = control EJ or T/ASK1-KD-S18 = treatment of ASK1-KD-S18 with drugs (PX-12 & G28-5) and C/ASK1-KD-S18 = Control ASK1-KD-S18. Bars correspond to mean values of 5-6 technical replicates ± SEM and results are representative of three independent experiments. Stats: ** $p<0.01$, paired student t-test, T/EJ vs C/EJ and T/ASK1-KD-S18 vs C/ASK1-KD-S18.

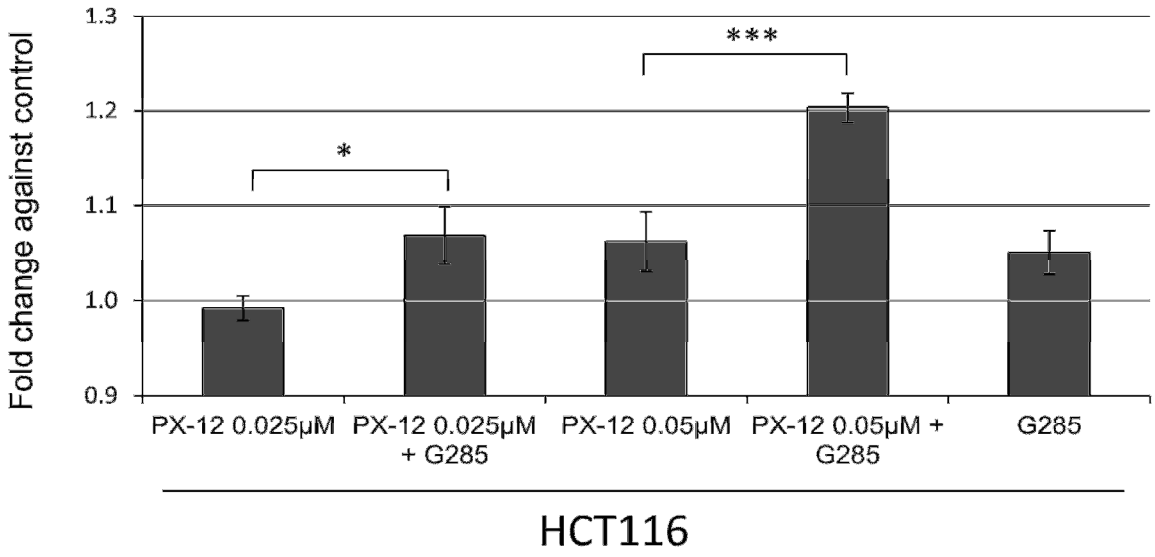


**Figure 5-29 Colorectal carcinoma cells are sensitive to PX-12/G28-5-mediated apoptosis**

HCT116 were seeded at a density of $8x10^3$ in DR/5%FCS/1%L-G in white 96-well plates. PX-12 was added at various concentrations (see graph) for one hour before the addition of G28-5 (10µg/ml). CytoTox-Glo substrate was added after 24 hours and RLU was assessed reflecting total levels of cell death. Results are presented as fold change (from generated RLU) by comparing T/HCT116 versus C/HCT116, where T/HCT116 = treatment of EJ with agonists (PX-12 & G28-5) and C/HCT116 = control HCT116. Bars correspond to mean values of 5-6 technical replicates ± SEM and results are representative of three independent experiments. Stats: * $p<0.05$, *** $p<0.001$, paired student t-test, T/HCT116 vs C/HCT116).

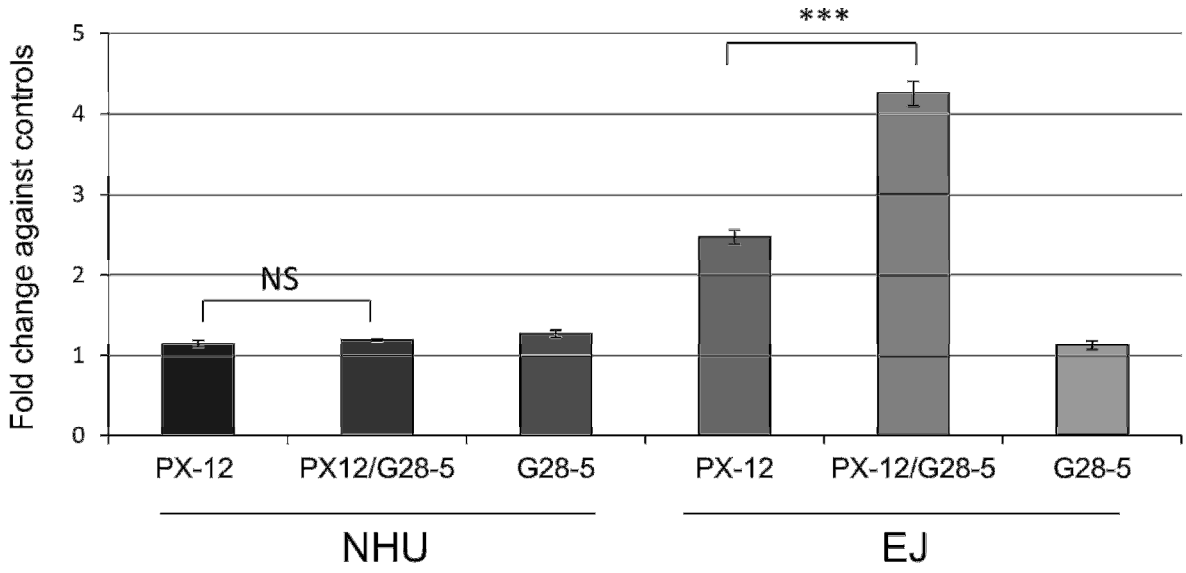


**Figure 5-30 PX-12/G28-5 mediated apoptosis is malignant cell-specific**

EJ were seeded at a density of $8x10^3$ in DR/5%FCS/1%L-G in white 96-well plates. NHU were seeded at a density $10^4$ in KSFMc. PX-12 was added at 2µM for one hour before the addition of G28-5 (10µg/ml) CytoTox-Glo substrate was added after 48 hours and RLU was assessed reflecting total levels of cell death. Results are presented as fold change (from generated RLU) by comparing T/EJ *versus* C/EJ or T/NHU versus C/NHU, where T/EJ= treatment of EJ with drugs (PX-12 & G28-5) and C/EJ = control EJ or T/NHU= treatment of NHU with drugs (PX-12 & G28-5) and C/NHU = Control NHU. Bars correspond to mean values of 5-6 technical replicates ± SEM and results are representative of three independent experiments. Stats: NS – non-significant *** $p<0.001$, paired student t-test, T/EJ vs C/EJ and T/NHU vs C/NHU.

### 5.6.7 The role of Glutathione (GSH) in mCD40L-mediated apoptosis

To investigate whether carcinoma cells may be sensitised to soluble CD40 agonists by pharmalogical inhibition of other target proteins, an experiment with Glutathione (GSH) inhibition was performed. Similarly to Trx, GSTp is important for cellular antioxidant defence and a plethora of studies have shown that it is also a biological inhibitor of JNK (Vasieva, 2011, Adler et al., 1999). Additionally some studies have shown that GSTp is also able to biologically inhibit ASK1 (Vasieva, 2011). Therefore as an alternative to Trx inhibition, it was proposed that GSTp inhibition would also sensitise UCC cell lines to the low apoptotic potential of soluble CD40 agonists by attenuating the apoptotic-signalling potential of ASK1, MKK4 and JNK, all of which have been shown (Chapter 4) essential for CD40-mediated killing.

The inhibition of GSH was achieved using pre-titrated concentrations Diethyl Maleate (DEM) a GSH depleting agent as previously described. DEM also causes a reduction in GSTp (Deneke and Fanburg, 1989) a member of the GSH family which inhibits by JNK activation under physiological conditions and is released during oxidative stress (Simic et al., 2009). It was hypothesised that DEM would sensitise cells to soluble CD40 agonists as it would decrease the antioxidant GSH and prevent JNK inhibition by GSTp during the CD40-mediated oxidative stress. The addition of DEM or G28-5 agonist alone again had minor effects on apoptosis as determined using CytoTox-Glo; however the combination of DEM/G28-5 led to significantly higher levels of apoptosis (Figure 5-31). This further demonstrated that the cellular response to CD40 engagement by soluble CD40 agonists is dependent on the redox status of the cell and also that this may be manipulated by pharmacological intervention.

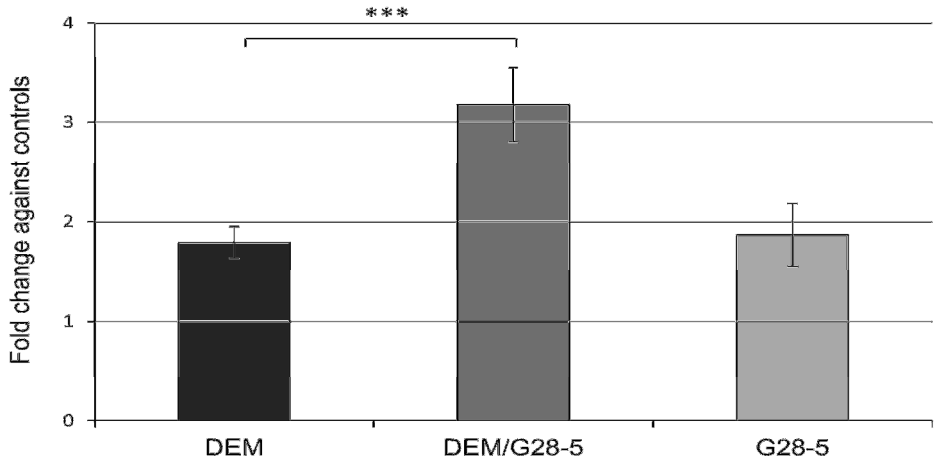


**Figure 5-31 Glutathione inhibition in combination with soluble CD40 agonist induces apoptosis in EJ carcinoma cells**

EJ were seeded at a density of $8x10^3$ in DR/5%FCS/1%L-G. DEM was added at 75µM for three hours before the addition of G28-5 (10µg/ml). CytoTox-Glo substrate was added after 48 hours and RLU was assessed reflecting total levels of cell death. Results are presented as fold change (from generated RLU) by comparing T/EJ versus C/EJ, where T/EJ = treatment of EJ with drugs (DEM and/or G28-5) and C/EJ = control EJ. Bars correspond to mean values of 5-6 technical replicates ± SEM and results are representative of three independent experiments. Stats: NS – non-significant *** $p<0.05$, paired student t-test, T/EJ vs C/EJ).

## 5.7 Summary

The results presented in this chapter provided a series of novel observations on the mechanisms of mCD40L-mediated apoptosis. One such observation is the finding that CD40 ligation and TRAF3 signalling induces activation of Nox to regulate oxidative stress. In light of the previously documented direct interaction of TRAF3 with p40phox, these results are suggestive of mCD40L-induced, TRAF3-mediated p40phox activation, as the latter is rapidly phosphorylated in response to mCD40L. CD40/TRAF3-mediated p40phox induction has been previously reported in B-cells (Ha and Lee, 2004), however this is the first time this has been demonstrated in an epithelial cell context. It is proposed that mCD40L utilises the aforementioned mechanism to relay a signal that rapidly induces ROS levels, which drive the CD40 intrinsic pathway of cell apoptosis, as loss of Nox activity by pharmacological inactivation abrogated Bax induction and apoptosis altogether. Thus, for the first time in carcinoma cells, this study has not only identified an important role for Nox in regulating cell apoptosis in response to the mCD40L-CD40 dyad, but also strongly suggests that the significant induction of TRAF3 drives ROS production via its interaction with p40-phox. Although a direct link between TRAF3 and p40phox was not formally demonstrated, future experiments using TRAF3 knockdown cells to examine phospho-p40-phox levels would provide further functional evidence. Finally, even though it cannot be excluded that ROS release via the mitochondria may also amplify apoptosis at later stages, clearly sustained Nox-induced ROS is critical, as shown in experiments where DPI introduced 24 hours post-ligation still attenuated cell death.

In agreement with accumulating recent evidence, the present data shows that the basal, steady-state intracellular ROS levels *in vitro* positively correlated with the tumour stage/grade and degree of malignant transformation of cells and that an increased ROS production could be associated with the degree of malignant behaviour, previously demonstrated in organotypic systems (Masters et al., 1986, Szatrowski and Nathan, 1991). The results presented here offer more evidence that the elevated basal ROS production in more malignant UCC cell lines also rendered them more susceptible to oxidative stress induced cell death by $H_2O_2$; however, in contrast to malignant cells, normal, NHU cells were highly refractory to oxidative

stress. These findings are in line with previous suggestions that higher-grade tumour cells are much more susceptible to $H_2O_2$ induced cell death (Lopez-Lazaro, 2007).

This study has also provided evidence for a critical pro-apoptotic ROS-associated threshold, which has long been hypothesised (Lopez-Lazaro, 2007). It has been shown that membrane CD40L, but not soluble CD40 agonists, efficiently generates ROS, thus demonstrating that there is a direct correlation between the ability to elevate ROS strong and a pro-apoptotic capacity and in carcinoma cells. Therefore, the increased ability of mCD40L to induce ASK1/MKK4/JNK, Bak/Bax activation and thus apoptosis is dependent on its ability to induce high levels of intracellular ROS. Additionally, as tumour cells maintain high ROS levels in support of proliferation, CD40 ligation 'pushes' cells past the critical ROS-related pro-apoptotic threshold and induces death.

Collectively considering the data, the results strongly suggest that the tumour cell-specific response to mCD40L is dependent on basal intracellular redox status, with more malignant cells showing increased susceptibility due to already elevated intracellular ROS concentrations, as exemplified by the differences between non-malignant RT4 and the highly anaplastic EJ cells in $H_2O_2$. These findings have therefore offered an insight as to why oxidative stress-resistant NHU are spared from mCD40L mediated apoptosis, compared with their oxidative stress-sensitive malignantly transformed counterparts (Bugajska et al., 2002, Shaw et al., 2005). Hence, it is strongly believed that this study has provided a mechanistic basis to explain the carcinoma cell-specific nature with regards to the CD40 'black-box'.

Finally, the mechanistic observations in this chapter have permitted the development and pre-clinical testing for a combinatorial therapeutic approach. ASK1 plays an essential role in CD40-mediated apoptosis (Chapter 4) and its activation is elegantly regulated by the redox protein Trx. Inhibition of Trx frees ASK1 for activation and also decreases the cells' defence against oxidative stress. mCD40L appears to be extremely efficient at ROS generation and downregulation of Trx (due extensive receptor cross-linking and subsequent TRAF/Nox activation) and requires no assistance in the induction of apoptosis; however, soluble agonists require exogenous intervention to raise ROS to a cytotoxic threshold. Whilst it is not understood how mCD40L-signals decrease Trx expression, it was on this hypothesis

that the combination of Trx inhibitor and soluble agonist was based. Trx inhibition appears to amplify the apoptotic stimulatory capacity of soluble CD40 agonists to levels observed for mCD40L. Combined with soluble CD40 agonist, the Trx permitted such essential pro-apoptotic ROS thresholds to be reached. The importance of ASK1 in this context was demonstrated by use of ASK1 knockdown cells. The attenuation of ASK1 via siRNA mediated knockdown not only abrogated apoptosis induced by membrane ligands (chapter 4), but also by the combinatorial Trx/soluble agonist treatment. These findings have underlined the value in understanding the precise CD40-mediated pathway of apoptosis in response to mCD40L, as it was exactly this knowledge that led to the combinatorial treatment that for the first time has permitted the use of soluble CD40 agonists to achieve equivalent effects to that of mCD40L.

The targeting of redox sensitive molecules may therefore represent a novel way to manipulate the tumour cell apoptotic response to CD40 agonists and may hold therapeutic potential for the future. In fact, this work has led to the submission of a patent application for the use of this concept as a carcinoma cell therapy (British Patent Application No. 1310349.4). This combinatorial approach showed not only quantitative but also qualitative similarities to mCD40L, as it was tumour cell specific, as shown in experiments in NHU cells. In line with the findings that NHUs are highly resistant to exogenous $H_2O_2$ insults, it was also found that they are equally resilient to ROS insults mediated by both mCD40L (also see chapter 6) and the combined use of soluble CD40 agonist with Trx inhibitor. Therefore, these findings provide the first paradigm of exploitation for a ROS susceptibility tumour-specific therapy based on the use of soluble CD40 agonists rendered highly pro-apoptotic by combinatorial use with Trx inhibitors.

# 6.0 The effect of CD40 ligation in 'para-malignant' epithelial cells: an investigation into the role of hTERT over-expression in regulating mCD40L-mediated responses

## 6.1 Background to malignant transformation and susceptibility to CD40 ligation

The ligation of CD40 by mCD40L causes extensive apoptosis in carcinoma cells but not in their normal epithelial counterparts. Georgopoulos and colleagues, using the urothelial model, have provided evidence that this differential susceptibility may be due to genetic alterations associated with the process of malignant transformation (Shaw et al., 2005, Bugajska et al., 2002). Functional studies revealed that normal cells (NHU) transduced with the human papilloma virus (HPV) 16 oncogene E6 are moderately susceptible to CD40-mediated killing during early stages of transformation however, following a stage of 'crisis' evident by extensive growth arrest and apoptosis, a new 'para-malignant' immortalised population arises that shows equal CD40-susceptibility to that observed with fully-malignant UCC cell lines (Bugajska et al., 2002). Further investigations showed that the ability of E6 to 'sensitise' NHU cells to CD40-mediated apoptosis is not due to its well characterised ability to inactivate p53, as independent p53 inactivation does not confer CD40 susceptibility (Shaw et al., 2005). Furthermore, p53 inactivation does not affect NHU life span or differentiation (Shaw et al., 2005, Georgopoulos et al., 2011) supporting the idea that p53 loss alone, although important in the process of urothelial carcinogenesis may not be as critical as anticipated. By contrast, p16 inactivation, the key modulator of the retinoblastoma-E2F (Rb-E2F) checkpoint complex, conferred a significant increase in susceptibility to CD40-mediated apoptosis. Although its loss in concert with p53 does not allow result in an immortalised phenotype, it is striking that NHU cells with functionally inactivated p16 become partially sensitised to CD40-killing (Shaw et al., 2005). Collectively, these observations suggest that apart from p53 and p16 loss of function, further mechanisms are required for both the induction of an infinite life span and CD40-sensitisation, one of which may perhaps be hTERT overexpression.

## 6.2 Background to human Telomerase Reverse Transcriptase (hTERT)

Telomerase is termed a reverse transcriptase ribonucleotide protein as it consists of an RNA component (TR) containing an antisense template for telomere synthesis, as well as a catalytic unit (hTERT) which functions to elongate and maintain DNA end repeats, known as telomeres. Telomeres are specialised structures that cap and preserve chromosomal integrity by preventing their rearrangement, end to end fusion and degradation (Greider, 1991). Telomeres are used to modulate the number of cell divisions, with each generation causing a reduction in telomere length and a loss in chromosomal stability. Telomere depletion causes the induction of cell senescence or apoptosis that is most likely mediated by p53 or p16/Rb when chromosomes are brought to catastrophic consequences (Harley, 2002, Shay and Wright, 2006, Geserick and Blasco, 2006).

*In vitro* the overexpression of hTERT can independently immortalise a plethora of normal cell lines (Harley, 2002) including NHU cells, which is one of the few cell phenotypes that shows basal hTERT expression (Georgopoulos et al., 2011). Primarily hTERT overexpression causes a cell population lag phase characterised by reduced growth rates but without signs of senescence, apoptosis or loss of differentiation. This phase is associated with an increase in p16 expression (Georgopoulos et al., 2011) (Chapman et al., 2006). Cells later on overcome the lag phase and show good recovery, which is coupled with reduced p16 expression, this most probably epigenetically modulated. Equally important, in contrast to lower passage cell populations, later ones are fully immortalised and progressively lose the ability to undergo terminal urothelial differentiation, this evident by the lack of expression of Uroplakin proteins or the ability to form a tight epithelial barrier (Georgopoulos et al., 2011).

Current research is providing evidence that the biological roles of telomerase extend beyond the maintenance of DNA telomeres and immortalisation, with a plethora of studies reporting regulatory roles in proliferation, resistance to apoptosis, DNA damage repair (Hanahan and Weinberg, 2011) and resistance to oxidative stress (Saretzki, 2009, Ding et al., 2013). A modern focus for bladder cancer therapy has been on the vulnerability of tumour cells to oxidative stress caused by the

accumulation of genetic alterations, particularly oncogene activation (Wang and Choudhary, 2011) and recent evidence demonstrates that telomerase also plays a fundamental role in such tumour cell resistance (Indran et al., 2011).

## 6.3 Tumour suppressor and oncogene ROS attenuation

The number of tumour suppressors and oncogenes implicated in oxidative stress are vast including; p53, Foxo, RB, p21, p16, breast cancer susceptibility genes -1, -2, EGFR, HER -1, -2, H-Ras and MT-CYB. There is a general consensus that a loss of tumour suppressors attenuate oxidative stress as they function to regulate cellular antioxidant defence, on the other hands oncogenes drive proliferation and create oxidative stress by a mounted cellular ATP demands in order to meet mitotic requirements (Vurusaner et al., 2012, Wang and Choudhary, 2011, Chung et al., 2009). In consideration that hTERT overexpression decreases p16, a tumour suppressor implicated in cellular redox control and that hTERT is implicated in oxidative stress defence, the current study focused on the current data available on these concepts.

## 6.4 p16 loss and hTERT over-expression and oxidative stress

Some report that p16 deficiency raises intrinsic ROS levels in melanocytes, keratinocytes and fibroblasts (Jenkins et al., 2010) whereas others have shown p16 loss has the opposite effect (Takahashi et al., 2006) therefore, the effects of tumour suppressor loss on cellular redox control remain controversial. However, if indeed p16 loss of function facilitates an elevation of basal ROS, the current work would provide support of this theory that loss of p16 function in NHU may cause an increased susceptibility to CD40-mediated apoptosis (Shaw et al., 2005) possibly due to its contributions towards crossing the ROS apoptotic-threshold.

Moreover, also hTERT over-expression has also been shown to regulate intrinsic basal ROS by improved cellular antioxidant defence, and an increase mitochondrial function by facilitating respiratory enzymes. Overall these cellular modifications protect cells from the intrinsic pathway of cell death via Bax inhibition,

maintained closure of PTPs and attenuated cytochrome c release (Indran et al., 2011). Interestingly, hTERT over-expression also reduces the *in vitro* sensitivity of cancer cells to TNFα (Gao and Chen, 2007a, Gao and Chen, 2007b) and TRAIL (Zhang et al., 2010) implying it generally offers protection against genotoxic insults including those by TNFRs. In fact, depletion of hTERT has also been shown to sensitise cells to cisplatin, etoposide, Mitomycin C and ROS-induced apoptosis via a p53 and Bax driven mechanism (Massard et al., 2006) and TRAIL via caspase-8 and -9 activation (Zhang et al., 2010).

## 6.5 Aim

The above intriguing findings, and in light of the previous work by Georgopoulos and colleagues showing that hTERT overexpression causes a reduction in p16 expression, nonetheless it is also proposed to regulate oxidative stress, led this study to determine the response of hTERT over-expressing NHU cells (HU-hTERT) to CD40-mediated apoptosis and oxidative stress. For this investigation, NHU and NU-hTERT cells were compared in a number of functional studies:

a) the co-culture method for CD40 ligation was used to activate CD40 receptors on the target cell line HU-hTERT (Figure 3-1) and apoptotic responses were examined using cell death detection assays and immunoblotting detection of pro-apoptotic markers

b) as this study has already shown differential susceptibility of urothelial cells to oxidative stress in normal versus non-malignant, moderately-malignant and highly anaplastic cells, we used this concept to determine HU-hTERT oxidative stress resilience compared with NHU cells and

c) basal levels of intrinsic ROS were quantified using the ROS detection molecule $H_2$DCFDA as detailed in Chapter 5.

## 6.6 Results

One aim of this section was to determine whether the immortalisation of NHU cells via hTERT overexpression alters their response to mCD40L-mediated CD40 ligation. We made use of HU-hTERT cells between passages 29-32 which have significant but not full loss of p16 expression yet are fully immortalised and have a loss of differentiation capacity - as previously detailed (Georgopoulos et al., 2011).

The immortalisation of NHU cells by hTERT significantly increased ($p<0.01$) the susceptibility of HU-hTERT cells to mCD40L-induced apoptosis compared with the NHU, and in most experiments the level of apoptosis observed were similar to that observed for EJ cells, as determined by CytoTox-Glo cell death detection assays (Figure 6-1). In line with this, hTERT over-expression increased mCD40L-induced caspase-3/7 activity, although this did not reach statistical significance compared with NHU, as shown in Figure 6-2. These findings suggested that hTERT-mediated NHU immortalisation renders normal urothelial cells susceptible to CD40 killing. Interestingly, and perhaps equally significant, in all apoptosis assays NHU cells were not only totally refractory to CD40-mediated apoptosis, but in fact, they exhibited a reduction (2-fold) in spontaneous levels of death, strongly implying a CD40-driven cyto-protection. This was shown using both CytoTox-Glo and caspase-3/7 death detection assays, which indicated that mCD40L-treated NHU cells had a decreased RLU and RFU respectively, when compared to their control - as shown in both Figure 6-1 and 6-2.

To corroborate the findings from the apoptosis detection assays, the levels of pro-apoptotic proteins Bak and Bax were examined following CD40 ligation. Results showed that there was an increase expression of pro-apoptotic markers Bak and Bax. Interestingly, the induction of Bak was much more pronounced than that of Bax and this is in agreement with a previous report showing that hTERT overexpression somehow prevents ROS induced Bax accumulation (Indran et al., 2010).

Previously (in Chapter 4), it was shown that mCD40L-induced apoptosis in UCC cell lines is dependent on the expression of TRAF3 which regulates the activation of JNK and the expression of Bak and Bax. Intriguingly, there was no induction in expression of TRAF3 in hTERT or NHU cells despite the former showing mCD40L susceptibility (not shown).

One hypothesis for the increased susceptibility of hTERT cells to mCD40L induced apoptosis could be that that hTERT overexpression increases sensitivity to oxidative stress by its reductive effects on p16, as reported by others (Jenkins et al., 2006). To investigate this NHU (negative control), hTERT and EJ (positive control) were treated with $H_2O_2$ and their growth/viability was assessed using the CellTiter 96® $AQ_{ueous}$ One Solution Cell proliferation assay. As shown in Figure 6-4 HU-hTERT did not show a dramatic susceptibility to $H_2O_2$ compared with NHU, however their levels of growth did decrease at higher concentrations (1600µM) where NHU still remained more proliferative. Unfortunately, due to the limited number of NHU cell passages and time constraints, it was not possible to investigate the effects of higher $H_2O_2$ concentrations which would provide a better and more detailed comparison in the exact oxidative stress resistance between NHU and HU-hTERT, and thus this remains yet to be fully explored.

An independent study has reported that hTERT overexpression decreases intracellular ROS levels (Indran et al., 2011), although conversely others report that p16 inactivation in numerous cell lines has been shown to increase ROS levels (Jenkins et al., 2010). In light that loss of p16 expression occurs in hTERT overexpressing NHU cells over passage 27 (Georgopoulos et al., 2011) the intrinsic ROS levels between HU-hTERT cells, NHU (negative control) and EJ (positive control) were compared to gain a further insight into the role of hTERT mediated ROS management. The measurement of intrinsic ROS between NHU, HU-hTERT and EJ was performed using the fluorescent marker 6-carboxy-2',7'-dichlorodihydrofluorescein diacetate ($H_2$DCFDA) as previously described in Chapter 5. As shown in Figure 6-5, EJ showed a significantly greater amount of intrinsic ROS over hTERT and NHU, conversely the immortalised NHU cell line HU-hTERT showed a decreased intrinsic ROS amount over both NHU and EJ. In finding that HU-hTERT cells have a decreased ROS over NHU it is possible to speculate from the results that hTERT acts intrinsically to reduce levels of intrinsic ROS, as implied by others (Indran et al., 2011), although the decrease is by no means dramatic. On the other hand it was interesting to observe that HU-hTERT cells showed intrinsic ROS levels that were more reminiscent of NHU than EJ, possibly confirming that these cells more closely resembled a ROS related phenotype to non-differentiated NHU cells over non-differentiated-malignant EJ cells. Collectively, these data and

those obtained from the $H_2O_2$ 'kill curve' experiments outlined the close relation between NU-hTERT and NHU cells, however ROS levels alone clearly cannot explain why hTERT cells showed a vulnerability to CD40-mediated apoptosis, thus implying the control of apoptosis is not simply dependant on intrinsic ROS concentrations but also other factors as discussed later.

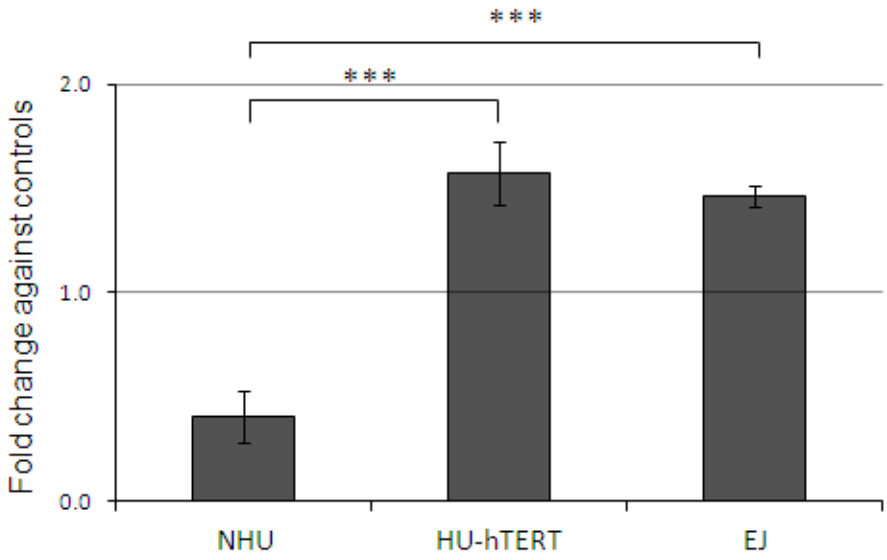


**Figure 6-1 The effect of CD40 ligation in normal and hTERT-immortalised urothelial cells: detection of cell death**

$8x10^3$ EJ, $10^4$ NHU and $10^4$ HU-hTERT cells were co-cultured with $10^4$ MMC treated mCD40L or Controls in DR/5%FCS/1%L-G or KFSMc in white 96-well plates. CytoTox-Glo substrate was added after 72 hours, luminescence was measured and background-corrected RLU readings deduced as described in Figure 3-7. Bars correspond to mean values of 5-6 technical replicates ± SEM and results are representative of three independent experiments. Stats: *** $p<0.001$, paired student t-test, EJ vs HU-hTERT or HU-hTERT vs NHU.

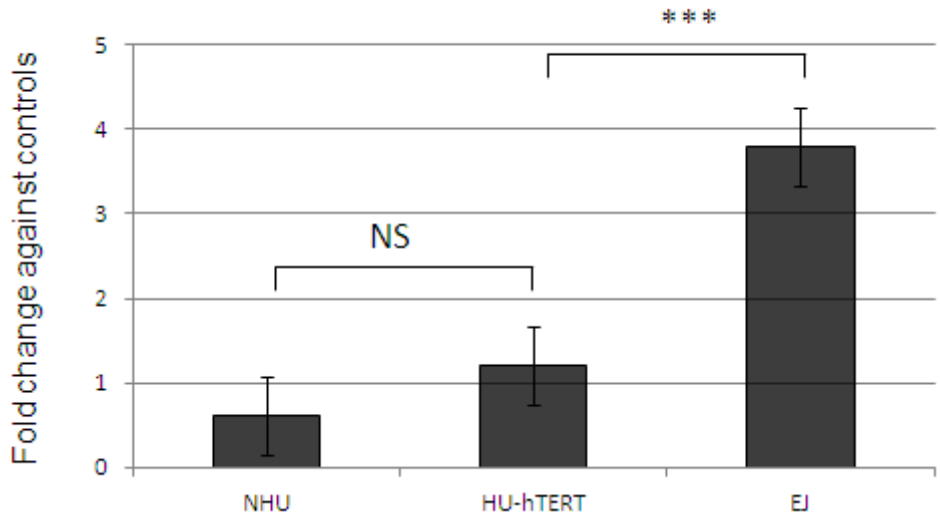


**Figure 6-2 The effect of CD40 ligation in normal and hTERT-immortalised urothelial cells: detection of caspase-3/7 activation**

$8x10^3$ EJ, $10^4$ NHU and HU-hTERT - were co-cultured with $10^4$ MMC treated mCD40L or Controls in DR/5%FCS/1%L-G or KSFMc in white 96-well plates. SensoLyte 3/7 reagent was added after 48 hours, fluorescence measured (as detailed in Section 2.11.3.1) and background-corrected RFU readings deduced by pair-wise subtraction of mCD40L and Control cell from the respective co-cultures. Bars represent mean RFU values for 5-6 technical replicates ± SEM, and results are representative of three independent experiments. Stats: *** $p<0.001$, paired student t-test, EJ vs HU-hTERT or HU-hTERT vs NHU.

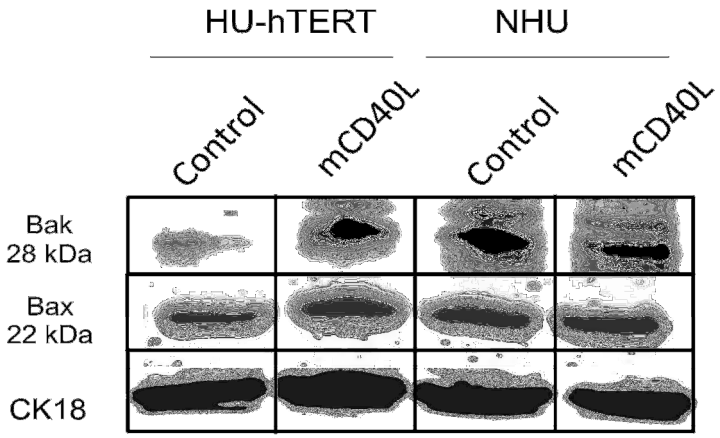


**Figure 6-3 CD40-mediated regulation of Bak and Bax expression in HU-hTERT and NHU cells**

$3x10^6$ NHU and hTERT cells were co-cultured with $3x10^6$ MMC treated mCD40L and Controls for 24 hours in KSFMc and $10cm^2$ culture dishes prior to lysis with 2X SDS-lysis buffer. 20µg of lysates were separated under denaturing conditions by SDS-PAGE using 4-12% (w/v) Bis-Tris gels and then immunoblotted onto a PVDF membrane. The PVDF membrane was probed overnight with an anti-BAK and an anti-BAX antibody (1:1000 dilution) and then with an anti-CK18 antibody (1:2000 dilution). The membrane was incubated for one hour with goat anti-mouse IgG AlexaFluor 680 (1:10,000 dilution) for the detection of Bax and CK18. Goat anti-rabbit IgG IRDye 800 (1:10,000 dilution) was used for the detection of Bak. Antibody binding was visualised at 700nm and 800nm using an Odyssey™ Infra-red Imaging system.

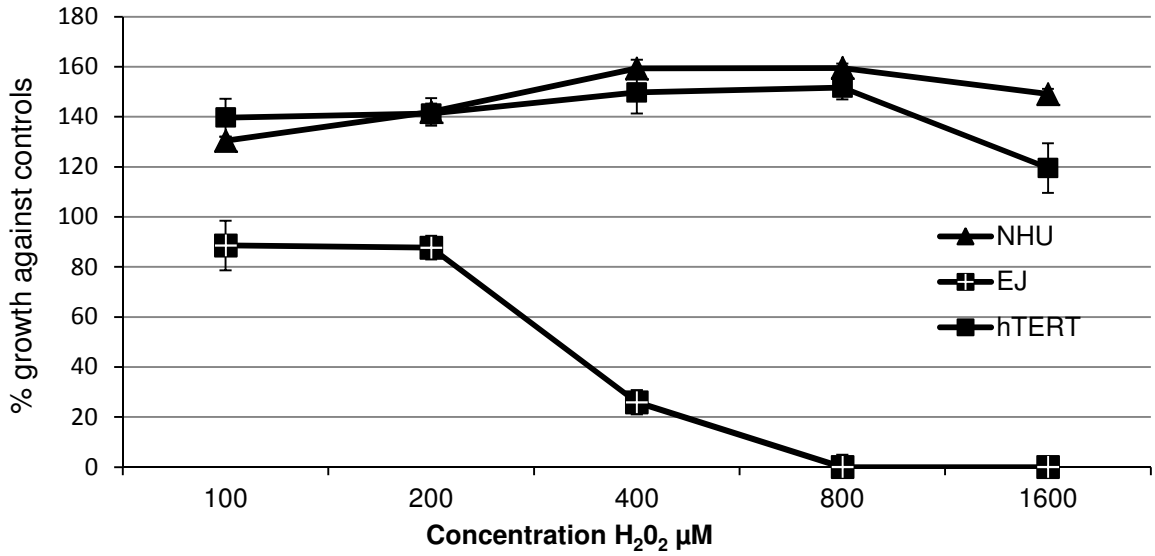


**Figure 6-4 The susceptibility of NHU, HU-hTERT and EJ cells to $H_2O_2$**

$8x10^3$ NHU, hTERT and EJ were seeded and allowed to adhere for 24 hours in KSFMc in transparent 96-well plates and subject to a range of $H_2O_2$ concentrations for 24 hours. 20µl of CellTiter 96® $AQ_{ueous}$ One Solution was added to appropriate wells and plates were incubated at 37℃ in 5% $CO_2$ for a total of 4 hours prior to the measurement of absorbance (Abs) at 492nm. Cell viability was calculated as percentage viability in comparison to controls using the following formula: (T/C) x100, where T= treated cells and C= controls cells. Bars represent mean absorbance values for 5-6 technical replicates ± SEM and results are representative of three independent experiments.

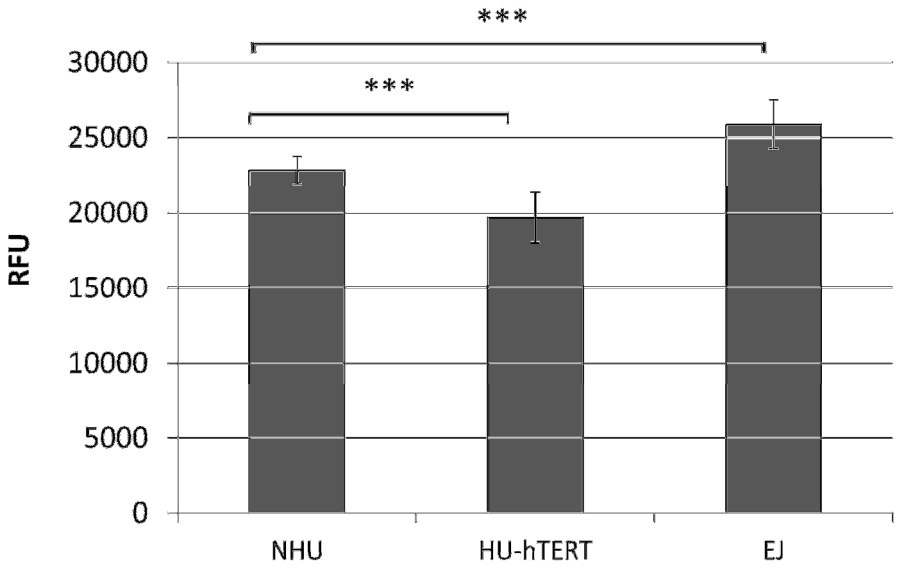


**Figure 6-5 Measurement of basal ROS levels of NHU, HU-hTERT and EJ cells**

$8x10^3$ NHU, hTERT and EJ cells were seeded for 24 hours in DR/5%FCS/1%L-G or KSFMc in white 96-well plates. Cells were first washed with PBS to remove any culture medium and were then treated with 1µM of $H_2$DCFDA in pre-warmed (37°C) PBS for 30 minutes 37°C in 5% $CO_2$. Cells were background corrected by subtraction of their relative autofluorescence (Figure 5-7). Bars represent mean RFU values for 35 technical replicates ± SEM and results are representative of three independent experiments. Stats: *** $p<0.001$ unpaired student t-test. EJ vs NHU, HU-hTERT vs NHU.

## 6.7 Summary

The current study has confirmed that normal (NHU) cells are resistant to CD40-mediated apoptosis in agreement with previous reports by Georgopoulos and colleagues, thus confirming the malignant cell specificity of CD40 (Bugajska et al., 2002, Shaw et al., 2005). The ligations of CD40 by mCD40L on NHU cells not only lead to un-detectable apoptosis, but instead CD40 ligation appeared to protect from spontaneous cell death in culture. This is in accordance to previous observations by Young, Eliopoulos and colleagues who reported that constitutive CD40 activation has the potential to transform fibroblasts *in vitro* (Baxendale et al., 2005). In agreement with the importance of ROS in CD40 death and combined with the observed ability of NHU cells to withstand high levels of exogenously provided ROS (in the form of H2O2), the results provide more evidence for the possibility that it is ROS activation that may underpin the tumour specificity of CD40. These observations also strengthen the more recently raised notion that oxidative stress insults may underpin tumour-targeted cell destruction in response to a variety of pro-apoptotic agents; yet ROS related signalling may also cause proliferative-survival response in NHU cells, which concords with the pro-survival role of ROS in normal cells and the potential role of sustained ROS activation during malignant transformation. Thus in summary, ROS whether exogenous or CD40-triggered, mediates UCC cell death but may cause the proliferation or increased survival of NHU cell lines. In addition to providing novel biological evidence for these hypotheses, our work constitutes a biological platform for the proposed clinical tumour cell specific targeting of bladder tumours by induced oxidative trauma (Wang and Choudhary, 2011).

In an attempt to shed more light on the ability of CD40 to induce death in para-malignant epithelial cells and to understand the role of malignant transformation in regulating the response to CD40 ligation, we examined for the first time the effect of CD40 on hTERT-immortalised urothelial cells. It has been reported that the over-expression of hTERT may decrease the susceptibility of cells to genotoxic stress and TNFR mediated apoptosis (Saretzki, 2009, Ding et al., 2013). Our results suggest that, compared with NHU cells HU-hTERT cells may have a lower amount of intrinsic ROS, however this does not appear to protect them from exogenous ROS insults in the form of H2O2, as they generally demonstrated decreased viability, and certainly

it does not protect them from CD40 killing, as we showed for the first time that HU-hTERT cells appear highly susceptible to CD40 ligation. Time constraints meant that it was not able to fully identify whether HU-hTERT cells show a more appreciable increased resistance to ROS insults in this context, but it would be very interesting for future studies to address this.

MCD40L-CD40 interactions were able to induce significant levels of apoptosis in HU-TERT cells when compared with NHU, in fact at times to a comparable extent observed in EJ cells. This is in disagreement with other reports that cell death mediated by TNFR members is abrogated by hTERT overexpression (Gao and Chen, 2007b, Gao and Chen, 2007a, Zhang et al., 2010), however the physiological relevance of other models of hTERT over-expression is not always clear due to experimental variables.

Not only are our HU-hTERT better- and fully-characterised (Georgopoulos et al., 2011) but also our findings resemble our observations on HPV E6 immortalised urothelial cells. Both HU-E6 and HU-hTERT cells are highly susceptible to CD40 death supported by the induction of pro-apoptotic Bak and Bax. Intriguingly, HPV E6 is a multifunctional oncoprotein that both inactivates p16 (Reznikoff et al., 1996) and triggers hTERT activation (Duffy et al., 2003). Our findings with p16 functional knockouts previously (Shaw et al., 2005) and hTERT over-expressers here may have therefore provided an explanation for the observations on HPV E6 and its ability to render urothelial cells susceptible to CD40 killing. Certainly the observation that HU-hTERT progressively lose p16 (Georgopoulos et al., 2011) implies that the combinatorial loss of p16 function and over-activation of hTERT may be the two main requirements that confer CD40 susceptibility. Of note also, future studies should examine the effect of CD40 ligation on later passage HU-hTERT cells (>p40) which appear to have ‘progressed’ further and showed even less p16 expression and have completely lost any ability to differentiate, thus representing an even more transformed phenotype. Loss of p16 is important (and occurs in HU-hTERT cells) but that alone is not enough to render NHU cells fully susceptible as previously demonstrated (Shaw et al., 2005). Thus additional changes to loss of p16 appear important and future studies will need to address this notion to fully explain reasons behind this intriguing concept.

Although according to the hypotheses raised in the study it was expected that differential susceptibility to CD40 in NHU vs hTERT vs UCC cells might be based on the different levels of ROS and thus a different pro-apoptotic ROS threshold, clearly the observation that ROS levels in HU-hTERT cells are not higher than those in NHU cells implies that the actual mechanisms may not be that simple. It should be noted that further optimisation experiments would be required to determine more sensitively the ROS basal level differences between NHU and hTERT cells. It is clear that although the ROS detection assay (using $H_2$DCFDA) employed in this study worked well, the reagent required extensive optimisation with regards to the concentration used, as too higher concentrations compromised its linear dynamic range (observations not shown).

However, and equally imperative, we believe these findings suggest a more fundamental principle, i.e. that ROS levels alone might not be adequate to determine apoptosis but another key factor might be the ability of cells to detoxify ROS. It would therefore be important to test whether mechanisms such as Trx and GSH might differ in normal epithelial cells. The observation that CD40 ligation down-regulated Trx expression, supported by the effectiveness of combinatorial use of Trx inhibitor and soluble agonist suggest that induction of ROS and concomitant down-regulation of detoxifying mechanisms may be interlinked and necessary for determining apoptotic susceptibility. Therefore, it would be important to examine the possible differences in Trx and GSH mechanisms in normal versus paramalignant cells and whether normal cells may be better at regulating ROS-related cytoprotective mechanisms.

# 7.0 General discussion

## 7.1 The mechanisms of mCD40L-mediated apoptotic death in malignant epithelial cells

The main aim of this thesis was to elucidate the molecular nature of the CD40 signalling 'black-box', i.e. the molecular signalling axis responsible for the activation of apoptosis in carcinoma cells. Whilst building on previous studies in our laboratory, this work has for the first time provided functional evidence for a TRAF3-Nox-ASK1-MKK4-JNK/AP-1 signalling pathway that drives intrinsic pathway regulated CD40-induced cell death. The following sections will discuss these observations in more detail. Besides the novelty of the observations presented in the general CD40 and TNFR field, it is equally important to emphasise the fact that unlike the vast majority of available studies reporting on the role of critical pro-apoptotic mediators such as ASK1, MKKs or JNK and their interactions in apoptotic signalling, the present study has uniquely analysed the expression and functional roles of such signalling mediators in a 'natural' system. This is based on endogenous protein expression and not any 'artificial' over-expression, which is often the case with most, if not (to our knowledge) virtually all CD40 studies in the literature.

### 7.1.1 Insights into the function of TRAF3 in mCD40L-induced apoptosis

TRAF3 is a CD40 adaptor protein which relays signals for activation of MAPKs. Such signals have generated multifaceted cell responses ranging from epithelial cell death to cell growth and survival (Hacker et al., 2011). TRAF3 has been shown in some instances to relay growth inhibition, yet in others apoptotic signals in epithelial based models, although the mechanistic explanations for this are largely unknown (Eliopoulos et al., 1996b, Dadgostar and Cheng, 2000). The ability of TRAF3 to mediate apoptotic signals is likely to be mediated by lipid raft formation (Dadgostar and Chen., 2000) with more recent evidence suggesting that this process is dependent on ROS-mediated receptor clustering via acid sphingomyelinase activation and ceramide production (Zhang et al., 2006, Zhang et al., 2007).

Based on expression detection analysis and stable shRNA-mediated knock-down experiments, this study has re-enforced the critical importance of TRAF3 in

apoptosis (Chapter 4) and has shown that mCD40L-CD40 interactions cause TRAF3 induction in UCC cell lines but not normal cells (not shown). Furthermore, soluble CD40 agonists do not stabilise TRAF3 as effectively as membrane agonists further suggesting CD40 cross-linking is also a key factor for high TRAF3 expression (Georgopoulos et al., 2006, Elmetwali et al., 2010b). As shown in Chapter 5 (and discussed in detail below) ROS plays an important role in CD40 killing. Although an unequivocal role for TRAF3 in the recruitment of Nox has not been provided, the work shown in this thesis has strongly implicated a TRAF3-Nox interaction in CD40-killing (also discussed below), which is in agreement with a previous study (Ha and Lee, 2004). In addition to performing co-immunoprecipitation studies to investigate whether TRAF3 and Nox do physically interact during mCD40L-induced signalling, the possible role of ROS in lipid raft formation should equally be explored in future work, as this study showed that malignant cells have a higher concentration of intrinsic ROS and are particularly susceptible to ROS-mediated death (exogenously induced or CD40-triggered).

Interestingly, not only has this study confirmed the critical role of TRAF3, but has also made some novel observations regarding its expression, which were not presented in Chapter 4 due to space limitations. Since detection of intracellular mediators in this study was based solely on an endogenous system following extensive optimisation of the immunoblotting techniques (and use of more sensitive PVDF membrane suitable for fluorescence measurements-based band detection (Li-Cor system), it became possible to more sensitively detect the expression of TRAF3. Moreover, during initial detection, it appeared that TRAF3 was present as an approximate 50kDa protein despite its full length being reported as 65kDa. This was an observation that was not unique to this project with UCC cells, but more recently we have confirmed this observation in colorectal carcinoma (CRC) cell lines in our laboratory (Mohammed and Georgopoulos, unpublished). Though this was not noted in previous reports by Georgopoulos (Georgopoulos et al., 2006) or Palmer and colleagues (Elmetwali et al., 2010b), it was not necessarily unexpected as TRAF3 does have a number of splice variants to produce various isoforms (Van Eyndhoven et al., 1999, Gamper et al., 2001). More importantly, siRNA mediated TRAF3 knockdown, not only attenuated apoptosis, but also abrogated detection of the 50kDa protein band. Furthermore, although cleavage of TRAF3 as a consequence of

caspase-3/7 activity has been reported (Lee et al., 2001), when co-cultures were performed in the presence of zVAD (pan-caspase inhibitor), no induction of the 65kDa band or loss of 50kDa bands was observed, in fact it appeared to enhance TRAF3 expression (not shown). The significance of this 50kDa isoform in an epithelial context remains unknown as many studies utilise B-cells for a TRAF3 investigations, however it has opened up an opportunity of novel investigation in its functional-epithelial role.

TRAF3 interacts with a variety of proteins (Hacker et al., 2011) and is frequently found in both cytoplasmic and nuclear subcellular regions (Urbich et al., 2001, Gamper et al., 2001, Van Eyndhoven et al., 1999). This is something we also observed in response to mCD40L-CD40 interaction using cell fractionation techniques followed by immunoblotting (Appendix III). TRAF3 localises to the nucleus in response to signalling triggered by other members of the TNFRSF such as LTβR, but the significance of this remains unknown (Force et al., 2000). The current study found no evidence that CD40 locates to the nucleus (not shown), and it was found only to be cytoplasmic despite a large TRAF3 nuclear expression. Although the presence of TRAF3 in the nucleus could be attributed to its over-expression, the presence of a DNA binding domain does indicate a biological reason for its nuclear localisation. TRAF3 is the only known TRAF molecule able to locate to the nucleus through the association with a nucleo-porin named p62, where it is proposed to modulate NF-κB activation (Gamper et al., 2000). Although NF-κB activity does not affect CD40-mediated apoptosis, it does occur following CD40 ligation (Georgopoulos et al., 2006). It would therefore be interesting to study whether a mutant TRAF3 molecule incapable of nuclear localisation can still function in CD40-killing. Studies have implied that TRAF3 may also directly alter AP-1 transcriptional activity in the nucleus in certain cell types offering protection against stress mediated apoptosis (Urbich et al., 2001), however the current study and others provide evidence that is also unlikely to occur in mCD40L induced apoptosis, as AP-1 inhibition attenuates this process (Georgopoulos et al., 2006).

Through stable, shRNA-mediated TRAF3 knockdown it has been shown by this study that mCD40L-induced phosphorylation of JNK and apoptosis is TRAF3 driven, thus confirming previous reports (Georgopoulos et al., 2006, Elmetwali et al., 2010b). The knockdown of TRAF3 also revealed that it positively regulates the

expression of pro-apoptotic Bcl-2 related family members Bak/Bax. Unquestionably, TRAF3 is a critical regulator of CD40-mediated apoptotic signals and requires more detailed functional investigations regarding its exact biological capabilities. As mentioned, it has been suggested that TRAF3 signalling may be dependent on lipid raft formation and its cell membrane interaction with Nox-2 to generate ROS (Ha and Lee, 2004, Wheeler and DeFranco, 2012, Bhogal et al., 2012). Thus, in light of the importance of ROS in apoptosis (discussed below) and the reports above, the current study determined whether a TRAF3-Nox functional link may underpin CD40-signalling responses.

### 7.1.2 The role of NADPH oxidase (Nox) in CD40-induced apoptosis

Nox represents an oxidoreductase enzyme, which is part of a family that transfer electrons from reduced molecules to oxidants. Nox is described as the "professional" ROS inducer, compared with any other oxidoreductases, as Nox-mediated ROS generation is intentional and not the result of respiratory by-production (Jiang et al., 2011). Nox-mediated ROS generation is used to regulate intrinsic, redox-sensitive signalling pathways via signalling protein modifications (Jiang et al., 2011, Bedard and Krause, 2007). Nox may induce ROS in response to chemotherapeutic agents and members of the TNRSF such as TNF-α or lymphotoxin, and this may be used to specifically target tumour cells due to their already raised oxidative stress state (Jin et al., 2008, Benhar et al., 2001).

It has been shown that CD40's intracellular domain recruits TRAF3 for NOX interaction via one of several sub-units, namely p40phox (Ha and Lee, 2004). These findings regarding TRAF3-Nox interactions were reported in B-cells via their overexpression. Exclusively however, in an endogenous system, results from the current study imply that this phenomenon may also occur in epithelial cells as through the use of an anti-phospho p40phox antibody combined with immunoblotting techniques it was also found that mCD40L treated cells also had a high degree of phosphorylation at the Nox-p40phox sun-unit, therefore directly reciprocating the situation reported in B-cells and confirming (to our knowledge) for only the 2$^{nd}$ time this biological phenonomenon (Ha and Lee, 2004).

Also in this study, through use of the Nox inhibitor DPI, it was shown that NOX inhibition prevents mCD40L-induced apoptosis and the expression of pro-apoptotic Bcl-2 members Bak/Bax, suggesting that either p40phox (or possibly another member of the Nox family) regulates CD40-mediated cell death via its manufacture of ROS. In support of this and others (Ha and Lee, 2004) there are more recent reports that phospho-p40phox has a specific role of ROS production in endothelial cells (Fan et al., 2009), thus enforcing this common mechanism between Nox mediated ROS production. Future work will look into the likelihood of a direct TRAF3-p40phox interaction in addition to determining whether p40phox phosphorylation is attenuated during TRAF3 knockout UCC cell mCD40L-CD40 ligation. Although time constraints meant that this experiment could not be performed, for the purpose of this study, it would generate more functional evidence in an endogenous system and not by means of overexpression employed by Ha and Lee (2004).

DPI is not a specific inhibitor of the p40phox sub-unit, but universal Nox, however this study shows that such inhibition can prevent CD40-induced ROS generation. This has provided a mechanistic insight that mCD40L-CD40-TRAF3-NOX interaction utilises ROS for the activation of pro-apoptotic pathways in UCC cell lines. Future work should target p40-phox specifically, possibly through shRNA knockdown, in order to precisely establish its role in context of CD40-mediated apoptosis.

### 7.1.3 A novel role for ASK1 in mCD40L-induced apoptosis

ASK1 is a MAPKKK that sits at the top of the MKK4/JNK signalling pathway responding primarily to oxidative cell stress mediated by reactive oxygen species (ROS). The deregulation of ASK1 constitutively activates inflammation, which leads to long term disorders such as neurogenative disease, cardiac disease, diabetes and cancer. ASK1 is normally suppressed by a redox protein known as thioredoxin (Trx) making it an inactive protein kinase. Trx binds ASK1 through a reduced intramolecular disulphide bridge, however the bonds are broken through oxidation, and in turn ASK1 auto-phosphorylates at Thr845 to become an active signalling kinase. ASK1 may also be phosphorylated at Ser367 causing its association with another biological inhibitor protein 14-3-3, and in line with Trx, oxidative stress also causes 14-3-3 release facilitating its autophosphorylation (Soga et al., 2012). One of the underlying factors which guided the exploration of the significance of ROS in the CD40 paradigm, was the fact that we observed that ASK1 is a critical regulator of CD40-mediated cell death combined with its recognition as a highly sensitive redox protein (Fujino et al., 2007). The current study generated functional evidence through shRNA-mediated protein knockdown, which showed that that ASK1 is positive regulator of CD40-mediated apoptosis.

The abrogation of ASK1 via shRNA mediated knockdown not only prevented mCD40L-induced apoptosis, but also abrogated the phosphorylation of JNK, which is essential for this outcome (Georgopoulos et al., 2006, Elmetwali et al., 2010a). This is the first time evidence has been generated that ASK1 has a functional role in the regulation of CD40-mediated apoptosis. In support, results by our group in CRC cell lines have implicated this may also hold true in other models (Mohammed and Georgopoulos, unpublished), thus suggesting that ASK1 is a critical regulator of the CD40-mCD40L response in carcinoma cells. Although due to time constraints we could not generate functional evidence to show that TRAF3-NOX interaction induces ASK1 activation, other studies do support that TRAF3 expression activates ASK1 via ROS enhancement, and that this leads to cell apoptosis (Chen et al., 2003). Additionally, it is widely reported that the ROS inductions play a regulatory role during this process via Trx and 14-3-3 release, and thus activation of ASK1 by CD40-TRAF3-NOX mediated ROS generations represents a valid evidence based hypothesis (Soga et al., 2012, Fujino et al., 2007).

Interestingly, in addition to identifying its novel pro-apoptotic role in CD40 signalling, and similarly to our observations for TRAF3, it was found in our endogenous system that ASK1 exists as a range of isoforms (not shown). The full length of ASK1 is reported to be 150kDa, however the current study and others on CRC cell lines by our group (Mohammed and Georgopoulos, unpublished) have observed a phosphorylated fragment at 39kDa during immunoblotting techniques. Moreover, in support, shRNA mediated ASK1 knockdown revealed that only the 39kDa fragment expression was attenuated (no other isoform was readily detectable or attenuated by the shRNAs), suggesting overall that this is the active signalling isoform involved in CD40-mediated apoptosis. The validity of our observations is supported by a previous publication that investigated ASK1 expression in cells using antibodies including the one used in this work (Stordal and Davey, 2008). The paper showed that ASK1 was cleaved to fragments of 39, 50, 75 and 110kDa when detected in carcinoma cells in an endogenous system but only following over-expression was the full-length 150kDa protein detectable (Stordal and Davey, 2008). The precise significance of this isoform and whether Trx has proficient binding capabilities for the 39kDa ASK1 isoform is unknown, and should be further investigated to determine its biological significance.

### 7.1.4 MAPKK activation and mCD40L-induced apoptosis: a critical role for MKK4 but not MKK7 in JNK activation and apoptosis

A number of reports based on protein over-expression studies have demonstrated that closely linked with the phosphorylation of JNK are MAPKKs MKK4 and MKK7 (Kim et al., 2005, Weston and Davis, 2002). The current study interestingly found that MKK4 but not MKK7 positively regulates mCD40L induced apoptosis via an ability to induce JNK phosphorylation. To date this is the first report that CD40 engagement uses a ASK-1-MKK4-JNK axis for the induction of cell death and mimics the signalling axis of cadmium induced neuronal cell apoptosis (Kim et al., 2005).

Due to difficulties encountered in its detection (very weak expression was observable) and time constraints it was not possible to demonstrate a direct functional link between ASK1 and MKK4, however as with ASK1, MKK4 knockdown

fully abolished JNK signalling overall implying that both are likely to regulate CD40-mediated apoptosis. To further validate the findings related to this model it is suggested that a phospho-MKK4 kinase assays are used as these are much more sensitive techniques for this type of assessment (Such as the AlphaScreen® SureFire® phospho-MKK4 Ser257/Thr261 Kit). This would strengthen the evidance of TRAF3-Nox-ASK1-MKK4 activation followed by JNK phosphorylation (see below) currently implied in CD40-mediated cell death.

Also noteworthy is the fact that MAPKKs, which include MKK4 and MKK7, are under tight regulation by a group of biological inhibitor proteins known as dual-specificity MAPK phosphatases (DS-MKPs) that are released during oxidative stress (Camps et al., 2000, Farooq and Zhou, 2004). Their regulatory role in CD40-mediated apoptosis is completely unexplored and thus represents another area of novel exploration in this field.

### 7.1.5 The role of JNK/AP-1 in mCD40L induced UCC cell apoptosis

JNK plays a multifaceted function with regards to cellular responses (Jing and Anning, 2005), however the current study has further cemented the notion that JNK plays a positive role in mCD40L induced apoptosis (Georgopoulos et al., 2006, Elmetwali et al., 2010b). Furthermore, it was confirmed that JNK induced apoptosis is mediated through the JNK/AP-1 axis, as not only did they augment mCD40L induced apoptosis, but were critical in the induction of the expression of pro-apoptotic Bak and Bax. Therefore, JNK/AP-1 regulate the intrinsic pathway of apoptosis, something which mirrors other findings on the redox regulation of JNK and pro-apoptotic Bcl-2 members (Jin et al., 2006).

It has been discussed (above) that Trx regulates ASK1 activity through a ROS dependent mechanism. Interestingly, JNK activation is also regulated by a redox sensitive biological inhibitor protein known as GSTp (Simic et al., 2009). The inhibitor used in this study (DEM) causes the depletion of GSTp and GSH (Deneke and Fanburg, 1989) and is less specific than Trx which, binds Trx only and no other Trx members, such as Trx reductase. Therefore, it cannot be ruled whether DEM was preventing GSTp mediated JNK biological inhibition to promote CD40-mediated

apoptosis or causing general oxidative stress via GSH abrogation. There is an implication however, that this conceptually similar method of pharmacological intervention may also promote soluble CD40 agonist pro-apoptotic responses, as this study showed that DEM-G28-5 induced levels of apoptosis were equal to Trx-G28-5 combinations. In support of this, studies have reported that GSH inhibitors also sensitise carcinoma cell lines to genotoxic ROS insults (Trachootham et al., 2006), thus suggesting that GSH or GSTp inhibition may be used to promote ROS mediated carcinoma apoptosis via a JNK associated mechanisms. Future work may involve the use of shRNA mediated JNK knockdown cells as we used a pharmacological inhibitor which, when added with the chemical inhibitor DEM may have produced non-specific cytotoxic effects. Moreover, many bladder cancers have an increased expression of GSH or GSTp (Pljesa-Ercegovac et al., 2011) further suggesting that malignant cells *in vivo* utilise this method of antioxidant overexpression for oxidative stress related cytoprotection.

### 7.1.6 CD40-mediated intrinsic apoptotic pathway regulation

It is well established that Bak and Bax mediate apoptosis through the alterations in MOMP, referred to as the intrinsic pathway of cell death (Chipuk and Green, 2008). It was previously reported and that mCD40L induces the expression of Bak and Bax (Georgopoulos et al., 2006, Bugajska et al., 2002), however the significance of this remained to be investigated. The current study has confirmed the pro-apoptotic role of Bak and Bax as their attenuation via shRNA mediated protein knockdown attenuated CD40-mediated apoptosis. This was more prominent in the case of Bax.

In addition to the observation that JNK/AP-1 directly regulate the induction of Bak/Bax expression, it was also confirmed in line with Elmetwali et al that cytochrome c is released as a result. A number of proteins located within the mitochondria that can induce apoptosis upon release including AIF, Endo G and Cytochrome C. The aforementioned are released from the mitochondria into the surrounding cytoplasm through the actions of Bak/Bax or through the actions of ROS on PTPs (Kroemer et al., 2007). As it was observed that cytochrome c was released during CD40-mediated apoptosis, it is likely that this creates a complex using Apaf-1

and procaspase-9, known as the caspase activating recruitment domain (CARD). The CARD would then proceed to activate caspase-9, caspase-3/7 and CAD through the intrinsic pathway of cell death (Shiozaki et al., 2002). These findings are supported by reports that caspase-9 or caspase-3/7 inhibition attenuates mCD40L induced apoptosis in UCC cell lines (Georgopoulos et al., 2006).

Despite the current findings on CD40-mediated apoptosis, it would be interesting to further investigate the role of mitochondria in apoptosis. Of interest would be the involvement of other mitochondrial death-related mediators, such as BH3-only proteins, or whether ROS open PTPs for release of AIF or Endo G or SMAC/DIABLO (Norberg et al., 2010) - SMAC/DIABLO shRNA-expressing retroviruses are available in our laboratory for future investigations. A good candidate for BH3-only protein exploration would be PUMA as it has been shown that it is important in p53-mediated induction of intrinsic apoptosis and it activates Bax during oxidative stress to induce apoptosis (Steckley et al., 2007).

## 7.2 The role of ROS in mCD40L-induced apoptosis

ROS were first thought to be molecules that caused cell damage, through lipid, protein and DNA oxidation. Intriguingly it is now recognised they also play a crucial secondary messenger role in activating cell signalling pathways (Terada, 2006). Furthermore, ROS species are implicated in virtually all the hallmarks of cancer proposed by Hanahan and Weinberg (2011) due to their diverse effects on cellular molecules and processes such as, angiogenesis, invasion and proliferation (Paletta-Silva et al., 2013). CD40 engagement, by sCD40Ls, triggers the production of ROS in B-cells and hepatocytes, which is mediated through the action of NOX (Bhogal et al., 2012, Ha and Lee, 2004, Wheeler and DeFranco, 2012). In line with the former, this study has shown for the first time that soluble CD40 agonists (mAb G28-5) trigger ROS in epithelial (urothelial) cells, but this is more pronounced following CD40 ligation by mCD40L. This may offer an explanation into the diverse range of responses that are seen in response to CD40 engagement over the past decade at least (Loskog and Eliopoulos, 2009), as this study shows that the ‘strength’ of the ROS signal directly influences the functional response.

A well established and characterised *in vitro* urothelial cell model system (Booth et al., 1997) was used to explore the hypothesis that malignant cell death by CD40 is underpinned by an increased susceptibility to ROS/oxidative stress induced cell death. Firstly, the proliferation rates of *in vitro* UCC cell lines (not shown) showed to positively correlated with the detectable levels of intrinsic ROS, as supported by other studies (Trachootham et al., 2006). Secondly, the increased ROS production by such cells may make them increasingly susceptible to $H_2O_2$ induced cell death, which is in agreement with previous hypotheses (Raj et al., 2011, Lopez-Lazaro, 2007, Wang and Choudhary, 2011, Trachootham et al., 2006). Meeting the abnormal energy demands of a tumour cell often leads to an inefficient way of energy production, which comes at the expense of increased intrinsic mitochondrial ROS leakage (Weinberg et al., 2010, Chung et al., 2009). Increased ROS leakage may promote the likelihood that further ROS insults will activate tumour cell pro-apoptotic pathways (Trachootham et al., 2006). This could be due to the widespread ability of ROS to activate oxidative stress sensitive pro-apoptotic and anti-apoptotic signalling pathways (Circu and Aw, 2010, Biswas et al., 2006). This is interesting as not only do cell lines holding more malignant potential show an increased CD40 susceptibility (Bugajska et al., 2002), but the *de novo* inactivation of p16 in NHU cells renders them CD40 susceptible (Shaw et al., 2005). The inactivation of p16 allows progression through G1-S phase via the Rb pathway, and may therefore place increased ATP demands for cell division, thus promoting the progression towards a CD40-associated pro-apoptotic threshold. This is further supported by findings that p53 inactivation, which participates in cell cycle progression after the Rb checkpoint, does not promote cell division or render NHU cells CD40 susceptible. Moreover, the combined inactivation of p16 and p53 (unpublished) further sensitises cells to CD40-mediated apoptosis possibly due an unrestricted passage though the G1-S phase, and thus further raises intrinsic ROS levels.

It is fascinating to observe that NHU cells are unharmed by CD40-mCD40L ligation and they are also unharmed by concentrations of $H_2O_2$ that completely apoptose their malignantly transformed counterparts which is possibly due to the fact they have no genetic alterations (Shaw et al., 2005, Bugajska et al., 2002). If anything the results in this study have for the first time shown that CD40 ligation by mCD40L is even cytoprotective thus providing supportive evidence for the previously

suggested cell-transforming potential of constitutive CD40 signalling (Baxendale et al., 2005). The ability to culture normal, NHU cells and observe the differences to direct ($H_2O_2$) or indirect (CD40) ROS signals has both provided support for the double-edged sword role of ROS in epithelial cell homeostasis and provided mechanistic evidence for the tumour-specific nature of mCD40L-CD40 ligation.

Current theories have suggested that the divided response between normal and malignant cells to oxidative stress is linked to oncogene activation and/or tumour suppressor loss, which may affect the cell intrinsic redox management (Wang and Choudhary, 2011, Vurusaner et al., 2012). To add to our previous knowledge on the role of changes associated with carcinogenesis on CD40 susceptibility this study investigated the effects of hTERT overexpression and immortalisation in NHU cells. It was found that HU-hTERT cells became sensitised to CD40-killing and a biological explanation for this may be that such cells show a reduction in p16 expression (Georgopoulos et al., 2011) However, loss of p16 alone is not adequate to sensitise to CD40 death (Shaw et al., 2005) and additional events may be responsible for conferring susceptibility. Furthermore, this study found that HU-hTERT cells also began to show signs of oxidative stress induced apoptosis in concentrations of $H_2O_2$ that NHU cells remained more viable. Some inconsistent findings were however observed, as the basal ROS levels of HU-hTERT cells was lower than NHU; it should nevertheless be noted that detection of ROS in NHU and hTERT using the ROS detection assay might not have been optimal and further investigation would be beneficial. Moreover, the lack of susceptibility of normal cells and increased susceptibility in malignant cells might not be acutely measured due to basal ROS levels but may also be dependent on cytoprotective mechanisms against ROS such as differences in Trx and GSH-related mechanisms. These hypotheses would be an interesting area of future work. In support of the importance of examining redox related mechanisms overall and not purely ROS levels alone, when colorectal cells were compared with UCC lines, it was found they had similar sensitivity to $H_2O_2$ yet CRC cells are much more sensitive to CD40-killing showing a high percentage of cell death after less than 24 hours post receptor ligation (Mohamed and Georgopoulos, unpublished).

## 7.3 A novel combinatorial therapy: targeting CD40-ASK1 mediated apoptosis by Trx inhibition

The findings of this study suggested that the inability of soluble agonists to induce any significant apoptosis may be related with their weak ability to elevate ROS, which in turn would modify Trx and inactivate it in order to allow phosphorylation of ASK1 for subsequent induction of apoptosis. Moreover, as the delivery of the mCD40L poses practical difficulties (and requires complex delivery strategies), it was hypothesised that it may be possible to combine a soluble CD40 agonist which might still be able to engage the CD40 signalling pathway when combined with a pharmacological inhibitor of Trx, to make up for the inability of soluble agonist to sufficiently raise ROS levels. It was hypothesised that by pharmacologically attenuating the protective Trx, sufficient TRAF3/ASK1/JNK activation would be achieved to allow ASK1-mediated CD40-killing. Thus, using the best characterised Trx inhibitor, PX-12, CD40-mediated apoptosis using a soluble agonist would be amplified via two biological mechanisms 1) it would facilitate an elevated amount of active ASK1, as Trx-ASK1 biological inhibition would be abolished and 2) it would increase oxidative stress (as Trx is an anti-oxidant) allowing CD40 generated ROS to exceed the CD40-induced, ROS-associated pro-apoptotic threshold, and thus activate apoptotic MAPK signalling pathways. Initial findings showed that Trx inhibition could not further enhance apoptosis mediated by mCD40L, which is in agreement with results observed with other CD40 sensitising agents such as the protein synthesis inhibitor CHX (Bugajska et al., 2002) and which also confirms that mCD40L represents the signal with the maximal pro-apoptotic capacity. Moreover, it was demonstrated that this is possibly due to the ability of mCD40L to endogenously down regulate Trx during CD40-mediated cell death, as mCD40L down-regulates Trx expression (Chapter 5).

We found for the first time that pharmacological Trx inhibition sensitised tumour cells to soluble CD40 agonists, that normally used alone are non-cytotoxic to UCC cell lines (Bugajska et al., 2002). Importantly, in support of the hypothesis that the soluble-agonist/PX-12 combinatorial treatment is functionally equivalent to mCD40L-induced CD40 ligation for ROS elevation, ASK1 knockdown resulted in resistance PX-12/G28-5 mAb induced cell death (as it did with mCD40L). Equally important, the current study not only demonstrates that the toxicity by the

aforementioned is ROS-ASK1 dependent, but also that the combinatorial treatment is, like mCD40L, also tumour cell-specific as NHU cells remained refractory. Importantly, the observation reported in numerous studies that tumour cells increase Trx expression and that this protects them ROS/oxidative stress mediated cell death (Qu et al., 2011, Kakolyris et al., 2001, Mitsui et al., 2002), strengthens the therapeutic potential of Trx inhibition in combination with soluble CD40 agonists for treatment of CD40 positive tumours, particularly those that progress with a dependence on Trx over-expression.

Even though this study primarily used urothelial cell lines to investigate Trx inhibitors and soluble CD40 agonists, additional experiments explored its potentially wider applicability. It was found that CRC cell lines were much more sensitive to Trx mediated cell toxicity and also that this was further enhanced by the addition of soluble CD40 agonists; in fact, some of the CRC lines underwent apoptosis rapidly following treatment with the combinatorial therapy (not shown). This observation was interesting as Trx inhibitors have been implicated to hold the most promise for the treatment of CRC over other epithelial tumours (Lincoln et al., 2003). Furthermore, studies performed in our laboratory have shown that CRC are extremely sensitive to mCD40L induced apoptosis showing large decreases in viability as early as 6 hours post-ligation (Mohamed and Georgopoulos, manuscript in preparation). Therefore the administration of Trx inhibitors combined with soluble CD40 agonists merits further pre-clinical testing to determine its universal efficacy not only against urothelial, but also other carcinomas, such as CRC.

## 7.4 The CD40 paradox: CD40 ligation as a double-edged sword underpinned by ROS?

Considering the amount of published evidence generated in the last nearly 30 years, none would argue whether CD40 and its cognate ligand (CD40L) have evolved as an important feature of normal immunoregulation and as key molecules in the body's fight against pathogenic infection and cancer, clearly placing the CD40/CD40L dyad in the "centre of the immune universe" (Grewal and Flavell, 1998). When CD40 'signals' are lost at the genetic level, individuals clinically manifest with a disease known as hyper IgM syndrome characterised by immunodeficiency and an increased risk of cancer (Eliopoulos and Young, 2004, Bereznaya and Chekhun, 2007). Aside from its important role in immunity however, clearly CD40 can regulate the fate of epithelial cells and particularly carcinoma-derived cells and its ability to inhibit carcinoma cell growth is well documented and reviewed (Young et al., 1998). Interestingly, its capacity to both facilitate tumour progression and/or mediate regression has raised the 'ingenious paradox' (Eliopoulos and Young, 2004) of CD40 being able to potentially have divergent roles on epithelial cell homeostasis, thus raising the possibility of CD40 having a key role in not only the immune but also the "epithelial universe".

Whether epithelial cells retain or lose CD40 expression during malignant transformation has been a point of debate. The observation that around 78% of some carcinomas (urothelial) retain CD40 expression (Cooke et al., 1999) implies that CD40 may have a tumour promoting role. It may be that throughout their malignant evolution, cancers may use the CD40 paradigm for advantageous signalling cascades, which aid their proliferation, survival and angiogenesis (Huang et al., 2011, Pham et al., 2002, Baxendale et al., 2005). Emerging evidence, including that generated by this study, suggests that this, in a normal cell context, may be attributed to chronic production of ROS (Waris and Ahsan, 2006, Behrend et al., 2003). ROS also possess the ability to induce genetic instability (Behrend et al., 2003, Radisky et al., 2005), activate JNK, p38 and NF-κB which have the ability to induce cancer cell proliferation, survival and thus malignant progression (Gallagher et al., 2002, Baxendale et al., 2005).

Yet, conversely, which exemplifies the complexity of the CD40 paradox, receptor ligation is clearly able to cause tumour regression (Loskog and Totterman, 2007) and there is plenty of evidence (here and elsewhere) for a growth-inhibitory or pro-apoptotic role in carcinoma cells. For instance, work using UCCs and CRCs cells in particular has shown that membrane CD40L has a high apoptotic potential (Elmetwali et al., 2010b, Bugajska et al., 2002, Georgopoulos et al., 2007, Georgopoulos et al., 2006, Hill et al., 2008b). This potential has been re-confirmed by the current study, using a range of assays to accomplish this. These observations thus raise the possibility for an immuno-surveillance role for the CD40/CD40L dyad, implying that loss of CD40 expression reported in carcinoma cells of bladder (Bugajska et al., 2002) or colorectal (Hill et al., 2008b) origins may provide an advantage during or, more likely, at late stages of carcinogenesis.

CD40L is physiologically expressed as a membrane ligand on activated T-cells (Elgueta et al., 2009), thus membrane ligand may represent a more natural ligand form (Bugajska et al., 2002), however it is more than likely that the release of matrix metalloproteinases (MMP) by malignant cells cleaves it into soluble form, thus attenuating its apoptotic, whilst activating its proliferative potential (Vardouli et al., 2009). This raises a prospect that the retention of CD40 expression by some tumours combined with their ability to cleave it from mCD40L to sCD40L may allow chronic ROS production and could confer transformational advantages in the long term. Therefore, as implied by Palmer and colleagues, a clinical system for mCD40L delivery as a therapy should contain a MMP cleavage-resistant motif, as this would render mCD40L non-cleavable and pro-apoptotic (Elmetwali et al., 2010b) ensuring that the ligand would remain membrane-bound as the induction of apoptosis is unquestionably linked to the strength (level of cross-linking) during CD40 ligation (Bugajska et al., 2002).

Collectively, it is clear that CD40 ligation represents as much a double-edged sword, as is the addiction of tumour cells to high levels of basal ROS levels. It is possible that despite being a proliferation signal in normal cells, as cells progress through paramalignant stages to full malignant transformation they paradoxically become sensitive to CD40 ligation. Similarly, although clearly tumour cells favour constitutive ROS production, this renders them more susceptible to signals that may ‘push’ them more easily past a critical pro-apoptotic threshold. The close connection

between ROS and CD40 and the clear importance of ROS in malignant cell killing is strongly suggestive that of a paradigm in which ROS underpins the tumour-specificity of the CD40/CD40L dyad, that in combination with CD40's ability to down-regulate ROS-related cytoprotective mechanisms, explains the pro-apoptotic capacity of CD40.

## 7.5 Concluding remarks

Through use of the urothelial model, this study has for the first time identified the intracellular signalling cascade that is triggered by CD40 ligation and results in extensive apoptosis in carcinoma cells (summarised schematically in Figure 7-1). It has identified a TRAF3-Nox-ROS-ASK1-MKK4-JNK/AP-1 pathway as being the driving force that triggers an intrinsic apoptotic pathway and results in carcinoma cell apoptosis. The prominent role of ROS in the pathway may have for the first time provided a mechanistic basis for the tumour-specificity of CD40 ligation. Equally vital, this new knowledge of the nature of the CD40 signalling 'black-box' has permitted the design of a combinatorial therapeutic strategy, involving soluble CD40 agonist in combination with pharmacological Trx inhibitor, that is functionally equivalent to the strongly pro-apoptotic membrane CD40L. The findings of this work have provided novel observations on the mechanisms of apoptosis triggered by TNSRF member CD40 as well as raising interesting questions for further biological studies; it has also provided a novel therapeutic avenue that may exploit CD40 as a targeted receptor for anticancer therapy.

## 7.6 Results subsequent to thesis completion

Although a previous implication, it was demonstrated subsequent to the completion of this thesis that;

a) TRAF3 regulates p40phox phosphorylation, ASK1 activation and MKK4 activation.
b) MKK4 is active at 3 hours and the knockdown cells MKK4-KD-S11 have a functional shRNA for siRNA mediated MKK4 protein knockdown.

Therefore overall an evidence based and very detailed pathway regulating mCD40L induced apoptosis was deciphered. (See appendix IIII for extra results and Figure 7-1).

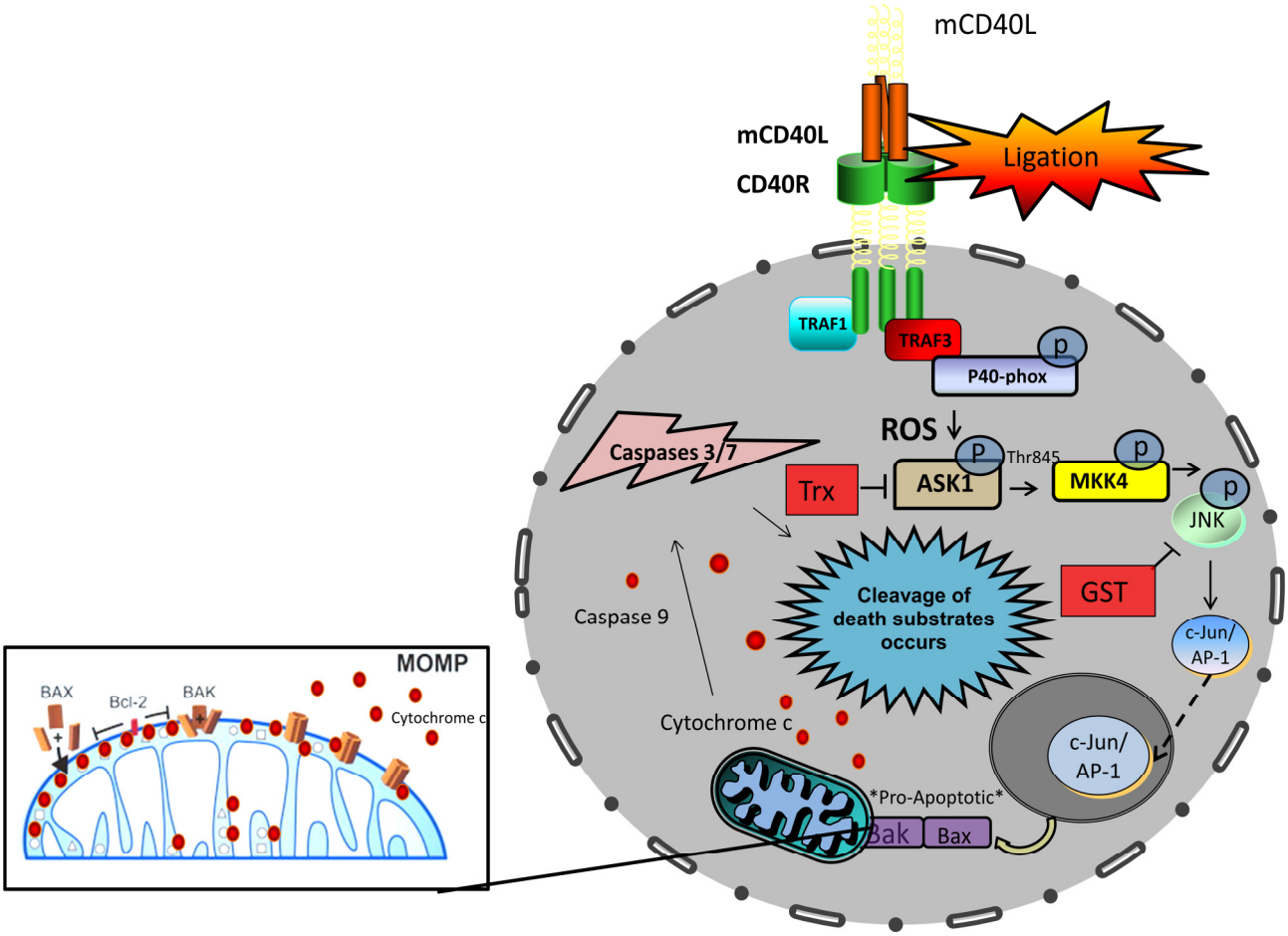


**Figure 7-1 – The CD40-mediated pathway of apoptosis**

Based on data from this study and published research, a tumour cell specific model of CD40-mediated apoptosis is proposed. CD40 ligation by mCD40L up-regulates and recruits a substantial amount of TRAF3, which phosphorylates NOX2 at the sub-unit p40phox. The rapid phosphorylation of p40phox by TRAF3 generates a ROS 'burst' which results in the dissociation of Trx from ASK1. ASK1 autophosphorylates at position Thr845 and activates MKK4 via its phosphorylation at Ser257. Active MKK4 phosphorylates JNK which in turn phosphorylates c-Jun to begin formation of AP-1. In the nucleus, AP-1 causes the transcriptional regulation of pro-apoptotic Bak and Bax, which mediate MOMP. MOMP leads to cytochrome c release which causes the formation of the CARD, activation of caspase-9 and subsequent activation of caspase-3/7 for the induction of apoptosis.

| Abbreviation | Actual |
|---|---|
| µg | Micro gram |
| µl | Micro litre |
| µM | Micro molar |
| aa | Amino acids |
| ACD | Accidental cell death |
| AIF | Apoptosis inducing factor |
| AIP | Inhibitor of apoptosis |
| AP-1 | Activator protein 1 |
| ASK1 | Apoptosis signalling kinase 1 |
| CAD | Caspase activated DNase |
| Carcinoma | Epithelial cancer |
| CARD | Caspase activation and recruitment domain |
| CDK | Cyclin dependant kinase |
| DC | Dendritic cell |
| DD | Death domain |
| DED | Death effector domain |
| DISC | Death inducing signalling complex |
| DEM | Diethyl Maleate |
| DPI | Diphenylene iodonium |
| FADD | Fas associated death domain |
| hTERT | Telomerase catalytic sub-unit |

| | |
|---|---|
| JNK | C-jun N-terminal kinase |
| mCD40L | Membrane CD40 ligand |
| mM | millimolar |
| MM | Malignant melanoma |
| MOMP | Mitochondrial outer membrane permeability |
| NAC | N-acetyl cysteine |
| NF-κB | nuclear factor kappa-light-chain-enhancer of activated B cells |
| NK | Natural killer |
| Nox | NADPH oxidase |
| OMM | Outer mitochondrial membrane |
| PCD | Programmed cell death |
| Rb | Retinoblastoma |
| redox | Reduction-oxidation |
| ROS | Reactive oxygen species |
| TCR | T-cell receptor |
| TIM | TRAF interacting motif |
| TNF (α) | Tumour necrosis factor (alpha) |
| TNFR | Tumour necrosis factor receptor |
| TNFR-I | Tumour necrosis factor receptor I |
| TRADD | TNFR-I associated death domain |
| TRAF | Tumour necrosis factor receptor associated factor |
| UCC | Urothelial cell carcinoma |

| | |
|---|---|
| UV | Ultra violet light |
| LMP1 | Latent membrane protein 1 |
| APC | Antigen presenting cell |
| TNFRSF | Tumour necrosis factor receptor super family |
| sCD40L | Soluble CD40 ligand |
| NHU | Normal urothelial cells |

# Appendix I

## List of Suppliers

| Supplier | Webpage/Address |
|---|---|
| | |
| Alpha labs | www.alphalabs.co.uk |
| Autogen Bioclear UK Ltd | Holly Ditch Farm, Mile Elm, |
| BD Biosciences | www.bdbiosciences.com/eu |
| BDH | Supplied by VWR |
| Bio-Rad Laboratories Ltd | *www.bio-rad.com* |
| Biosera | www.biosera.com |
| Calbiochem | Supplied by Merck |
| Cambridge Bioscience | www.bioscience.co.uk |
| Clontech (Takara Bio Inc) | www.clontech.com |
| ENZO | www.enzolifesciences.com |
| Falcon | Supplied by VWR |
| Fisher Scientific UK Ltd | *www.fisher.co.uk* |
| Gompels healthcare | www.gompels.co.uk |
| Greiner Bio-one Ltd | www.greinerbioone.com/en/england/start/ |
| Insight Biotechnology Ltd | www.insightbio.com |
| Invitrogen Ltd | www.invitrogen .com |
| Invivogen | www.invivogen.com |
| Jencons-PLS | Supplied by VWR International |
| Li-Cor Biosciences UK Ltd | www.licor.com |
| Merck | www.merck.co.uk |
| Microsoft Corporation | www.microsoft.com |
| Millipore | www.merckmillipore.co.uk |
| Molecular Probes | Supplied by Invitrogen |
| Nalgene Europe Ltd | Supplied by Fisher Scientific |
| New England Biolabs (UK) Ltd | www.neb.uk.com |
| Pierce | Supplied by Thermo Scientific |
| Promega UK Ltd | www.promega.com |
| Qiagen Ltd | www.qiagen.com |
| Roche Diagnostics Ltd | www.roche.co.uk/portal/uk/diagnostics |
| Santa Cruz Biotechnology | Supplied by Insight Biotechnology Ltd |
| Sigma-Aldrich Company Ltd | www.sigmaaldrich.com |
| Starstedt Ltd | www.sarstedt.com |
| Statebourne Cryogenics Ltd | *www.statebourne.com* |
| Sterilin Ltd | Supplied by Fisher |
| Tebu-bio | www.tebu-bio.co.uk |
| ThermoFisher Scientific Inc | www.fisher.com |
| VWR international | www.vwr.com |

# Appendix II

## Stock solutions

### General Solutions:

#### Phosphate Buffered Saline (PBS)

137mM NaCl, 2.7mM KCl, 3.2mM $Na_2HPO_4$ and 147mM $KH_2PO_4$, pH7.2 in autoclaved $dH_2O$. Prepared from x10 solution (Invitrogen: 14200-067).

#### Tris Buffered Saline (TBS)

50mM Tris-HCl (pH7.4) and 150mM NaCl in $dH_2O$

### Western Blotting Solutions:

#### 2x SDS lysis buffer

125mM Tris-HCl (pH6.8), 20% (w/v) glycerol, 2% (w/v) SDS, 200mM Sodium fluoride, 2mM Sodium Orthovanadate, 40mM Tetra-sodium pyrophosphate and made to 50ml in $dH_2O$.

#### "Towbin" Transfer Buffer

12mM Tris, 38mM Glycine, 20% (v/v) Methanol made to 1l in $dH_2O$.

## Appendix III

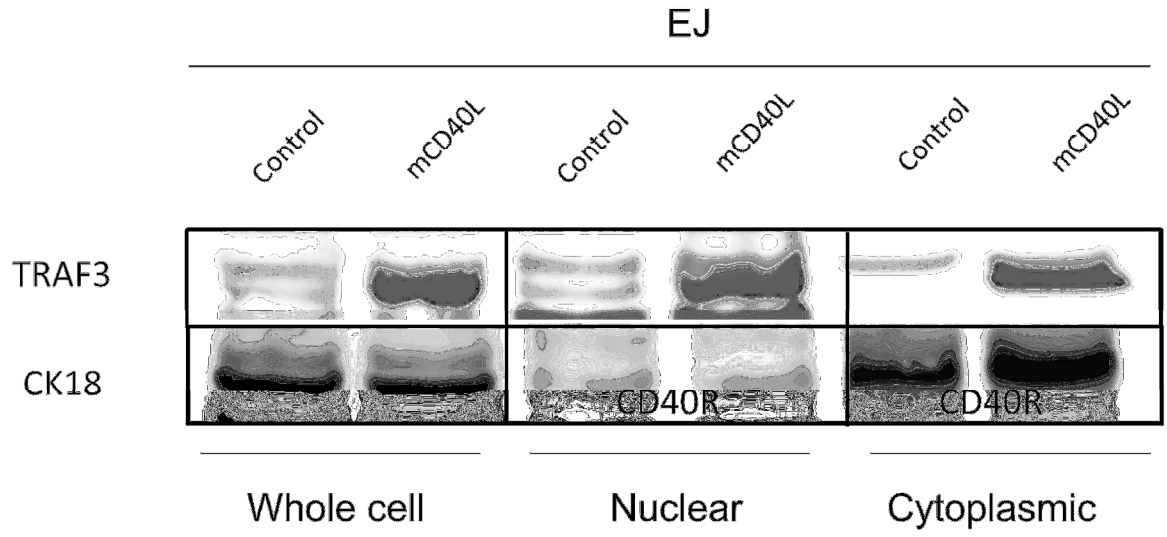


**TRAF3 locates to the nucleus and Cytoplasm in response to mCD40L**

EJ were co-cultured with MMC treated mCD40L and Controls in DR/5%FCS/1%L-G for 24 hours before cells were harvested using Trypsin-EDTA and processed accordingly to the manufacturers protocol for the Fisher nuclear extraction kit. 20µg of full, nuclear and cytoplasmic lysates were separated under denaturing conditions by SDS-PAGE using 4-12% (w/v) Bis-Tris gels and then immunoblotted onto a PVDF membrane. The PVDF membrane was probed overnight with an antibody raised against TRAF3 (1:500) and then for an antibody rose against epithelia specific Cytokeratin 18 (1:2000) for full lysates. CD40 was used to confirm the separation between the nuclear and cytoplasmic proteins. The membrane was incubated for one hour with goat anti-mouse IgG AlexaFluor 680 (1:10,000 dilution) for the detection of CK18 and CD40. Goat anti-rabbit IgG IRDye 800 (1:10,000 dilution) was used for the detection of TRAF3. Antibody binding was visualised at 700nm and 800nm using an Odyssey$^{TM}$ Infra-red Imaging system.

# Appendix IIII results subsequent to thesis completion

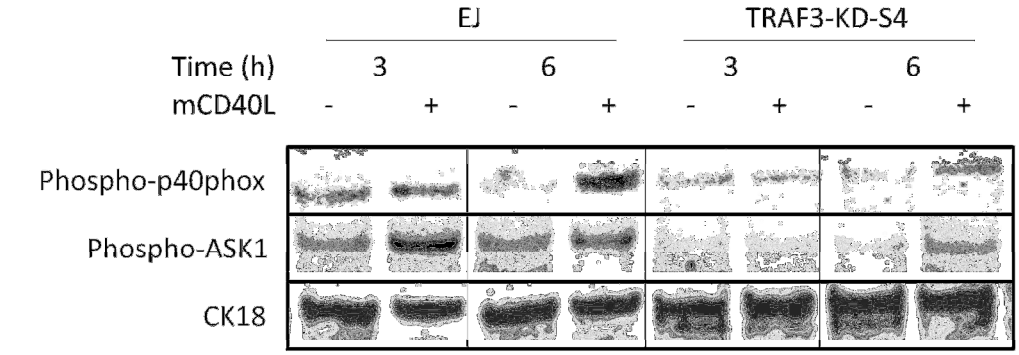


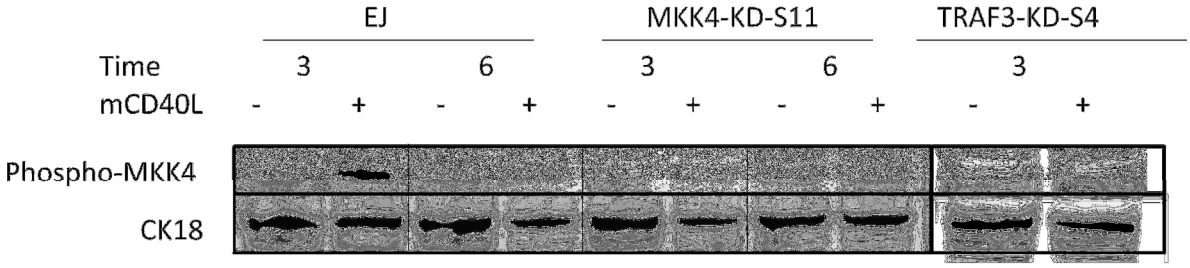

## References:

ADLER, V., YIN, Z., FUCHS, S. Y., BENEZRA, M., ROSARIO, L., TEW, K. D., PINCUS, M. R., SARDANA, M., HENDERSON, C. J. & WOLF, C. R. (1999) Regulation of JNK signaling by GSTp. *The EMBO journal,* 18**,** 1321-1334.

AFFORD, S. C., AHMED-CHOUDHURY, J., RANDHAWA, S., RUSSELL, C., YOUSTER, J., CROSBY, H. A., ELIOPOULOS, A., HUBSCHER, S. G., YOUNG, L. S. & ADAMS, D. H. (2001) CD40 activation-induced, Fas-dependent apoptosis and NF-ÎºB/AP-1 signaling in human intrahepatic biliary epithelial cells. *The FASEB Journal,* 15**,** 2345-2354.

AHMED-CHOUDHURY, J., RUSSELL, C. L., RANDHAWA, S., YOUNG, L. S., ADAMS, D. H., AFFORD, S. C. & CHOUDHURY, J. A. (2003) Differential induction of nuclear factor-kappaB and activator protein-1 activity after CD40 ligation is associated with primary human hepatocyte apoptosis or intrahepatic endothelial cell proliferation. *Mol Biol Cell,* 14**,** 1334-45.

AMAKATA, Y., FUJIYAMA, Y., ANDOH, A., HODOHARA, K. & BAMBA, T. (2001) Mechanism of NK cell activation induced by coculture with dendritic cells derived from peripheral blood monocytes. *Clinical & Experimental Immunology,* 124**,** 214-222.

AMEYAR, M., WISNIEWSKA, M. & WEITZMAN, J. B. (2003) A role for AP-1 in apoptosis: the case for and against. *Biochimie,* 85**,** 747-752.

ANGKEOW, P., DESHPANDE, S. S., QI, B., LIU, Y. X., PARK, Y. C., JEON, B. H., OZAKI, M. & IRANI, K. (2002) Redox factor-1: an extra-nuclear role in the regulation of endothelial oxidative stress and apoptosis. *Cell death and differentiation,* 9**,** 717-725.

AON, M. A., STANLEY, B. A., SIVAKUMARAN, V., KEMBRO, J. M., O'ROURKE, B., PAOLOCCI, N. & CORTASSA, S. (2012) Glutathione/thioredoxin systems modulate mitochondrial H2O2 emission: An experimental-computational study. *The Journal of general physiology,* 139**,** 479-491.

APEL, K. & HIRT, H. (2004) Reactive oxygen species: metabolism, oxidative stress, and signal transduction. *Annu. Rev. Plant Biol.,* 55**,** 373-399.

ARCIPOWSKI, K. M. & BISHOP, G. A. (2012) Roles of the kinase TAK1 in TRAF6-dependent signaling by CD40 and its oncogenic viral mimic, LMP1. *PloS one,* 7**,** e42478.

ARMITAGE, R. J. (1994) Tumor necrosis factor receptor superfamily members and their ligands. *Curr Opin Immunol,* 6**,** 407-13.

ARMITAGE, R. J., FANSLOW, W. C., STROCKBINE, L., SATO, T. A., CLIFFORD, K. N., MACDUFF, B. M., ANDERSON, D. M., GIMPEL, S. D., DAVIS-SMITH, T. & MALISZEWSKI, C. R. (1992) Molecular and biological characterization of a murine ligand for CD40. *Nature,* 357**,** 80-82.

ATOCHINA, O. & HARN, D. (2005) LNFPIII/LeX-stimulated macrophages activate natural killer cells via CD40-CD40L interaction. *Clinical and diagnostic laboratory immunology,* 12**,** 1041-1049.

BAKER, A. F., DRAGOVICH, T., TATE, W. R., RAMANATHAN, R. K., ROE, D., HSU, C.-H., KIRKPATRICK, D. L. & POWIS, G. (2006) The antitumor thioredoxin-1 inhibitor PX-12 (1-methylpropyl 2-imidazolyl disulfide) decreases thioredoxin-1 and VEGF levels in cancer patient plasma. *Journal of Laboratory and Clinical Medicine,* 147**,** 83-90.

BAKER, R. L., WAGNER JR, D. H. & HASKINS, K. (2008) CD40 on NOD CD4 T cells contributes to their activation and pathogenicity. *Journal of autoimmunity,* 31**,** 385-392.

BANCHEREAU, J., BAZAN, F., BLANCHARD, D., BRIE, F., GALIZZI, J. P., VAN KOOTEN, C., LIU, Y. J., ROUSSET, F. & SAELAND, S. (1994) The CD40 antigen and its ligand. *Annual review of immunology,* 12**,** 881-926.

BATLLE, A., PAPADOPOULOU, V., GOMES, A. R., WILLIMOTT, S., MELO, J. V., NARESH, K., LAM, E. W. F. & WAGNER, S. D. (2009) CD40 and B-cell receptor signalling induce MAPK family members that can either induce or repress Bcl-6 expression. *Molecular immunology,* 46**,** 1727-1735.

BAUD, V. R. & KARIN, M. (2001) Signal transduction by tumor necrosis factor and its relatives. *Trends in cell biology,* 11**,** 372-377.

BAXENDALE, A. J., DAWSON, C. W., STEWART, S. E., MUDALIAR, V., REYNOLDS, G., GORDON, J., MURRAY, P. G., YOUNG, L. S. & ELIOPOULOS, A. G. (2005) Constitutive activation of the CD40 pathway promotes cell transformation and neoplastic growth. *Oncogene,* 24**,** 7913-7923.

BEDARD, K. & KRAUSE, K.-H. (2007) The NOX family of ROS-generating NADPH oxidases: physiology and pathophysiology. *Physiological reviews,* 87**,** 245-313.

BEHREND, L., HENDERSON, G. & ZWACKA, R. M. (2003) Reactive oxygen species in oncogenic transformation. *Biochemical Society Transactions,* 31**,** 1441.

BENHAR, M., DALYOT, I., ENGELBERG, D. & LEVITZKI, A. (2001) Enhanced ROS production in oncogenically transformed cells potentiates c-Jun N-terminal kinase and p38 mitogen-activated protein kinase activation and sensitization to genotoxic stress. *Molecular and cellular biology,* 21**,** 6913-6926.

BEREZNAYA, N. M. & CHEKHUN, V. F. (2007) Expression of CD40 and CD40L on tumor cells: the role of their interaction and new approach to immunotherapy. *Exp Oncol,* 29**,** 2-12.

BERMUDEZ, O., PAGES, G. & GIMOND, C. (2010) The dual-specificity MAP kinase phosphatases: critical roles in development and cancer. *American Journal of Physiology-Cell Physiology,* 299**,** C189-C202.

BHOGAL, R. H., WESTON, C. J., CURBISHLEY, S. M., ADAMS, D. H. & AFFORD, S. C. (2012) Activation of CD40 with platelet derived CD154 promotes reactive oxygen species dependent death of human hepatocytes during hypoxia and reoxygenation. *PloS one,* 7**,** e30867.

BISHOP, G. A. (2004) The multifaceted roles of TRAFs in the regulation of B-cell function. *Nature Reviews Immunology,* 4**,** 775-786.

BISHOP, G. A., MOORE, C. R., XIE, P., STUNZ, L. L. & KRAUS, Z. J. (2007) TRAF proteins in CD40 signaling. *TNF Receptor Associated Factors (TRAFs).* Springer.

BISWAS, S., CHIDA, A. S. & RAHMAN, I. (2006) Redox modifications of proteinâ€“thiols: emerging roles in cell signaling. *Biochemical pharmacology,* 71**,** 551-564.

BITTON-WORMS, K., PIKARSKY, E. & ARONHEIM, A. (2010) The AP-1 repressor protein, JDP2, potentiates hepatocellular carcinoma in mice. *Molecular cancer,* 9**,** 54.

BOOTH, C., HARNDEN, P., TREJDOSIEWICZ, L. K., SCRIVEN, S., SELBY, P. J. & SOUTHGATE, J. (1997) Stromal and vascular invasion in an human in vitro

bladder cancer model. *Laboratory investigation; a journal of technical methods and pathology,* 76**,** 843-857.

BUGAJSKA, U., GEORGOPOULOS, N. T., SOUTHGATE, J., JOHNSON, P. W. M., GRABER, P., GORDON, J., SELBY, P. J. & TREJDOSIEWICZ, L. K. (2002) The effects of malignant transformation on susceptibility of human urothelial cells to CD40-mediated apoptosis. *Journal of the National Cancer Institute,* 94**,** 1381-1395.

BUHTOIAROV, I. N., LUM, H., BERKE, G., PAULNOCK, D. M., SONDEL, P. M. & RAKHMILEVICH, A. L. (2005) CD40 ligation activates murine macrophages via an IFN-Î³-dependent mechanism resulting in tumor cell destruction in vitro. *The Journal of Immunology,* 174**,** 6013-6022.

BUSH, T. J. V. & BISHOP, G. A. (2008) TLR7 and CD40 cooperate in ILâ€ 6 production via enhanced JNK and APâ€ 1 activation. *European journal of immunology,* 38**,** 400-409.

CALLARD, R. E., ARMITAGE, R. J., FANSLOW, W. C. & SPRIGGS, M. K. (1993) CD40 ligand and its role in X-linked hyper-IgM syndrome. *Immunology today,* 14**,** 559-564.

CAMPS, M., NICHOLS, A. & ARKINSTALL, S. (2000) Dual specificity phosphatases: a gene family for control of MAP kinase function. *The FASEB Journal,* 14**,** 6-16.

CARGNELLO, M. & ROUX, P. P. (2011) Activation and function of the MAPKs and their substrates, the MAPK-activated protein kinases. *Microbiology and Molecular Biology Reviews,* 75**,** 50-83.

CHAMBERS, J. W. & LOGRASSO, P. V. (2011) Mitochondrial c-Jun N-terminal kinase (JNK) signaling initiates physiological changes resulting in amplification of reactive oxygen species generation. *Journal of Biological Chemistry,* 286**,** 16052-16062.

CHANDEL, N. S., SCHUMACKER, P. T. & ARCH, R. H. (2001) Reactive oxygen species are downstream products of TRAF-mediated signal transduction. *Journal of Biological Chemistry,* 276**,** 42728-42736.

CHAPMAN, E. J., HURST, C. D., PITT, E., CHAMBERS, P., AVEYARD, J. S. & KNOWLES, M. A. (2006) Expression of hTERT immortalises normal human urothelial cells without inactivation of the p16/Rb pathway. *Oncogene,* 25**,** 5037-5045.

CHEN, M.-C., HWANG, M.-J., CHOU, Y.-C., CHEN, W.-H., CHENG, G., NAKANO, H., LUH, T.-Y., MAI, S.-C. & HSIEH, S.-L. (2003) The role of apoptosis signal-regulating kinase 1 in lymphotoxin-Î² receptor-mediated cell death. *Journal of Biological Chemistry,* 278**,** 16073-16081.

CHENG, G., CLEARY, A. M., YE, Z.-S., HONG, D. I., LEDERMAN, S. & BALTIMORE, D. (1995) Involvement of CRAF1, a relative of TRAF, in CD40 signaling. *Science,* 267**,** 1494-1498.

CHIPUK, J. E. & GREEN, D. R. (2008) How do BCL-2 proteins induce mitochondrial outer membrane permeabilization? *Trends in cell biology,* 18**,** 157-164.

CHO, S.-G., LEE, Y. H., PARK, H.-S., RYOO, K., KANG, K. W., PARK, J., EOM, S.-J., KIM, M. J., CHANG, T.-S. & CHOI, S.-Y. (2001) Glutathione S-transferase mu modulates the stress-activated signals by suppressing apoptosis signal-regulating kinase 1. *Journal of Biological Chemistry,* 276**,** 12749-12755.

CHOPRA, B., GEORGOPOULOS, N. T., NICHOLL, A., HINLEY, J., OLEKSIEWICZ, M. B. & SOUTHGATE, J. (2009) Structurally diverse peroxisome proliferatorâ€ activated receptor agonists induce apoptosis in human

uroâ€ epithelial cells by a receptorâ€ independent mechanism involving storeâ€ operated calcium channels. *Cell proliferation,* 42**,** 688-700.
CHOUDHARY, S., RATHORE, K. & WANG, H.-C. R. (2010) FK228 and oncogenic H-Ras synergistically induce Mek1/2 and Nox-1 to generate reactive oxygen species for differential cell death. *Anti-cancer drugs,* 21**,** 831-840.
CHOUDHARY, S., RATHORE, K. & WANG, H.-C. R. (2011) Differential induction of reactive oxygen species through Erk1/2 and Nox-1 by FK228 for selective apoptosis of oncogenic H-Ras-expressing human urinary bladder cancer J82 cells. *Journal of cancer research and clinical oncology,* 137**,** 471-480.
CHOUDHARY, S. & WANG, H.-C. R. (2007) Proapoptotic ability of oncogenic H-Ras to facilitate apoptosis induced by histone deacetylase inhibitors in human cancer cells. *Molecular cancer therapeutics,* 6**,** 1099-1111.
CHOUDHARY, S. & WANG, H.-C. R. (2009) Role of reactive oxygen species in proapoptotic ability of oncogenic H-Ras to increase human bladder cancer cell susceptibility to histone deacetylase inhibitor for caspase induction. *Journal of cancer research and clinical oncology,* 135**,** 1601-1613.
CHUNG, J. S., LEE, S. B., PARK, S. H., KANG, S. T., NA, A. R., CHANG, T.-S., KIM, H. J. & YOO, Y. D. (2009) Mitochondrial reactive oxygen species originating from Romo1 exert an important role in normal cell cycle progression by regulating p27Kip1 expression. *Free radical research,* 43**,** 729-737.
CIRCU, M. L. & AW, T. Y. (2010) Reactive oxygen species, cellular redox systems, and apoptosis. *Free Radical Biology and Medicine,* 48**,** 749-762.
COOKE, P. W., JAMES, N. D., GANESAN, R., WALLACE, M., BURTON, A. & YOUNG, L. S. (1999) CD40 expression in bladder cancer. *The Journal of pathology,* 188**,** 38-43.
CRALLAN, R. A., GEORGOPOULOS, N. T. & SOUTHGATE, J. (2006) Experimental models of human bladder carcinogenesis. *Carcinogenesis,* 27**,** 374-81.
D'AUTREAUX, B. T. & TOLEDANO, M. B. (2007) ROS as signalling molecules: mechanisms that generate specificity in ROS homeostasis. *Nature Reviews Molecular Cell Biology,* 8**,** 813-824.
DADGOSTAR, H. & CHENG, G. (2000) Membrane localization of TRAF 3 enables JNK activation. *Journal of Biological Chemistry,* 275**,** 2539-2544.
DAMDIMOPOULOS, A. E., MIRANDA-VIZUETE, A., PELTO-HUIKKO, M., GUSTAFSSON, J.-Ã. K. & SPYROU, G. (2002) Human mitochondrial thioredoxin involvement in mitochondrial membrane potential and cell death. *Journal of Biological Chemistry,* 277**,** 33249-33257.
DANG, C. V. (2012) Links between metabolism and cancer. *Genes & Development,* 26**,** 877-890.
DANIAL, N. N. & KORSMEYER, S. J. (2004) Cell death: critical control points. *Cell,* 116**,** 205-219.
DASGUPTA, S., HOQUE, M. O., UPADHYAY, S. & SIDRANSKY, D. (2008) Mitochondrial cytochrome B gene mutation promotes tumor growth in bladder cancer. *Cancer research,* 68**,** 700-706.
DAVIES, C. C., MASON, J., WAKELAM, M. J. O., YOUNG, L. S. & ELIOPOULOS, A. G. (2004) Inhibition of phosphatidylinositol 3-kinase-and ERK MAPK-regulated protein synthesis reveals the pro-apoptotic properties of CD40 ligation in carcinoma cells. *Journal of Biological Chemistry,* 279**,** 1010-1019.

DENEKE, S. M. & FANBURG, B. L. (1989) Regulation of cellular glutathione. *American Journal of Physiology-Lung Cellular and Molecular Physiology,* 257**,** L163-L173.

DEWAS, C. D., DANG, P. M.-C., GOUGEROT-POCIDALO, M.-A. & EL-BENNA, J. (2003) TNF-Î± induces phosphorylation of p47phox in human neutrophils: partial phosphorylation of p47phox is a common event of priming of human neutrophils by TNF-Î± and granulocyte-macrophage colony-stimulating factor. *The Journal of Immunology,* 171**,** 4392-4398.

DHANASEKARAN, D. N. & JOHNSON, G. L. (2007) MAPKs: function, regulation, role in cancer and therapeutic targeting. *Oncogene,* 26**,** 3097-3099.

DHANASEKARAN, D. N. & REDDY, E. P. (2008) JNK signaling in apoptosis. *Oncogene,* 27**,** 6245-6251.

DICKSON, M. A., HAHN, W. C., INO, Y., RONFARD, V., WU, J. Y., WEINBERG, R. A., LOUIS, D. N., LI, F. P. & RHEINWALD, J. G. (2000) Human keratinocytes that express hTERT and also bypass a p16INK4a-enforced mechanism that limits life span become immortal yet retain normal growth and differentiation characteristics. *Molecular and cellular biology,* 20**,** 1436-1447.

DING, D., ZHOU, J., WANG, M. & CONG, Y. S. (2013) Implications of telomereâ€  independent activities of telomerase reverse transcriptase in human cancer. *FEBS Journal*.

DORION, S., LAMBERT, H. & LANDRY, J. (2002) Activation of the p38 signaling pathway by heat shock involves the dissociation of glutathione S-transferase Mu from Ask1. *Journal of Biological Chemistry,* 277**,** 30792-30797.

DUFFY, C. L., PHILLIPS, S. L. & KLINGELHUTZ, A. J. (2003) Microarray analysis identifies differentiation-associated genes regulated by human papillomavirus type 16 E6. *Virology,* 314**,** 196-205.

EFERL, R. & WAGNER, E. F. (2003) AP-1: a double-edged sword in tumorigenesis. *Nature Reviews Cancer,* 3**,** 859-868.

ELGUETA, R., BENSON, M. J., DE VRIES, V. C., WASIUK, A., GUO, Y. & NOELLE, R. J. (2009) Molecular mechanism and function of CD40/CD40L engagement in the immune system. *Immunological reviews,* 229**,** 152-172.

ELIOPOULOS, A. G., DAVIES, C., BLAKE, S. S. M., MURRAY, P., NAJAFIPOUR, S., TSICHLIS, P. N. & YOUNG, L. S. (2002) The oncogenic protein kinase Tpl-2/Cot contributes to Epstein-Barr virus-encoded latent infection membrane protein 1-induced NF-ÎºB signaling downstream of TRAF2. *Journal of virology,* 76**,** 4567-4579.

ELIOPOULOS, A. G., DAVIES, C., KNOX, P. G., GALLAGHER, N. J., AFFORD, S. C., ADAMS, D. H. & YOUNG, L. S. (2000a) CD40 induces apoptosis in carcinoma cells through activation of cytotoxic ligands of the tumor necrosis factor superfamily. *Molecular and cellular biology,* 20**,** 5503-5515.

ELIOPOULOS, A. G., DAVIES, C., KNOX, P. G., GALLAGHER, N. J., AFFORD, S. C., ADAMS, D. H. & YOUNG, L. S. (2000b) CD40 induces apoptosis in carcinoma cells through activation of cytotoxic ligands of the tumor necrosis factor superfamily. *Mol Cell Biol,* 20**,** 5503-15.

ELIOPOULOS, A. G., DAWSON, C. W., MOSIALOS, G., FLOETTMANN, J. E., ROWE, M., ARMITAGE, R. J., DAWSON, J., ZAPATA, J. M., KERR, D. J. & WAKELAM, M. J. (1996a) CD40-induced growth inhibition in epithelial cells is mimicked by Epstein-Barr Virus-encoded LMP1: involvement of TRAF3 as a common mediator. *Oncogene,* 13**,** 2243-2254.

ELIOPOULOS, A. G., DAWSON, C. W., MOSIALOS, G., FLOETTMANN, J. E., ROWE, M., ARMITAGE, R. J., DAWSON, J., ZAPATA, J. M., KERR, D. J., WAKELAM, M. J., REED, J. C., KIEFF, E. & YOUNG, L. S. (1996b) CD40-induced growth inhibition in epithelial cells is mimicked by Epstein-Barr Virus-encoded LMP1: involvement of TRAF3 as a common mediator. *Oncogene,* 13**,** 2243-54.

ELIOPOULOS, A. G. & YOUNG, L. S. (2004) The role of the CD40 pathway in the pathogenesis and treatment of cancer. *Current opinion in pharmacology,* 4**,** 360-367.

ELMETWALI, T., SEARLE, P. F., MCNEISH, I., YOUNG, L. S. & PALMER, D. H. (2010a) CD40 ligand induced cytotoxicity in carcinoma cells is enhanced by inhibition of metalloproteinase cleavage and delivery via a conditionally-replicating adenovirus. *Molecular cancer,* 9**,** 52.

ELMETWALI, T., YOUNG, L. S. & PALMER, D. H. (2010b) CD40 ligand-induced carcinoma cell death: a balance between activation of TNFR-associated factor (TRAF) 3-dependent death signals and suppression of TRAF6-dependent survival signals. *The Journal of Immunology,* 184**,** 1111-1120.

ELMORE, S. (2007) Apoptosis: a review of programmed cell death. *Toxicologic pathology,* 35**,** 495-516.

ELSBY, R., KITTERINGHAM, N. R., GOLDRING, C. E., LOVATT, C. A., CHAMBERLAIN, M., HENDERSON, C. J., WOLF, C. R. & PARK, B. K. (2003) Increased constitutive c-Jun N-terminal kinase signaling in mice lacking glutathione S-transferase Pi. *Journal of Biological Chemistry,* 278**,** 22243-22249.

ESPOSTI, M. D. & DIVE, C. (2003) Mitochondrial membrane permeabilisation by Bax/Bak. *Biochemical and biophysical research communications,* 304**,** 455-461.

ESTRELA, J. M., ORTEGA, A. & OBRADOR, E. (2006) Glutathione in cancer biology and therapy. *Critical reviews in clinical laboratory sciences,* 43**,** 143-181.

FAN, L. M., TENG, L. & LI, J.-M. (2009) Knockout of p47phox uncovers a critical role of p40phox in reactive oxygen species production in microvascular endothelial cells. *Arteriosclerosis, thrombosis, and vascular biology,* 29**,** 1651-1656.

FAN, M. & CHAMBERS, T. C. (2001) Role of mitogen-activated protein kinases in the response of tumor cells to chemotherapy. *Drug Resistance Updates,* 4**,** 253-267.

FAROOQ, A. & ZHOU, M.-M. (2004) Structure and regulation of MAPK phosphatases. *Cellular signalling,* 16**,** 769-779.

FLEMING, Y., ARMSTRONG, C., MORRICE, N., PATERSON, A., GOEDERT, M. & COHEN, P. (2000) Synergistic activation of stress-activated protein kinase 1/c-Jun N-terminal kinase (SAPK1/JNK) isoforms by mitogen-activated protein kinase kinase 4 (MKK4) and MKK7. *Biochem. j,* 352**,** 145-154.

FONSATTI, E., MAIO, M., ALTOMONTE, M. & HERSEY, P. (2010) Biology and clinical applications of CD40 in cancer treatment. *Seminars in oncology.* Elsevier.

FORCE, W. R., GLASS, A. A., BENEDICT, C. A., CHEUNG, T. C., LAMA, J. & WARE, C. F. (2000) Discrete signaling regions in the lymphotoxin-Î² receptor for tumor necrosis factor receptor-associated factor binding, subcellular localization, and activation of cell death and NF-Î¹B pathways. *Journal of Biological Chemistry,* 275**,** 11121-11129.

FUJINO, G., NOGUCHI, T., MATSUZAWA, A., YAMAUCHI, S., SAITOH, M., TAKEDA, K. & ICHIJO, H. (2007) Thioredoxin and TRAF family proteins regulate reactive oxygen species-dependent activation of ASK1 through reciprocal modulation of the N-terminal homophilic interaction of ASK1. *Molecular and cellular biology,* 27**,** 8152-8163.

FUNAKOSHI, S., LONGO, D. L. & MURPHY, W. J. (1996) Differential in vitro and in vivo antitumor effects mediated by anti-CD40 and anti-CD20 monoclonal antibodies against human B-cell lymphomas. *Journal of Immunotherapy,* 19**,** 93-101.

GALLAGHER, N. J., ELIOPOULOS, A. G., AGATHANGELO, A., OATES, J., CROCKER, J. & YOUNG, L. S. (2002) CD40 activation in epithelial ovarian carcinoma cells modulates growth, apoptosis, and cytokine secretion. *Molecular Pathology,* 55**,** 110-120.

GALLUZZI, L., AARONSON, S. A., ABRAMS, J., ALNEMRI, E. S., ANDREWS, D. W., BAEHRECKE, E. H., BAZAN, N. G., BLAGOSKLONNY, M. V., BLOMGREN, K. & BORNER, C. (2009) Guidelines for the use and interpretation of assays for monitoring cell death in higher eukaryotes. *Cell Death & Differentiation,* 16**,** 1093-1107.

GALY, A. H. & SPITS, H. (1992) CD40 is functionally expressed on human thymic epithelial cells. *The Journal of Immunology,* 149**,** 775-782.

GAMPER, C., OMENE, C. O., VAN EYNDHOVEN, W. G., GLASSMAN, G. D. & LEDERMAN, S. (2001) Expression and function of TRAF-3 splice-variant isoforms in human lymphoma cell lines. *Human immunology,* 62**,** 1167-1177.

GAMPER, C., VAN EYNDHOVEN, W. G., SCHWEIGER, E., MOSSBACHER, M., KOO, B. & LEDERMAN, S. (2000) TRAF-3 interacts with p62 nucleoporin, a component of the nuclear pore central plug that binds classical NLS-containing import complexes. *Molecular immunology,* 37**,** 73-84.

GAO, X.-D. & CHEN, Y.-R. (2007a) Inhibition of telomerase with human telomerase reverse transcriptase antisense enhances tumor necrosis factor-alpha-induced apoptosis in bladder cancer cells. *CHINESE MEDICAL JOURNAL-BEIJING-ENGLISH EDITION-,* 120**,** 755.

GAO, X. D. & CHEN, Y. R. (2007b) Inhibition of telomerase with hTERT antisense enhances TNF-alpha-induced apoptosis in prostate cancer cells PC3]. *Zhonghua nan ke xue= National journal of andrology,* 13**,** 723.

GEORGOPOULOS, N. T., KIRKWOOD, L. A., VARLEY, C. L., MACLAINE, N. J., AZIZ, N. & SOUTHGATE, J. (2011) Immortalisation of normal human urothelial cells compromises differentiation capacity. *European urology,* 60**,** 141-149.

GEORGOPOULOS, N. T., MERRICK, A., SCOTT, N., SELBY, P. J., MELCHER, A. & TREJDOSIEWICZ, L. K. (2007) CD40â€ mediated death and cytokine secretion in colorectal cancer: A potential target for inflammatory tumour cell killing. *International journal of cancer,* 121**,** 1373-1381.

GEORGOPOULOS, N. T., STEELE, L. P., THOMSON, M. J., SELBY, P. J., SOUTHGATE, J. & TREJDOSIEWICZ, L. K. (2006) A novel mechanism of CD40-induced apoptosis of carcinoma cells involving TRAF3 and JNK/AP-1 activation. *Cell Death & Differentiation,* 13**,** 1789-1801.

GESERICK, C. & BLASCO, M. A. (2006) Novel roles for telomerase in aging. *Mechanisms of ageing and development,* 127**,** 579-583.

GHAMANDE, S., HYLANDER, B. L., OFLAZOGLU, E., LELE, S., FANSLOW, W. & REPASKY, E. A. (2001) Recombinant CD40 ligand therapy has significant

antitumor effects on CD40-positive ovarian tumor xenografts grown in SCID mice and demonstrates an augmented effect with cisplatin. *Cancer Res,* 61**,** 7556-62.

GHIRINGHELLI, F., MACNARD, C., MARTIN, F. & ZITVOGEL, L. (2006) The role of regulatory T cells in the control of natural killer cells: relevance during tumor progression. *Immunological reviews,* 214**,** 229-238.

GODWIN, A. K., MEISTER, A., O'DWYER, P. J., HUANG, C. S., HAMILTON, T. C. & ANDERSON, M. E. (1992) High resistance to cisplatin in human ovarian cancer cell lines is associated with marked increase of glutathione synthesis. *Proceedings of the National Academy of Sciences,* 89**,** 3070-3074.

GOLDMAN, E. H., CHEN, L. & FU, H. (2004) Activation of apoptosis signal-regulating kinase 1 by reactive oxygen species through dephosphorylation at serine 967 and 14-3-3 dissociation. *Journal of Biological Chemistry,* 279**,** 10442-10449.

GRAMMER, A. C. & LIPSKY, P. E. (2001) CD40-mediated regulation of immune responses by TRAF-dependent and TRAF-independent signaling mechanisms. *Advances in immunology,* 76**,** 61-178.

GREIDER, C. W. (1991) Telomerase is processive. *Molecular and cellular biology,* 11**,** 4572-4580.

GREWAL, I. S. & FLAVELL, R. A. (1998) CD40 and CD154 in cell-mediated immunity. *Annual review of immunology,* 16**,** 111-135.

GRIENDLING, K. K. & USHIO-FUKAI, M. (2000) Reactive oxygen species as mediators of angiotensin II signaling. *Regulatory peptides,* 91**,** 21-27.

GUICCIARDI, M. E. & GORES, G. J. (2009) Life and death by death receptors. *The FASEB Journal,* 23**,** 1625-1637.

GUPTA, A., ROSENBERGER, S. F. & BOWDEN, G. T. (1999) Increased ROS levels contribute to elevated transcription factor and MAP kinase activities in malignantly progressed mouse keratinocyte cell lines. *Carcinogenesis,* 20**,** 2063-2073.

GUPTA, S. (2003) Molecular signaling in death receptor and mitochondrial pathways of apoptosis (Review). *International journal of oncology,* 22**,** 15.

GUSTAFSON, S. J., DUNLAP, K. L., MCGILL, C. M. & KUHN, T. B. (2012) A Nonpolar Blueberry Fraction Blunts NADPH Oxidase Activation in Neuronal Cells Exposed to Tumor Necrosis Factor-Î±. *Oxidative medicine and cellular longevity,* 2012.

HA, Y. J. & LEE, J. R. (2004) Role of TNF receptor-associated factor 3 in the CD40 signaling by production of reactive oxygen species through association with p40phox, a cytosolic subunit of nicotinamide adenine dinucleotide phosphate oxidase. *The Journal of Immunology,* 172**,** 231-239.

HA, Y. J., SEUL, H. J. & LEE, J. R. (2011) Ligation of CD40 receptor in human B lymphocytes triggers the 5-lipoxygenase pathway to produce reactive oxygen species and activate p38 MAPK. *Experimental & molecular medicine,* 43**,** 101-110.

HACKER, H., TSENG, P.-H. & KARIN, M. (2011) Expanding TRAF function: TRAF3 as a tri-faced immune regulator. *Nature Reviews Immunology,* 11**,** 457-468.

HAEUSGEN, W., HERDEGEN, T. & WAETZIG, V. (2011) The bottleneck of JNK signaling: molecular and functional characteristics of MKK4 and MKK7. *European journal of cell biology,* 90**,** 536-544.

HALLIWELL, B. (2007) Oxidative stress and cancer: have we moved forward? *Biochem. j,* 401**,** 1-11.

HAN, J., LEE, J. D., BIBBS, L. & ULEVITCH, R. J. (1994) A MAP kinase targeted by endotoxin and hyperosmolarity in mammalian cells. *Science,* 265**,** 808-811.

HAN, S. I., KIM, Y.-S. & KIM, T.-H. (2008) Role of apoptotic and necrotic cell death under physiologic conditions. *BMB Rep,* 41**,** 1-10.

HANAHAN, D. & WEINBERG, R. A. (2011) Hallmarks of cancer: the next generation. *Cell,* 144**,** 646-674.

HARLEY, C. B. (2002) Telomerase is not an oncogene. *Oncogene,* 21**,** 494-502.

HAYWARD, A. R., LEVY, J., FACCHETTI, F., NOTARANGELO, L., OCHS, H. D., ETZIONI, A., BONNEFOY, J.-Y., COSYNS, M. & WEINBERG, A. (1997) Cholangiopathy and tumors of the pancreas, liver, and biliary tree in boys with X-linked immunodeficiency with hyper-IgM. *The Journal of Immunology,* 158**,** 977-983.

HEHLGANS, T. & PFEFFER, K. (2005) The intriguing biology of the tumour necrosis factor/tumour necrosis factor receptor superfamily: players, rules and the games. *Immunology,* 115**,** 1-20.

HEMPEL, N., YE, H., ABESSI, B., MIAN, B. & MELENDEZ, J. A. (2009) Altered redox status accompanies progression to metastatic human bladder cancer. *Free Radical Biology and Medicine,* 46**,** 42-50.

HENGARTNER, M. O. (2000) The biochemistry of apoptosis. *Nature,* 407**,** 770-776.

HESS, J., ANGEL, P. & SCHORPP-KISTNER, M. (2004) AP-1 subunits: quarrel and harmony among siblings. *Journal of cell science,* 117**,** 5965-5973.

HESS, S. & ENGELMANN, H. (1996) A novel function of CD40: induction of cell death in transformed cells. *The Journal of experimental medicine,* 183**,** 159-167.

HIBI, M., LIN, A., SMEAL, T., MINDEN, A. & KARIN, M. (1993) Identification of an oncoprotein-and UV-responsive protein kinase that binds and potentiates the c-Jun activation domain. *Genes & Development,* 7**,** 2135-2148.

HILL, K. S., ERRINGTON, F., STEELE, L. P., MERRICK, A., MORGAN, R., SELBY, P. J., GEORGOPOULOS, N. T., O'DONNELL, D. M. & MELCHER, A. A. (2008a) OK432-activated human dendritic cells kill tumor cells via CD40/CD40 ligand interactions. *J Immunol,* 181**,** 3108-15.

HILL, K. S., ERRINGTON, F., STEELE, L. P., MERRICK, A., MORGAN, R., SELBY, P. J., GEORGOPOULOS, N. T., O'DONNELL, D. M. & MELCHER, A. A. (2008b) OK432-activated human dendritic cells kill tumor cells via CD40/CD40 ligand interactions. *The Journal of Immunology,* 181**,** 3108-3115.

HIRAI, H., ADACHI, T. & TSUBATA, T. (2003) Involvement of cell cycle progression in survival signaling through CD40 in the B-lymphocyte line WEHI-231. *Cell Death & Differentiation,* 11**,** 261-269.

HIRANO, A., LONGO, D. L., TAUB, D. D., FERRIS, D. K., YOUNG, L. S., ELIOPOULOS, A. G., AGATHANGGELOU, A., CULLEN, N., MACARTNEY, J. & FANSLOW, W. C. (1999) Inhibition of human breast carcinoma growth by a soluble recombinant human CD40 ligand. *Blood,* 93**,** 2999-3007.

HIROTA, K., MURATA, M., SACHI, Y., NAKAMURA, H., TAKEUCHI, J., MORI, K. & YODOI, J. (1999) Distinct Roles of Thioredoxin in the Cytoplasm and in the Nucleus A TWO-STEP MECHANISM OF REDOX REGULATION OF TRANSCRIPTION FACTOR NF-ÎºB. *Journal of Biological Chemistry,* 274**,** 27891-27897.

HOEFLICH, K. P., YEH, W.-C., YAO, Z., MAK, T. W. & WOODGETT, J. R. (1999) Mediation of TNF receptor-associated factor effector functions by apoptosis signal-regulating kinase-1 (ASK1). *Oncogene,* 18**,** 5814-5820.

HOLLSTEIN, M., SIDRANSKY, D., VOGELSTEIN, B. & HARRIS, C. S. C. (1991) p53 mutations in human cancers. *Science,* 253**,** 49-53.

HOSTAGER, B. S., CATLETT, I. M. & BISHOP, G. A. (2000) Recruitment of CD40 and tumor necrosis factor receptor-associated factors 2 and 3 to membrane microdomains during CD40 signaling. *Journal of Biological Chemistry,* 275**,** 15392-15398.

HU, W. H., JOHNSON, H. & SHU, H. B. (1999) Tumor necrosis factor-related apoptosis-inducing ligand receptors signal NF-kappaB and JNK activation and apoptosis through distinct pathways. *J Biol Chem,* 274**,** 30603-10.

HUANG, Q., QU, Q.-X., XIE, F., ZHANG, T., HU, J.-M., CHEN, Y.-G. & ZHANG, X.-G. (2011) CD40 is overexpressed by HPV16/18-E6 positive cervical carcinoma and correlated with clinical parameters and vascular density. *Cancer Epidemiology,* 35**,** 388-392.

ICHIJO, H., NISHIDA, E., IRIE, K., TEN DIJKE, P., SAITOH, M., MORIGUCHI, T., TAKAGI, M., MATSUMOTO, K., MIYAZONO, K. & GOTOH, Y. (1997) Induction of apoptosis by ASK1, a mammalian MAPKKK that activates SAPK/JNK and p38 signaling pathways. *Science,* 275**,** 90-94.

IGNEY, F. H. & KRAMMER, P. H. (2002) Death and anti-death: tumour resistance to apoptosis. *Nature Reviews Cancer,* 2**,** 277-288.

IMAIZUMI, K., KAWABE, T., ICHIYAMA, S., KIKUTANI, H., YAGITA, H., SHIMOKATA, K. & HASEGAWA, Y. (1999) Enhancement of tumoricidal activity of alveolar macrophages via CD40-CD40 ligand interaction. *American Journal of Physiology-Lung Cellular and Molecular Physiology,* 277**,** L49-L57.

INDRAN, I. R., HANDE, M. P. & PERVAIZ, S. (2011) hTERT overexpression alleviates intracellular ROS production, improves mitochondrial function, and inhibits ROS-mediated apoptosis in cancer cells. *Cancer research,* 71**,** 266-276.

INOUE, Y., OTSUKA, T., NIIRO, H., NAGANO, S., ARINOBU, Y., OGAMI, E., AKAHOSHI, M., MIYAKE, K., NINOMIYA, I. & SHIMIZU, S. (2004) Novel regulatory mechanisms of CD40-induced prostanoid synthesis by IL-4 and IL-10 in human monocytes. *The Journal of Immunology,* 172**,** 2147-2154.

JACKAMAN, C., CORNWALL, S., GRAHAM, P. T. & NELSON, D. J. (2010) CD40-activated B cells contribute to mesothelioma tumor regression. *Immunology and cell biology,* 89**,** 255-267.

JACKAMAN, C., LEW, A. M., ZHAN, Y., ALLAN, J. E., KOLOSKA, B., GRAHAM, P. T., ROBINSON, B. W. S. & NELSON, D. J. (2008) Deliberately provoking local inflammation drives tumors to become their own protective vaccine site. *International immunology,* 20**,** 1467-1479.

JACOBS-HELBER, S. M., WICKREMA, A., BIRRER, M. J. & SAWYER, S. T. (1998) AP1 regulation of proliferation and initiation of apoptosis in erythropoietin-dependent erythroid cells. *Molecular and cellular biology,* 18**,** 3699-3707.

JENKINS, N. C., LIU, T., CASSIDY, P., LEACHMAN, S. A., BOUCHER, K. M., GOODSON, A. G., SAMADASHWILY, G. & GROSSMAN, D. (2010) The p16INK4A tumor suppressor regulates cellular oxidative stress. *Oncogene,* 30**,** 265-274.

JIANG, F., ZHANG, Y. & DUSTING, G. J. (2011) NADPH oxidase-mediated redox signaling: roles in cellular stress response, stress tolerance, and tissue repair. *Pharmacological Reviews,* 63**,** 218-242.

JIN, H. O., PARK, I. C., AN, S., LEE, H. C., WOO, S. H., HONG, Y. J., LEE, S. J., PARK, M. J., YOO, D. H. & RHEE, C. H. (2006) Upâ€ regulation of Bak and

Bim via JNK downstream pathway in the response to nitric oxide in human glioblastoma cells. *Journal of cellular physiology,* 206**,** 477-486.
JIN, S., RAY, R. M. & JOHNSON, L. R. (2008) TNF-Î±/cycloheximide-induced apoptosis in intestinal epithelial cells requires Rac1-regulated reactive oxygen species. *American Journal of Physiology-Gastrointestinal and Liver Physiology,* 294**,** G928-G937.
JING, L. I. U. & ANNING, L. (2005) Role of JNK activation in apoptosis: a double-edged sword. *Cell research,* 15**,** 36-42.
JOCHUM, W., PASSEQUE, E. & WAGNER, E. F. (2001) AP-1 in mouse development and tumorigenesis. *Oncogene,* 20**,** 2401-2412.
JUNDI, M., NADIRI, A., AL-ZOOBI, L., HASSAN, G. S. & MOURAD, W. (2012) CD40-mediated cell death requires TRAF6 recruitment. *Immunobiology,* 217**,** 375-383.
JYOTHI, M. D. & KHAR, A. (2000) Regulation of CD40L expression on natural killer cells by interleukin-12 and interferon Î³: its role in the elicitation of an effective antitumor immune response. *Cancer Immunology, Immunotherapy,* 49**,** 563-572.
KAHL, R., KAMPKOTTER, A., WÃ¤TJEN, W. & CHOVOLOU, Y. (2004) Antioxidant Enzymes and Apoptosis#. *Drug metabolism reviews,* 36**,** 747-762.
KAKOLYRIS, S., GIATROMANOLAKI, A., KOUKOURAKIS, M., POWIS, G., SOUGLAKOS, J., SIVRIDIS, E., GEORGOULIAS, V., GATTER, K. C. & HARRIS, A. L. (2001) Thioredoxin expression is associated with lymph node status and prognosis in early operable non-small cell lung cancer. *Clinical cancer research,* 7**,** 3087-3091.
KAMATA, H., HONDA, S.-I., MAEDA, S., CHANG, L., HIRATA, H. & KARIN, M. (2005) Reactive oxygen species promote TNFÎ±-induced death and sustained JNK activation by inhibiting MAP kinase phosphatases. *Cell,* 120**,** 649-661.
KASHIWADA, M., SHIRAKATA, Y., INOUE, J.-I., NAKANO, H., OKAZAKI, K., OKUMURA, K., YAMAMOTO, T., NAGAOKA, H. & TAKEMORI, T. (1998) Tumor necrosis factor receptorâ€“associated factor 6 (TRAF6) stimulates extracellular signalâ€“regulated kinase (ERK) activity in CD40 signaling along a ras-independent pathway. *The Journal of experimental medicine,* 187**,** 237-244.
KATO, M., SHIMADA, Y., TANAKA, H., HOSOTANI, R., OHSHIO, G., ISHIZAKI, K. & IMAMURA, M. (1999) Characterization of six cell lines established from human pancreatic adenocarcinomas. *Cancer,* 85**,** 832-840.
KATO, T., DUFFEY, D. C., ONDREY, F. G., DONG, G., CHEN, Z., COOK, J. A., MITCHELL, J. B. & VAN WAES, C. (2000) Cisplatin and radiation sensitivity in human head and neck squamous carcinomas are independently modulated by glutathione and transcription factor NFâ€ ÎºB. *Head & neck,* 22**,** 748-759.
KAWABE, T., MATSUSHIMA, M., HASHIMOTO, N., IMAIZUMI, K. & HASEGAWA, Y. (2011) CD40/CD40 ligand interactions in immune responses and pulmonary immunity. *Nagoya journal of medical science,* 73**,** 69-78.
KAWABE, T., NAKA, T., YOSHIDA, K., TANAKA, T., FUJIWARA, H., SUEMATSU, S., YOSHIDA, N., KISHIMOTO, T. & KIKUTANI, H. (1994) The immune responses in CD40-deficient mice: impaired immunoglobulin class switching and germinal center formation. *Immunity,* 1**,** 167-178.
KENNEDY, N. J. & DAVIS, R. J. (2003) Role of JNK in tumor development. *Cell Cycle,* 2**,** 199-201.

KHONG, A., NELSON, D. J., NOWAK, A. K., LAKE, R. A. & ROBINSON, B. W. S. (2012) The use of agonistic anti-CD40 therapy in treatments for cancer. *International reviews of immunology,* 31**,** 246-266.

KIM, E. Y., SEO, J. M., CHO, K. J. & KIM, J. H. (2009) Ras-induced invasion and metastasis are regulated by a leukotriene B4 receptor BLT2-linked pathway. *Oncogene,* 29**,** 1167-1178.

KIM, H.-J., LEE, J.-H., KIM, S.-J., OH, G. S., MOON, H.-D., KWON, K.-B., PARK, C., PARK, B. H., LEE, H.-K. & CHUNG, S.-Y. (2010) Roles of NADPH oxidases in cisplatin-induced reactive oxygen species generation and ototoxicity. *The Journal of Neuroscience,* 30**,** 3933-3946.

KIM, S. D., MOON, C. K., EUN, S.-Y., RYU, P. D. & JO, S. A. (2005) Identification of ASK1, MKK4, JNK, c-Jun, and caspase-3 as a signaling cascade involved in cadmium-induced neuronal cell apoptosis. *Biochemical and biophysical research communications,* 328**,** 326-334.

KIM, Y.-S., MORGAN, M. J., CHOKSI, S. & LIU, Z.-G. (2007) TNF-induced activation of the Nox1 NADPH oxidase and its role in the induction of necrotic cell death. *Molecular cell,* 26**,** 675-687.

KIYONO, T., FOSTER, S. A., KOOP, J. I., MCDOUGALL, J. K., GALLOWAY, D. A. & KLINGELHUTZ, A. J. (1998) Both Rb/p16INK4a inactivation and telomerase activity are required to immortalize human epithelial cells. *Nature,* 396**,** 84-88.

KROEMER, G., GALLUZZI, L. & BRENNER, C. (2007) Mitochondrial membrane permeabilization in cell death. *Physiological reviews,* 87**,** 99-163.

KUWANA, T. & NEWMEYER, D. D. (2003) Bcl-2-family proteins and the role of mitochondria in apoptosis. *Current opinion in cell biology,* 15**,** 691-699.

KYRIAKIS, J. M. & AVRUCH, J. (2001) Mammalian mitogen-activated protein kinase signal transduction pathways activated by stress and inflammation. *Physiological reviews,* 81**,** 807-869.

KYRIAKIS, J. M. & AVRUCH, J. (2012) Mammalian MAPK signal transduction pathways activated by stress and inflammation: a 10-year update. *Physiological reviews,* 92**,** 689-737.

LAW, C.-L., GORDON, K. A., COLLIER, J., KLUSSMAN, K., MCEARCHERN, J. A., CERVENY, C. G., MIXAN, B. J., LEE, W. P., LIN, Z. & VALDEZ, P. (2005) Preclinical antilymphoma activity of a humanized anti-CD40 monoclonal antibody, SGN-40. *Cancer research,* 65**,** 8331-8338.

LAWLER, S., FLEMING, Y., GOEDERT, M. & COHEN, P. (1998) Synergistic activation of SAPK1/JNK1 by two MAP kinase kinases< i> in vitro</i>. *Current biology,* 8**,** 1387-1391.

LEE, N. K. & LEE, S. Y. (2002) Modulation of life and death by the tumor necrosis factor receptor-associated factors (TRAFs). *Journal of biochemistry and molecular biology,* 35**,** 61-66.

LEE, Z. H., LEE, S. E., KWACK, K., YEO, W., LEE, T. H., BAE, S. S., SUH, P.-G. & KIM, H.-H. (2001) Caspase-mediated cleavage of TRAF3 in FasL-stimulated Jurkat-T cells. *Journal of leukocyte biology,* 69**,** 490-496.

LEI, K. & DAVIS, R. J. (2003) JNK phosphorylation of Bim-related members of the Bcl2 family induces Bax-dependent apoptosis. *Proceedings of the National Academy of Sciences,* 100**,** 2432-2437.

LEI, K., NIMNUAL, A., ZONG, W.-X., KENNEDY, N. J., FLAVELL, R. A., THOMPSON, C. B., BAR-SAGI, D. & DAVIS, R. J. (2002) The Bax subfamily

of Bcl2-related proteins is essential for apoptotic signal transduction by c-Jun NH2-terminal kinase. *Molecular and cellular biology,* 22**,** 4929-4942.

LI, J.-M., FAN, L. M., CHRISTIE, M. R. & SHAH, A. M. (2005) Acute tumor necrosis factor alpha signaling via NADPH oxidase in microvascular endothelial cells: role of p47phox phosphorylation and binding to TRAF4. *Molecular and cellular biology,* 25**,** 2320-2330.

LI, J. & YUAN, J. (2008) Caspases in apoptosis and beyond. *Oncogene,* 27**,** 6194-6206.

LI, Q., SPENCER, N. Y., OAKLEY, F. D., BUETTNER, G. R. & ENGELHARDT, J. F. (2009) Endosomal Nox2 facilitates redox-dependent induction of NF-Î¤B by TNF-Î±. *Antioxidants & redox signaling,* 11**,** 1249-1263.

LINCOLN, D. T., EMADI, E. M., TONISSEN, K. F. & CLARKE, F. M. (2003) The thioredoxin-thioredoxin reductase system: over-expression in human cancer. *Anticancer research,* 23**,** 2425-2433.

LIU, H., ZHANG, H., ILES, K. E., RINNA, A., MERRILL, G., YODOI, J., TORRES, M. & FORMAN, H. J. (2006) The ADP-stimulated NADPH oxidase activates the ASK-1/MKK4/JNK pathway in alveolar macrophages. *Free radical research,* 40**,** 865-874.

LIU, Y. & MIN, W. (2002) Thioredoxin promotes ASK1 ubiquitination and degradation to inhibit ASK1-mediated apoptosis in a redox activity-independent manner. *Circulation research,* 90**,** 1259-1266.

LOPEZ-LAZARO, M. (2007) Dual role of hydrogen peroxide in cancer: possible relevance to cancer chemoprevention and therapy. *Cancer letters,* 252**,** 1-8.

LOSKOG, A. & TOTTERMAN, T. H. (2007) CD40L-a multipotent molecule for tumor therapy. *Endocrine, Metabolic & Immune Disorders-Drug Targets (Formerly Current Drug Targets-Immune, Endocrine & Metabolic Disorders),* 7**,** 23-28.

LOSKOG, A. S. I. & ELIOPOULOS, A. G. (2009) The Janus faces of CD40 in cancer. *Seminars in immunology.* Elsevier.

LOWE, S. W., CEPERO, E. & EVAN, G. (2004) Intrinsic tumour suppression. *Nature,* 432**,** 307-315.

MA, D. Y. & CLARK, E. A. (2009) The role of CD40 and CD154/CD40L in dendritic cells. *Seminars in immunology.* Elsevier.

MACKEY, M. F., GUNN, J. R., TING, P. P., KIKUTANI, H., DRANOFF, G., NOELLE, R. J. & BARTH, R. J. (1997) Protective immunity induced by tumor vaccines requires interaction between CD40 and its ligand, CD154. *Cancer research,* 57**,** 2569-2574.

MANDAL, M., OLSON, D. J., SHARMA, T., VADLAMUDI, R. K. & KUMAR, R. (2001) Butyric acid induces apoptosis by up-regulating Bax expression via stimulation of the c-Jun N-terminal kinase/activation protein-1 pathway in human colon cancer cells. *Gastroenterology,* 120**,** 71-78.

MARKS, P. A. & XU, W. S. (2009) Histone deacetylase inhibitors: Potential in cancer therapy. *Journal of cellular biochemistry,* 107**,** 600-608.

MASSARD, C., ZERMATI, Y., PAULEAU, A. L., LAROCHETTE, N., METIVIER, D., SABATIER, L., KROEMER, G. & SORIA, J. C. (2006) hTERT: a novel endogenous inhibitor of the mitochondrial cell death pathway. *Oncogene,* 25**,** 4505-4514.

MASTERS, J. R. W., HEPBURN, P. J., WALKER, L., HIGHMAN, W. J., TREJDOSIEWICZ, L. K., POVEY, S., PARKAR, M., HILL, B. T., RIDDLE, P. R. & FRANKS, L. M. (1986) Tissue culture model of transitional cell

carcinoma: characterization of twenty-two human urothelial cell lines. *Cancer research,* 46**,** 3630-3636.
MATHUR, R. K., AWASTHI, A., WADHONE, P., RAMANAMURTHY, B. & SAHA, B. (2004) Reciprocal CD40 signals through p38MAPK and ERK-1/2 induce counteracting immune responses. *Nature medicine,* 10**,** 540-544.
MATSUURA, H., NISHITOH, H., TAKEDA, K., MATSUZAWA, A., AMAGASA, T., ITO, M., YOSHIOKA, K. & ICHIJO, H. (2002) Phosphorylation-dependent Scaffolding Role of JSAP1/JIP3 in the ASK1-JNK Signaling Pathway A NEW MODE OF REGULATION OF THE MAP KINASE CASCADE. *Journal of Biological Chemistry,* 277**,** 40703-40709.
MATSUZAWA, A., TSENG, P.-H., VALLABHAPURAPU, S., LUO, J.-L., ZHANG, W., WANG, H., VIGNALI, D. A. A., GALLAGHER, E. & KARIN, M. (2008) Essential cytoplasmic translocation of a cytokine receptorâ€“assembled signaling complex. *Science,* 321**,** 663-668.
MICHEAU, O. & TSCHOPP, J. R. (2003) Induction of TNF receptor I-mediated apoptosis via two sequential signaling complexes. *Cell,* 114**,** 181-190.
MITSUI, A., HAMURO, J., NAKAMURA, H., KONDO, N., HIRABAYASHI, Y., ISHIZAKI-KOIZUMI, S., HIRAKAWA, T., INOUE, T. & YODOI, J. (2002) Overexpression of human thioredoxin in transgenic mice controls oxidative stress and life span. *Antioxidants and Redox Signaling,* 4**,** 693-696.
MOLL, R., ACHTSTATTER, T., BECHT, E., BALCAROVA-STÃ¤NDER, J., ITTENSOHN, M. & FRANKE, W. W. (1988) Cytokeratins in normal and malignant transitional epithelium. Maintenance of expression of urothelial differentiation features in transitional cell carcinomas and bladder carcinoma cell culture lines. *The American journal of pathology,* 132**,** 123.
MORAN, A. E., KOVACSOVICS-BANKOWSKI, M. & WEINBERG, A. D. (2013) The TNFRs OX40, 4-1BB, and CD40 as targets for cancer immunotherapy. *Curr Opin Immunol*.
MORGAN, M. J. & LIU, Z.-G. (2010) Crosstalk of reactive oxygen species and NF-ÎºB signaling. *Cell research,* 21**,** 103-115.
MORRIS, A. E., REMMELE, R. L., KLINKE, R., MACDUFF, B. M., FANSLOW, W. C. & ARMITAGE, R. J. (1999) Incorporation of an isoleucine zipper motif enhances the biological activity of soluble CD40L (CD154). *Journal of Biological Chemistry,* 274**,** 418-423.
MUNROE, M. E. & BISHOP, G. A. (2007) A costimulatory function for T cell CD40. *The Journal of Immunology,* 178**,** 671-682.
NAKANO, H., SAKON, S., KOSEKI, H., TAKEMORI, T., TADA, K., MATSUMOTO, M., MUNECHIKA, E., SAKAI, T., SHIRASAWA, T. & AKIBA, H. (1999) Targeted disruption of Traf5 gene causes defects in CD40-and CD27-mediated lymphocyte activation. *Proceedings of the National Academy of Sciences,* 96**,** 9803-9808.
NI, C.-Z., WELSH, K., LEO, E., CHIOU, C.-K., WU, H., REED, J. C. & ELY, K. R. (2000) Molecular basis for CD40 signaling mediated by TRAF3. *Proceedings of the National Academy of Sciences,* 97**,** 10395-10399.
NILES, A. L., MORAVEC, R. A., ERIC HESSELBERTH, P., SCURRIA, M. A., DAILY, W. J. & RISS, T. L. (2007) A homogeneous assay to measure live and dead cells in the same sample by detecting different protease markers. *Analytical biochemistry,* 366**,** 197-206.

NISHITOH, H., SAITOH, M., MOCHIDA, Y., TAKEDA, K., NAKANO, H., ROTHE, M., MIYAZONO, K. & ICHIJO, H. (1998) ASK1 is essential for JNK/SAPK activation by TRAF2. *Molecular cell,* 2**,** 389-395.

NOIKE, T., MIWA, S., SOEDA, J., KOBAYASHI, A. & MIYAGAWA, S.-I. (2008) Increased expression of thioredoxin-1, vascular endothelial growth factor, and redox factor-1 is associated with poor prognosis in patients with liver metastasis from colorectal cancer. *Human pathology,* 39**,** 201-208.

NORBERG, E., ORRENIUS, S. & ZHIVOTOVSKY, B. (2010) Mitochondrial regulation of cell death: processing of apoptosis-inducing factor (AIF). *Biochemical and biophysical research communications,* 396**,** 95-100.

ORTEGA, A. L., MENA, S. & ESTRELA, J. M. (2011) Glutathione in cancer cell death. *Cancers,* 3**,** 1285-1310.

OTT, M., GOGVADZE, V., ORRENIUS, S. & ZHIVOTOVSKY, B. (2007) Mitochondria, oxidative stress and cell death. *Apoptosis,* 12**,** 913-922.

PALETTA-SILVA, R., ROCCO-MACHADO, N. L. & MEYER-FERNANDES, J. R. (2013) NADPH oxidase biology and the regulation of tyrosine kinase receptor signaling and cancer drug cytotoxicity. *International journal of molecular sciences,* 14**,** 3683-3704.

PAN, J.-S., HONG, M.-Z. & REN, J.-L. (2009) Reactive oxygen species: a double-edged sword in oncogenesis. *World journal of gastroenterology: WJG,* 15**,** 1702.

PARK, S.-M., KIM, H.-S., CHOE, J. & LEE, T. H. (1999) Differential induction of cytokine genes and activation of mitogen-activated protein kinase family by soluble CD40 ligand and TNF in a human follicular dendritic cell line. *The Journal of Immunology,* 163**,** 631-638.

PARK, S., HAHM, E. R., LEE, D. K. & YANG, C. H. (2004) Inhibition of APâ€ 1 transcription activator induces mycâ€ dependent apoptosis in HL60 cells. *Journal of cellular biochemistry,* 91**,** 973-986.

PAULIE, S., EHLIN-HENRIKSSON, B., MELLSTEDT, H. K., KOHO, H., BEN-AISSA, H. & PERLMANN, P. (1985) A p50 surface antigen restricted to human urinary bladder carcinomas and B lymphocytes. *Cancer Immunology, Immunotherapy,* 20**,** 23-28.

PAULIE, S., KOHO, H., BEN-AISSA, H., HANSSON, Y., LUNDBLAD, M.-L. & PERLMANN, P. (1984) Monoclonal antibodies to antigens associated with transitional cell carcinoma of the human urinary bladder. *Cancer Immunology, Immunotherapy,* 17**,** 173-179.

PEGUET-NAVARRO, J., DALBIEZ-GAUTHIER, C., MOULON, C., BERTHIER, O., RÃ©ANO, A., GAUCHERAND, M., BANCHEREAU, J., ROUSSET, F. & SCHMITT, D. (1997) CD40 ligation of human keratinocytes inhibits their proliferation and induces their differentiation. *The Journal of Immunology,* 158**,** 144-152.

PENN, I. (1990) Occurrence of cancers in immunosuppressed organ transplant recipients. *Clinical transplants***,** 53.

PFEFFER, K. (2003) Biological functions of tumor necrosis factor cytokines and their receptors. *Cytokine & growth factor reviews,* 14**,** 185-191.

PHAM, L. V., TAMAYO, A. T., YOSHIMURA, L. C., LO, P., TERRY, N., REID, P. S. & FORD, R. J. (2002) A CD40 signalosome anchored in lipid rafts leads to constitutive activation of NF-Îºb and autonomous cell growth in B cell lymphomas. *Immunity,* 16**,** 37-50.

PINCHUK, L. M., KLAUS, S. J., MAGALETTI, D. M., PINCHUK, G. V., NORSEN, J. P. & CLARK, E. A. (1996) Functional CD40 ligand expressed by human blood dendritic cells is up-regulated by CD40 ligation. *The Journal of Immunology,* 157**,** 4363-4370.

PLJESA-ERCEGOVAC, M., SAVIC-RADOJEVIC, A., DRAGICEVIC, D., MIMIC-OKA, J., MATIC, M., SASIC, T., PEKMEZOVIC, T., VUKSANOVIC, A. & SIMIC, T. (2011) Enhanced GSTP1 expression in transitional cell carcinoma of urinary bladder is associated with altered apoptotic pathways. *Urologic Oncology: Seminars and Original Investigations.* Elsevier.

POUND, J. D., CHALLA, A., HOLDER, M. J., ARMITAGE, R. J., DOWER, S. K., FANSLOW, W. C., KIKUTANI, H., PAULIE, S., GREGORY, C. D. & GORDON, J. (1999) Minimal cross-linking and epitope requirements for CD40-dependent suppression of apoptosis contrast with those for promotion of the cell cycle and homotypic adhesions in human B cells. *Int Immunol,* 11**,** 11-20.

PULLEN, S. S., MILLER, H. G., EVERDEEN, D. S., DANG, T. T. A., CRUTE, J. J. & KEHRY, M. R. (1998) CD40-tumor necrosis factor receptor-associated factor (TRAF) interactions: regulation of CD40 signaling through multiple TRAF binding sites and TRAF hetero-oligomerization. *Biochemistry,* 37**,** 11836-11845.

QI, C. J., ZHENG, L., ZHOU, X., TAO, Y., GE, Y., ZHUANG, Y. M., XU, Y., YU, G. & ZHANG, X. G. (2004) Cross-linking of CD40 using anti-CD40 antibody, 5C11, has different effects on XG2 multiple myeloma cells. *Immunol Lett,* 93**,** 151-8.

QU, Y., WANG, J., RAY, P. S., GUO, H., HUANG, J., SHIN-SIM, M., BUKOYE, B. A., LIU, B., LEE, A. V. & LIN, X. (2011) Thioredoxin-like 2 regulates human cancer cell growth and metastasis via redox homeostasis and NF-ÎºB signaling. *The Journal of clinical investigation,* 121**,** 212.

RADISKY, D. C., LEVY, D. D., LITTLEPAGE, L. E., LIU, H., NELSON, C. M., FATA, J. E., LEAKE, D., GODDEN, E. L., ALBERTSON, D. G. & NIETO, M. A. (2005) Rac1b and reactive oxygen species mediate MMP-3-induced EMT and genomic instability. *Nature,* 436**,** 123-127.

RAFFEL, J., BHATTACHARYYA, A. K., GALLEGOS, A., CUI, H., EINSPAHR, J. G., ALBERTS, D. S. & POWIS, G. (2003) Increased expression of thioredoxin-1 in human colorectal cancer is associated with decreased patient survival. *Journal of Laboratory and Clinical Medicine,* 142**,** 46-51.

RAINGEAUD, J., WHITMARSH, A. J., BARRETT, T., DERIJARD, B. & DAVIS, R. J. (1996) MKK3-and MKK6-regulated gene expression is mediated by the p38 mitogen-activated protein kinase signal transduction pathway. *Molecular and cellular biology,* 16**,** 1247-1255.

RAJ, L., IDE, T., GURKAR, A. U., FOLEY, M., SCHENONE, M., LI, X., TOLLIDAY, N. J., GOLUB, T. R., CARR, S. A. & SHAMJI, A. F. (2011) Selective killing of cancer cells by a small molecule targeting the stress response to ROS. *Nature,* 475**,** 231-234.

RAMANATHAN, R. K., ABBRUZZESE, J., DRAGOVICH, T., KIRKPATRICK, L., GUILLEN, J. M., BAKER, A. F., PESTANO, L. A., GREEN, S. & VON HOFF, D. D. (2011) A randomized phase II study of PX-12, an inhibitor of thioredoxin in patients with advanced cancer of the pancreas following progression after a gemcitabine-containing combination. *Cancer chemotherapy and pharmacology,* 67**,** 503-509.

RAMANATHAN, R. K., DRAGOVICH, T., RICHARDS, D., STEPHENSON, J., PESTANO, L., HISCOX, A., LEOS, R., CHOW, S., MILLARD, J. & KIRKPATRICK, L. (2009) Results from phase Ib studies of PX-12, a thioredoxin inhibitor in patients with advanced solid malignancies. *J Clin Oncol (Meeting Abstracts).*

RAMIREZ, S. H., FAN, S., DYKSTRA, H., REICHENBACH, N., DEL VALLE, L., POTULA, R., PHIPPS, R. P., MAGGIRWAR, S. B. & PERSIDSKY, Y. (2010) Dyad of CD40/CD40 ligand fosters neuroinflammation at the bloodâ€“brain barrier and is regulated via JNK signaling: implications for HIV-1 encephalitis. *The Journal of Neuroscience,* 30**,** 9454-9464.

RAO, D. D., VORHIES, J. S., SENZER, N. & NEMUNAITIS, J. (2009) siRNA vs. shRNA: similarities and differences. *Advanced drug delivery reviews,* 61**,** 746-759.

RASTOGI, R. P. & SINHA, R. P. (2010) Apoptosis: molecular mechanisms and pathogenicity.

RAY, P. D., HUANG, B.-W. & TSUJI, Y. (2012) Reactive oxygen species (ROS) homeostasis and redox regulation in cellular signaling. *Cellular signalling,* 24**,** 981-990.

REZNIKOFF, C. A., YEAGER, T. R., BELAIR, C. D., SAVELIEVA, E., PUTHENVEETTIL, J. A. & STADLER, W. M. (1996) Elevated p16 at senescence and loss of p16 at immortalization in human papillomavirus 16 E6, but not E7, transformed human uroepithelial cells. *Cancer research,* 56**,** 2886-2890.

RIEDL, S. J. & SHI, Y. (2004) Molecular mechanisms of caspase regulation during apoptosis. *Nature Reviews Molecular Cell Biology,* 5**,** 897-907.

ROWLAND, S. L., TREMBLAY, M. M., ELLISON, J. M., STUNZ, L. L., BISHOP, G. A. & HOSTAGER, B. S. (2007) A novel mechanism for TNFR-associated factor 6-dependent CD40 signaling. *The Journal of Immunology,* 179**,** 4645-4653.

SACKS, D. & NOBEN-TRAUTH, N. (2002) The immunology of susceptibility and resistance to Leishmania major in mice. *Nature Reviews Immunology,* 2**,** 845-858.

SARETZKI, G. (2009) Telomerase, mitochondria and oxidative stress. *Experimental gerontology,* 44**,** 485-492.

SATO, S., SANJO, H., TAKEDA, K., NINOMIYA-TSUJI, J., YAMAMOTO, M., KAWAI, T., MATSUMOTO, K., TAKEUCHI, O. & AKIRA, S. (2005) Essential function for the kinase TAK1 in innate and adaptive immune responses. *Nature immunology,* 6**,** 1087-1095.

SCAFFIDI, C., FULDA, S., SRINIVASAN, A., FRIESEN, C., LI, F., TOMASELLI, K. J., DEBATIN, K.-M., KRAMMER, P. H. & PETER, M. E. (1998) Two CD95 (APO-1/Fas) signaling pathways. *The EMBO journal,* 17**,** 1675-1687.

SCARLETT, U. K., CUBILLOS-RUIZ, J. R., NESBETH, Y. C., MARTINEZ, D. G., ENGLE, X., GEWIRTZ, A. T., AHONEN, C. L. & CONEJO-GARCIA, J. R. (2009) In situ stimulation of CD40 and Toll-like receptor 3 transforms ovarian cancerâ€“infiltrating dendritic cells from immunosuppressive to immunostimulatory cells. *Cancer research,* 69**,** 7329-7337.

SCHMIELAU, J. & FINN, O. J. (2001) Activated granulocytes and granulocyte-derived hydrogen peroxide are the underlying mechanism of suppression of T-cell function in advanced cancer patients. *Cancer research,* 61**,** 4756-4760.

SCHNEIDER, P., HOLLER, N., BODMER, J. L., HAHNE, M., FREI, K., FONTANA, A. & TSCHOPP, J. (1998) Conversion of membrane-bound Fas(CD95) ligand to its soluble form is associated with downregulation of its proapoptotic activity and loss of liver toxicity. *J Exp Med,* 187**,** 1205-13.

SCORRANO, L. & KORSMEYER, S. J. (2003) Mechanisms of cytochrome< i> c</i> release by proapoptotic BCL-2 family members. *Biochemical and biophysical research communications,* 304**,** 437-444.

SENA, L. A. & CHANDEL, N. S. (2012) Physiological roles of mitochondrial reactive oxygen species. *Molecular cell,* 48**,** 158-167.

SHANNON, A. M., BOUCHIER-HAYES, D. J., CONDRON, C. M. & TOOMEY, D. (2003) Tumour hypoxia, chemotherapeutic resistance and hypoxia-related therapies. *Cancer treatment reviews,* 29**,** 297-307.

SHARMA, R., YANG, Y., SHARMA, A., AWASTHI, S. & AWASTHI, Y. C. (2004) Antioxidant role of glutathione S-transferases: protection against oxidant toxicity and regulation of stress-mediated apoptosis. *Antioxidants and Redox Signaling,* 6**,** 289-300.

SHAW, N. J., GEORGOPOULOS, N. T., SOUTHGATE, J. & TREJDOSIEWICZ, L. K. (2005) Effects of loss of p53 and p16 function on life span and survival of human urothelial cells. *Int J Cancer,* 116**,** 634-9.

SHAY, J. W. & WRIGHT, W. E. (2006) Telomerase therapeutics for cancer: challenges and new directions. *Nature Reviews Drug Discovery,* 5**,** 577-584.

SHEN, H.-M. & PERVAIZ, S. (2006) TNF receptor superfamily-induced cell death: redox-dependent execution. *The FASEB Journal,* 20**,** 1589-1598.

SHERR, C. J. & MCCORMICK, F. (2002) The RB and p53 pathways in cancer. *Cancer cell,* 2**,** 103-112.

SHIMADA, K., NAKAMURA, M., ANAI, S., DE VELASCO, M., TANAKA, M., TSUJIKAWA, K., OUJI, Y. & KONISHI, N. (2009) A novel human AlkB homologue, ALKBH8, contributes to human bladder cancer progression. *Cancer research,* 69**,** 3157-3164.

SHIOZAKI, E. N., CHAI, J. & SHI, Y. (2002) Oligomerization and activation of caspase-9, induced by Apaf-1 CARD. *Proceedings of the National Academy of Sciences,* 99**,** 4197-4202.

SIMIC, T., SAVIC-RADOJEVIC, A., PLJESA-ERCEGOVAC, M., MATIC, M. & MIMIC-OKA, J. (2009) Glutathione S-transferases in kidney and urinary bladder tumors. *Nature Reviews Urology,* 6**,** 281-289.

SOGA, M., MATSUZAWA, A. & ICHIJO, H. (2012) Oxidative stress-induced diseases via the ASK1 signaling pathway. *International journal of cell biology,* 2012.

SOUTHGATE, J., MASTERS, J. R. W. & TREJDOSIEWICZ, L. K. (2002) Culture of human urothelium. *Culture of epithelial cells***,** 381-400.

STAMENKOVIC, I., CLARK, E. A. & SEED, B. (1989) A B-lymphocyte activation molecule related to the nerve growth factor receptor and induced by cytokines in carcinomas. *The EMBO journal,* 8**,** 1403.

STECKLEY, D., KARAJGIKAR, M., DALE, L. B., FUERTH, B., SWAN, P., DRUMMOND-MAIN, C., POULTER, M. O., FERGUSON, S. S. G., STRASSER, A. & CREGAN, S. P. (2007) Puma is a dominant regulator of oxidative stress induced Bax activation and neuronal apoptosis. *The Journal of Neuroscience,* 27**,** 12989-12999.

STEELE, L. P., GEORGOPOULOS, N. T., SOUTHGATE, J., SELBY, P. J. & TREJDOSIEWICZ, L. K. (2006) Differential susceptibility to TRAIL of normal versus malignant human urothelial cells. *Cell Death Differ,* 13**,** 1564-76.

STORDAL, B. & DAVEY, R. (2008) A 39 kDa fragment of endogenous ASK1 suggests specific cleavage not degradation by the proteasome. *IUBMB life,* 60**,** 180-184.

SUN, X.-M., BRATTON, S. B., BUTTERWORTH, M., MACFARLANE, M. & COHEN, G. M. (2002) Bcl-2 and Bcl-xL inhibit CD95-mediated apoptosis by preventing mitochondrial release of Smac/DIABLO and subsequent inactivation of X-linked inhibitor-of-apoptosis protein. *Journal of Biological Chemistry,* 277**,** 11345-11351.

SUTTLES, J., MILHORN, D. M., MILLER, R. W., POE, J. C., WAHL, L. M. & STOUT, R. D. (1999) CD40 Signaling of Monocyte Inflammatory Cytokine Synthesis through an ERK1/2-dependent Pathway A TARGET OF INTERLEUKIN (IL)-4 AND IL-10 ANTI-INFLAMMATORY ACTION. *Journal of Biological Chemistry,* 274**,** 5835-5842.

SYMONS, A., BEINKE, S. & LEY, S. C. (2006) MAP kinase kinase kinases and innate immunity. *Trends in immunology,* 27**,** 40-48.

SZATROWSKI, T. P. & NATHAN, C. F. (1991) Production of large amounts of hydrogen peroxide by human tumor cells. *Cancer research,* 51**,** 794-798.

TAI, Y.-T., LI, X.-F., CATLEY, L., COFFEY, R., BREITKREUTZ, I., BAE, J., SONG, W., PODAR, K., HIDESHIMA, T. & CHAUHAN, D. (2005) Immunomodulatory drug lenalidomide (CC-5013, IMiD3) augments anti-CD40 SGN-40â€“induced cytotoxicity in human multiple myeloma: clinical implications. *Cancer research,* 65**,** 11712-11720.

TAKAHASHI, A., OHTANI, N., YAMAKOSHI, K., IIDA, S.-I., TAHARA, H., NAKAYAMA, K., NAKAYAMA, K. I., IDE, T., SAYA, H. & HARA, E. (2006) Mitogenic signalling and the p16INK4aâ€“Rb pathway cooperate to enforce irreversible cellular senescence. *Nature cell biology,* 8**,** 1291-1297.

TAYLOR, E. L., MEGSON, I. L., HASLETT, C. & ROSSI, A. G. (2003) Nitric oxide: a key regulator of myeloid inflammatory cell apoptosis. *Cell Death & Differentiation,* 10**,** 418-430.

TAYLOR, R. C., CULLEN, S. P. & MARTIN, S. J. (2008) Apoptosis: controlled demolition at the cellular level. *Nature Reviews Molecular Cell Biology,* 9**,** 231-241.

TERADA, L. S. (2006) Specificity in reactive oxidant signaling: think globally, act locally. *The Journal of cell biology,* 174**,** 615-623.

TOBIUME, K., MATSUZAWA, A., TAKAHASHI, T., NISHITOH, H., MORITA, K.-I., TAKEDA, K., MINOWA, O., MIYAZONO, K., NODA, T. & ICHIJO, H. (2001) ASK1 is required for sustained activations of JNK/p38 MAP kinases and apoptosis. *EMBO reports,* 2**,** 222-228.

TOMIYAMA, A., SERIZAWA, S., TACHIBANA, K., SAKURADA, K., SAMEJIMA, H., KUCHINO, Y. & KITANAKA, C. (2006) Critical role for mitochondrial oxidative phosphorylation in the activation of tumor suppressors Bax and Bak. *Journal of the National Cancer Institute,* 98**,** 1462-1473.

TONG, A. W., PAPAYOTI, M. H., NETTO, G., ARMSTRONG, D. T., ORDONEZ, G., LAWSON, J. M. & STONE, M. J. (2001) Growth-inhibitory effects of CD40 ligand (CD154) and its endogenous expression in human breast cancer. *Clinical cancer research,* 7**,** 691-703.

TONG, A. W. & STONE, M. J. (2003) Prospects for CD40-directed experimental therapy of human cancer. *Cancer gene therapy,* 10**,** 1-13.

TORRES, M. & FORMAN, H. J. (2003) Redox signaling and the MAP kinase pathways. *Biofactors,* 17**,** 287-296.

TRACHOOTHAM, D., ALEXANDRE, J. & HUANG, P. (2009) Targeting cancer cells by ROS-mediated mechanisms: a radical therapeutic approach? *Nature Reviews Drug Discovery,* 8**,** 579-591.

TRACHOOTHAM, D., ZHOU, Y., ZHANG, H., DEMIZU, Y., CHEN, Z., PELICANO, H., CHIAO, P. J., ACHANTA, G., ARLINGHAUS, R. B. & LIU, J. (2006) Selective killing of oncogenically transformed cells through a ROS-mediated mechanism by Î²-phenylethyl isothiocyanate. *Cancer cell,* 10**,** 241-252.

TRAPANI, J. A. & SMYTH, M. J. (2002) Functional significance of the perforin/granzyme cell death pathway. *Nature Reviews Immunology,* 2**,** 735-747.

TURNER, J. G., RAKHMILEVICH, A. L., BURDELYA, L., NEAL, Z., IMBODEN, M., SONDEL, P. M. & YU, H. (2001) Anti-CD40 antibody induces antitumor and antimetastatic effects: the role of NK cells. *The Journal of Immunology,* 166**,** 89-94.

UENO, M., MASUTANI, H., ARAI, R. J., YAMAUCHI, A., HIROTA, K., SAKAI, T., INAMOTO, T., YAMAOKA, Y., YODOI, J. & NIKAIDO, T. (1999) Thioredoxin-dependent redox regulation of p53-mediated p21 activation. *Journal of Biological Chemistry,* 274**,** 35809-35815.

URBICH, C., MALLAT, Z., TEDGUI, A., CLAUSS, M., ZEIHER, A. M. & DIMMELER, S. (2001) Upregulation of TRAF-3 by shear stress blocks CD40-mediated endothelial activation. *Journal of Clinical Investigation,* 108**,** 1451-1458.

VALKO, M., IZAKOVIC, M., MAZUR, M., RHODES, C. J. & TELSER, J. (2004) Role of oxygen radicals in DNA damage and cancer incidence. *Molecular and cellular biochemistry,* 266**,** 37-56.

VAN EYNDHOVEN, W. G., GAMPER, C. J., CHO, E., MACKUS, W. J. M. & LEDERMAN, S. (1999) TRAF-3 mRNA splice-deletion variants encode isoforms that induce NF-ÎºB activation. *Molecular immunology,* 36**,** 647-658.

VARDOULI, L., LINDQVIST, C., VLAHOU, K., LOSKOG, A. S. & ELIOPOULOS, A. G. (2009) Adenovirus delivery of human CD40 ligand gene confers direct therapeutic effects on carcinomas. *Cancer Gene Ther*.

VASIEVA, O. (2011) The many faces of glutathione transferase pi. *Current Molecular Medicine,* 11**,** 129.

VELA, L., GONZALO, O., NAVAL, J. & MARZO, I. (2013) Direct Interaction of Bax and Bak Proteins with Bcl-2 Homology Domain 3 (BH3)-only Proteins in Living Cells Revealed by Fluorescence Complementation. *Journal of Biological Chemistry,* 288**,** 4935-4946.

VON LEOPRECHTING, A., VAN DER BRUGGEN, P., PAHL, H. L., ARUFFO, A. & SIMON, J. C. (1999) Stimulation of CD40 on immunogenic human malignant melanomas augments their cytotoxic T lymphocyte-mediated lysis and induces apoptosis. *Cancer research,* 59**,** 1287-1294.

VONDERHEIDE, R. H. (2007) Prospect of targeting the CD40 pathway for cancer therapy. *Clinical cancer research,* 13**,** 1083-1088.

VURUSANER, B., POLI, G. & BASAGA, H. (2012) Tumor suppressor genes and ROS: complex networks of interactions. *Free Radical Biology and Medicine,* 52**,** 7-18.

WAGNER, E. F. & NEBREDA, Ã. N. R. (2009) Signal integration by JNK and p38 MAPK pathways in cancer development. *Nature Reviews Cancer,* 9**,** 537-549.
WANG, H.-C. R. & CHOUDHARY, S. (2011) Reactive oxygen species-mediated therapeutic control of bladder cancer. *Nature Reviews Urology,* 8**,** 608-616.
WANG, X., DESTRUMENT, A. & TOURNIER, C. (2007) Physiological roles of MKK4 and MKK7: insights from animal models. *Biochimica et Biophysica Acta (BBA)-Molecular Cell Research,* 1773**,** 1349-1357.
WARIS, G. & AHSAN, H. (2006) Reactive oxygen species: role in the development of cancer and various chronic conditions. *Journal of carcinogenesis,* 5**,** 14.
WEINBERG, F., HAMANAKA, R., WHEATON, W. W., WEINBERG, S., JOSEPH, J., LOPEZ, M., KALYANARAMAN, B., MUTLU, G. K. M., BUDINGER, G. R. S. & CHANDEL, N. S. (2010) Mitochondrial metabolism and ROS generation are essential for Kras-mediated tumorigenicity. *Proceedings of the National Academy of Sciences,* 107**,** 8788-8793.
WELSH, S. J., WILLIAMS, R. R., BIRMINGHAM, A., NEWMAN, D. J., KIRKPATRICK, D. L. & POWIS, G. (2003) The Thioredoxin Redox Inhibitors 1-Methylpropyl 2-Imidazolyl Disulfide and Pleurotin Inhibit Hypoxia-induced Factor 1Î± and Vascular Endothelial Growth Factor Formation 1. *Molecular cancer therapeutics,* 2**,** 235-243.
WESTON, C. R. & DAVIS, R. J. (2002) The JNK signal transduction pathway. *Current opinion in genetics & development,* 12**,** 14-21.
WHEELER, M. L. & DEFRANCO, A. L. (2012) Prolonged production of reactive oxygen species in response to B cell receptor stimulation promotes B cell activation and proliferation. *The Journal of Immunology,* 189**,** 4405-4416.
WINGETT, D. G., VESTAL, R. E., FORCIER, K., HADJOKAS, N. & NIELSON, C. P. (1998) CD40 is functionally expressed on human breast carcinomas: variable inducibility by cytokines and enhancement of Fas-mediated apoptosis. *Breast cancer research and treatment,* 50**,** 27-36.
WINTERBOURN, C. C. (2008) Reconciling the chemistry and biology of reactive oxygen species. *Nature chemical biology,* 4**,** 278-286.
WOELFLE, U., SAUTER, G., SANTJER, S., BRAKENHOFF, R. & PANTEL, K. (2004) Down-regulated expression of cytokeratin 18 promotes progression of human breast cancer. *Clinical cancer research,* 10**,** 2670-2674.
WYLLIE, A. H. (2010) â€œWhere, O death, is thy sting?â€ A brief review of apoptosis biology. *Molecular neurobiology,* 42**,** 4-9.
XIE, P. (2013) TRAF molecules in cell signaling and in human diseases. *Journal of molecular signaling,* 8**,** 7.
XIE, P., HOSTAGER, B. S., MUNROE, M. E., MOORE, C. R. & BISHOP, G. A. (2006) Cooperation between TNF receptor-associated factors 1 and 2 in CD40 signaling. *The Journal of Immunology,* 176**,** 5388-5400.
XU, X. P., ZHAI, D., KIM, E., SWIFT, M., REED, J. C., VOLKMANN, N. & HANEIN, D. (2013) Three-dimensional structure of Bax-mediated pores in membrane bilayers. *Cell Death & Disease,* 4**,** e683.
YIN, Y., WANG, S., SUN, Y., MATT, Y., COLBURN, N. H., SHU, Y. & HAN, X. (2009) JNK/AP-1 pathway is involved in tumor necrosis factor-Î± induced expression of vascular endothelial growth factor in MCF7 cells. *Biomedicine & Pharmacotherapy,* 63**,** 429-435.
YOULE, R. J. & STRASSER, A. (2008) The BCL-2 protein family: opposing activities that mediate cell death. *Nature Reviews Molecular Cell Biology,* 9**,** 47-59.

YOUNG, L. S., DAWSON, C. W., BROWN, K. W. & RICKINSON, A. B. (1989) Identification of a human epithelial cell surface protein sharing an epitope with the C3d/epsteinâ€ barr virus receptor molecule of B lymphocytes. *International journal of cancer,* 43**,** 786-794.

YOUNG, L. S., ELIOPOULOS, A. G., GALLAGHER, N. J. & DAWSON, C. W. (1998) CD40 and epithelial cells: across the great divide. *Immunology today,* 19**,** 502-506.

ZHANG, A. Y., YI, F., JIN, S., XIA, M., CHEN, Q.-Z., GULBINS, E. & LI, P.-L. (2007) Acid sphingomyelinase and its redox amplification in formation of lipid raft redox signaling platforms in endothelial cells. *Antioxidants & redox signaling,* 9**,** 817-828.

ZHANG, A. Y., YI, F., ZHANG, G., GULBINS, E. & LI, P.-L. (2006) Lipid raft clustering and redox signaling platform formation in coronary arterial endothelial cells. *Hypertension,* 47**,** 74-80.

ZHANG, R.-G., ZHAO, J.-J., YANG, L.-Q., YANG, S.-M., WANG, R.-Q., CHEN, W.-S., PENG, G.-Y. & FANG, D.-C. (2010) RNA interference-mediated hTERT inhibition enhances TRAIL-induced apoptosis in resistant hepatocellular carcinoma cells. *Oncology reports,* 23**,** 1013-1019.

ZHANG, R., AL-LAMKI, R., BAI, L., STREB, J. W., MIANO, J. M., BRADLEY, J. & MIN, W. (2004a) Thioredoxin-2 inhibits mitochondria-located ASK1-mediated apoptosis in a JNK-independent manner. *Circulation research,* 94**,** 1483-1491.

ZHANG, X. D., GILLESPIE, S. K. & HERSEY, P. (2004b) Staurosporine induces apoptosis of melanoma by both caspase-dependent and-independent apoptotic pathways. *Molecular cancer therapeutics,* 3**,** 187-197.

ZITVOGEL, L., TESNIERE, A. & KROEMER, G. (2006) Cancer despite immunosurveillance: immunoselection and immunosubversion. *Nature Reviews Immunology,* 6**,** 715-727.

ZUCKERMAN, V., WOLYNIEC, K., SIONOV, R. V., HAUPT, S. & HAUPT, Y. (2009) Tumour suppression by p53: the importance of apoptosis and cellular senescence. *The Journal of pathology,* 219**,** 3-15.